

LUND UNIVERSITY

Lignin Conversion to Value-Added Small-Molecule Chemicals

Towards Integrated Forest Biorefineries

Abdelaziz, Omar Y.

2021

Document Version:
Publisher's PDF, also known as Version of record

Link to publication

Citation for published version (APA):
Abdelaziz, O. Y. (2021). *Lignin Conversion to Value-Added Small-Molecule Chemicals: Towards Integrated Forest Biorefineries.* [Doctoral Thesis (compilation), Division of Chemical Engineering]. Department of Chemical Engineering, Faculty of Engineering (LTH), Lund University.

Total number of authors:
1

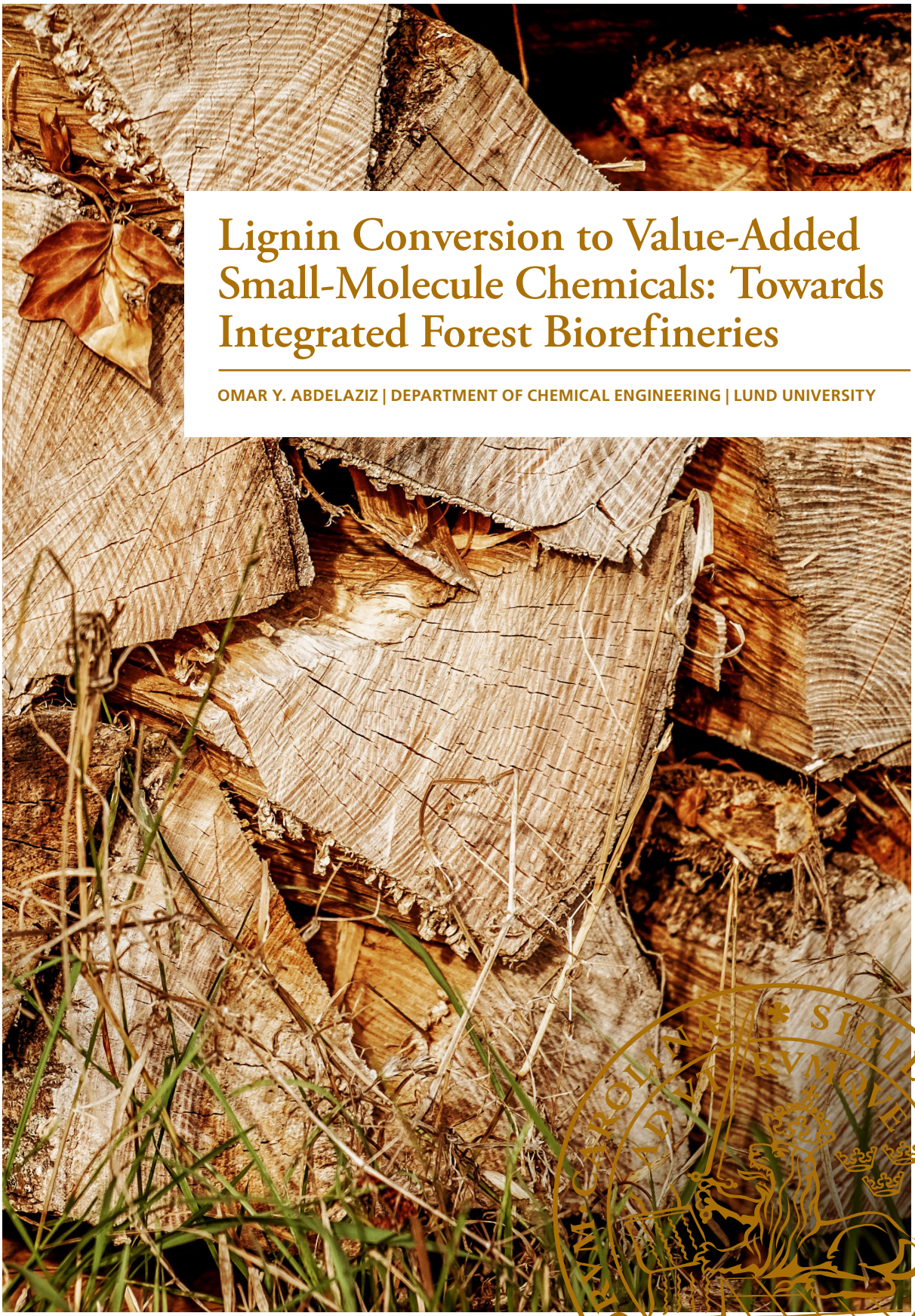
General rights
Unless other specific re-use rights are stated the following general rights apply:
Copyright and moral rights for the publications made accessible in the public portal are retained by the authors and/or other copyright owners and it is a condition of accessing publications that users recognise and abide by the legal requirements associated with these rights.
• Users may download and print one copy of any publication from the public portal for the purpose of private study or research.
• You may not further distribute the material or use it for any profit-making activity or commercial gain
• You may freely distribute the URL identifying the publication in the public portal

Read more about Creative commons licenses: https://creativecommons.org/licenses/

Take down policy
If you believe that this document breaches copyright please contact us providing details, and we will remove access to the work immediately and investigate your claim.

LUND UNIVERSITY

PO Box 117
221 00 Lund
+46 46-222 00 00



Lignin Conversion to Value-Added Small-Molecule Chemicals: Towards Integrated Forest Biorefineries

OMAR Y. ABDELAZIZ | DEPARTMENT OF CHEMICAL ENGINEERING | LUND UNIVERSITY

Lignin Conversion to Value-Added Small-Molecule Chemicals

Towards Integrated Forest Biorefineries

Omar Y. Abdelaziz



LUND UNIVERSITY

DOCTORAL DISSERTATION
by due permission of the Faculty of Engineering, Lund University, Sweden.
To be defended in Lecture Hall KC:B at the Center for Chemistry and Chemical Engineering, Naturvetarvägen 14, Lund, Sweden, on March 15, 2021 at 09:00.

Faculty opponent
Dr. Richard J.A. Gosselink
Wageningen Food & Biobased Research, the Netherlands

Organization LUND UNIVERSITY Department of Chemical Engineering P.O. Box 124 SE-221 00 Lund Sweden	**Document name** DOCTORAL DISSERTATION **Date of issue** 2021-02-19
Author Omar Y. Abdelaziz	**Sponsoring organizations** Swedish Foundation for Strategic Research Swedish Energy Agency

Title and subtitle

Lignin Conversion to Value-Added Small-Molecule Chemicals: Towards Integrated Forest Biorefineries

Abstract

Lignin is the most abundant aromatic biopolymer on Earth and has significant potential as a feedstock for industrial use. Due to its intrinsic heterogeneity and recalcitrance, lignin has been regarded as a low-value side-product in the pulp and paper industry and in second-generation biorefineries. However, novel technologies are currently being explored to utilize lignin as a renewable resource for bio-based chemicals, fuels, and materials. The efficient valorization of lignin would also improve the economics and sustainability of forest-based industries. Deriving value from lignin, beyond low-value heat and power, is thus essential for the success of a global circular bioeconomy employing lignocellulosic biomass as a raw material.

This thesis discusses the possibility of producing high-value chemicals from technical lignin streams via thermochemical–biological methods. The work deals with four major research themes: (1) providing insights into the physicochemical properties of technical lignins that could be valuable in designing routes for their valorization, (2) developing technologies for the thermochemical depolymerization of lignin under batch and continuous-flow conditions, (3) developing strategies for the biological valorization of lignin by combining thermochemical depolymerization with microbial conversion, and (4) assessing the techno-economic viability of lignin as a feedstock for sustainable chemical production in a biorefinery.

Comprehensive physicochemical characterization of technical lignins is crucial in the development of molecularly tailored lignin-based applications. Elucidating the structural and compositional features can facilitate the matching of technical lignin streams with suitable valorization strategies, including thermochemical depolymerization. Two thermochemical depolymerization approaches were investigated for the production of low-molecular-weight aromatics from technical lignin: base-catalyzed depolymerization and oxidative depolymerization. Both approaches were also found to be effective means of pretreatment enabling the microbial conversion of kraft lignin.

Continuous processing allowed hydrothermal lignin treatment at exceptionally short residence times, and this is anticipated to be an important stepping-stone toward technical lignin valorization. Membrane filtration appeared to be a practical method of separating complex depolymerized lignin mixtures for product fractionation and upgrading. Bimetallic catalyst systems based on Cu, Mn, and V improved the oxidative conversion of lignosulfonate and kraft lignins into value-added aromatic compounds. Techno-economic analysis underlined the viability of large-scale chemical production from kraft lignin by oxidative depolymerization, offering opportunities for process integration with traditional pulp mills.

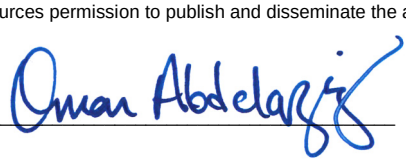
Keywords

aromatic monomers; biorefinery; catalysis; kraft lignin; lignin depolymerization; lignin valorization; microbial conversion; renewable chemicals; techno-economic analysis

Classification system and/or index terms (if any)

Supplementary bibliographical information		**Language** English
ISSN and key title		**ISBN** 978-91-7422-782-6 (Printed version) 978-91-7422-783-3 (Digital version)
Recipient's notes	**Number of pages** 169	**Price**
	Security classification	

I, the undersigned, being the copyright owner of the abstract of the above-mentioned dissertation, hereby grant to all reference sources permission to publish and disseminate the abstract of the above-mentioned dissertation.

Signature  Date 2021-02-01

Lignin Conversion to Value-Added Small-Molecule Chemicals

Towards Integrated Forest Biorefineries

Omar Y. Abdelaziz



LUND
UNIVERSITY

Cover image from Pixabay

Copyright pp 1–64 (Omar Y. Abdelaziz)
Paper 1 © The Authors (Open Access)
Paper 2 © The Authors (Open Access)
Paper 3 © The Authors (Open Access)
Paper 4 © The Authors (Open Access)
Paper 5 © American Chemical Society (Open Access, ACS AuthorChoice)
Paper 6 © American Chemical Society (Open Access, ACS AuthorChoice)
Paper 7 © The Royal Society of Chemistry

Faculty of Engineering
Department of Chemical Engineering

ISBN 978-91-7422-782-6 (Printed version)
ISBN 978-91-7422-783-3 (Digital version)

Printed in Sweden by Media-Tryck, Lund University
Lund 2021

Media-Tryck is a Nordic Swan Ecolabel certified provider of printed material. Read more about our environmental work at www.mediatryck.lu.se

MADE IN SWEDEN

وَفَوْقَ كُلِّ ذِى عِلْمٍ عَلِيمٌ ﴿يوسف:٧٦﴾

But over all endued with knowledge is
One, the All-Knowing ﴿Yusuf:76﴾

Abstract

Lignin is the most abundant aromatic biopolymer on Earth and has significant potential as a feedstock for industrial use. Due to its intrinsic heterogeneity and recalcitrance, lignin has been regarded as a low-value side-product in the pulp and paper industry and in second-generation biorefineries. However, novel technologies are currently being explored to utilize lignin as a renewable resource for bio-based chemicals, fuels, and materials. The efficient valorization of lignin would also improve the economics and sustainability of forest-based industries. Deriving value from lignin, beyond low-value heat and power, is thus essential for the success of a global circular bioeconomy employing lignocellulosic biomass as a raw material.

This thesis discusses the possibility of producing high-value chemicals from technical lignin streams via thermochemical–biological methods. The work deals with four major research themes: (1) providing insights into the physicochemical properties of technical lignins that could be valuable in designing routes for their valorization, (2) developing technologies for the thermochemical depolymerization of lignin under batch and continuous-flow conditions, (3) developing strategies for the biological valorization of lignin by combining thermochemical depolymerization with microbial conversion, and (4) assessing the techno-economic viability of lignin as a feedstock for sustainable chemical production in a biorefinery.

Comprehensive physicochemical characterization of technical lignins is crucial in the development of molecularly tailored lignin-based applications. Elucidating the structural and compositional features can facilitate the matching of technical lignin streams with suitable valorization strategies, including thermochemical depolymerization. Two thermochemical depolymerization approaches were investigated for the production of low-molecular-weight aromatics from technical lignin: base-catalyzed depolymerization and oxidative depolymerization. Both approaches were also found to be effective means of pretreatment enabling the microbial conversion of kraft lignin.

Continuous processing allowed hydrothermal lignin treatment at exceptionally short residence times, and this is anticipated to be an important stepping-stone toward technical lignin valorization. Membrane filtration appeared to be a practical method of separating complex depolymerized lignin mixtures for product fractionation and upgrading. Bimetallic catalyst systems based on Cu, Mn, and V improved the oxidative conversion of lignosulfonate and kraft lignins into value-added aromatic compounds. Techno-economic analysis underlined the viability of large-scale chemical production from kraft lignin by oxidative depolymerization, offering opportunities for process integration with traditional pulp mills.

Populärvetenskaplig sammanfattning

Det finns en djupt rotad tro att man kan göra vad som helst med lignin utom att tjäna pengar, men stämmer det fortfarande? Fastän detta gamla talesätt antyder att värdeskapande från lignin är svårt, undersöks flera tekniska koncept för att producera ligninbaserade kemikalier, bränslen och material. Dessa framväxande tekniker kommer att hjälpa oss att härleda mesta möjliga värde från lignin, något som är nödvändigt i en cirkulär, biobaserad ekonomi som utnyttjar biomassa som ett förnybart material. Vad är då lignin, var återfinns det, och hur kan vi använda det för att skapa mest värde?

Lignin är en polymer med högt kolinnehåll som återfinns i växters cellväggar. Det hjälper till att hålla ihop växten och bidrar till funktionaliteten. I princip fungerar lignin som det lim som håller ihop de två andra huvudsakliga komponenterna i biomassa, cellulosa och hemicellulosa. Vid produktion av papper och biobränslen betraktas lignin allt som oftast som en biprodukt och eldas lokalt för att producera energi. Lignin är dock för värdefullt för att eldas i syfte att skapa energi och denna avhandling beskriver strategier som kan användas för att omvandla denna industriella biprodukt till högvärdiga produkter.

Först användes välkända tekniker för att karakterisera de fysikaliska och kemiska egenskaperna hos olika kommersiella ligniner. Det är viktigt att ha en god grund att stå på för att kunna matcha olika ligninströmmar med lämpliga metoder och tekniker för att öka värdet på ligninet. Bland dessa metoder framstår kombinationen av termokemisk och biologisk omvandling som en metod med signifikant potential att överkomma de utmaningar som finns i uppgradering av denna fascinerande, men komplexa biopolymer, till högvärdiga produkter. Biologisk omvandling med syfte att öka värdet på lignin inkluderar ofta ett förbehandlingssteg där ligninmakromolekylen bryts ner till mindre delar, vilka blir tillgängliga för mikroorganismen. Denna förbehandling kan göras med enzymer, vilket ofta är en långsam process, eller med termokemiska metoder som producerar en blandning av värdefulla ämnen.

För att producera mindre molekyler från industriella ligninsubstrat har två metoder använts i detta arbete, baskatalyserad- och oxidativdepolymerisering. Den förstnämnda metoden utfördes i en flödesreaktor, vilket gjorde det möjligt att använda mycket korta reaktionstider. Den senare metoden förlitar sig på användning av syrgas och ger en mer hållbar och gynnsam process än tidigare rapporterats. Genom att använda bimetalliska katalysatorer förbättrades den oxidativa ligninomvandlingsprocessen och genom teknoekonomisk analys visades det att storskalig kemikalieproduktion skulle kunna vara lönsam med denna process.

List of papers

This thesis is based on the research papers listed below, which are referred to in the text by their Roman numerals. The papers are appended at the end of this thesis.

I. Physicochemical characterisation of technical lignins for their potential valorisation

Abdelaziz, O.Y. & Hulteberg, C.P. (2017)

Waste and Biomass Valorization, 8(3), 859–869

II. Continuous catalytic depolymerisation and conversion of industrial kraft lignin into low-molecular-weight aromatics

Abdelaziz, O.Y., Li, K., Tunå, P. & Hulteberg, C.P. (2018)

Biomass Conversion and Biorefinery, 8, 455–470

III. Membrane filtration of alkali-depolymerised kraft lignin for biological conversion

Abdelaziz, O.Y., Ravi, K., Nöbel, M., Tunå, P., Turner, C. & Hulteberg, C.P. (2019)

Bioresource Technology Reports, 7, 100250

IV. Oxidative depolymerisation of lignosulphonate lignin into low-molecular-weight products with Cu–Mn/δ-Al_2O_3

Abdelaziz, O.Y., Meier, S., Prothmann, J., Turner, C., Riisager, A. & Hulteberg, C.P. (2019)

Topics in Catalysis, 62(7-11), 639–648

V. Oxidative depolymerization of kraft lignin for microbial conversion

Abdelaziz, O.Y., Ravi, K., Mittermeier, F., Meier, S., Riisager, A., Lidén, G. & Hulteberg, C.P. (2019)

ACS Sustainable Chemistry & Engineering, 7(13), 11640–11652

VI. Conceptual design of a kraft lignin biorefinery for the production of valuable chemicals via oxidative depolymerization

Abdelaziz, O.Y., Al-Rabiah, A.A., El-Halwagi, M.M. & Hulteberg, C.P. (2020)

ACS Sustainable Chemistry & Engineering, 8(23), 8823–8829

VII. Oxidative depolymerization of kraft lignin to high-value aromatics using a homogeneous vanadium–copper catalyst

Walch, F., Abdelaziz, O.Y., Meier, S., Bjelić, S., Hulteberg, C.P. & Riisager, A. (2021)

Catalysis Science & Technology, DOI: 10.1039/d0cy02158j

My contributions to the studies

The papers appended to this thesis were coauthored. My contributions to the studies were as follows.

I. I designed and performed the study. I evaluated the results and wrote the manuscript, together with the coauthor.

II. I contributed to the conceptualization and construction of the continuous-flow reactor setup. I participated in the planning of the study, the experimental work, and the interpretation of the results. I wrote the manuscript, with input from the other authors.

III. I participated in the conceptualization and design of the study, the experimental work, and the interpretation of the results. I wrote the manuscript, together with the other authors.

IV. I participated in the design of the study. I performed the catalytic oxidation reactions. I evaluated the results and wrote the manuscript, with input from the other authors. I handled the submission.

V. I participated in the conceptualization and design of the study and performed the oxidative depolymerization experiments. I evaluated the results and wrote the manuscript, with input from the other authors.

VI. I participated in the conceptualization and design of the study, and contributed to the modeling and simulation of the process. I performed the analysis of process efficiency, sustainability, and economics. I interpreted the results and wrote the manuscript, with input from the other authors.

VII. I participated in the conceptualization and design of the study. I coordinated the catalytic depolymerization experiments and chemical analysis. I was involved in the interpretation of the results, and I critically reviewed the manuscript.

Associated publications

I have also contributed to the following peer-reviewed publications, which are not included in this thesis:

P1. Biological valorization of low molecular weight lignin

Abdelaziz, O.Y., Brink, D.P., Prothmann, J., Ravi, K., Sun, M., García-Hidalgo, J., Sandahl, M., Hulteberg, C.P., Turner, C., Lidén, G. & Gorwa-Grauslund, M.F. (2016)

Biotechnology Advances, 34(8), 1318–1346

P2. Bacterial conversion of depolymerized Kraft lignin

Ravi, K., Abdelaziz, O.Y., Nöbel, M., García-Hidalgo, J., Gorwa-Grauslund, M.F., Hulteberg, C.P. & Lidén, G. (2019)

Biotechnology for Biofuels, 12:56

P3. Green solvents-based fractionation process for kraft lignin with controlled dispersity and molecular weight

Ajao, O., Jeaidi, J., Benali, M., Abdelaziz, O.Y. & Hulteberg, C.P. (2019)

Bioresource Technology, 291, 121799

P4. New synthetic approaches to biofuels from lignocellulosic biomass

Zhu, P., Abdelaziz, O.Y., Hulteberg, C.P. & Riisager, A. (2020)

Current Opinion in Green and Sustainable Chemistry, 21, 16–21

P5. Lignin depolymerization under continuous-flow conditions: highlights of recent developments

Abdelaziz, O.Y. & Hulteberg, C.P. (2020)

ChemSusChem, 13(17), 4382–4384

Abbreviations

2D	Two-dimensional
ACD	Acid-catalyzed depolymerization
BCD	Base-catalyzed depolymerization
BET	Brunauer–Emmett–Teller
BJH	Barrett–Joyner–Halenda
CFR	Continuous-flow reactor
DIK	Depolymerized Indulin AT kraft lignin
DS	Dry solids content
EDS	Energy-dispersive spectroscopy
FTIR	Fourier transform infrared spectroscopy
HMBC	Heteronuclear multiple-bond correlation
HMW	High molecular weight
HRMS	High-resolution mass spectrometry
HSQC	Heteronuclear single-quantum correlation
ICP–OES	Inductively coupled plasma–optical emission spectrometry
IK	Indulin AT kraft lignin
LB	LignoBoost kraft lignin
LMW	Low molecular weight
MISR	Metric for inspecting sales and reactants
MWD	Molecular weight distribution
M_n	Number-average molecular weight
M_w	Weight-average molecular weight
NaLS	Sodium lignosulfonate lignin
NMR	Nuclear magnetic resonance
NPV	Net present value
ODLB	Oxidatively depolymerized LignoBoost lignin
OD_{620}	Optical density at 620 nm
PSD	Particle size distribution
ROI	Return on investment
SEM	Scanning electron microscopy
SEC	Size-exclusion chromatography
TEA	Techno-economic analysis
TGA	Thermogravimetric analysis
UHPLC	Ultra-high-performance liquid chromatography
UHPSFC	Ultra-high-performance supercritical fluid chromatography
UV–Vis	Ultraviolet–visible absorption spectroscopy
WBL	Weak black liquor
wt%	Weight percent
XPS	X-ray photoelectron spectroscopy
XRD	X-ray diffraction

Contents

1 Introduction 1

1.1 Background 1

1.2 Aims and approach 2

1.3 Outline of the thesis 3

2 Lignin – a fascinating macromolecule for biorefineries 4

2.1 Lignin in a biorefinery context 4

2.2 Lignin structure and composition 5

2.3 Technical lignin 7

2.3.1 Kraft lignin 8

2.3.2 Lignosulfonates 10

2.3.3 Alkali lignin 11

2.3.4 Organosolv lignin 11

2.3.5 Hydrolysis lignin 12

2.4 Market potential for lignin 13

2.5 Technologies for lignin conversion 15

2.5.1 Acid-catalyzed depolymerization 16

2.5.2 Base-catalyzed depolymerization 17

2.5.3 Oxidative depolymerization 17

2.5.4 Reductive depolymerization 18

2.5.5 Thermal depolymerization 18

2.5.6 Other depolymerization strategies 19

3 Base-catalyzed depolymerization of technical lignin 20

3.1 Understanding the physicochemical properties 20

3.2 Depolymerization under continuous-flow conditions 23

3.3 Bioconversion of alkali-treated kraft lignin 28

4 Oxidative depolymerization of technical lignin 32

4.1 Searching for a heterogeneous catalyst 32

4.2 Bioconversion of oxygen-treated kraft lignin 36

4.3 Process design and techno-economics 42

4.4 On the yields of phenolic monomers 47

5 Conclusions and outlook 52

Acknowledgments 55

References 58

1 Introduction

This thesis is composed of a summary and seven papers. The summary presents an overview of my research, discusses it in the perspective of lignin valorization research, and summarizes the key findings and conclusions. The seven papers describe the details of the scientific approaches used, including lignin characterization, depolymerization, and upgrading through thermochemical and biochemical processes. The focus is on aligning these aspects of a technological biorefinery to provide pathways for the utilization of lignin as a renewable resource for value-added chemicals. In this chapter, an introduction is given to the research subject, the overall aims of the work performed are described, and a brief outline of the thesis is given.

1.1 Background

The conversion of lignocellulosic biomass to chemicals, fuels, and materials is a promising alternative to traditional processes based on diminishing fossil resources. Terrestrial (nonedible) plant biomass in the form of lignocellulose comprises polymeric carbohydrates and lignin; both of which have been recognized as attractive renewable sources of carbon that can largely cover the future demand for clean energy, and hence help us meet the targets for sustainable development [1]. To achieve this goal, it is essential to overcome the resistance of plant cell walls to chemical and biological deconstruction, so-called biomass recalcitrance [2]. The first step in a biorefinery is usually fractionation either based on delignification or carbohydrate conversion to reduce the recalcitrance and the complexity of lignocellulosic biomass [3].

The success of the pulp and paper industry and second-generation biorefineries relies on the efficient separation and utilization of the lignin fraction of biomass. Vast amounts of lignin are processed in pulp mills, where its main use today is limited to combustion for energy recovery [4,5]. It is, however, anticipated that in an advanced biorefinery, i.e., in the production of second-generation ethanol, considerable amounts of lignin will be generated, surplus to that required to power the biorefining operation [6,7]. Therefore, making better use of this renewable aromatic resource is a major goal in the lignin valorization community. The efficient utilization of lignin will not only enable the production of value-added chemicals,

fuels, and materials, but will also improve the economic viability as well as the sustainability profiles of the pulp and paper and the biofuel sectors.

1.2 Aims and approach

The scope of this thesis covers the thermochemical depolymerization of lignin macromolecules into smaller fragments that could be exploited in various kinds of microbial metabolism. The work presented here was carried out as part of a larger project funded by the *Swedish Foundation for Strategic Research*, and aims to explore novel high-value applications of lignin through tailoring microbial hosts for the biological valorization of low-molecular-weight (LMW) lignin (Figure 1.1).

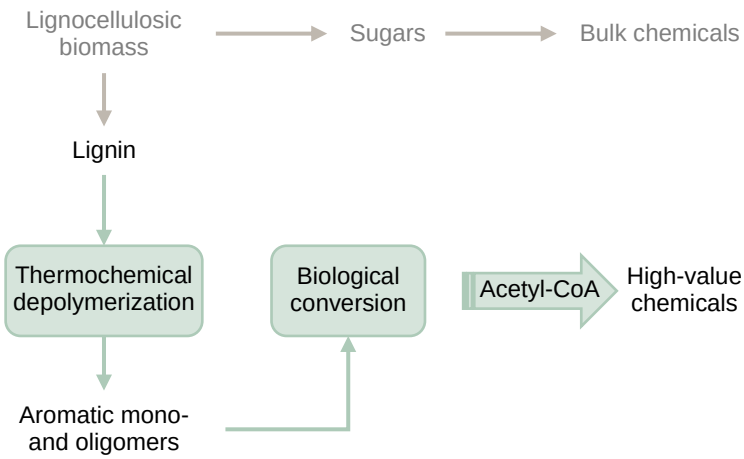


Figure 1.1. An overview of the proposed approach for biological lignin valorization to value-added chemicals.

The overall goal of the project was to demonstrate a strategy for the biological valorization of lignin to high-value chemicals by transforming the aromatic mono- and oligomers derived from thermochemical depolymerization into central metabolites, e.g. acetyl-CoA, for internal product biosynthesis. Lignin, recovered primarily from industrial sources, can be depolymerized by thermochemical methods to produce a mixture of LMW aromatic compounds. This mixture of aromatics serves as a source of carbon and energy for microorganisms to enable further conversion into value-added products. Potential products and metabolic intermediates that could be obtained with this strategy include, among others, vanillin, *cis*,*cis*-muconate, adipic acid, 2-pyrone-4,6-dicarboxylic acid, polyhydroxyalkanoate, and triacylglycerols.

The specific research goals of the work described in this thesis were:

- to provide insights into the physicochemical properties of technical lignins that could be valuable in designing routes for their valorization,
- to develop technologies for the thermochemical depolymerization of lignin under batch and continuous-flow conditions,
- to develop strategies for the biological valorization of lignin by combining thermochemical depolymerization with microbial conversion, and
- to assess the techno-economic viability of lignin as a feedstock for sustainable chemical production in a biorefinery.

1.3 Outline of the thesis

This thesis is divided into five chapters and seven appended papers. Chapter 1 presents a brief background on the scope of the research and introduces the aims of the work. Chapter 2 gives a general overview of lignin, its presence in the biosphere, and the chemistry behind this intriguing macromolecule, including the main types of lignin, possible applications, and technologies for their conversion. Chapter 3 summarizes the work carried out on lignin characterization (**Paper I**) and the base-catalyzed depolymerization and conversion of kraft lignin (**Papers II** and **III**). **Paper I** presents the tools that can be used for the characterization of technical lignin, and describes the effect of pretreatment severity on the chemical composition and functional properties of lignin as a raw material. **Paper II** describes a method for the base-catalyzed depolymerization of lignin in a continuous-flow reactor system, and the impact of operating conditions on the conversion of kraft lignin into LMW phenolics. The study described in **Paper III** builds on the findings presented in **Paper II**, in which a process concept combining depolymerization, nanofiltration, and bioconversion is demonstrated, and its potential for integration into existing pulp and paper mills is discussed. Chapter 4 outlines the work performed on the oxidative depolymerization of lignin (**Papers IV**, **V**, **VI**, and **VII**). **Paper IV** describes experiments employing various heterogeneous catalysts to determine their ability to depolymerize lignosulfonate lignin into LMW products. **Paper V** demonstrates the potential of oxidative depolymerization as a means of pretreatment for the biological conversion of kraft lignin. The findings of **Paper V** were used as the basis of the work presented in **Paper VI** to design a conceptual process and assess the techno-economics of large-scale production of value-added chemicals from kraft lignin. **Paper VII** describes a strategy for converting kraft lignin into LMW phenolics with a high bio-oil yield under oxidative conditions using a vanadium–copper catalyst. Finally, the conclusions drawn from the findings of this work and suggestions for future research are presented in Chapter 5.

2 Lignin – a fascinating macromolecule for biorefineries

Lignin is a complex and abundant natural polymer with high aromaticity and, as such, is a potential raw material for sustainable conversion into value-added chemicals and fuels. Being found in the cell wall of terrestrial plants, lignin provides strength and rigidity, facilitates the transport of water and nutrients in plant tissues, and forms a recalcitrant barrier to pathogens [8]. Lignin is also obtained from the pulp and paper industry and various other sources. Interest in this multifaceted macromolecule arises from different fields of knowledge, such as biology, chemistry, chemical engineering, environmental science, and economics; this diversity implies that a comprehensive view about lignin should come from a multidisciplinary approach [9].

2.1 Lignin in a biorefinery context

Wood and other lignocellulosic materials are composed mainly of three different polymers, namely cellulose, hemicellulose, and lignin. These three polymers are found in wood plant cell walls, where they form lignin–carbohydrate complexes, which have been suggested to play a vital role in recalcitrance during biomass fractionation and processing [10]. These complexes are believed to assemble through covalent and non-covalent binding between lignin and carbohydrates (mainly with hemicellulose), and are responsible for the strength and structure of the plant cell wall (Figure 2.1), posing an obstacle in the separation and utilization of plant-based resources [11,12]. However, the extraction and subsequent chemical transformation of the three constituent polymers can provide a broad and multifunctional array of valuable chemicals, fuels, and materials. If obtained through an integrated system of reaction pathways, a so-called biorefinery, the optimal potential of each constituent, and thus the maximum gain, can be achieved from the whole biomass feedstock [13].

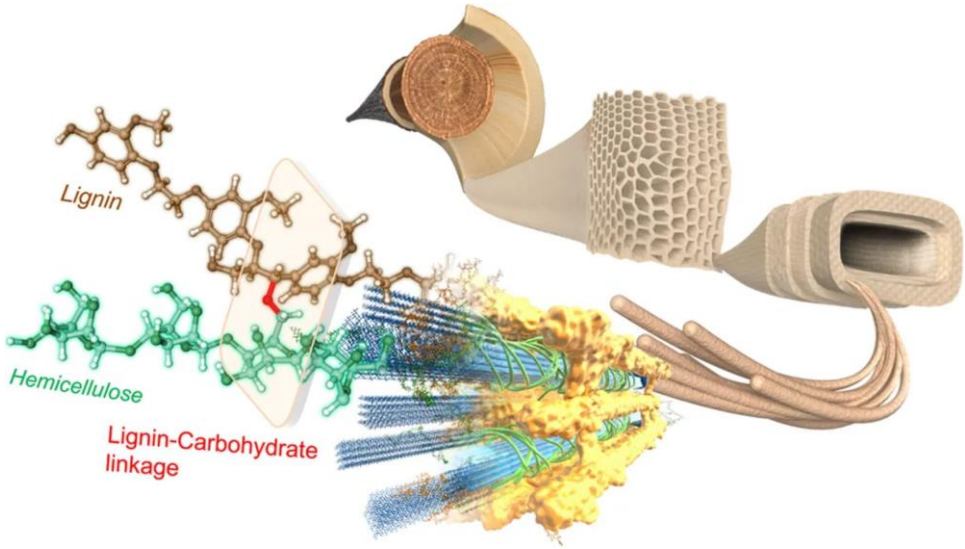


Figure 2.1. A three-dimensional illustration of the lignin–carbohydrate complex in the wood plant cell wall. (Reproduced from Nishimura et al. [11], under a Creative Commons Attribution 4.0 International License)

2.2 Lignin structure and composition

Lignin biosynthesis occurs through the oxidative radical polymerization of three major *p*-hydroxycinnamyl alcohols: sinapyl alcohol, coniferyl alcohol, and *p*-coumaryl alcohol [14], the so-called monolignols (Figure 2.2). Phenoxyl radials generated from these three monolignols are randomly polymerized to produce a lignin polymer with a three-dimensional network [15]. In contrast to most other biopolymers, the structure of lignin lacks regular and ordered repeating units, making it recalcitrant to depolymerization [14]. Following incorporation into lignin, the monolignols give rise to three basic structural units, abbreviated S (syringyl), G (guaiacyl), and H (*p*-hydroxyphenyl), which vary in their number of methoxy functionalities on the aromatic ring. Hardwood lignin is composed of both S and G units, softwood lignin is composed of mainly G units with minor amounts of H units, and herbaceous plant lignin comprises all three structural units. Typically, softwoods contain the highest amount of lignin (21–29 wt%), followed by hardwoods (18–25 wt%), and herbaceous plants (15–24 wt%), although variations also occur in different regions of the cell wall, with cell type, and the stage in the cell cycle [3]. For example, the weight-average molecular weight (*M*w) of milled wood lignin from Southern pine is 14.9, while that of Norway spruce is 23.5 kDa, showing that the molecular weight of lignin varies considerably depending on the source of the biomass, pretreatment conditions, and the method of isolation [16].

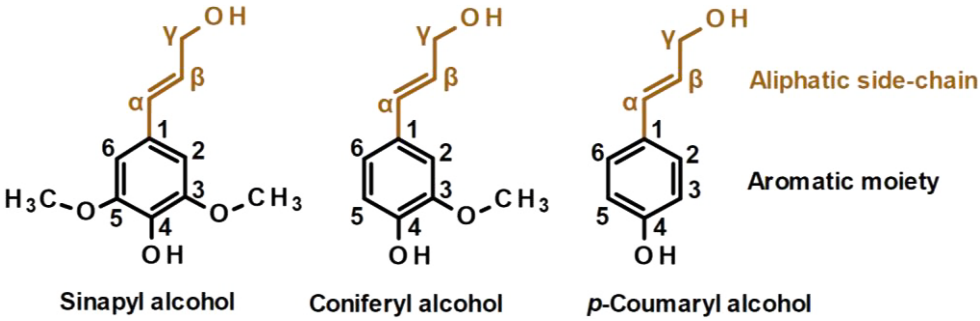


Figure 2.2. Structures of the three monolignols. The numbering of carbon atoms in the benzene ring and the notation on the aliphatic propylene side-chain are shown.

The variations in lignin structure originate not only from the presence of different monolignols as building blocks, but also from the way in which the monolignols are bound to each other to produce the lignin complex, for example, C–O and C–C interunit bonds in the biopolymer. The arylglycerol-β-aryl ether (β-O-4) is the most common and well-known interunit linkage, which accounts for 45–60% in softwood and hardwood lignins [17]. Other known interunit linkages include α-O-4, 4-O-5, β-β, β-5, β-1, and 5-5 (Figure 2.3). Recently discovered units may also include dibenzodioxocin (5-5/β-O-4/α-O-4), spirodienone (β-1/α-O-α), and benzodioxane (β-O-4/α-O-5, called C-Lignin) linkages [15]. The linkages and functional groups common in lignin are given in Table 2.1, together with their relative proportions.

Table 2.1. Relative proportions of the main linkages and functional groups in lignin (Adapted from Abdelaziz et al. [4])

Linkage	Softwood lignin (%)	Hardwood lignin (%)
β-O-4	45–50	60
α-O-4	2–8	7
4-O-5	4–8	7–9
β-β	2–6	3–12
β-5	9–12	6
β-1	7–10	1–7
5-5	10–27	3–9
Functional group abundance per 100 C_9 units		
Aliphatic hydroxyl	115–120	88–166
Methoxyl	90–97	139–158
Phenolic hydroxyl	15–30	10–15
Carbonyl	10–20	17–24

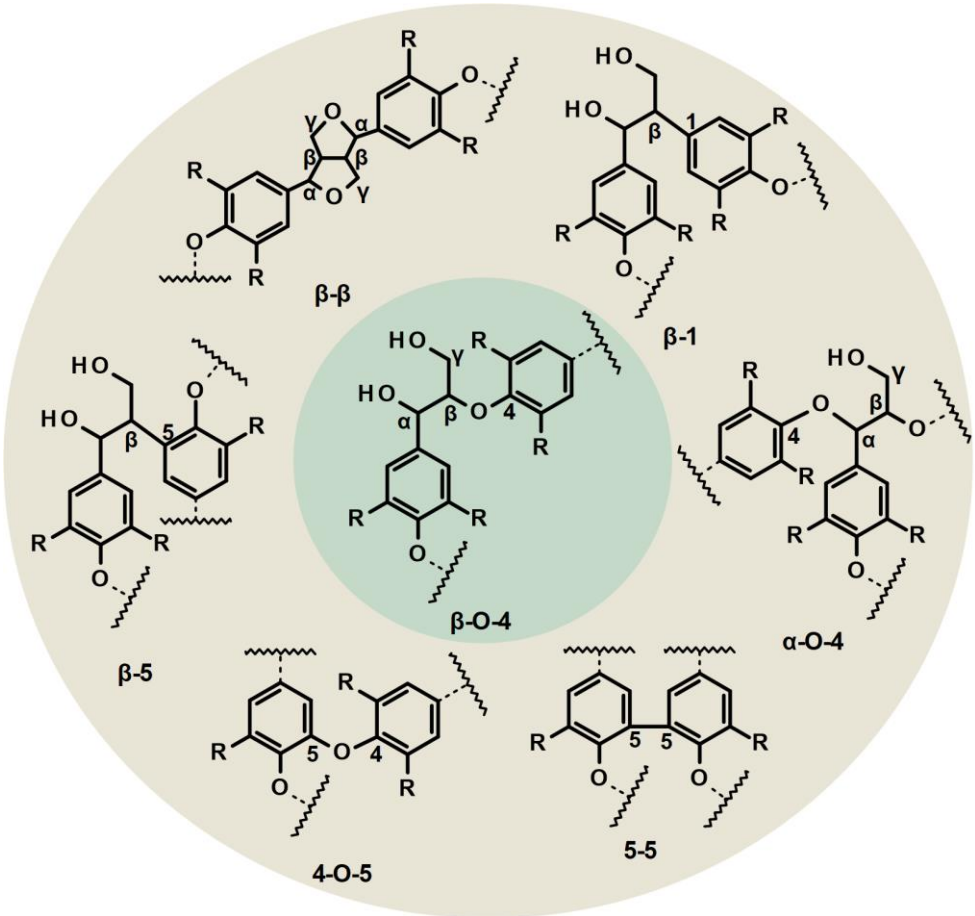


Figure 2.3. Main interunit linkages in lignin.

2.3 Technical lignin

The term technical lignin (also referred to as industrial or commercial lignin) is used to denote lignin streams that are generated from the pulp and paper industry, or from the developing cellulosic ethanol industry. Technical lignin presents a potentially sustainable bulk feedstock and, depending on the delignification procedure, it can be broadly divided into two different categories: sulfur-containing lignin and sulfur-free lignin (Figure 2.4). Each kind of technical lignin is unique with respect to its chemical structure, molecular weight, dispersity, and purity [18,19]. It is therefore important to have knowledge on the entire pathway through which a technical lignin stream is generated. Compared to native lignin, technical lignin is characterized by

its low abundance of cleavable β-ether linkages and its highly condensed nature, aspects that must be considered when developing strategies for lignin valorization including depolymerization and material applications [20].

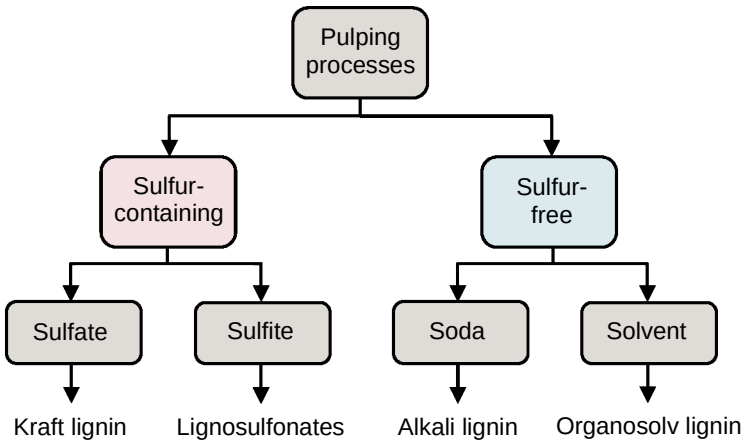


Figure 2.4. Common chemical pulping processes and their corresponding technical lignin products.

2.3.1 Kraft lignin

Kraft (sulfate) pulping (Figure 2.5) is the main process used to produce chemical pulp, accounting for about 90% of the global production. The annual production of kraft pulp worldwide is on the order of 130 million tons [13], of which approximately 50 million tons of lignin is generated [21,22]. Wood chips are transformed into pulp by cooking in an aqueous solution of NaOH and Na_2S, so-called white liquor, at a temperature of 155–175 °C [23]. After delignification, the cellulosic fibers are washed and chemically bleached, often using ClO_2 as a bleaching agent [24]. The fibers are then drained, pressed, and thermally dried to obtain the kraft pulp product. The spent delignification liquor from the washing step (weak black liquor, WBL, containing 12–20% solids), is concentrated by evaporation to reduce the water content to about 15–25% [25]. The resulting stream, concentrated black liquor, is then incinerated in the recovery boiler to provide energy and recover the inorganic cooking chemicals. The spent inorganic chemicals form a smelt consisting of a mixture of molten salts, mainly Na_2CO_3 and Na_2S. This smelt is dissolved to form a green liquor, and then recausticized with quick-lime (CaO) to regenerate the pulping liquor, that is, white liquor. The lime mud ($CaCO_3$) resulting from caustization is sent to a lime kiln to regenerate CaO for reuse.

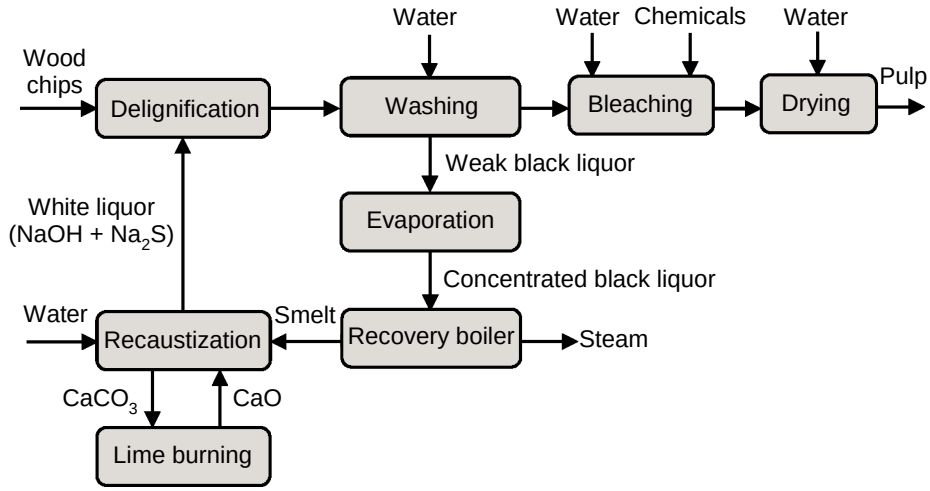


Figure 2.5. Simplified block flow diagram of the kraft pulping process. (Adapted from Bonhivers and Stuart [24])

Various techniques can be used to isolate lignin from kraft black liquor. Indulin AT, lignin precipitated from the kraft black liquor of linerboard pulp, has been the only source of technical lignin from the kraft process on the market for a long time. It was commercialized by the West Virginia Pulp and Paper Company MeadWestvaco in the 1950s (now merged to form WestRock), with applications in rubber reinforcement, and as asphalt emulsifiers, etc. [18].

The LignoBoost process is another example of a lignin extraction technology from black liquor, exploiting the energy surplus of modern kraft pulping [26,27]. The technology is based on acid precipitation, and was developed jointly by Chalmers University of Technology, Sweden, and Innventia (now part of RISE, Research Institutes of Sweden). The main steps in the LignoBoost process include precipitation, filtration, reslurrying, and washing (Figure 2.6). Partially evaporated black liquor containing ~40% dry solids content (DS) is acidified with CO_2 to a pH of about 10, followed by filtration and dewatering of the precipitated lignin. The filter cake is then reslurried with dilute aqueous H_2SO_4 to equilibrate at pH ~2; this acidified lignin slurry is then fed to a second chamber filter press. Finally, the filter cake is washed and dewatered, resulting in a purified lignin stream. The lignin material obtained with this method has low ash and carbohydrate contents and a high DS, and some 2–3% sulfur is usually present, about half being chemically bound to the lignin [28]. LignoBoost lignin has broad applications, e.g., in the production of fuels, dispersants, adhesives, carbon fibers, and bioplastics.

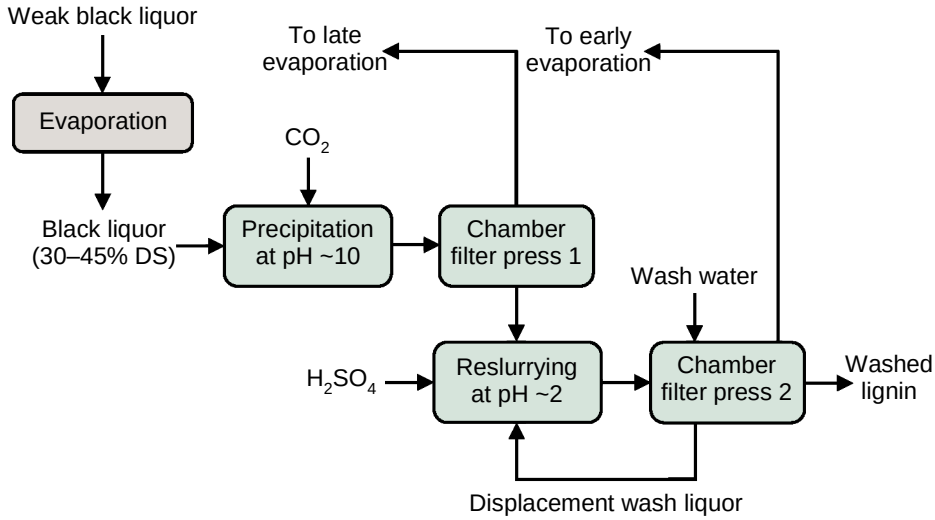


Figure 2.6. Simplified block flow diagram of the LignoBoost process for kraft lignin extraction. (Adapted from [18,26])

Other examples of recent technologies for extracting lignin from kraft black liquor include the LignoForce process and the Sequential Liquid–Lignin Recovery and Purification (SLRP) process [18]. All the above mentioned technologies are in current industrial use, except for SLRP, which has been demonstrated on pilot scale [29]. Such technologies allow pulp and paper manufacturers to broaden their portfolio of bio-based products, together with lignin production.

2.3.2 Lignosulfonates

Lignins from sulfite pulping are referred to as lignosulfonates due to the presence of sulfonate groups in their structure. Lignosulfonates are produced using sulfurous acid and/or its salts containing Ca^{2+}, Mg^{2+}, NH_4^+, or Na^+ cations at different pH levels [30]. Cooking can be acidic, neutral, or alkaline, depending on the combination of salts (Table 2.2). Acid (bi)sulfite pulps are used in the production of newsprint, tissue, and some printing paper grades, while pulps from neutral and alkaline sulfite processes are used in the manufacture of corrugated medium and packaging grades.

Compared to kraft lignin, lignosulfonates have lower purity, relatively higher molecular weight, and contain higher amounts of sulfur (4–8%) [3,9]. Nevertheless, lignosulfonates have a unique property that differentiates them from most other kinds of lignin: they are water-soluble, even at low pH. The global production of lignosulfonates is about 1 million metric tons per annum; Borregaard LignoTech in Norway being the biggest producer, and they are used mainly as binders and

dispersants in a broad range of applications [28,31]. However, sulfite pulping is declining drastically due to the higher versatility and efficiency of the kraft process, which is expected to result in reduced availability of lignosulfonates in the future.

Table 2.2. Sulfite pulping methods for lignin extraction from wood (Adapted from Calvo-Flores et al. [9])

Cooking process	Reactive agent(s)	pH	Temperature (°C)
Acid sulfite	SO_2/HSO_3^-	1–2	125–145
Bisulfite	HSO_3^-	3–5	150–175
Neutral sulfite	HSO_3^-/SO_3^{2-}	6–7	150–175
Alkaline sulfite/anthraquinone	$NaSO_3$	9–13	50–175

2.3.3 Alkali lignin

Alkali lignin is generated from the soda or soda-anthraquinone pulping processes. Such soda-based cooking approaches are used chiefly for cooking of nonwood plant fibers such as bagasse, straw, flax, but also, to some extent, hardwood [32]. The biomass is digested using an aqueous solution of NaOH or $Ca(OH)_2$ at temperatures up to about 160 °C [9]. Anthraquinone can also be used as an additive to reduce the degradation (peeling) of carbohydrates [33]. Compared to kraft lignin and lignosulfonates, alkali lignin is sulfur-free, implying that the native lignin structure is relatively least altered by soda pulping. Nonetheless, alkali lignin shares some structural similarities with kraft lignin due to common lignin solubilization mechanisms. Alkali lignin can also be extracted from soda black liquor through acidification, filtration, and washing, similar to kraft black liquor. The largest producer of sulfur-free alkali lignin worldwide is GreenValue SA, Switzerland, and it is used in wood adhesives, thermoplastic composites, animal feed, etc.

2.3.4 Organosolv lignin

Organosolv pulping is based on the treatment of biomass with organic solvents such as methanol, ethanol, butanol, formic acid, acetic acid, and peroxyformic acid, or in combination with water at temperatures in the range 180–200 °C [33]. In this process, lignin is solubilized in the organic medium, after which it is separated from the hemicellulose fraction by precipitation from the pulping liquor, resulting in organosolv lignin. Solubilization enables a lignin fraction to be obtained with a low degree of structural alterations and dispersity. For instance, the homogeneity of organosolv lignin is generally higher than that of lignosulfonates or alkali lignin [32,34]. Organosolv lignin is characterized by being sulfur-free and by its considerably lower carbohydrate and ash contents, making it a suitable substrate for catalytic transformation into valuable chemicals or materials [18,20].

2.3.5 Hydrolysis lignin

The cellulosic ethanol industry is emerging as a source of technical lignin. Within lignocellulosic ethanol production, hydrolysis lignin can be isolated prior to downstream carbohydrate conversion or after ethanol separation (Figure 2.7). Hydrolysis lignin can be divided into two major categories, namely acid hydrolysis lignin and enzymatic hydrolysis lignin. It can also be differentiated by plant origin, i.e. softwood, hardwood, or nonwood sources. After fermentation, lignin is liberated as a solid residue with a highly condensed structure, containing significant amounts of unprocessed material and components of carbohydrate origin [28]. Its high sorption ability and difficulties in dewatering allow the utilization of such lignin as a sorbent [32]. Nonetheless, the relatively high molecular weight and dispersity index of hydrolysis lignin pose considerable challenges in its effective valorization into higher-value products. Hydrolysis lignin could, however, probably be used in value-added markets if the lignin were to be recovered at an early stage. Provided that the pretreatment processes, e.g. organosolv, ionic liquids, etc., are not excessively expensive, the extra cost of prerecovery could be compensated by its unique material properties [6].

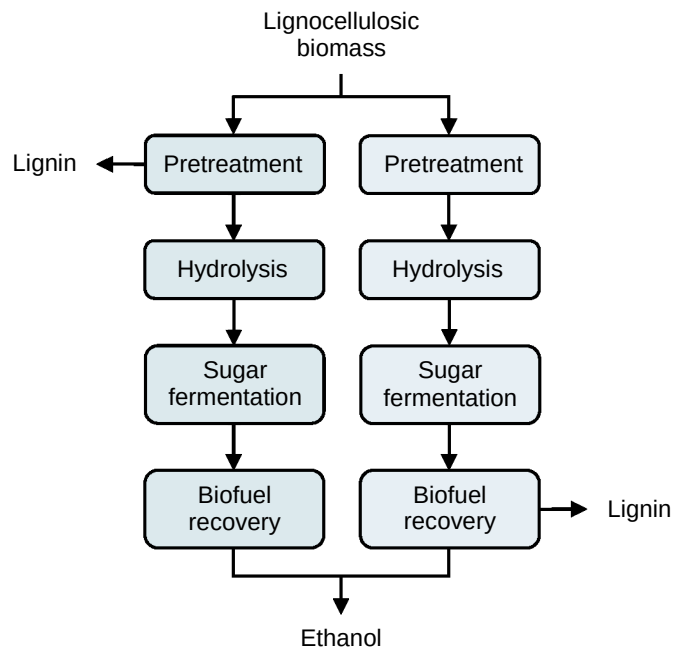


Figure 2.7. Paths for the recovery of lignin in lignocellulosic ethanol production. This can be done either after hydrolysis and fermentation, or through pretreatment before carbohydrate conversion. Enzymatic or chemical (acid) hydrolysis is usually employed to convert the complex carbohydrates into simple sugars. (Adapted from [6,25])

2.4 Market potential for lignin

Over the past decades, lignin has proved valuable to the pulp and paper industry and to emerging second-generation biorefineries. Lignin is a versatile macromolecule, and thus has the potential to serve as a raw material for several applications. The role of lignin as a renewable feedstock has been extensively described in both the generation of process heat and power, and in the production of value-added products [35]. Apart from its traditional use in pulp mills as a solid fuel for energy generation in the recovery boilers, other applications include the production of syngas products, hydrocarbons, phenols, and phenol substitutes, oxidized products, and macromolecules (Figure 2.8). The market is thus gradually expanding through new product development.

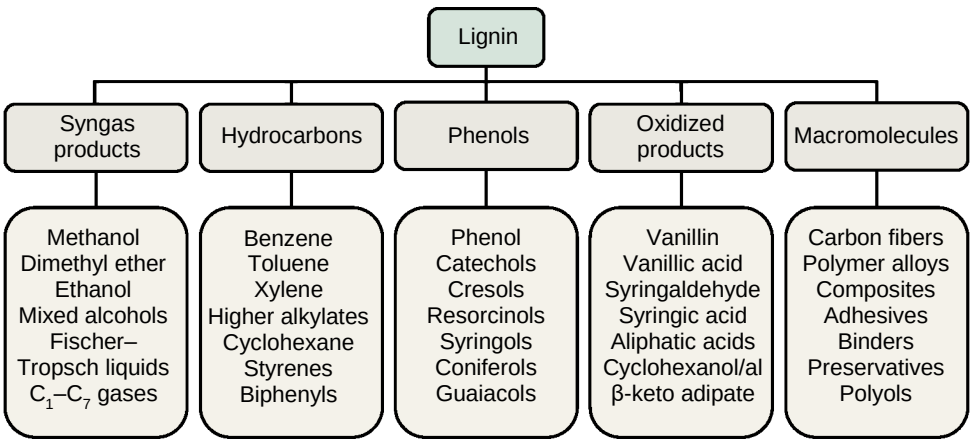


Figure 2.8. Products that could potentially be made from lignin. (Adapted from [35,36])

The focus of the work presented in this thesis is on the production of phenol derivatives and oxidized products from lignin, which are discussed in detail in Chapters 3 and 4. Such products are suitable for applications in the fine chemical industry, and are of high market value (Figure 2.9). These two applications employ technologies that break down the lignin structure into simple phenolic monomers, such as guaiacol and vanillin, while preserving the intrinsic aromatic structure. Depending on the quality and functionality of the parent lignin, the conversion of lignin into value-added chemicals via depolymerization can provide niche opportunities, most likely over the medium to long-term timeframes.

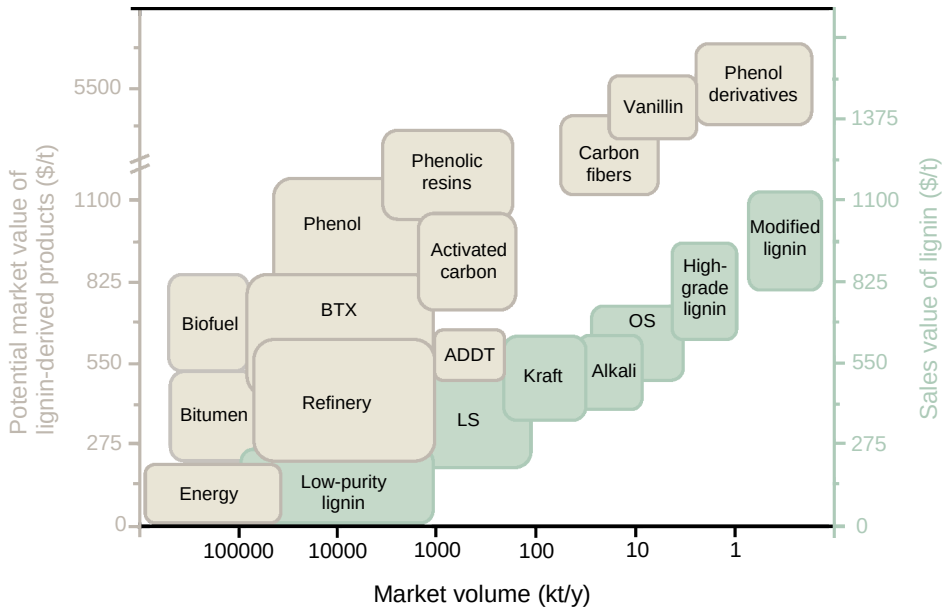


Figure 2.9. Potential market volume and estimated values of lignin and lignin-derived products. Low-purity lignin includes black liquor and nonfermentables. (BTX-benzene, toluene, and xylene; ADDT-additives; LS-lignosulfonates; OS-organosolv) (Adapted from [25,36,37])

The sales value of lignin on the market depends on various factors, such as the initial source of the lignin, the extraction process, the structural modifications, the treatment after extraction, and the end-use application. Low-purity lignin, representing the lowest sales value on the market is mainly burned to produce heat or energy (Figure 2.9), e.g. the nonfermentable fraction resulting after hydrolysis and fermentation in the production of lignocellulosic ethanol and the lignin dissolved in black liquor in pulp mills [36]. Lignosulfonates and kraft lignin are also in the low-value segment compared to other types of lignin (Figure 2.9); however, they can be produced at higher levels of purity depending on the end-use. On the other hand, the high market share of lignosulfonates and kraft lignin increases their potential for upgrading to higher-value products [25]. Although organosolv and other high-grade lignin streams (e.g. hydrolysis and ionic liquid lignins) constitute a small share of lignin production, they are more suitable for conversion to higher-value products. It is anticipated that the market share of high-purity lignin will increase in the future, especially with the development of second-generation biorefineries [38,39]. Notably, kraft and organosolv lignins have been identified as interesting starting materials with considerable potential in the production of value-added chemicals [37]. Kraft lignin was used as the starting raw material for most of the work presented in this thesis.

The long-standing belief in industry that one can make anything out of lignin except money is no longer true; there are now several opportunities for making money out of lignin (Figure 2.9). Nevertheless, it is important to use the right kind of lignin for the right application [36]. It should be borne in mind that there is a rather high degree of uncertainty concerning the value of lignin-derived products, and as a result, the commercial application of lignin conversion technologies is still limited. On the other hand, the sales value of lignin on the market appears to be reasonably stable [40], in contrast fossil resources, the prices of which can fluctuate significantly. Lignin-derived products can be produced either by exploiting the macromolecular structure of lignin or via lignin depolymerization and upgrading to value-added products. In the present work, the possibility of producing value-added chemicals such as vanillin, guaiacol, and other phenolic derivatives, from kraft and lignosulfonate lignins was investigated, as a substantial increase in their value can be foreseen based on the value chains of the feedstocks and the products. It is, however, important that such lignin conversion technologies are optimized and assessed to ensure profitability and cost-effectiveness.

2.5 Technologies for lignin conversion

The development of viable strategies for lignin valorization requires efficient technologies for lignin depolymerization and conversion. The lignin macromolecule can be deconstructed into LMW fragments by thermochemical or biological means for further upgrading, or for direct use as a platform for value-added chemicals and fuels. The focus of this thesis is on the development of thermochemical technologies that can break the complex macromolecular structure of technical lignin into LMW fragments suitable for applications, mainly in the fine chemical industry. Novel approaches that combine thermochemical treatment and biological conversion were also investigated.

Thermochemical technologies for lignin conversion rely on thermal energy to drive the transformation towards valuable lignin-derived phenolic intermediates. Such technologies can be broadly classified into acid- or base-catalyzed depolymerization (hydrothermal treatment), chemical oxidation (oxidative depolymerization), hydroprocessing and liquid-phase reforming, pyrolysis, and gasification. Figure 2.10 presents an overview of the various process technologies used for the thermochemical conversion of lignin. The temperature regime and the initial reaction environment define the lignin conversion process. The reactions can take place in an oxidizing atmosphere (with air, O_2, or H_2O_2, as common oxidants), in a reducing atmosphere (with an external H_2 or a hydrogen-donating solvent as a reductant), or in a neutral initial reaction atmosphere.

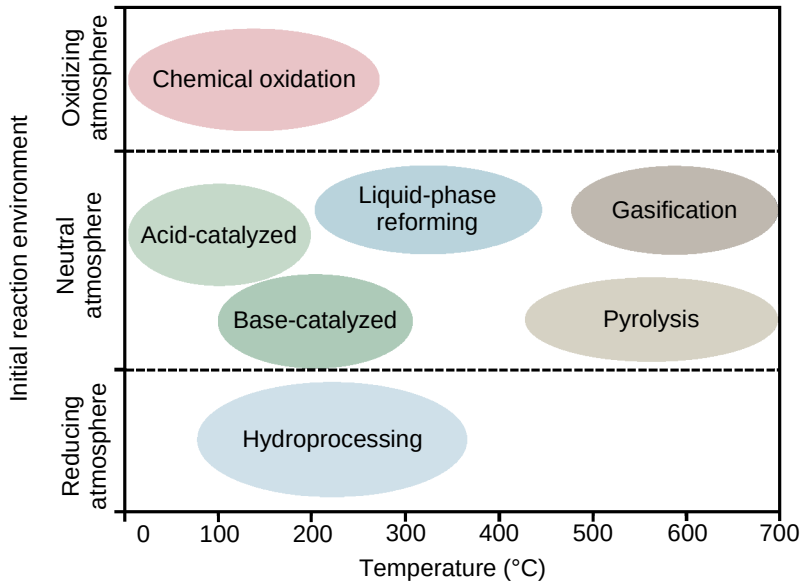


Figure 2.10. An overview of process technologies for the thermochemical conversion of lignin. The typical temperature ranges for different processes are shown on the abscissa. (Adapted from [41])

2.5.1 Acid-catalyzed depolymerization

Acid-catalyzed depolymerization (ACD), or acidolysis, of lignin has attracted attention due to its relevance to the biorefinery concept. The use of acid catalysts to depolymerize and dehydrate the plant cell wall polysaccharides is common in many processes for lignocellulosic biomass pretreatment. The approach has been used historically in structural investigations, and more recently for the synthesis of well-defined aromatic compounds [42,43]. ACD is usually carried out at temperatures between roughly 0 and 200 °C [41], sometimes higher (≥250 °C) [3], to break the C–O or C–C linkages between lignin units, providing smaller segments that include phenolic monomers. The mechanism of ACD is primarily based on the hydrolytic cleavage of α- and β-aryl ether linkages; the former being more rapidly depolymerized due to their lower activation energy. Lewis acids or soluble/solid Brønsted acids can be used to drive such a conversion, in water, in an organic solvent, or in a mixture. Products of ACD are often prone to condensation, and the reactive intermediates generated tend to repolymerize and form more complex lignin structures, thus making the selective deconstruction of lignin to LMW products challenging. However, repolymerization can be minimized by conducting ACD under the mildest possible operating conditions, normally by using organic solvents capable of solubilizing lignin fragments, such as alcohols, tetrahydrofuran, 1,4-dioxane, and γ-valerolactone [44].

2.5.2 Base-catalyzed depolymerization

Base-catalyzed depolymerization (BCD) of lignin, i.e. hydrothermal lignin treatment below the critical temperature of water in alkaline media, is regarded as a promising method for lignin conversion. Valuable products with a narrow product specification can be obtained from lignin and lignin-containing streams via BCD [45]. The fact that base chemicals are employed in the pulping process is also favorable from a process integration perspective. BCD is commonly conducted at elevated temperatures in the range of 100–300 °C in which methoxyphenols are the prevailing products, and also ≥300 °C, at which catechol and alkylcatechols can be obtained [3,41]. The catalytic reagents are commercially available bases such as NaOH, $Ca(OH)_2$, LiOH, and KOH. Although in most cases soluble bases are used in BCD, solid bases can also be used, e.g., MgO, CaO, and basic zeolites. As in the case of ACD, effective BCD of lignin is severely hampered by repolymerization of the reactive intermediates. Therefore, minimizing the rate of undesirable condensation reactions during BCD is key to ensuring high yields of the products. Additional challenges can arise due to the fairly high degree of complexity, diversity, and variability of the reaction mixtures generated, which impedes their direct exploitation. An ideal BCD process would thus lead to high yields of phenolic monomers, while at the same time allowing their easy separation from the reaction mixture. BCD of kraft lignin is one subject of research described in this thesis (**Papers II** and **III**), and is discussed in further detail in Chapter 3.

2.5.3 Oxidative depolymerization

Oxidative depolymerization, or chemical oxidation, of lignin constitutes an energy-efficient means of lignin deconstruction, while generating targeted products with multiple functionalities, including valuable chemicals such as phenolic aldehydes, phenolic acids, and carboxylic acids [37,46]. Lignin oxidation is usually performed at relatively low temperatures, 0–250 °C, in an oxidizing atmosphere, and a radical chemistry mechanism is usually applied in the production of such functionalized aromatics [41]. Common oxidizing agents used for lignin oxidation include molecular O_2, H_2O_2, peracetic acid, and air; and the reactions can occur in alkaline, acidic, or pH-neutral media employing homogeneous or heterogeneous catalysis. Research into the oxidative depolymerization of lignin can complement new developments in biorefinery research, helping to solve the riddle of lignin complexity [47]. Furthermore, oxidative depolymerization has been recommended as one of the most promising techniques for converting lignin into value-added chemicals, principally phenolic aldehydes/acids or mono- and dicarboxylic acids (e.g. formic, acetic, oxalic, malonic, and succinic acids), that are suitable for production on an industrial scale [48]. Oxidative depolymerization of lignosulfonates (**Paper IV**) and kraft lignin (**Papers V**, **VI**, and **VII**) was investigated in this work, and is discussed in further detail in Chapter 4.

2.5.4 Reductive depolymerization

Reductive depolymerization of lignin has the potential to generate simple bulk aromatics such as phenols, benzene, toluene, and xylene, and alkane fuels. Lignin is deconstructed in the presence of a redox catalyst and a reducing agent (mainly H_2) through reductive depolymerization. Hydrogen can either be supplied as an external gas, or can be derived from hydrogen-donor species, normally the solvent, but it can also be the lignin macromolecule itself [3]. When an external H_2 source is used, the process is termed hydroprocessing; while when the hydrogen is derived from the solvent/lignin, the process is called liquid-phase reforming. Lignin hydroprocessing involves thermal reduction at temperatures typically in the range of 100–350 °C, whereas temperatures ranging from 250 to 400 °C are used for liquid-phase reforming [41]. In reductive depolymerization, lignin is frequently deoxygenated with the aid of hydrogen via hydrodeoxygenation, where the degree of deoxygenation depends on the process characteristics, and the catalyst used [3]. The range of products generated by reductive lignin depolymerization also varies depending on the method applied, i.e. mild/harsh hydroprocessing, bifunctional catalysis, or liquid-phase reforming. Phenols with C3 side-chains (C3-phenols) have been cited as an example of the most promising lignin-derived chemicals for industrial production, and these could be produced via mild reductive depolymerization (typically at 160–250 °C) [48].

2.5.5 Thermal depolymerization

The pyrolysis of lignin is a method of primary thermal depolymerization used to produce a liquid product known as biocrude at high temperatures (typically 450–700 °C) [41]. The reactions usually take place in the absence of oxygen to generate a mixture of noncondensable gases, liquid oil, and solid char, with or without a catalyst. The effect of the pyrolysis temperature on the aromatic substitution pattern of lignin-derived G-type phenolic products is shown in Figure 2.11. The primary pyrolysis of lignin (at 200–400 °C) results mainly in 4-substituted guaiacols, while in secondary pyrolysis (>400 °C), guaiacols are rapidly transformed into catechols and *o*-cresols, together with phenols [49]. Phenols and *o*-cresols are relatively stable during high-temperature pyrolysis. Pyrolysis can provide a means of obtaining lignin-derived phenolic monomers and oligomers; however, it is necessary to have an understanding of the reaction kinetics to maximize the yields of the desired products, and to design appropriate upgrading processes. Gasification is another form of thermal depolymerization that can be used to produce synthesis gas (H_2 and CO) from a range of lignin feedstocks or model compounds. In high-temperature gasification, H_2 results from cracking of aromatic rings, while CO results from cracking of the C–O–C and C=O functional groups [50]. The synthesis gas can then be converted into various other chemicals, e.g. methanol, using conventional process technologies.

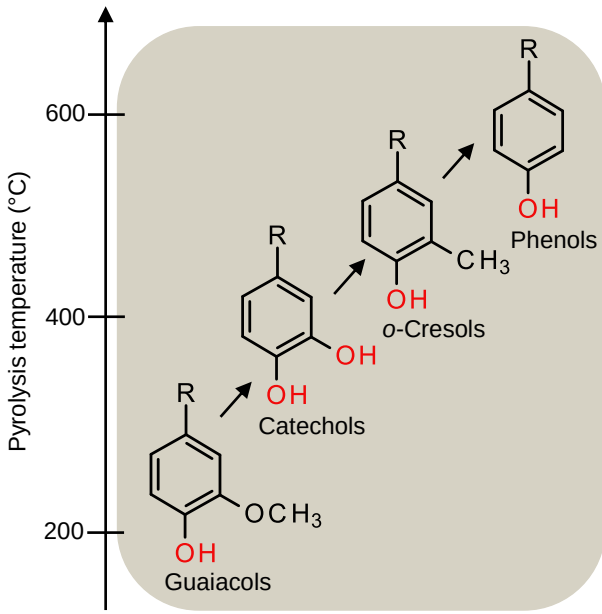


Figure 2.11. Influence of pyrolysis temperature on the aromatic substitution pattern of lignin-derived phenolic monomers. (Adapted from [49])

2.5.6 Other depolymerization strategies

Apart from the lignin-depolymerization methods mentioned above, other strategies include biological depolymerization, electrochemical depolymerization, microwave-assisted depolymerization, and two-step depolymerization. In biological depolymerization, biocatalysts such as enzymes or microbes are employed to transform lignin into value-added products. Such nature-inspired solutions hold promise as environmentally friendly alternatives to chemical catalysis and thermochemical methods [51]. Electrochemical depolymerization is another green strategy for transforming lignin into value-added commodities, relying on the power of electrocatalysis [52]. Microwave technology has also been applied in lignin conversion, and can be divided into microwave-assisted pyrolysis and solvolysis, depending on the reaction conditions [49]. Finally, two-step strategies have also been investigated for lignin conversion, in which the objective of the first step is generally to weaken the β-O-4 linkages, enabling subsequent depolymerization under milder conditions in the second step, which thus favors the rate of depolymerization over repolymerization [3]. Two-step protocols could provide flexibility for renewable aromatic production by applying different depolymerization or conversion sequences.

3 Base-catalyzed depolymerization of technical lignin

In this chapter, the key results reported in **Papers I-III** are summarized and discussed. Firstly, the physicochemical nature of various kinds of technical lignin is touched upon by providing insights into their structure and composition, and potential valorization routes are proposed in a biorefinery context. Secondly, the BCD of kraft lignin into LMW phenolics under continuous-flow conditions is presented. Finally, membrane separation is discussed as an approach to facilitate biological conversion of the LMW compounds obtained from the continuous BCD of kraft lignin. This chapter poses two core research questions:

> RQ3.1. Which physicochemical tools can be used to assist in conceptualizing efficient valorization routes for technical lignin?
>
> RQ3.2. Is it possible to generate molecules that are compatible with biological upgrading from the continuous BCD of technical lignin?

The first of these was the subject of the study presented in **Paper I**, and is discussed in Section 3.1, while the second is addressed in **Papers II** and **III**, and is discussed in Sections 3.2 and 3.3.

3.1 Understanding the physicochemical properties

In order to develop efficient bio- or thermochemical valorization strategies for technical lignin, it is important to have sound knowledge of their physicochemical properties. The structure, content, purity, and reactivity of lignin differ widely as a result of variations in origin, pretreatment conditions, and the isolation methods used to produce technical lignin (Sections 2.2 and 2.3). In the study described in **Paper I**, kraft and alkali lignins were subjected to structural characterization using various physicochemical analysis techniques. These two types of technical lignin originate from common industrial pulping methods, and their structural and functional properties were determined to investigate the physicochemical differences that could result from the pretreatment conditions. The aim of this was to provide support in determining suitable conditions for the better valorization of

technical lignin, with emphasis on the biological valorization of lignin to produce value-added chemicals. The analysis techniques applied and their purposes are given in Figure 3.1.

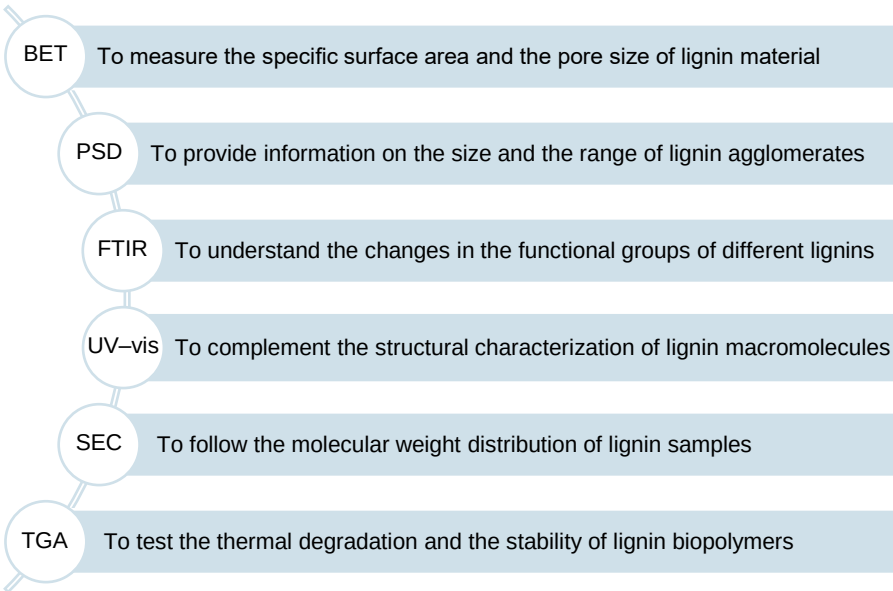


Figure 3.1. The characterization techniques used to provide insights into the structure-related properties of technical lignins (Paper I). (BET, Brunauer–Emmett–Teller; PSD, particle size distribution; FTIR, Fourier transform infrared spectroscopy; UV–vis, ultraviolet–visible absorption spectroscopy; SEC, size-exclusion chromatography; TGA, thermogravimetric analysis)

The specific surface area, pore size, and pore volume of both lignins were determined by N_2 physisorption using the Brunauer–Emmett–Teller (BET) and Barrett–Joyner–Halenda (BJH) methods [53,54]. Variations were observed in the textural properties of the kraft and alkali lignins, indicating that the pretreatment conditions influenced the textural parameters of isolated lignins (**Paper I**). Lignins with a large surface area and pore size are favorable in biological lignin valorization, as they would be more accessible to bacterial enzymes. The BET and BJH methods were also used for catalyst characterization (**Paper IV**) and to determine the textural properties of depolymerized lignin (**Paper V**).

The particle size distribution (PSD) of lignins was determined by laser diffraction. PSD provides an indication of the degree of aggregation of lignin macromolecules. Although both lignins exhibited a geometric PSD in the micron size range, the two kinds of pretreatment resulted in different size distributions of the lignin particles (**Paper I**). Smaller lignin and lignin-derived products may serve as better substrates for further microbial assimilation.

Fourier transform infrared (FTIR) spectroscopy and ultraviolet–visible absorption (UV–vis) spectroscopy were used to investigate the differences in lignin composition and structural changes, relying on the specific absorbance of individual phenolic species. Similarities were observed in the functional groups of kraft and alkali lignins in the FTIR spectra, and both lignins exhibited the characteristic vibrations of G-type units (**Paper I**). No significant differences were observed in the UV spectra acquired from the lignins; both showing absorption maxima at λ=280 nm, which is typical for technical lignins (**Paper I**). More considerations should thus be made when tailoring valorization routes for these lignins, and more detailed insight into the lignin macromolecular structure is required. Nuclear magnetic resonance (NMR) spectroscopy could perhaps be used to provide information on the different interunit linkages and aromatic moieties in the lignin structure. NMR was not used in the physicochemical characterization study described in **Paper I**, but it was used to elucidate the structure and functional group decoration of lignin and lignin-derived products in later studies (**Papers II**, **IV**, **V**, and **VII**).

The molecular weight of lignin is a fundamental property that governs the recalcitrance of biomass and lignin valorization. Among different characterization techniques, size-exclusion chromatography (SEC) is the most common method used to determine the molecular weight of technical lignins [16,55,56]. SEC was carried out using polyethylene glycol standards and NaOH as eluent to determine the molecular weight distribution (MWD) of the kraft and alkali lignins. They showed different MWD profiles; the kraft lignin exhibiting a lower apparent molecular weight and a narrower MWD (**Paper I**). There are several ways of catabolizing LMW lignin to form value-added end products using the natural metabolic products of microorganisms and metabolic engineering combined with thermochemical depolymerization [4]. SEC was also used in this work to determine the molecular weight, dispersity, and MWD of lignin and lignin-derived products (**Papers II**-**V** and **VII**).

Thermogravimetric analysis (TGA) was conducted in an inert atmosphere to compare the thermal stability of the two lignin materials. Thermal degradation of the lignins was carried out over a wide range of temperatures between 225 °C and 600 °C (**Paper I**). At 600 °C, the amounts of nonvolatile residue were determined to be around 50%, indicating the high thermal stability of both lignins (**Paper I**). This can be attributed to the high degree of branching and condensation of such technical lignins, as the more the lignin is condensed, the more easily it can be converted to char [57].

RQ3.1 was partly answered by the application of well-known methods to characterize the physicochemical properties of two commercial lignins (**Paper I**). However, in order to match suitable technical lignin streams with various valorization routes, these tools must be combined with other characterization techniques, such as NMR, elemental analysis, and high-resolution mass spectrometry (HRMS).

3.2 Depolymerization under continuous-flow conditions

The development of successful strategies for biological lignin valorization depends on designing effective depolymerization protocols. Most of the research in the field of lignin depolymerization has focused on batch-mode processing, while very few studies have been reported employing continuous reactor systems [58]. Among the different technologies available for lignin conversion, BCD holds promise in converting complex lignin streams into valuable phenolic intermediates with process integration opportunities suitable for the pulp and paper industry. BCD can be carried out under continuous-flow conditions, enabling efficient lignin conversion with only short residence times (typically <1 h). Repolymerization leading to the formation of undesirable solid products, such as char and residual lignin, can also be avoided to a large extent.

Indulin AT kraft lignin (IK), a softwood kraft lignin that is precipitated from the black liquor of linerboard-grade pulp, was subjected to continuous BCD to produce LMW phenolics (**Paper II**). The reactions were carried out in an in-house-built continuous-flow reactor (CFR) system using NaOH as catalyst, at temperatures from 170 to 250 °C and residence times of 1–4 min. The storage stability of the depolymerized Indulin AT kraft lignin (DIK) fractions was investigated, and the products were characterized using SEC, ultra-high-performance supercritical fluid chromatography (UHPSFC) combined with HRMS, and ^{1}H and two-dimensional (2D) ^{1}H–^{13}C heteronuclear single-quantum correlation (HSQC) NMR spectroscopy techniques. A schematic diagram of the experimental setup designed for the continuous BCD of lignin is shown in Figure 3.2.

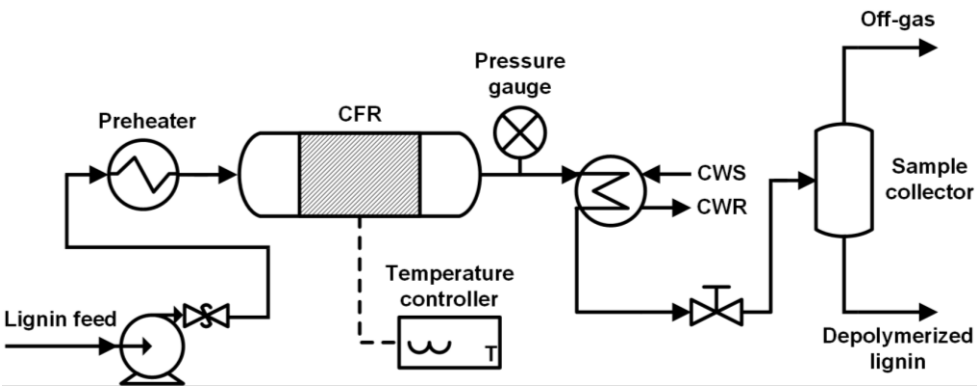


Figure 3.2. Schematic of the experimental setup used in the study described in Paper II. (CFR, continuous-flow reactor; CWS, cooling water supply; CWR, cooling water return)

The lignin feed (5 wt% IK dissolved in 1.25 M NaOH aqueous solution) was pumped to a bench-scale tubular CFR where the BCD reactions occur. The reactor was equipped with a preheater to heat the feed mixture to the desired depolymerization temperature. The temperature was adjusted using a temperature controller, and the pressure was controlled using a backpressure regulator. The stream exiting the CFR was condensed using a circulating water bath, and a pressure control valve made of a nickel–molybdenum–chromium superalloy (Hastelloy® C276) was used to regulate the pressure during the course of the reaction. Hastelloy C276 is also used in the reactor tubes, instead of the ordinary stainless steel tubes, for better corrosion resistance in such a highly alkaline environment (pH ≥12). After condensation, a filter was connected to the inlet of the pressure control valve to protect it from possible char deposition. Prior to each experimental run, the setup was heated and pressurized to the desired operating conditions by maintaining a continuous flow of deionized water in the entire system. The total operating volume of the system is about 50 mL. After exiting the reaction zone and throttling the effluent to atmospheric pressure, the liquid depolymerized lignin product was collected continuously for chemical analysis and stability tests.

SEC was carried out to assess the changes in the MWD of lignin samples before and after reaction at temperatures in the range 170–250 °C and residence times of 1, 2, and 4 min (**Paper II**). The MWD of IK was wide, extending from 1 to 100 kDa, with a peak at about 4 kDa, representing the main part of the high-molecular-weight (HMW) complexes, and a minor peak at about 0.9 kDa, representing a fraction of LMW oligomers. In general, a gradual shift toward LMW compartments was observed for the DIK fractions with increasing reaction temperature. Components with molecular weight greater than 10 kDa almost disappeared as the temperature approached 250 °C. The peaks at about 0.2–0.4 kDa, likely representing LMW monomers and dimers, were observed at reaction temperatures above approximately 220 °C (at τ = 1 min) or 190 °C (at τ = 2 min); and the higher the temperature, the higher the concentration of the LMW fractions. The peaks representing LMW compounds were found to be more distinct when the reactions were performed for 2 min than those performed for 1 min; however, char was formed at 250 °C. No significant shift toward LMW fractions was seen upon increasing the residence time further, indicating that repolymerization could be a problem at a τ of 4 min and above. Based on the above observations, a reaction temperature of 240 °C and a residence time of 2 min were chosen as the optimal conditions for the BCD of IK in continuous-mode operation.

The stability of the lignin and lignin-derived products was investigated by studying the effects of long-term storage and storage temperature on their properties (**Paper II**). IK appeared to be quite stable when stored at room temperature for up to 3 months. However, changes were observed in the MWDs of DIK fractions stored under the same conditions, suggesting that repolymerization of reactive product intermediates may have occurred. This is probably the reason for the formation of

heavier compounds in the lignin-derived products during long-term storage, in agreement with previous observations [59]. However, during long-term storage at a low temperature (4 °C), the DIK fractions were deemed to be stable, showing almost no changes in MWD. Low-temperature storage is therefore recommended to improve the stability of depolymerized lignin fractions.

UHPSFC-HRMS was performed to determine the most abundant monomeric compounds in IK and the DIK obtained from the continuous BCD process at the optimal conditions (240 °C; 2 min). The major compounds identified in the samples included guaiacol, vanillin, acetovanillone, *p*-hydroxyacetophenone, vanillic acid, *p*-hydroxybenzoic acid, and *p*-hydroxybenzaldehyde (**Paper II**). The last three monomers were detected in the parent IK, but with relatively lower peak intensities. Conversely, guaiacol, vanillin, and acetovanillone were the main phenolic monomers generated in the DIK fraction. The higher concentration of LMW compounds in the DIK stream is consistent with the interpretation of the MWD from the SEC analysis discussed above.

NMR spectroscopy was performed to elucidate the structural and functional aspects of IK and the DIK (**Paper II**). The ^{1}H NMR spectra obtained from DIK showed higher intensities (sharper peaks) for the proton chemical shifts than the spectra from IK, which confirms the expected increase in the degree of depolymerization; and thus the formation of LMW species. A lower methoxy group content was observed in DIK than in IK, consistent with the literature on the hydrothermal treatment of lignin catalyzed by alkaline pH [60,61]. In coexistence with the methoxy and aldehyde groups, the main ^{1}H NMR signals were attributed to typical proton chemical shifts in the aromatic region, that is, signals between 6.0 and 8.0 ppm, confirming the presence of LMW aromatic species in DIK, which is in line with the findings of SEC and UHPSFC-HRMS.

The 2D ^{1}H–^{13}C HSQC NMR spectra were divided into an aliphatic region (δ_C/δ_H 8.0–52.5/0.5–4.5 ppm), an aliphatic oxygenated side-chain region (δ_C/δ_H 52.5–90.0/2.8–5.7 ppm), and an aromatic region (δ_C/δ_H 105–155/6.0–9.2 ppm). Chemical shifts were referenced to the residual solvent signal at 2.5 and 39.5 ppm for ^{1}H and ^{13}C, respectively. The tentative assignments of ^{1}H–^{13}C correlation cross-peaks in the 2D NMR spectra were revealed for IK and DIK, based on literature data [20,62]. Figure 3.3 shows the aliphatic oxygenated side-chain region in the 2D HSQC NMR spectra from IK and DIK (the other spectral regions can be found in **Paper II**).

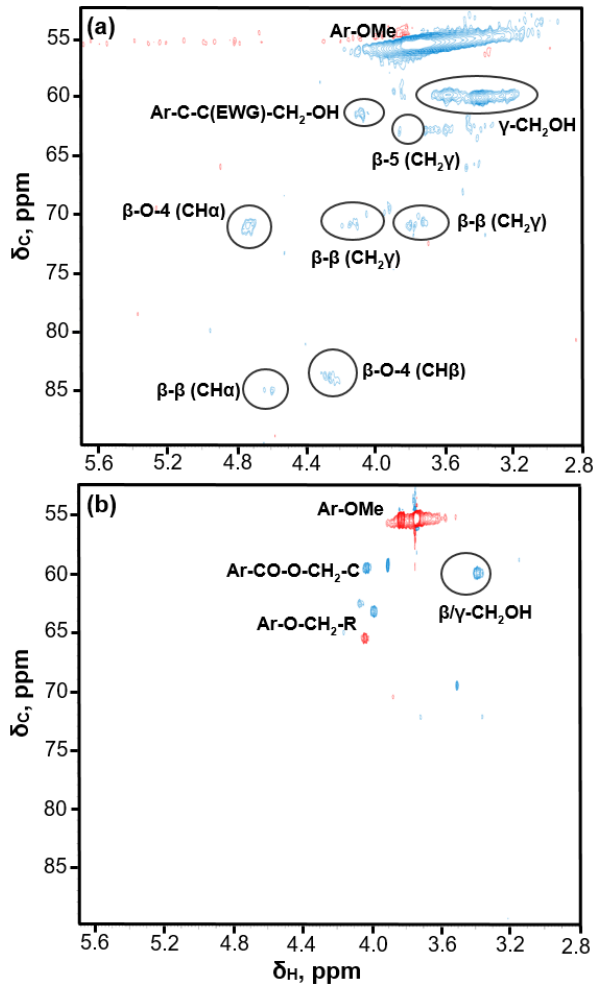


Figure 3.3. The aliphatic oxygenated side-chain region (δ_C/δ_H 52.5–90.0/2.8–5.7 ppm) in the 2D HSQC NMR spectra from (a) IK and (b) DIK samples. Reaction conditions: 50 g/L IK, 1.25 M NaOH aqueous solution, 240 °C, 130 bar, 2 min. (Adapted from Paper II)

The common interunit linkages β-O-4 (β-aryl ether), β-β (pinoresinol), β-β (secoisolariciresinol), and β-5 (phenylcoumaran) were identified in the basic structure of IK. However, the β-1 (diphenyl ethane), α-O-4 (α-aryl ether), and dibenzodioxocin (5-5-α, β-O-4) linkages were not detected, as they were apparently hydrolyzed during the pulping process [63]. It was found that practically all the interunit/C–O linkages identified in IK had disappeared after the BCD reaction, implying that such bonds were cleaved under the conditions used (240 °C; 2 min; continuous mode). This is an important finding, as it clearly indicates that the IK starting material was effectively depolymerized under basic conditions using the CFR system.

A limited number of studies have been carried out on the hydrothermal BCD of technical lignin into phenolics using continuous tubular reactors (Table 3.1). BCD of organosolv lignin has been reported in a continuous-reactor setup equipped with a water preheater and a cooler, showing that phenolic monomers are the primary products under alkaline conditions, while the oligomers are the result of consecutive condensation reactions between these highly reactive products [64]. BCD of kraft lignin in a continuous-flow reactor electrically heated with a molten eutectic potassium nitrate/nitrite salt has also been described, indicating that NaOH is efficient as a catalyst in obtaining monomers that are suitable for the production of liquid chemicals [65]. The continuous BCD of kraft lignin for the synthesis of a sustainable carbon fiber precursor has also been demonstrated, where an oily liquid phase containing catechol and methylated derivatives was generated [66]. The upscaling of continuous BCD of organosolv and kraft lignins to pilot plant dimensions has been reported, where bio-oils rich in phenolic monomers, including guaiacol, catechol, and/or syringol were obtained [67]. In another pilot study, the conversion of kraft lignin into bio-oil and chemicals in near-critical water has been demonstrated, where BCD was carried out in a continuous fixed-bed reactor using ZrO_2 as a heterogeneous catalyst, K_2CO_3 as a homogeneous co-catalyst, and phenol as both a co-solvent and a capping agent [68].

Table 3.1. Overview of hydrothermal BCD of technical lignin in continuous tubular reactors (Adapted from Abdelaziz and Hulteberg [58])

Lignin	Conc. (wt%)	Temperature (°C)	Pressure (bar)	Residence time (min)	Ref.
Organosolv	2.5–10	240–340	250–315	2.5–15	[64]
Organosolv; Kraft	2.5–10	250–340	250	7.5–15	[67]
Kraft	10	270, 290, 315	130	15, 23, 43	[65]
Kraft	12	300	180	8–24	[66]
Kraft	5.5	350	250	11	[68]
Kraft	5	170–250	120–130	1, 2, 4	**Paper II**

In the light of progress on the above, the findings presented in **Paper II** contribute to the state of the art in continuous lignin depolymerization, describing an effective approach for the conversion of kraft lignin into LMW phenolics with a short residence time, at a relatively low reaction temperature, and without using any organic solvent or capping agent. This approach also offers opportunities for process integration with traditional pulp and paper mills. Understanding and improving the transformation of technical lignin under continuous-flow conditions could facilitate the transition towards industrial applications. Moreover, the findings presented in **Paper II** contribute to partly answering RQ3.2 in the scope of this thesis, as these LMW phenolic derivatives represent potential substrates for further biological conversion and upgrading.

3.3 Bioconversion of alkali-treated kraft lignin

Kraft lignin is highly heterogeneous, and several pieces of its puzzling structure are still missing. The inherent heterogeneity of native lignin is complicated by the variability and complex chemistry of the delignification process [69]. During the kraft process, lignin undergoes significant structural changes, during which several labile bonds (e.g., C–O) in the native structure are replaced by new, more strong and recalcitrant ones (e.g., C–C) [70]. Additional challenges can arise from the high degree of complexity, variability, and diversity of the product mixtures generated, making them barely suitable for direct utilization. All these factors impede the efficient conversion of kraft lignin into value-added products.

The above-mentioned challenges call for innovative separation and upgrading solutions. Membrane separation of complex depolymerized lignin streams represents a promising approach for product fractionation, to obtain well-defined fractions with improved functionalities [71]. Compared to other approaches for the separation of depolymerized lignin, such as acidification, solvent extraction, and adsorption, membranes have the advantage of extracting compounds based on molecular weight, while minimizing the need for solvents. Biological lignin valorization is another promising approach that exploits the multitude of compounds resulting from thermochemical depolymerization by funneling the depolymerized lignin mixture into one or two intermediates [4,8]. This strategy employs engineered microbial platforms that are able to metabolize the lignin-derived intermediates for subsequent conversion into value-added compounds.

Membrane separation and biological conversion were combined with thermochemical depolymerization to develop a possible biorefinery concept for kraft lignin valorization, as described in **Paper III**. The continuous BCD approach described in **Paper II** was used to generate a DIK stream at a slightly lower reaction temperature of 220 °C and a residence time of 2 min, using a NaOH:IK weight ratio of 1 with 5 wt% IK loading. Although a temperature of 240 °C was used previously for the BCD of IK (Section 3.2), the lower temperature of 220 °C was used in these experiments to ensure operational stability and to control char formation. Membrane filtration was used to obtain a fraction containing mainly LMW phenolic species from the DIK stream for use in biological conversion. A polymeric membrane with a molecular weight cut-off of 0.5–0.7 kDa was used to fractionate the DIK into a permeate stream (DIKP) rich in LMW species, and a retentate stream (DIKR) rich in HMW substances. The DIKP was used as a carbon source for three bacterial strains: *Pseudomonas fluorescens*, *Pseudomonas putida*, and *Rhodococcus opacus*, and the growth of these microorganisms was investigated. Figure 3.4 provides an overview of the process concept described in **Paper III** in relation to the continuous BCD process of **Paper II**.

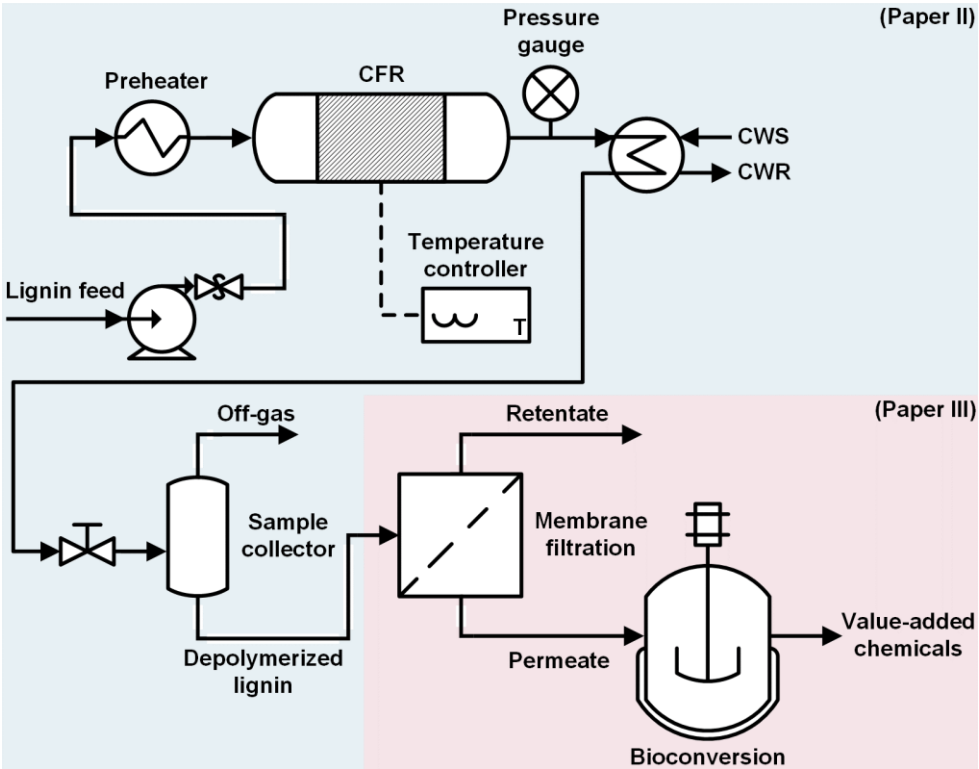


Figure 3.4. Overview of the process concept presented in Paper III in relation to that described in Paper II. (CFR, continuous-flow reactor; CWS, cooling water supply; CWR, cooling water return)

The yields of the phenolic monomers guaiacol, vanillin, acetovanillone, vanillic acid, and *p*-hydroxybenzoic acid in the DIK stream before being subjected to membrane filtration were 3.5, 1.3, 0.95, 0.31, and 0.27 wt%, respectively [72], corresponding to a total yield of 6.3 wt% (Figure 3.5). A polymeric flat nano-filtration membrane was used to recover the LMW phenolics and was chosen to withstand the highly alkaline DIK mixture (pH ~13.5). The average membrane flux, J (L/m^{2}h), was determined by weighing the permeate samples on a digital scale, and calculated according to:

$$J = Q_p/A_m \qquad (3.1)$$

where Q_p denotes the permeate flow rate through the membrane (L/h), and A_m the membrane surface area (m^2). The permeate was collected continuously and the accumulated weight was recorded every 20 s. The total filtration time was 3.7 h. The DIKP and DIKR fractions were stored at 4 °C prior to chemical analysis and bacterial cultivation. Cultivation using the DIKP fraction (after adjusting the pH to

~7) proceeded for 7 days, and bacterial growth was monitored spectrophotometrically by measuring the optical density (OD) at 620 nm.

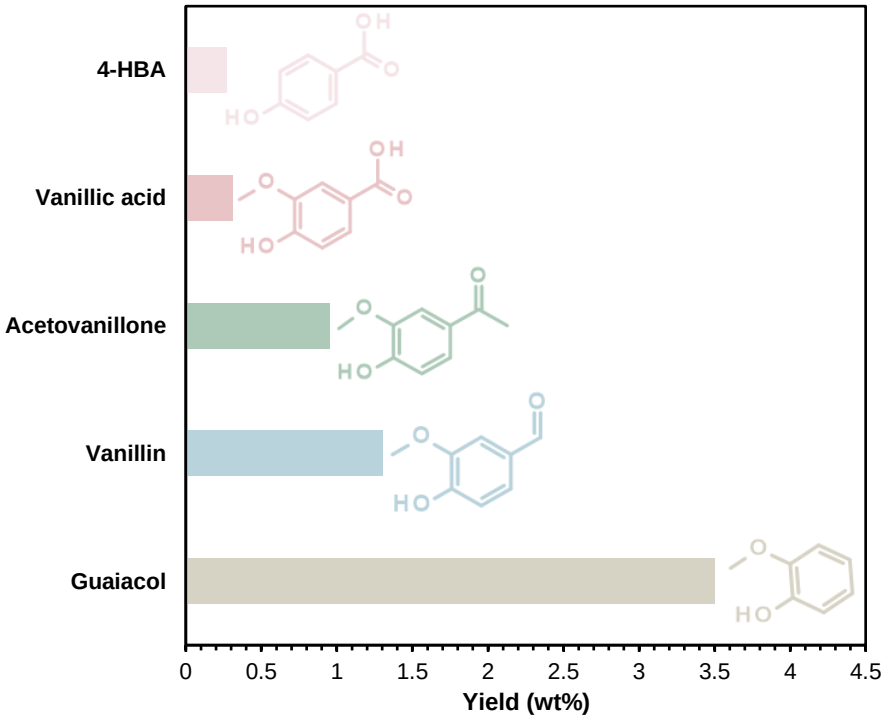


Figure 3.5. Yields of phenolic monomers from the continuous base-catalyzed depolymerization of IK. Reaction conditions: 50 g/L IK, 1.25 M NaOH aqueous solution, 220 °C, 120 bar, 2 min. (4-HBA, *p*-hydroxybenzoic acid)

The MWD of the DIKP and the DIKR were measured using SEC to evaluate the efficacy of membrane nanofiltration in treating the DIK stream. The ratio between LMW species and HMW lignin was clearly different in the separated fractions (Figure 3.6). The LMW fraction of the DIK mixture passed through the membrane while the larger components were retained. This allowed the DIKP fraction, containing most of the LMW species (0.25–0.45 kDa), to be used at a higher concentration without the precipitation of solids in subsequent biological conversion.

The volumetric fraction of DIKP at the end of the filtration cycle was 70%. The initial average permeate flux was about 13 L/m^{2}h; after which it gradually decreased, reaching a minimum of about 8 L/m^{2}h by the end of the cycle. The decrease in the permeate flux may be due to the increasing concentration of HMW material in the retentate. About 32% permeation of the initial lignin by weight was attained over the entire filtration cycle (**Paper III**).

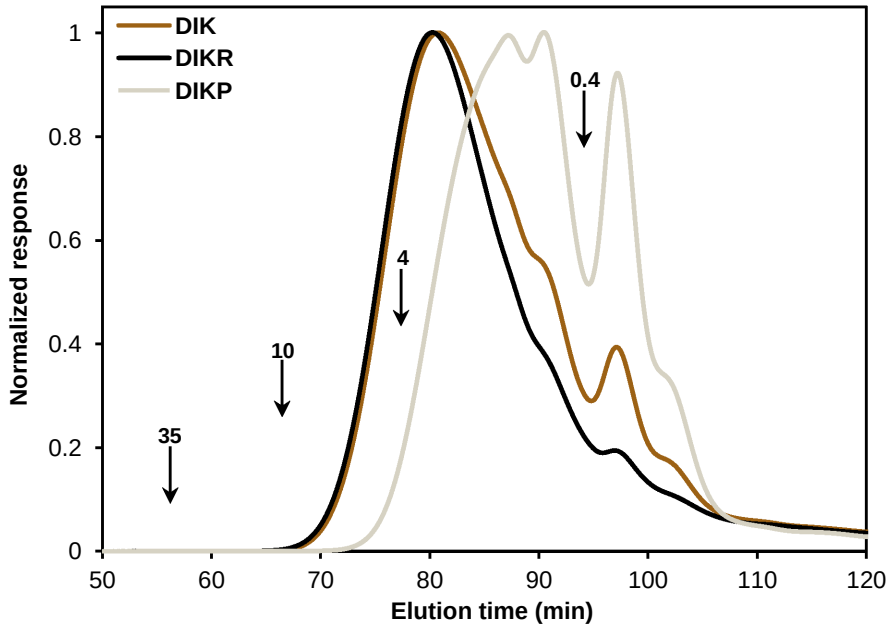


Figure 3.6. Size-exclusion chromatograms of depolymerized Indulin AT kraft lignin (DIK) and the membrane-filtered retentate (DIKR) and permeate (DIKP), showing characteristic UV absorption at 280 nm. The arrows indicate the molecular weights (kDa) of the polyethylene glycol standards used for calibration. (Adapted from Paper III)

An increase in the OD of almost 0.1 was observed in the *Pseudomonas* cultures on day 1 (**Paper III**), which was probably able to grow by the consumption of the readily available phenolic monomers, vanillin, vanillic acid, and *p*-hydroxybenzoic acid [73]. The OD of *Pseudomonas* cultures increased further after the addition of extra substrate (1 mL DIKP on days 2 and 4), giving a final OD of 0.3. In contrast, no practical growth was observed for the *Rhodococcus* strain on the DIKP, probably due to inhibition by higher concentrations of LMW phenolics, salts, or other compounds present in the DIKP medium (**Paper III**).

The findings presented in **Paper III** indicate that membrane filtration is a promising method of separating complex depolymerized lignin streams in order to enable biological conversion of LMW phenolics at increased concentrations, and thus contributes to answering RQ3.2. Biocompatible molecules suitable for biological conversion could be produced from kraft lignin by combining thermochemical depolymerization with nanofiltration. Such a strategy for technical lignin valorization may be integrated into existing pulp and paper facilities (as described in **Paper III**); however, the key to a self-sustaining operation is the downstream neutralization of the permeate before biological upgrading, as this could constrain the atomic balance in the pulp mill.

4 Oxidative depolymerization of technical lignin

In this chapter, the major findings reported in **Papers IV-VII** are summarized and discussed. The generation of LMW phenolic chemicals from sodium lignosulfonates with heterogeneous catalysts in an oxidative environment is discussed first. Oxidative depolymerization is then presented as a possible pretreatment step to enable the biological conversion of kraft lignin. The economic viability of a process for the oxidative depolymerization of kraft lignin to provide a feedstock for large-scale biochemical production is analyzed and discussed. Finally, the production of LMW phenolics and high-quality bio-oil from kraft lignin employing homogeneous catalysts under oxidative conditions is presented.

This chapter poses three main research questions:

> RQ4.1. Can an efficient catalytic system be developed to depolymerize technical lignin under oxidative conditions?
>
> RQ4.2. Is it possible to produce molecules suitable for biological upgrading by the oxidative depolymerization of technical lignin?
>
> RQ4.3. Is biochemical production from technical lignin subjected to oxidative depolymerization economically viable?

The first question was investigated in the studies presented in **Papers IV** and **VII**, and is discussed in Sections 4.1 and 4.4, the second was the focus of **Paper V**, and is discussed in Section 4.2, and the third was the focus of the study described in **Paper VI**, and is discussed in Section 4.3.

4.1 Searching for a heterogeneous catalyst

Oxidative depolymerization is a promising strategy in the conversion of complex lignin streams into highly functionalized chemicals under relatively mild operating conditions. Oxidative lignin depolymerization can be carried out in the presence of homogeneous, heterogeneous, or enzymatic catalytic systems. Heterogeneous catalysts offer a number of advantages in the oxidative depolymerization of technical

lignin, including ease of separation and recyclability, making them interesting for industrial applications.

Alumina-supported copper–manganese and nickel–molybdenum catalysts were investigated in the oxidative depolymerization of sodium lignosulfonate lignin (NaLS) to enable the production of value-added LMW phenolics (**Paper IV**). Lignosulfonates have a high MWD, low purity, and a high sulfur content, which make their conversion a challenging task. However, lignosulfonates are water-soluble, in contrast to almost all other technical lignins. This was the main reason for choosing this as raw material, as the reactions could be performed at near-neutral pH, which may benefit the investigated heterogeneous catalytic systems.

Catalytic oxidative depolymerization of NaLS was carried out at an elevated temperature using molecular O_2 as an oxidant in batch mode. The catalysts used were based on an extruded δ-Al_2O_3 support and were synthesized by incipient wetness impregnation. A mixture of Cu and Mn acetate salts was used to prepare the Cu-Mn/δ-Al_2O_3 catalyst (Cu-Mn), while the nitrate salts of Ni and Mo were used to prepare a Ni-Mo/δ-Al_2O_3 catalyst (Ni-Mo). A sulfided form of Ni-Mo was also prepared by treating the active metals with H_2S and further waxing using a C_{18}-saturated hydrocarbon to ensure intactness. After reaction, the product mixtures were analyzed with SEC, 2D ^{1}H–^{13}C HSQC NMR spectroscopy, and UHPSFC-HRMS. The best performing catalyst was characterized before and after use with N_2 physisorption, scanning electron microscopy (SEM), energy dispersive spectroscopy (EDS), TGA, X-ray diffraction (XRD), X-ray photoelectron spectroscopy (XPS), and inductively coupled plasma optical emission spectrometry (ICP–OES).

To investigate possible differences between the NaLS substrate and the reaction products generated, the samples were analyzed and compared with respect to MWD and chemical structure. According to SEC analysis, the Cu-Mn system exhibited the best performance, converting the HMW NaLS into LMW products with a much narrower MWD. The better catalytic performance of Cu-Mn compared to the other catalyst systems was attributed to the ability of Cu and Mn ions to form highly oxidized metallo–oxo complexes upon reaction with the molecular O_2 (**Paper IV**). The product mixtures generated with the Ni-Mo and sulfided Ni-Mo systems had slightly lower MWDs than the mixture from the control experiment (no catalyst); however, the changes were not significant, and Cu-Mn was therefore chosen for detailed analysis.

NMR measurements revealed variations in the chemical structures of NaLS and the product mixture from the Cu-Mn system. Spectral comparison indicated that the proposed catalytic oxidative depolymerization pathway vastly abolishes the methoxy group signals ($\delta^{1}H$ ~3.5-4 ppm, $\delta^{13}C$ ~55 ppm) and other signals in the aliphatic oxygenated side-chain region at $\delta^{13}C$ ~60-90 ppm (**Paper IV**). The spectrum from the water-soluble post-reaction mixture was also largely devoid of

aromatic $^{1}H–^{13}C$ HSQC signals, consistent with reports on a chelator-mediated Fenton reaction [74].

Molecular information was obtained on the NaLS substrate and sample of the Cu-Mn-derived product using UHPSFC-HRMS. Figure 4.1 shows the base peak ion chromatograms of NaLS and the oxidatively depolymerized product generated with the Cu-Mn. As can be seen, the catalytically treated sample contained more monomers than the NaLS sample, indicating effective transformation of NaLS into LMW compounds. Four lignin monomers; vanillin, *p*-hydroxybenzaldehyde, vanillic acid, and *p*-hydroxybenzoic acid, were identified in the catalytically treated sample, based on the retention time, exact mass, and detected fragments. Vanillic acid was identified in both samples, although the significant difference in the peak intensities of the extracted ion chromatograms indicated that more vanillic acid was produced through Cu-Mn-catalyzed oxidative depolymerization.

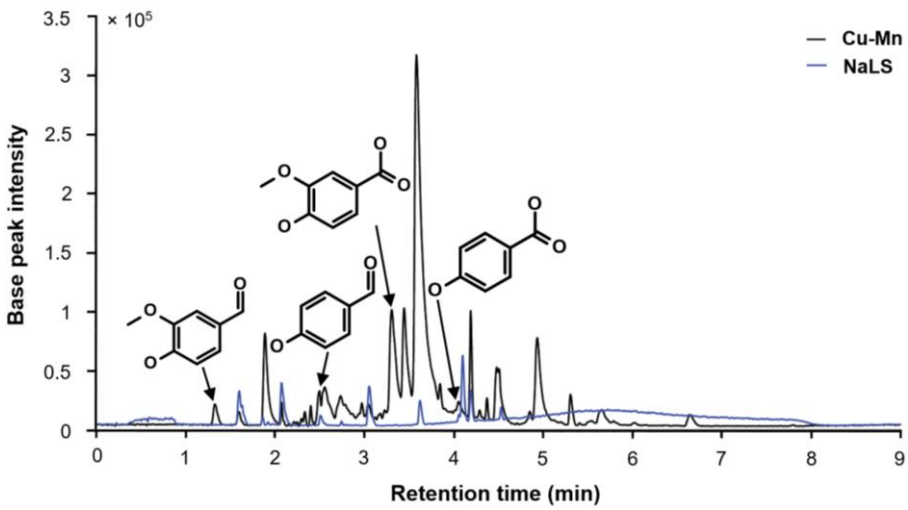


Figure 4.1. Base peak ion chromatograms of sodium lignosulfonate lignin (NaLS) and the oxidatively depolymerized product generated with the Cu-Mn/δ-Al_2O_3 catalyst (Cu-Mn). Reaction conditions: 20 g/L NaLS, 300 mg catalyst, 160 °C, 15 bar O_2, 60 min. (Adapted from Paper IV)

Characterization is indispensable in catalyst development, and constitutes an essential part of research into heterogeneous catalysis. Various techniques were used to characterize the fresh and spent samples of Cu-Mn and the δ-Al_2O_3 support. N_2 physisorption showed that the δ-Al_2O_3 support had a BET specific surface area of 128 m^2/g and a pore volume of 0.54 cm^3/g. Dispersing the active phase over the support reduced the measured surface area slightly (118 m^2/g for the fresh Cu-Mn). The spent catalyst otherwise showed a higher surface area than the fresh one (145 m^2/g), which was believed to be due to the formation of carbon deposits in the catalyst pores (**Paper IV**).

SEM images were obtained of the fresh Cu-Mn (Figure 4.2a) and the spent Cu-Mn (Figure 4.2b) to visualize the change in morphology of the catalyst samples. Significant differences were observed between the fresh and the spent catalysts, in that an uneven surface layer (dark grey areas) appeared on the spent catalyst. Observations from the spent sample using BET and SEM were further elucidated by TGA, showing that the weight of the spent catalyst decreased by almost 10% between 300 and 450 °C, compared to the fresh catalyst (**Paper IV**). The additional material loss of the spent catalyst was attributed to the vaporization of heavier organic compounds and, at higher temperatures, the oxidation of solid carbon, probably seen as the surface layer in SEM, leading to variations in the BET surface area, as discussed above.

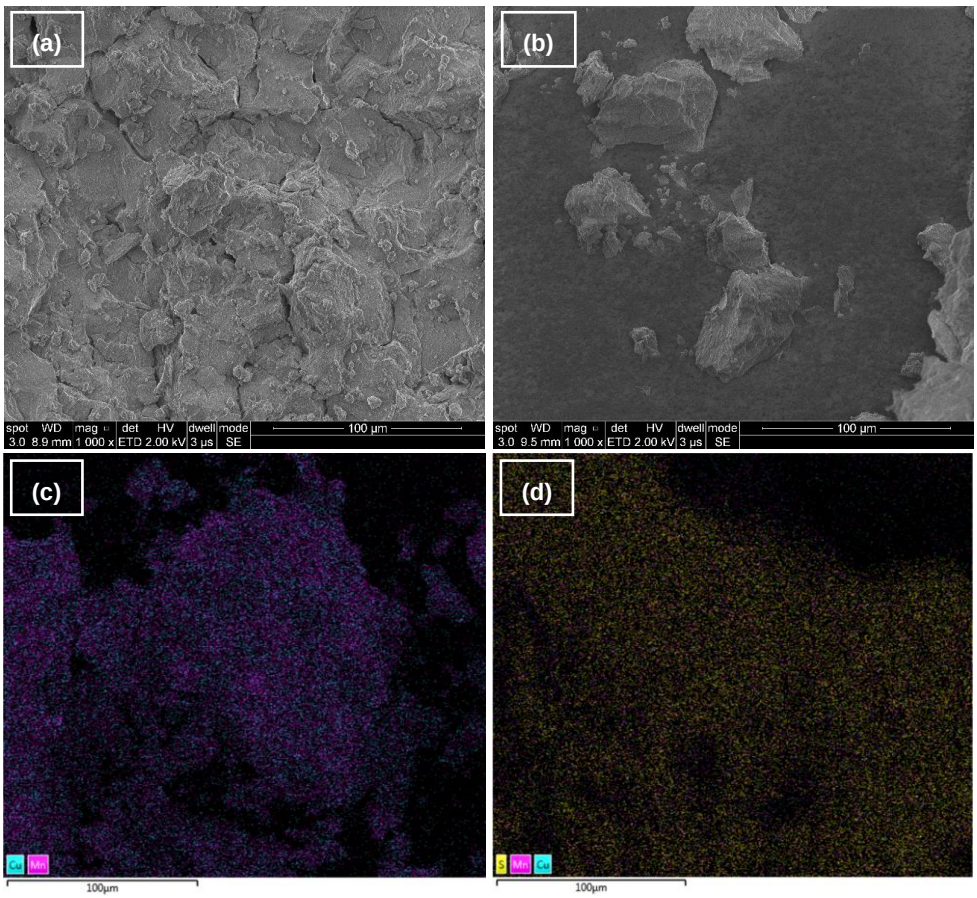


Figure 4.2. SEM images (a-b) and EDS elemental mapping (c-d) of the Cu-Mn catalyst. Images of the fresh catalyst are shown on the left, and spent catalyst on the right. (Adapted from Paper IV)

Furthermore, SEM-EDS elemental mapping revealed a significant increase in the amount of sulfur in the spent catalyst (Figure 4.2d) compared to the fresh catalyst (Figure 4.2c). The signal intensities of Mn and Cu also appeared to be lower in the spent catalyst (see **Paper IV** for map sum spectra). However, no changes were observed in the powder XRD patterns obtained from the bulk of the catalyst, both exhibiting diffractions peaks consistent with the delta phase of alumina [75].

The surface composition of Cu-Mn was determined using XPS, revealing differences between the fresh and spent catalyst (**Paper IV**). A high surface sulfur content of 1.7 atomic% was detected in the spent catalyst after the reaction, implying that the deposition of sulfur on the surface of the catalyst may be a problem. The spent catalyst also showed a lower surface concentration of Mn (0.4 atomic% versus 3.3 atomic% in the fresh catalyst), while the surface concentration of Cu remained essentially unchanged. This decrease in Mn content indicates possible leaching of Mn species from the supported catalyst during the reaction. The leaching of Mn species was further confirmed and quantified by ICP–OES (**Paper IV**). The composition of the fresh Cu-Mn was determined to be about 3.2 wt% Mn and 2.3 wt% Cu, together with no or very low amounts of sulfur. After the reaction, the metal contents had decreased to about 0.3 wt% Mn and 0.5 wt% Cu, indicating that Cu species had also been leached from the catalyst, despite the surface concentration apparently remaining unaltered, as suggested by XPS analysis. In addition, the sulfur content had increased considerably, to approximately 0.4 wt%. Taken together, the results of the material characterization indicated that the catalyst was not stable under the operating conditions used, which prevented investigations of catalyst reusability.

The results presented in **Paper IV** show that Cu-Mn is an efficient heterogeneous catalyst for the conversion of NaLS into LMW phenolic compounds under oxidative conditions, and thus contributes to partly answering RQ4.1. These LMW compounds could potentially be utilized in various value-added applications in the fast-growing biobased chemical industry. However, the stability of the catalyst during operation was poor, and must be investigated further, as being able to reuse the catalyst will be key in successful industrial operation.

4.2 Bioconversion of oxygen-treated kraft lignin

As mentioned above, oxidative depolymerization appears to be a promising approach for the conversion of technical lignin into highly functionalized LMW chemicals under fairly mild operating conditions. Valuable chemical compounds can be generated through oxidative depolymerization, including phenolic aldehydes and phenolic acids, and used as sources of carbon and energy in bioconversion.

Paper V describes the investigation of alkaline oxidative depolymerization as a form of pretreatment to enable the biological conversion of softwood-based LignoBoost kraft lignin (LB). The reactions were performed in batch mode at various temperatures (120–200 °C) and O_2 partial pressures (3–15 bar) to identify the optimal conditions for obtaining a biocompatible, oxidatively depolymerized LignoBoost lignin (ODLB) stream. The effect of reaction severity on MWD and the formation of LMW compounds was evaluated. The growth of four aromatic-catabolizing microbial strains, namely *Pseudomonas putida* KT2440, *Pseudomonas fluorescens*, *Rhodococcus opacus*, and *Sphingobium* sp. SYK-6, was investigated on product mixtures, utilizing the oxygen-treated LB stream as the sole source of carbon and energy.

The molecular weight of the depolymerized LB samples produced under different reaction conditions was evaluated using SEC. Table 4.1 lists the different conditions used, while the variation in the relative mass abundance of corresponding oxygen-treated LB samples is shown in Figure 4.3 (the variation in MWD and dispersity index can be found in **Paper V**).

Table 4.1. Reaction conditions and product yields from the oxidative depolymerization of LB (Adapted from Paper V)

Reaction[a]	Temperature (°C)	P_{O_2} (bar)	Monophenols + Acids (%)[b]	pH
1	120	3	5.2	13.1
2	120	9	6.3	12.6
3	120	15	9.4	10.1
4	160	3	8.3	12.3
5	160	9	10.5	8.3
6	160	15	10.4	7.6
7	200	3	6.8	12.0
8	200	9	13.1	8.4
9	200	15	14.2	7.0
Blank	–	–	3.2	13.4

[a]Fixed reaction parameters: 20 g/L LB, 0.2 M NaOH aqueous solution, 30 min. [b]Based on the total lignin substrate.

A significant reduction in molecular weight and lower dispersity indices were observed after oxidative depolymerization, the general trend being improved lignin breakdown into LMW species at higher temperature and O_2 pressure. Based on sodium polystyrene sulfonate calibration, approximately half of the LB substrate consisted of molecules with M_w >10 kDa, while the LMW fraction (<1 kDa) represented less than 1% of the total mass abundance (Figure 4.3). On the other hand, the abundance of HMW fractions (>10 kDa) was mostly less than 5% after reactions at 160 °C and 200 °C (reactions 4–9). The fraction rich in phenolic monomers, dimers, and trimers (<1 kDa) also increased to 4–12%, confirming that both high temperature and high O_2 pressure were needed to effectively depolymerize the LB substrate into LMW products.

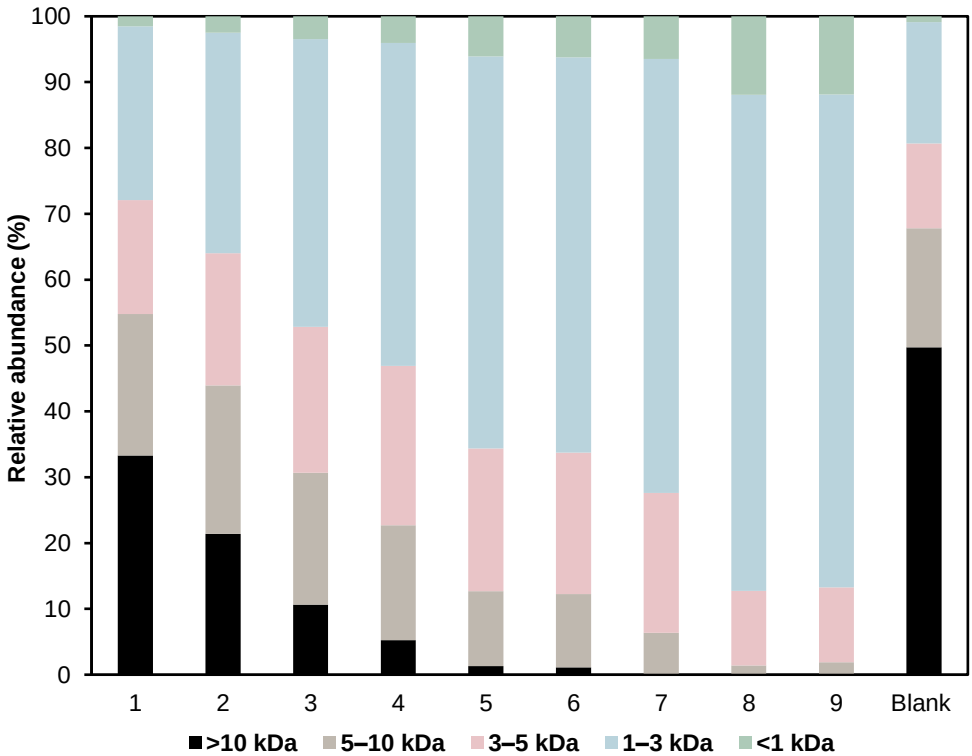


Figure 4.3. Relative mass abundance in differently oxygen-treated LB samples. The reaction number according to Table 4.1 is given on the abscissa. (Adapted from Paper V)

The distribution and yields of lignin-derived phenolic products resulting from oxidative depolymerization are known to vary depending on the lignin source and isolation method [76], processing conditions [77], and the kind of treatment prior to conversion [78]. The phenolic monomers and carboxylic acids produced by the oxidative depolymerization of LB under different treatment conditions were identified and quantified using liquid chromatography (see Table 4.1). The main phenolic monomers identified in the oxygen-treated samples were vanillin, vanillic acid, guaiacol, and acetovanillone; the highest total yield of 3.2 wt% being observed after treatment at 160 °C and 3 bar O_2 (reaction 4, Figure 4.4). The yields obtained for vanillin and vanillic acid were higher than in the blank sample (up to five-fold higher), confirming that molecular oxygen promoted their formation [79]. The amount of guaiacol produced increased with increasing reaction temperature. Formic and acetic acids were the predominant carboxylic acids found in the oxygen-treated samples (4–13 wt%), together with minor amounts of succinic acid (see **Paper V** for details). The formation of carboxylic acids lowered the pH of the product mixtures (Table 4.1), providing favorable conditions for further biological conversion due to enhanced solubility at near-neutral pH.

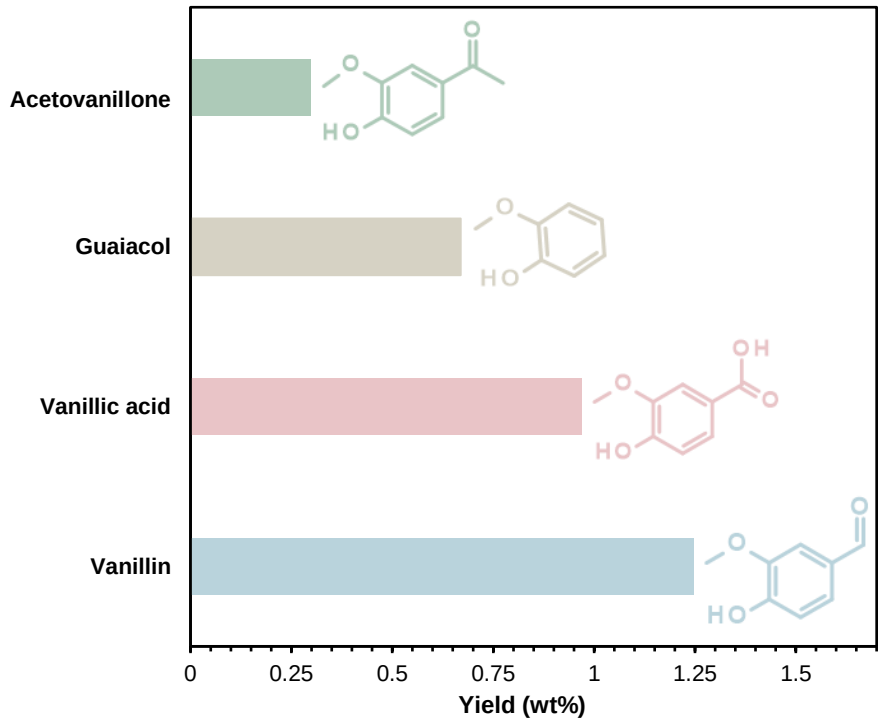


Figure 4.4. Yields of phenolic monomers from the oxidative depolymerization of LB. Reaction conditions: 20 g/L LB, 0.2 M NaOH aqueous solution, 160 °C, 3 bar O_2, 30 min.

As the overarching goal of the work described in this thesis was the biological conversion of phenolic species, the ODLB stream generated at 160 °C and 3 bar O_2 was characterized in detail with NMR, SEM, and BET, and used in microbial cultivations. The reactor was scaled up to prepare a larger batch of the product mixture under these conditions.

The presence of phenolic aldehydes, ketones, and carboxylic acids detected by liquid chromatography analysis was confirmed by 2D ^{1}H–^{13}C heteronuclear multiple-bond correlation (HMBC)- and HSQC-based NMR analyses (**Paper V**). The structural differences between LB and ODLB produced under selected conditions were demonstrated by HMBC, particularly concerning aliphatic and aromatic aldehydes, ketones, and acids ($\delta^{13}C$ ~170–215 ppm). The HSQC data also revealed a decrease in the methoxy resonance at $\delta^{13}C/\delta^{1}H$ ≈56/3.7 ppm, whereas the aromatic motifs ($\delta^{13}C/\delta^{1}H$ 105–140/6.0–8.0 ppm) were rather resistant to degradation. This structural stability implies that lignin depolymerization could be possible without oxidative cleavage of the aromatic rings under suitable conditions.

The changes in the surface morphology of the LB substrate observed after oxidative depolymerization were examined using SEM (see **Paper V** for SEM images). The surface of LB was rather smooth, underlining the highly recalcitrant nature of the untreated lignin material. However, after the reaction, the surface of the ODLB sample was fragmented into smaller particles, and needle-like structures were seen together with multi-layer eroded regions. Such changes in morphology likely reduce the surface integrity of the material and increase the surface area, making it more accessible to subsequent biological conversion [80].

N_2 physisorption measurements were carried out to obtain quantitative estimates of the changes in pore structure and surface area of the lignin material following oxidative depolymerization. The textural properties of the LB and ODLB samples are summarized in Table 4.2.

Table 4.2. Textural properties of lignin samples before and after oxidative depolymerization (Adapted from Paper V)

Sample	BET surface area (m^2/g)	Pore size (nm)	Pore volume (cm^3/g)
LB	1.23	4.90	0.0015
ODLB[a]	4.35	5.49	0.0060

[a]Reaction conditions: 20 g/L LB, 0.2 M NaOH aqueous solution, 160 °C, 3 bar O_2, 30 min.

The untreated LB had a BET specific surface area of 1.23 m^2/g and a pore volume of 0.0015 cm^3/g, and assuming cylindrical pores, the average pore size was calculated to be 4.9 nm. The ODLB sample showed a significant increase in BET specific surface area (4.35 m^2/g, nearly four-fold higher) together with increases in both pore volume (0.0060 cm^3/g) and pore size (5.49 nm), all of which are in line with the interpretation of the SEM images discussed above. The fact that the ODLB sample had a greater pore size and surface area could improve the access of microbial enzymes and reactive mediators, which would further facilitate the biological lignin conversion process.

Bacterial growth on agar plates was evaluated using LB and oxygen-treated LB samples (blank and reactions 1–9, Table 4.1) as the sole carbon and energy sources (see **Paper V** for growth patterns). The bacterial strains *Pseudomonas putida* KT2440, *Pseudomonas fluorescens*, *Rhodococcus opacus* and *Sphingobium* sp. SYK-6 have previously been reported to metabolize related lignin substrates and lignin-derived phenolic compounds [81]. It was found that neither LB nor the oxygen-treated LB samples was toxic to bacterial growth at the concentrations used. However, less growth was observed on the untreated LB than on the oxygen-treated LB samples, which is consistent with the higher amount of readily available LMW phenolics for direct consumption in the oxygen-treated LB samples (Table 4.1; Figure 4.3). Abundant growth was observed on the samples treated under harsh conditions, i.e. high temperature and O_2 pressure, which may be due to the higher concentrations of carboxylic acids, supporting growth of the microorganisms [82,83].

High-cell-density cultivations (OD ≈4) were performed to assess the utilization of LMW compounds in 2 g/L ODLB as carbon source for the four abovementioned bacterial strains (Figure 4.5). A slight decrease in OD was detected for all the microorganisms initially after inoculation, after which the OD was maintained throughout the cultivation of *Pseudomonas putida* KT2440, *Rhodococcus opacus*, and *Sphingobium* sp. SYK-6. However, in the case of *Pseudomonas fluorescens*, a decrease in OD (from 3.7 to 2.5) was observed during the first 45 h, probably due to the formation of cell aggregates. The tendency of *Pseudomonas fluorescens* to form aggregates when exposed to toxic environments has been reported previously [84], and was also observed with the DIKP material (**Paper III**).

Pseudomonas putida KT2440 and *Sphingobium* sp. SYK-6 were then cultivated in higher substrate concentrations (10 g/L ODLB; initial OD <0.01) in order to assess their growth and tolerance under such conditions (**Paper V**). Growth of both strains was clearly observed, and the consumption of phenolic monomers by the micro-organisms was in agreement with that in the high-cell-density cultivations.

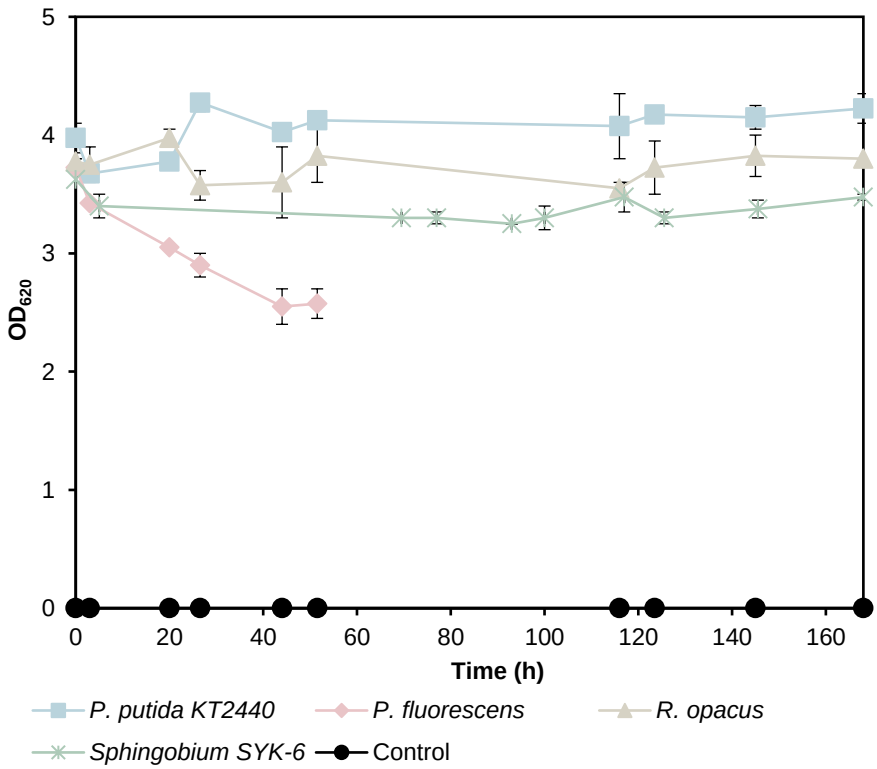


Figure 4.5. Cell density of bacterial species cultivated on minimal growth medium supplemented with 2 g/L ODLB as the sole carbon source. Reaction conditions: 20 g/L LB, 0.2 M NaOH aqueous solution, 160 °C, 3 bar O_2, 30 min. (Adapted from Paper V)

The findings presented in **Paper V** indicate that oxidative depolymerization is an effective method of converting technical lignin streams into LMW phenolics under rather mild operating conditions. Biocompatible molecules suitable for biological conversion at increased concentrations could be produced from kraft lignin by means of oxygen treatment, and this contributes to answering RQ4.2. This combined approach can hopefully shape the future forest biorefinery, allowing valorization of kraft lignin on a large scale. However, the yield of phenolic monomers must be enhanced, the fermentation conditions optimized, and the economic viability of full-scale applications assessed to accelerate the introduction of green processes and product development.

4.3 Process design and techno-economics

Techno-economic analysis (TEA) is essential for the successful development of integrated biorefinery concepts. The technical and economic performance of a given biorefinery can be evaluated through a TEA framework involving process modeling, simulation, engineering design, and economics. The results of TEA can then be used to prioritize certain areas of research and development. Assessing the commercial viability of a process at an early-stage will reduce the risks involved in scale-up and improve cost-competitiveness. In the context of lignin conversion to value-added products, high product yields and low separation costs are key drivers for economic viability, including biological upgrading, in future biorefineries [85].

The results of the study described in **Paper V** were used as the basis for the design and TEA of large-scale production of value-added chemicals from lignin by oxidative depolymerization (**Paper VI**). The viability of chemical production preceding biological conversion was investigated as another potential route for lignin processing in a biorefinery. A conceptual process design was developed using the Aspen Plus simulation software, and process profitability was assessed using different price ranges of lignin and lignin-derived products. Process sustainability was also investigated in an integrated forest biorefinery context. The overall objective was to identify possible limitations in the process and to determine whether the process would be economically and environmentally viable.

The feed to the process was assumed to be a WBL. The ODLB produced at 160 °C and 3 bar O_2 (reaction 4, Table 4.1) was chosen as the target product stream for the process due to its higher yield of valuable LMW phenolics (Figure 4.4). Carboxylic acids generated by the reaction were treated as useful co-products. The process was designed to be integrated into an existing kraft pulp mill. A simplified block flow diagram showing the major unit operations of the proposed process modeled in **Paper VI** is presented in Figure 4.6.

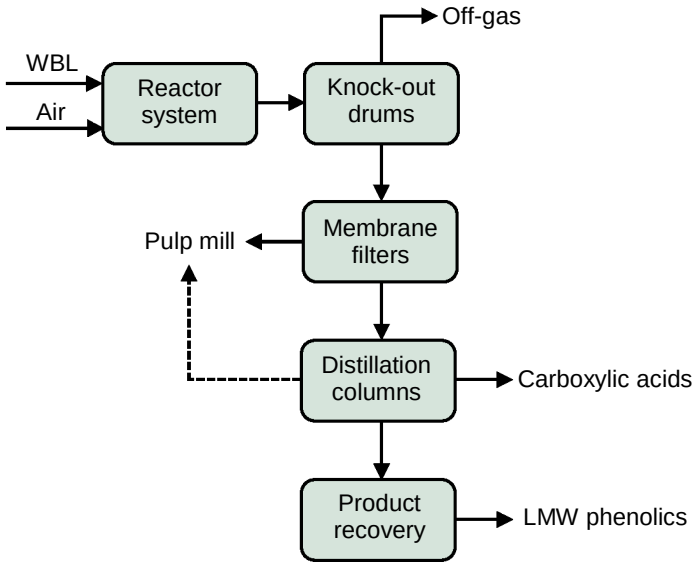


Figure 4.6. Simplified block flow diagram of the kraft lignin biorefinery process modeled in Paper VI. (WBL, weak black liquor; LMW, low molecular weight)

After specifying the input streams and unit operations, mass and energy balances were calculated, and the main design data were determined for a 700 t/y kraft lignin-based biorefinery. The nonrandom two-liquid thermodynamic property model was used to describe the phase equilibrium between different components of the process. Aspen Energy Analyzer was used to estimate the total utility requirements for heating and cooling in the process. A heat-integrated design was also proposed with the aim of maximizing the process-to-process heat recovery, thus minimizing the total utility requirements. The amount of CO_2 emitted, corresponding to burning a certain amount of fuel, Q_{fuel}, was calculated for the proposed process designs using the equation below:

$$[CO_2]_{emitted} = (Q_{fuel}/NHV) \times (C\%/100) \times \alpha \qquad (4.1)$$

where α is the ratio of the molar masses of CO_2 and C, and *NHV* denotes the net heating value of a fuel with a carbon content of *C*% [86,87].

A quantitative investigation of process sustainability and greenness was performed through the environmental factor (E-factor), which determines the weight of waste per unit weight of product [88]. The higher the value of the E-factor, the more waste will be generated by a given process or reaction.

$$\text{E-factor} = m\,(waste)/m\,(product) \qquad (4.2)$$

The E-factor allows the material efficiency, defined as the total weight of useful products divided by the total weight of useful products + waste [89], to be estimated.

$$\text{Material efficiency} = 1/(\text{E-factor} + 1) \quad (4.3)$$

Stoichiometric–economic targeting, a useful tool in guiding early-stage decisions concerning a proposed process design, was used to provide benchmarks for the flows of reactants and products coupled with chemical pricing data [90]. The metric for inspecting sales and reactants (MISR) was used to determine whether the proposed process had the potential for economic viability or not, and is defined as:

$$\text{MISR} = \frac{\sum_{p=1}^{N_{\text{products}}} F_p \times S_p}{\sum_{r=1}^{N_{\text{reactants}}} F_r \times C_r} \quad (4.4)$$

where F_p is the annual production rate of product p, S_p is the selling price of product p, F_r is the annual feed rate of reactant r, and C_r is the cost price of reactant r. If the MISR value is greater than one, the process may be considered for more detailed TEA to evaluate its profitability, and higher values of MISR are typically desirable. If the value of MISR is less than one, the process is not economically viable.

For detailed TEA, the total capital and operating costs were estimated using the CAPCOST software [91] in order to assess the economic viability of the proposed process designs. All costs were estimated in US dollars (US$) and updated to 2019 prices, taking into account the annual Chemical Engineering Plant Cost Index. Return on investment (ROI) and net present value (NPV) were the indices calculated to evaluate the profitability of the process. The major assumptions used in the TEA are summarized in Table 4.3.

Table 4.3. Main assumptions used in the techno-economic analysis of the kraft lignin biorefinery process described in Paper VI

Component	Basis/Price
Year of evaluation	2019
Plant lifetime	10 years
Construction period	2 years
Yearly operation time	8400 hours
Corporate taxation rate[a]	21.4%
Working capital	10.5% of FCI[b]
Salvage value	10% of FCI[b]
Electricity	$50/MWh
Low-pressure steam	$4/GJ
High-pressure steam	$7/GJ
Cooling water	$0.05/m^3
Lignin	$0.25/kg
Carboxylic acids	$0.75/kg
Phenolic monomers	$20/kg

[a]As applied in Sweden (the assumed location of the biorefinery) from 1 January 2019. [b]FCI, fixed capital investment.

Based on the block flow diagram in Figure 4.6, a computer-aided simulation model was developed to evaluate the mass and energy balances for the proposed process (see **Paper VI** for process flow diagram and data related to the main process streams and unit operations). Heat integration reduced the energy requirements for heating and cooling utilities by 22% and 21%, respectively, in relation to the base case, and led to a further reduction in CO_2 emissions of about 9,500 kg/d or 14,100 kg/d, depending on whether the fuel used was natural gas or heavy fuel oil.

The E-factor of the process was estimated to be ~1.6, which is in the range for the bulk chemical industrial sector [88]. The material efficiency was hence calculated to be 38%, which is a satisfactory value for a biomass-based synthetic pathway [92]. Notwithstanding these indicators, establishing the true environmental impact of such an early-stage technology requires a detailed life cycle assessment, where other metrics, such as acidification, ozone depletion, smog formation, and societal impact, can be evaluated.

The MISR was used to assess the economic potential of the process based on actual stoichiometric calculations, taking into account actual product yields and separation losses. The effect of the cost of lignin on the MISR for the proposed kraft biorefinery process is shown in Figure 4.7.

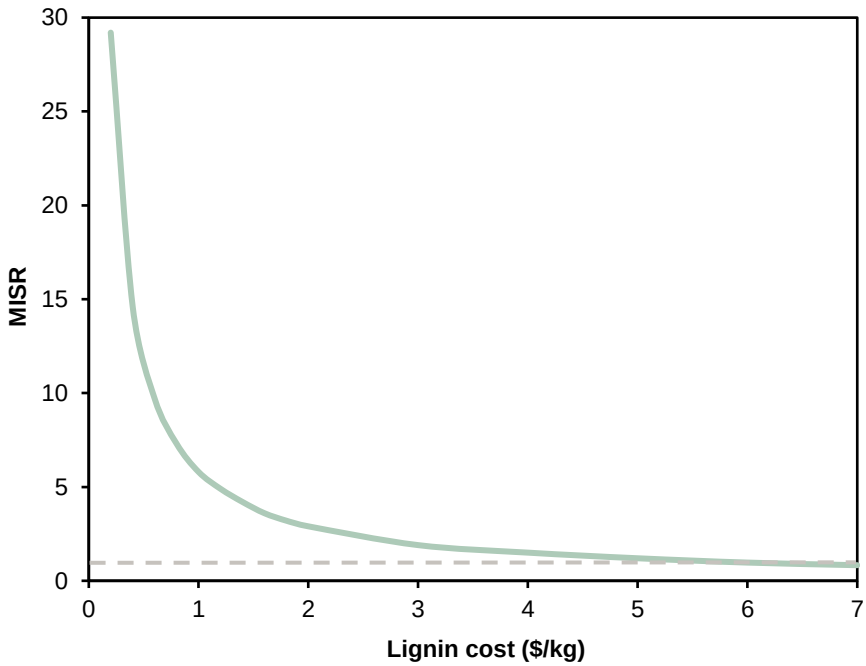


Figure 4.7. Effect of the cost of lignin on MISR in the proposed kraft biorefinery process. (MISR, metric for inspecting sales and reactants) (Adapted from Paper VI)

The process becomes economically infeasible when the cost of lignin exceeds $5.6/kg. The process may still not be economically feasible at lower lignin costs as other costs, such as capital cost, utilities, etc., must be considered, and the profitability of the plant must be assessed. Therefore, a more detailed economic analysis was undertaken, in which the profitability of the various process schemes was evaluated based on the ROI and NPV (the economic results obtained for the base case and the heat-integrated design can be found in **Paper VI**).

The total capital cost of the heat-integrated design was estimated to be about 2.5% higher than in the base case. However, a significant reduction in the cost of utilities was realized through applying heat integration (22% compared with the base case), which influenced the overall profitability of the process. The ROI and NPV of the base case were 10.4% and $3.6MM, respectively, while the corresponding values for the heat-integrated design were 14% and $5MM. Acceptable values of ROI for forest biorefineries are higher than in traditional forest-based industries, and have been reported to be in the range of 10–15% [93]. The acceptable value is lower in Scandinavia than in other countries, signifying the future potential of establishing forest-based biorefineries. Furthermore, a sensitivity analysis was carried out to evaluate the impact of changes in the cost of lignin and the selling price of vanillin on the profitability of the process. Figure 4.8 shows the ROI as a function of the selling price of vanillin for the heat-integrated design.

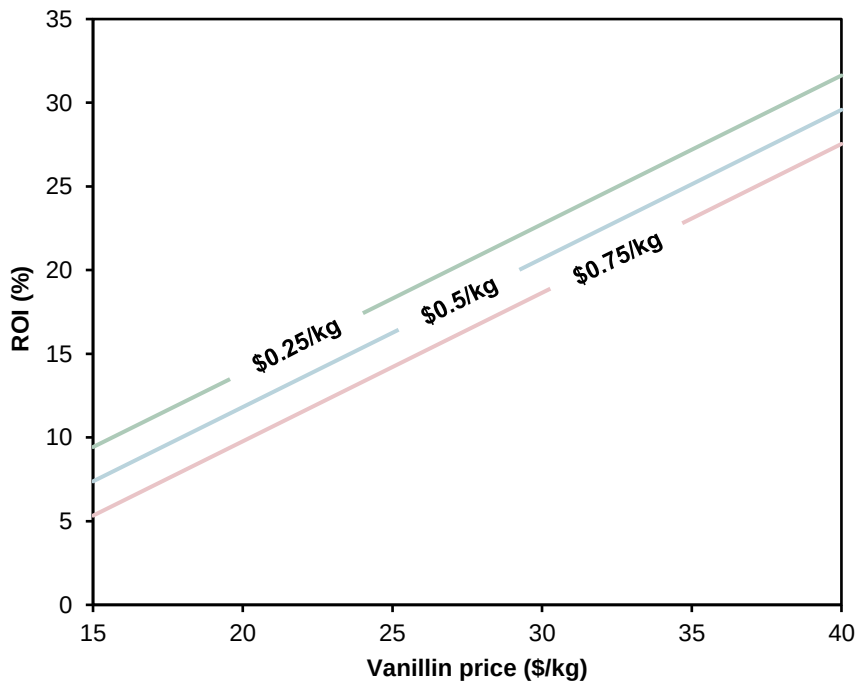


Figure 4.8. Sensitivity analysis for the ROI of the heat-integrated design of the proposed kraft biorefinery, for various lignin costs and vanillin prices. (ROI, return on investment) (Adapted from Paper VI)

The selling price of vanillin had a considerable influence on the ROI of the process, resulting in values ranging from 5% to 32%, depending on the lignin cost and the product price specified. At the higher lignin cost, the heat-integrated design exhibited an average increase in ROI of approximately 3.4%, compared to the base case (see **Paper VI** for detailed comparison).

After heat integration, and assuming a lignin cost of $0.25/kg, the proposed biorefinery was deemed economically viable, with values of ROI in the range of 9–32%, depending on the product selling price. This finding contributes to answering RQ4.3, as an economically viable process for biochemical production from kraft lignin via oxidative depolymerization can be envisioned. It should, however, be pointed out that the process described in **Paper VI** is still in its infancy, and there is a fairly high degree of uncertainty associated with the market value of the products generated. The process plant should be co-located and integrated with an existing kraft pulp mill, as this would substantially reduce the operating costs. Improving the yield of phenolic monomers would also improve the profitability of the process. The commercial application of lignin conversion processes is still limited, which makes the assessment of such early-stage technologies desirable to promote further technological development toward the practical realization of an integrated biorefinery for valorizing technical lignin.

4.4 On the yields of phenolic monomers

Catalysis could play a fundamental role in improving oxidative depolymerization strategies by enabling new chemical transformations and reaction regimes, and thus contribute to more sustainable use of lignin. **Paper VII** describes a study in which the impact of employing various homogeneous transition-metal catalysts on the oxidative depolymerization of LB was investigated. The primary aim was to enhance the yields of LMW phenolics obtained from LB, thus providing potentially better substrates for biological conversion, and improving the overall profitability of the process, aspects that are discussed in **Papers V** and **VI**, respectively.

Initial screening of homogeneous catalytic systems, including $Cu(OAc)_2$, $Mn(OAc)_2$, $VO(acac)_2$, and their combinations, was conducted to evaluate their ability to catalyze the oxidative depolymerization of LB for the production of high-value LMW phenolics, using molecular O_2 as an environmentally benign oxidant, and an aqueous NaOH solution as solvent. The reactions were carried out in batch mode, and the catalytic performance was evaluated based on the selectivity for vanillin and vanillic acid.

After each reaction, a dedicated workup procedure was performed on the reaction mixtures generated to separate the bio-oil, the aqueous phase, and the solid residue (Figure 4.9). An aliquot of reaction mixture (pH >13) was first acidified with aqueous HCl to pH ≤1 in order to precipitate the HMW lignin fragments, followed by centrifugation to separate the solid residue from the liquid phase. The liquid phase was then transferred to a separatory funnel, where it was extracted three times with ethyl acetate to separate the aqueous phase from the organic phase. The organic phase was then dried over anhydrous Na_2SO_4, and the ethyl acetate evaporated under vacuum to yield a brownish bio-oil.

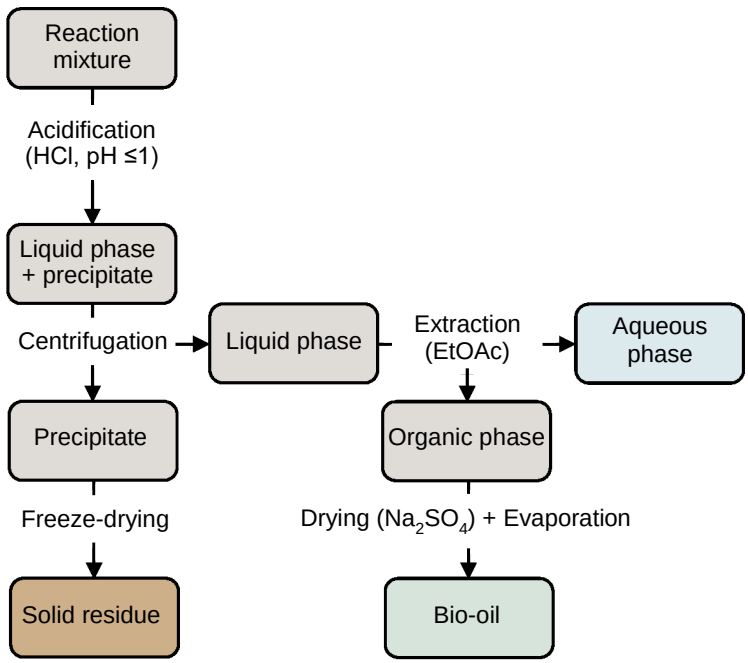


Figure 4.9. A schematic of the workup procedure described in Paper VII, following the oxidative depolymerization of LB. (EtOAc, ethyl acetate)

The yield of bio-oil was calculated gravimetrically based on the weight of lignin fed into the reactor. The resulting dry bio-oil was also used to quantify the phenolic monomers. The monomer yields were calculated using data from $^{1}H–^{13}C$ HSQC NMR spectroscopy, according to the following equation:

$$\text{Monomer yield (wt\%)} = \frac{m\,(monomer)_{NMR}}{m\,(bio\text{-}oil)_{NMR}} \times \frac{m\,(bio\text{-}oil)_{E} \times \text{AF}}{m\,(lignin)_{I}} \times 100 \quad (4.5)$$

where *m (monomer)*$_{NMR}$ is the weight of the phenolic monomer in the NMR sample, *m (bio-oil)*$_{NMR}$ is the weight of the bio-oil in the NMR sample, *m (bio-oil)*$_{E}$ is the weight of the bio-oil extracted after workup, *m (lignin)*$_{I}$ is the initial weight of the lignin, and AF is an aliquot factor that accounts for the aliquot volume used in workup in relation to the total volume of the reaction mixture. SEC, ^{13}C and 2D HSQC NMR spectroscopy, and ultra-high-performance liquid chromatography (UHPLC)–HRMS were used for the complete characterization of LB and the various LB-derived products.

The $VO(acac)_2$-$Cu(OAc)_2$ (V-Cu) catalyst system exhibited the highest vanillin yield (~3.5 wt%), together with a total yield of identified phenolic monomers of ~7 wt% (Figure 4.10). Compared to the control reaction (no added catalyst) and the Cu-catalyzed reaction, the V-Cu system showed improvements in the total monomer yield of 27% and 8%, respectively. These findings imply a combined effect that enhances the catalytic activity of the V-Cu system, which is consistent with previous observations on lignin model compounds and commercial lignin sources [94,95].

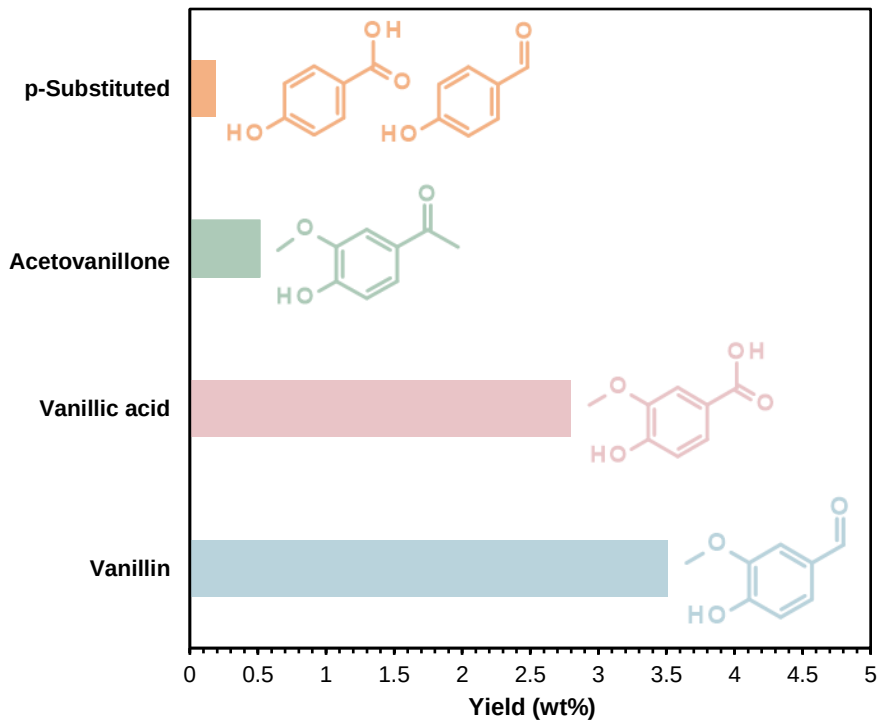


Figure 4.10. Yields of phenolic monomers from the oxidative depolymerization of LB using a V-Cu catalyst. Reaction conditions: 25 g/L LB, 2 M NaOH aqueous solution, 1.4 mmol $VO(acac)_2$-$Cu(OAc)_2$ catalyst, 150 °C, 5 bar O_2, 10 min. Reactions were performed in duplicate, and the average values are given. The *para*-substituted phenolics represent a combination of *p*-hydroxybenzoic acid and *p*-hydroxybenzaldehyde.

The reaction mechanism probably proceeds via a combination of C–C and C–O bond cleavages. Selective oxidative C–C bond cleavages in lignin model compounds have been described when using homogeneous copper [96] and vanadium [97] catalysts. The selectivity between C–C and C–O bond cleavage has also been shown to be dependent on the nature of the vanadium catalyst [98]. Furthermore, the highly functionalized phenolic monomers produced by molecular oxygen lignin depolymerization in aqueous alkaline media are often not stable, due to secondary reaction mechanisms that have not yet been identified [99]. Together, the reaction pathways can depend on various parameters, including the chemical nature of the vanadium/copper catalyst, the type of lignin (model compound or technical lignin), the reaction conditions employed, and the oxidant and the solvent used. A dedicated mechanistic investigation will be required to gain detailed insights into the combined effect of the V-Cu system and probable metal–metal interactions, and to elucidate specific cleavages of interunit linkages.

SEC analysis was carried out using sodium polystyrene sulfonate calibration standards to follow the degree of depolymerization and MWDs for the LB feed and the V-Cu-derived samples (**Paper VII**). M_w decreased notably from 5.98 kDa for the LB feed to 1.14 kDa for the V-Cu-derived product, with a corresponding decrease in M_n from 1.67 kDa to 0.79 kDa. A narrower MWD was observed in the V-Cu-derived product, showing a dispersity index of 1.44, compared to 3.58 for the LB feed. A rather high concentration of LB-derived oligomers was also observed in the V-Cu-derived product, as indicated by the relatively higher UV absorbance in the 0.7–0.8 kDa region, assuming that molar absorptivity is constant for the different eluted fractions (see **Paper VII** for SEC–UV profiles).

^{1}H–^{13}C HSQC NMR spectroscopy was performed on the LB substrate and the bio-oils obtained after oxidative depolymerization and workup (**Paper VII**). Most of the interunit linkages detected in LB disappeared after the reaction, suggesting the effective cleavage of these bonds, as well as the efficient separation of the desired LMW monomers from higher molecular fragments during workup. Different structural motifs were also seen in the spectra of the catalytically-derived bio-oils (see **Paper VII** for spectral comparison). The spectrum of the bio-oil obtained with the V-Cu catalyst contained signals characteristic of structural motifs in individual spectra for both V- and Cu-derived bio-oils, providing evidence of a combined effect of V and Cu. The observation of different reactivity patterns resulting from V-Cu catalysis, in comparison to their monometallic analogues, indicates the potential of this catalytic system for the oxidative depolymerization of complex lignin streams.

UHPLC–HRMS was carried out on the LB substrate, and on the organic (bio-oil) and aqueous fractions obtained from the control experiment and from V-Cu catalysis (**Paper VII**). Clustering analysis revealed that the vast majority of the organic species present in the LB feed were successfully converted during oxidative

depolymerization, which is consistent with the observations from NMR analysis, and was also demonstrated by higher bio-oil yields.

In total, 161 chemical species in aqueous fractions fulfilled the cut-off criteria set, and were classified into 14 mainly present in the V-Cu-derived sample, 56 mostly present in the control sample, and 91 species that were statistically indistinguishable (see **Paper VII** for volcano plots). Of the 37 molecular species detected in the organic fractions, 9 new species were formed in the control experiment, leaving 16 species statistically indistinguishable. The V-Cu-catalyzed process, on the other hand, was able to generate 13 new species, probably via different reaction pathways, thus reducing the number of indistinguishable species from 16 to 12. Interestingly, more than a 30-fold increase was seen in two aromatic molecules with an oxoacetic functional group and oxalic acid, when using the V-Cu catalyst. This may indicate new routes for the production of platform chemicals with oxoacetic functionalities.

Parametric optimization of the operating conditions was performed including reaction temperature, O_2 partial pressure, and residence time, as well as the V:Cu molar ratio and the catalyst:lignin ratio (the results and a discussion on the influence of various parameters on the yields of phenolic monomers can be found in **Paper VII**). The recyclability of the V-Cu catalyst was also investigated; unfortunately, a rather poor catalytic activity (considerably lower vanillin yield) was observed after its reuse. There is therefore a need for further research into catalyst recyclability.

The findings presented in **Paper VII** underline the potential of the vanadium–copper bimetallic catalytic system in the efficient conversion of technical lignin into value-added LMW chemicals under oxidative conditions, and contribute to answering RQ4.1. A combined effect was seen between V and Cu, affecting the cleavage of various lignin linkages and enhancing the product yields and qualities. The closed-ended research questions RQ4.2 and RQ4.3 may be transformed into open-ended questions, where the suitability of the products generated for biological conversion could be examined, and the economic viability of the process for sustainable chemical production could be assessed.

5 Conclusions and outlook

From the findings presented in this thesis, it can be concluded that thermochemical–biological approaches for lignin valorization hold significant potential in overcoming the problems associated with the heterogeneity of technical lignin, for the production of value-added chemicals. A wide range of high-value products could be derived from complex lignin substrates by combining thermochemical depolymerization with microbial conversion, thus improving the economics of the forest biorefinery. The work described in this thesis has focused on the conversion of technical lignin streams into small-molecule chemicals via thermochemical depolymerization methods. Five specific research questions were addressed.

Which physicochemical tools can be used to assist in conceptualizing efficient valorization routes for technical lignin?

Determining the physicochemical properties of technical lignin streams is essential for the rational development of molecularly tailored lignin-based applications. In order to match technical lignin streams with suitable valorization routes, it is necessary to have information on their chemical composition, functional groups, molecular weight, skeletal structure and relative distribution of interunit linkages, thermal stability, and the size and the range of lignin agglomerates. Such information, aided by recent advances in SEC, 2D NMR, FTIR, and HRMS, for example, will help future valorization efforts for the conversion of lignin into chemicals, fuels, or materials.

Is it possible to generate molecules that are compatible with biological upgrading from the continuous BCD of technical lignin?

An effective BCD process has been developed for the continuous conversion of IK into LMW phenolics at a relatively low reaction temperature (<250 °C), with an exceptionally short residence time (~2 min), without the need for an organic solvent or capping agent. Following membrane filtration, the produced LMW phenolics have been found suitable for microbial conversion at increased concentrations, with possibilities for process integration with traditional pulp and paper mills. Future work may include investigating different kinds of lignin, feeding higher concentrations of lignin into the CFR, varying the NaOH concentration, controlling char deposition, investigating different membrane materials and bacterial strains, reactor

design for scale-up and commercialization, and the design of energy-recovery solutions.

Can an efficient catalytic system be developed to depolymerize technical lignin under oxidative conditions?

The oxidative depolymerization of NaLS into LMW phenolics over a heterogeneous Cu-Mn catalyst has been demonstrated, showing promising results. Harnessing the NaLS substrate for such conversion has, however, been challenging due to its low purity, wide MWD, and high sulfur content (almost 8%). For instance, the leaching of metals and the deposition of carbon- and sulfur-containing compounds on the surface of the catalyst have been observed. Further optimization is therefore needed to ensure long-term stability of the catalyst. Other catalyst preparation methods, such as deposition–precipitation, as well as other catalyst formulations, could be tested. Other technical lignin streams with higher purity and lower sulfur content, such as organosolv lignin or hydrolysis lignin, could also be investigated.

A homogeneous V-Cu catalytic system has also been developed for the oxidative depolymerization of LB into LMW phenolic monomers; vanillin and vanillic acid being the primary products. A combined effect of V and Cu was seen, influencing the cleavage of various lignin linkages, and the V-Cu system showed an improvement in the total monomer yield of ~27%, compared to the control reaction. New routes for the synthesis of platform chemicals with oxoacetic functionalities are also envisaged via V-Cu catalysis. However, the recycling and reuse of V-Cu should be the subject of future research, as this is essential for successful implementation under industrially relevant conditions. A mechanistic investigation will also be required to gain detailed insights into the combined effect of V-Cu and probable metal–metal interactions, and to elucidate specific cleavages of lignin linkages.

Is it possible to produce molecules suitable for biological upgrading by the oxidative depolymerization of technical lignin?

Oxidative depolymerization has been shown to be an effective thermochemical approach for converting kraft lignin into LMW phenolic monomers suitable for biological conversion at increased concentrations. Vanillin, vanillic acid, guaiacol, and acetovanillone have been identified as the main phenolic monomers in the oxygen-treated LB. The growth of various aromatic-catabolizing bacterial strains has been demonstrated on product mixtures, utilizing the oxygen-treated LB as the sole source of carbon and energy. Although the direct uptake of LB-derived monomers has been shown by various bacterial species, the yield of monomers (<5 wt%) is probably too low for an industrial application. Future work must therefore include enhancing the yield of phenolic monomers, optimizing the fermentation conditions, and assessing the viability of large-scale applications toward bioproduct development.

Is biochemical production from technical lignin subjected to oxidative depolymerization economically viable?

The techno-economic viability of a process for the oxidative depolymerization of kraft lignin as a resource for sustainable chemical production has been analyzed. The proposed biorefinery process was evaluated on a scale of 700 t/y of fresh lignin feed. After heat integration, and assuming a lignin cost of $0.25/kg, the proposed process can be regarded as economically viable, with values of ROI in the range of 9–32%, depending on the selling price of the product. Co-locating and integrating the process with an existing kraft pulp mill would considerably reduce the overall operating costs. Future work should include improving the yield and selectivity to phenolic products as this would significantly improve the profitability of the process. A detailed life cycle assessment would also be required in order to establish the true environmental footprint of such early-stage technology.

The findings of the work described in this thesis have thus contributed to the development of thermochemical–biological approaches for the valorization of technical lignin, a largely underexploited feedstock in the pulp and paper and biofuel industries. The utilization of technical lignin for the production of value-added chemicals is key to ensure progress in the transition to a low-carbon economy and to ensure the success of future biorefineries.

Acknowledgments

I would like to express my deepest gratitude to my supervisor, *Prof. Christian Hulteberg*, for his invaluable guidance, continuous encouragement, and endless support throughout my PhD journey. Thank you *Christian* for introducing me to the world of lignin, for giving me the freedom to develop and implement new research ideas, and for providing me with many remarkable learning opportunities. I enjoyed our countless meetings, and I am grateful for the practical suggestions and valuable advice you have provided at all times. It is impossible to say how much I have learnt from you *Christian*; not only regarding the work in this thesis, but also for my professional development, and for that I am deeply grateful and truly appreciative.

I would also like to acknowledge my co-supervisors, *Prof. Charlotta Turner* and *Prof. Ola Wallberg*; your professional support and guidance were crucial in completing this work. Thank you *Lotta* for your valuable insights into lignin analysis and for providing feedback when needed, and thank you *Ola* for all the knowledge you shared and for the long hours we spent trying to get various simulations to converge.

I would like to extend my thanks to *Dr. Per Tunå* for giving me the lowdown on the technicalities of flow chemistry; and to *Dr. Helena Svensson* for being such a great example of a course coordinator and for her constructive feedback, which helped me improve my teaching skills. Special thanks to *Dr. Meher Sanku* for helping to maintain a pleasant working environment, and for many great activities and excursions; I really enjoyed sharing an office with you *Meher*.

I am grateful to the current and former members of the *Innovative Process Engineering Group*: *Prof. Hans Karlsson*, *Dr. Fredric Bauer*, *Dr. Sara Blomberg*, *Dr. Laura Malek*, *Lucy Jensen*, *Hanna Karlsson*, *Linnéa Kollberg*, and *Kena Li*, for all our scientific and nonscientific discussions, both inside and outside the workplace. It has been a pleasure to be part of this group.

I am also grateful to the current and former members of the *Lignin Group* at Lund University: *Prof. Marie Gorwa-Grauslund*, *Prof. Gunnar Lidén*, *Dr. Henrik Almqvist*, *Dr. Daniel Brink*, *Dr. Magnus Carlquist*, *Dr. Javier García-Hidalgo*, *Dr. Jens Prothmann*, *Dr. Krithika Ravi*, *Dr. Margareta Sandahl*, *Dr. Mingzhe Sun*, *Fabian Mittermeier*, and *Matthias Nöbel*, for our fruitful collaboration and discussions on such an intriguing macromolecule.

I wish to thank all my colleagues at the Department of Chemical Engineering, LTH, for instilling a high-standard work culture. Special thanks to *Mia Hedin*, *Maria Messer*, *Lena Nilsson*, and *Gity Yahoo*, for all their help with administrative matters. To *Lena*, you are greatly missed! Thanks also to *Dr. Mats Galbe* for always finding the time to discuss my study plan; to *Michaël Grimsberg* for fixing things, including software and memorable hiking trips; and to *Paula Leckius* for her ingenious insights and suggestions on the art of typography.

During my PhD studies, I was fortunate to spend six months at the Centre for Catalysis and Sustainable Chemistry, Technical University of Denmark (DTU), with the group of *Prof. Anders Riisager*. I would like to sincerely thank *Anders* for giving me the opportunity to work in his lab, for supporting and guiding me during my stay at DTU, and the indispensable contribution this made to my work. It was a privilege to work with you *Anders*, and I am grateful for everything I have learned from you. Special thanks to *Dr. Sebastian Meier*, who never wavered in his ambition to get the best out of my lignin samples by NMR, or to offer constructive feedback. Thank you *Sebastian* for our productive collaboration, working with you has been a great pleasure. I wish to thank all my colleagues at DTU Chemistry for welcoming me into their scientific sphere and making me feel at home.

Many thanks to all my coauthors and coworkers for their important contributions to this work: *Prof. Mahmoud El-Halwagi (Texas A&M University)*, for constantly sharing his extensive knowledge and insightful suggestions on process economics; *Dr. Olumoye Ajao* and *Dr. Marzouk Benali (Natural Resources Canada)*, for coauthorship of a research paper on lignin fractionation and excellent cooperation; *Dr. Abdulrahman Al-Rabiah (King Saud University)*, for his valuable experience in process simulation and successful collaboration; *Dr. Saša Bjelić (Paul Scherrer Institute)*, for his immense knowledge of mass spectrometry, which contributed to a positive outcome; *Florian Walch (DTU)*, for his hard work and commitment (it has been amazing to see how my passion for lignin has passed on to you, and I wish you all the best in the future); and *Ping Zhu (DTU)*, for coauthorship of a review on the trends in lignocellulose conversion (I wish you the best of luck with your PhD).

I also wish to thank *Prof. Fatma Ashour (Cairo University)* and *Prof. Mamdouh Gadalla (The British University in Egypt)*, for their continued support and encouragement and for all the knowledge they have provided me with since my undergraduate studies; and *Prof. Tamer Ahmed (Cairo University)*, for broadening my horizons within the chemical engineering field and for always checking on the progress of my PhD studies.

The *Swedish Foundation for Strategic Research* and the *Swedish Energy Agency* are gratefully acknowledged for their financial support of this work.

I am indebted to *my parents*, for all their efforts in raising me and all their sacrifices; your prayers mean so much! Thank you to *my mother*, for unconditional love and care; whatever I do for you, I will forever be in your debt. Thank you to *my father*, for teaching me to aim high in my ambitions and to work hard to achieve them. Thank you to my sister, *Yomna*, for always being there for me; I wish you and your lovely family a wonderful life, full of happiness and success.

To *my mother-in-law*, *father-in-law*, and *brothers-in-law*, thank you for your constant support and encouragement; I sincerely appreciate everything you have done for me. To *my grandmother*, who passed away while I was working on my PhD, thank you for being an outstanding teacher and an enduring source of inspiration; I hope I have made you proud!

Last, but certainly not least, I would like to wholeheartedly thank my wife, *Aisha*, and my son, *Yusuf*, for being the light of my life and the driving force behind essentially every successful endeavor. *Aisha*, I could write several chapters expressing my love and gratitude, but I will simply say here that I am blessed to be married to a woman like you!

*** الْحَمْدُ لِلَّهِ الَّذِي بِنِعْمَتِهِ تَتِمُّ الصَّالِحَاتُ ***

References

1. Zhu P, Abdelaziz OY, Hulteberg CP, Riisager A: **New synthetic approaches to biofuels from lignocellulosic biomass**. *Curr Opin Green Sustain Chem* 2020, **21**:16–21.
2. Himmel ME, Ding S-Y, Johnson DK, Adney WS, Nimlos MR, Brady JW, Foust TD: **Biomass recalcitrance: engineering plants and enzymes for biofuels production**. *Science* 2007, **315**:804–807.
3. Schutyser W, Renders T, Van den Bosch S, Koelewijn S-F, Beckham GT, Sels BF: **Chemicals from lignin: an interplay of lignocellulose fractionation, depolymerisation, and upgrading**. *Chem Soc Rev* 2018, **47**:852–908.
4. Abdelaziz OY, Brink DP, Prothmann J, Ravi K, Sun M, García-Hidalgo J, Sandahl M, Hulteberg CP, Turner C, Lidén G, et al.: **Biological valorization of low molecular weight lignin**. *Biotechnol Adv* 2016, **34**:1318–1346.
5. Abu-Omar MM, Barta K, Beckham GT, Luterbacher JS, Ralph J, Rinaldi R, Román-Leshkov Y, Samec JSM, Sels BF, Wang F: **Guidelines for performing lignin-first biorefining**. *Energy Environ Sci* 2021, **14**:262–292.
6. Ragauskas AJ, Beckham GT, Biddy MJ, Chandra R, Chen F, Davis MF, Davison BH, Dixon RA, Gilna P, Keller M, et al.: **Lignin valorization: improving lignin processing in the biorefinery**. *Science* 2014, **344**:1246843.
7. Moretti C, Corona B, Hoefnagels R, Vural-Gürsel I, Gosselink R, Junginger M: **Review of life cycle assessments of lignin and derived products: Lessons learned**. *Sci Total Environ* 2021, **770**:144656.
8. Beckham GT, Johnson CW, Karp EM, Salvachúa D, Vardon DR: **Opportunities and challenges in biological lignin valorization**. *Curr Opin Biotechnol* 2016, **42**:40–53.
9. Calvo-Flores FG, Dobado JA, Isac-García J, Martín-Martínez FJ: *Lignin and Lignans as Renewable Raw Materials: Chemistry, Technology and Applications*. John Wiley & Sons, Ltd; 2015.
10. Giummarella N, Pu Y, Ragauskas AJ, Lawoko M: **A critical review on the analysis of lignin carbohydrate bonds**. *Green Chem* 2019, **21**:1573–1595.
11. Nishimura H, Kamiya A, Nagata T, Katahira M, Watanabe T: **Direct evidence for α ether linkage between lignin and carbohydrates in wood cell walls**. *Sci Rep* 2018, **8**:6538.
12. Zhao Y, Shakeel U, Saif Ur Rehman M, Li H, Xu X, Xu J: **Lignin-carbohydrate complexes (LCCs) and its role in biorefinery**. *J Clean Prod* 2020, **253**:120076.
13. Rinaldi R, Jastrzebski R, Clough MT, Ralph J, Kennema M, Bruijnincx PCA,

Weckhuysen BM: **Paving the Way for Lignin Valorisation: Recent Advances in Bioengineering, Biorefining and Catalysis**. *Angew Chemie Int Ed* 2016, **55**:8164–8215.

14. del Río JC, Rencoret J, Gutiérrez A, Elder T, Kim H, Ralph J: **Lignin Monomers from beyond the Canonical Monolignol Biosynthetic Pathway: Another Brick in the Wall**. *ACS Sustain Chem Eng* 2020, **8**:4997–5012.
15. Katahira R, Elder TJ, Beckham GT: **A Brief Introduction to Lignin Structure**. In *Lignin Valorization: Emerging Approaches*. Edited by Beckham GT. The Royal Society of Chemistry; 2018:1–20.
16. Tolbert A, Akinosho H, Khunsupat R, Naskar AK, Ragauskas AJ: **Characterization and analysis of the molecular weight of lignin for biorefining studies**. *Biofuels, Bioprod Biorefining* 2014, **8**:836–856.
17. Zakzeski J, Bruijnincx PCA, Jongerius AL, Weckhuysen BM: **The catalytic valorization of lignin for the production of renewable chemicals**. *Chem Rev* 2010, **110**:3552–3599.
18. Li T, Takkellapati S: **The current and emerging sources of technical lignins and their applications**. *Biofuels, Bioprod Biorefining* 2018, **12**:756–787.
19. Balakshin MY, Capanema EA, Sulaeva I, Schlee P, Huang Z, Feng M, Borghei M, Rojas OJ, Potthast A, Rosenau T: **New Opportunities in the Valorization of Technical Lignins**. *ChemSusChem* 2021, doi:10.1002/cssc.202002553.
20. Constant S, Wienk HLJ, Frissen AE, de Peinder P, Boelens R, van Es DS, Grisel RJH, Weckhuysen BM, Huijgen WJJ, Gosselink RJA, et al.: **New insights into the structure and composition of technical lignins: a comparative characterisation study**. *Green Chem* 2016, **18**:2651–2665.
21. Bruijnincx PCA, Rinaldi R, Weckhuysen BM: **Unlocking the potential of a sleeping giant: lignins as sustainable raw materials for renewable fuels, chemicals and materials**. *Green Chem* 2015, **17**:4860–4861.
22. Hu J, Zhang Q, Lee D-J: **Kraft lignin biorefinery: A perspective**. *Bioresour Technol* 2018, **247**:1181–1183.
23. Sjöström E: *Wood Chemistry: Fundamentals and Applications*. Academic Press, Inc., San Diego, California; 1993.
24. Bonhivers J-C, Stuart PR: **Applications of Process Integration Methodologies in the Pulp and Paper Industry**. In *Handbook of Process Integration (PI): Minimisation of Energy and Water Use, Waste and Emissions*. Edited by Klemeš JJ. Woodhead Publishing Limited/Elsevier; 2013:765–798.
25. Rodrigues A, Pinto P, Barreiro F, Costa CAE, Mota MIF, Fernandes I: *An Integrated Approach for Added-Value Products from Lignocellulosic Biorefineries: Vanillin, Syringaldehyde, Polyphenols and Polyurethane*. Springer Nature Switzerland AG; 2018.
26. Tomani P: **The LignoBoost process**. *Cellul Chem Technol* 2010, **44**:53–58.
27. Öhman F, Theliander H, Tomani P, Axegård P: *Method for separating lignin from black liquor*. US Patent 8,486,224 B2. 2013.
28. Gellerstedt G, Tomani P, Axegård P, Backlund B: **Lignin recovery and lignin-**

based products. In *Integrated Forest Biorefineries: Challenges and Opportunities*. Edited by Christopher L. The Royal Society of Chemistry; 2013:180–210.

29. Hubbe MA, Alén R, Paleologou M, Kannangara M, Kihlman J: **Lignin recovery from spent alkaline pulping liquors using acidification, membrane separation, and related processing steps: A review**. *BioResources* 2019, **14**:2300–2351.
30. Aro T, Fatehi P: **Production and Application of Lignosulfonates and Sulfonated Lignin**. *ChemSusChem* 2017, **10**:1861–1877.
31. Biddy MJ: **Adding Value to the Biorefinery with Lignin: An Engineer's Perspective**. In *Lignin Valorization: Emerging Approaches*. Edited by Beckham GT. The Royal Society of Chemistry; 2018:499–518.
32. Vishtal A, Kraslawski A: **Challenges in industrial applications of technical lignins**. *BioResources* 2011, **6**:3547–3568.
33. Galkin MV, Samec JSM: **Lignin Valorization through Catalytic Lignocellulose Fractionation: A Fundamental Platform for the Future Biorefinery**. *ChemSusChem* 2016, **9**:1544–1558.
34. El Mansouri N-E, Salvadó J: **Structural characterization of technical lignins for the production of adhesives: Application to lignosulfonate, kraft, soda-anthraquinone, organosolv and ethanol process lignins**. *Ind Crops Prod* 2006, **24**:8–16.
35. Holladay JE, White JF, Bozell JJ, Johnson D: *Top Value-Added Chemicals from Biomass - Volume II—Results of Screening for Potential Candidates from Biorefinery Lignin*. Pacific Northwest National Laboratory; 2007.
36. Gosselink RJA: *Lignin as a renewable aromatic resource for the chemical industry*. PhD thesis. Wageningen University; 2011.
37. Behling R, Valange S, Chatel G: **Heterogeneous catalytic oxidation for lignin valorization into valuable chemicals: what results? What limitations? What trends?** *Green Chem* 2016, **18**:1839–1854.
38. Gillet S, Aguedo M, Petitjean L, Morais ARC, da Costa Lopes AM, Łukasik RM, Anastas PT: **Lignin transformations for high value applications: towards targeted modifications using green chemistry**. *Green Chem* 2017, **19**:4200–4233.
39. Rumpf J, Do XT, Burger R, Monakhova YB, Schulze M: **Extraction of High-Purity Lignins via Catalyst-free Organosolv Pulping from Low-Input Crops**. *Biomacromolecules* 2020, **21**:1929–1942.
40. Ľudmila H, Michal J, Andrea Š, Aleš H: **Lignin, potential products and their market value**. *Wood Res* 2015, **60**:973–986.
41. Li C, Zhao X, Wang A, Huber GW, Zhang T: **Catalytic Transformation of Lignin for the Production of Chemicals and Fuels**. *Chem Rev* 2015, **115**:11559–11624.
42. Sturgeon MR, Kim S, Lawrence K, Paton RS, Chmely SC, Nimlos M, Foust TD, Beckham GT: **A Mechanistic Investigation of Acid-Catalyzed Cleavage of Aryl-Ether Linkages: Implications for Lignin Depolymerization in Acidic Environments**. *ACS Sustain Chem Eng* 2014, **2**:472–485.
43. Lahive CW, Deuss PJ, Lancefield CS, Sun Z, Cordes DB, Young CM, Tran F, Slawin AMZ, de Vries JG, Kamer PCJ, et al.: **Advanced Model Compounds for**

Understanding Acid-Catalyzed Lignin Depolymerization: Identification of Renewable Aromatics and a Lignin-Derived Solvent. *J Am Chem Soc* 2016, **138**:8900–8911.

44. Questell-Santiago YM, Galkin MV, Barta K, Luterbacher JS: **Stabilization strategies in biomass depolymerization using chemical functionalization**. *Nat Rev Chem* 2020, **4**:311–330.
45. Rößiger B, Unkelbach G, Pufky-Heinrich D: **Base-Catalyzed Depolymerization of Lignin: History, Challenges and Perspectives**. In *Lignin - Trends and Applications*. Edited by Poletto M. IntechOpen; 2018:99–120.
46. Tarabanko VE, Tarabanko N: **Catalytic Oxidation of Lignins into the Aromatic Aldehydes: General Process Trends and Development Prospects**. *Int J Mol Sci* 2017, **18**:2421.
47. Vangeel T, Schutyser W, Renders T, Sels BF: **Perspective on Lignin Oxidation: Advances, Challenges, and Future Directions**. *Top Curr Chem* 2018, **376**:30.
48. Ren T, Qi W, Su R, He Z: **Promising Techniques for Depolymerization of Lignin into Value-added Chemicals**. *ChemCatChem* 2019, **11**:639–654.
49. Agarwal A, Rana M, Park J-H: **Advancement in technologies for the depolymerization of lignin**. *Fuel Process Technol* 2018, **181**:115–132.
50. Pandey MP, Kim CS: **Lignin Depolymerization and Conversion: A Review of Thermochemical Methods**. *Chem Eng Technol* 2011, **34**:29–41.
51. Chio C, Sain M, Qin W: **Lignin utilization: A review of lignin depolymerization from various aspects**. *Renew Sustain Energy Rev* 2019, **107**:232–249.
52. Garedew M, Lin F, Song B, DeWinter TM, Jackson JE, Saffron CM, Lam CH, Anastas PT: **Greener Routes to Biomass Waste Valorization: Lignin Transformation Through Electrocatalysis for Renewable Chemicals and Fuels Production**. *ChemSusChem* 2020, **13**:4214–4237.
53. Brunauer S, Emmett PH, Teller E: **Adsorption of Gases in Multimolecular Layers**. *J Am Chem Soc* 1938, **60**:309–319.
54. Barrett EP, Joyner LG, Halenda PP: **The Determination of Pore Volume and Area Distributions in Porous Substances. I. Computations from Nitrogen Isotherms**. *J Am Chem Soc* 1951, **73**:373–380.
55. Ringena O, Lebioda S, Lehnen R, Saake B: **Size-exclusion chromatography of technical lignins in dimethyl sulfoxide/water and dimethylacetamide**. *J Chromatogr A* 2006, **1102**:154–163.
56. Salanti A, Orlandi M, Zoia L: **Fluorescence Labeling of Technical Lignin for the Study of Phenolic Group Distribution as a Function of the Molecular Weight**. *ACS Sustain Chem Eng* 2020, **8**:8279–8287.
57. Kim J-Y, Oh S, Hwang H, Kim U-J, Choi JW: **Structural features and thermal degradation properties of various lignin macromolecules obtained from poplar wood (Populus albaglandulosa)**. *Polym Degrad Stab* 2013, **98**:1671–1678.
58. Abdelaziz OY, Hulteberg CP: **Lignin Depolymerization under Continuous-Flow Conditions: Highlights of Recent Developments**. *ChemSusChem* 2020, **13**:4382–4384.

59. Nguyen Lyckeskog H, Mattsson C, Åmand L-E, Olausson L, Andersson S-I, Vamling L, Theliander H: **Storage Stability of Bio-oils Derived from the Catalytic Conversion of Softwood Kraft Lignin in Subcritical Water**. *Energy & Fuels* 2016, **30**:3097–3106.

60. Matsushita Y, Jo E-K, Inakoshi R, Yagami S, Takamoto N, Fukushima K, Lee S-C: **Hydrothermal reaction of sulfuric acid lignin generated as a by-product during bioethanol production using lignocellulosic materials to convert bioactive agents**. *Ind Crops Prod* 2013, **42**:181–188.

61. Toor SS, Rosendahl L, Rudolf A: **Hydrothermal liquefaction of biomass: A review of subcritical water technologies**. *Energy* 2011, **36**:2328–2342.

62. Mattsson C, Andersson S-I, Belkheiri T, Åmand L-E, Olausson L, Vamling L, Theliander H: **Using 2D NMR to characterize the structure of the low and high molecular weight fractions of bio-oil obtained from LignoBoost™ kraft lignin depolymerized in subcritical water**. *Biomass and Bioenergy* 2016, **95**:364–377.

63. Santos RB, Hart PW, Jameel H, Chang H: **Wood Based Lignin Reactions Important to the Biorefinery and Pulp and Paper Industries**. *BioResources* 2013, **8**:1456–1477.

64. Roberts VM, Stein V, Reiner T, Lemonidou A, Li X, Lercher JA: **Towards Quantitative Catalytic Lignin Depolymerization**. *Chem - A Eur J* 2011, **17**:5939–5948.

65. Beauchet R, Monteil-Rivera F, Lavoie JM: **Conversion of lignin to aromatic-based chemicals (L-chems) and biofuels (L-fuels)**. *Bioresour Technol* 2012, **121**:328–334.

66. Otromke M, Shuttleworth PS, Sauer J, White RJ: **Hydrothermal base catalysed treatment of Kraft Lignin for the preparation of a sustainable carbon fibre precursor**. *Bioresour Technol Reports* 2019, **5**:251–260.

67. Rößiger B, Röver R, Unkelbach G, Pufky-Heinrich D: **Production of Bio-Phenols for Industrial Application: Scale-Up of the Base-Catalyzed Depolymerization of Lignin**. *Green Sustain Chem* 2017, **7**:193–202.

68. Nguyen TDH, Maschietti M, Belkheiri T, Åmand L-E, Theliander H, Vamling L, Olausson L, Andersson S-I: **Catalytic depolymerisation and conversion of Kraft lignin into liquid products using near-critical water**. *J Supercrit Fluids* 2014, **86**:67–75.

69. Crestini C, Lange H, Sette M, Argyropoulos DS: **On the structure of softwood kraft lignin**. *Green Chem* 2017, **19**:4104–4121.

70. Lancefield CS, Wienk HLJ, Boelens R, Weckhuysen BM, Bruijnincx PCA: **Identification of a diagnostic structural motif reveals a new reaction intermediate and condensation pathway in kraft lignin formation**. *Chem Sci* 2018, **9**:6348–6360.

71. Polizzi V, Servaes K, Vandezande P, Kouris PD, Panaite AM, Jacobs G, Hensen EJM, Boot MD, Vanbroekhoven K: **Molecular weight-based fractionation of lignin oils by membrane separation technology**. *Holzforschung* 2020, **74**:166–174.

72. Ravi K, Abdelaziz OY, Nöbel M, García-Hidalgo J, Gorwa-Grauslund MF,

Hulteberg CP, Lidén G: **Bacterial conversion of depolymerized Kraft lignin**. *Biotechnol Biofuels* 2019, **12:56**.

73. Ravi K, García-Hidalgo J, Gorwa-Grauslund MF, Lidén G: **Conversion of lignin model compounds by Pseudomonas putida KT2440 and isolates from compost**. *Appl Microbiol Biotechnol* 2017, **101**:5059–5070.

74. Kent MS, Zeng J, Rader N, Avina IC, Simoes CT, Brenden CK, Busse ML, Watt J, Giron NH, Alam TM, et al.: **Efficient conversion of lignin into a water-soluble polymer by a chelator-mediated Fenton reaction: optimization of H2O2 use and performance as a dispersant**. *Green Chem* 2018, **20**:3024–3037.

75. Sieber M, Mehner T, Dietrich D, Alisch G, Nickel D, Meyer D, Scharf I, Lampke T: **Wear-resistant coatings on aluminium produced by plasma anodising-A correlation of wear properties, microstructure, phase composition and distribution**. *Surf Coatings Technol* 2014, **240**:96–102.

76. Das A, Rahimi A, Ulbrich A, Alherech M, Motagamwala AH, Bhalla A, da Costa Sousa L, Balan V, Dumesic JA, Hegg EL, et al.: **Lignin Conversion to Low-Molecular-Weight Aromatics via an Aerobic Oxidation-Hydrolysis Sequence: Comparison of Different Lignin Sources**. *ACS Sustain Chem Eng* 2018, **6**:3367–3374.

77. Pacek AW, Ding P, Garrett M, Sheldrake G, Nienow AW: **Catalytic Conversion of Sodium Lignosulfonate to Vanillin: Engineering Aspects. Part 1. Effects of Processing Conditions on Vanillin Yield and Selectivity**. *Ind Eng Chem Res* 2013, **52**:8361–8372.

78. Yao SG, Mobley JK, Ralph J, Crocker M, Parkin S, Selegue JP, Meier MS: **Mechanochemical Treatment Facilitates Two-Step Oxidative Depolymerization of Kraft Lignin**. *ACS Sustain Chem Eng* 2018, **6**:5990–5998.

79. Bjelić S, Garbuio L, Arturi KR, van Bokhoven JA, Jeschke G, Vogel F: **Oxidative Biphasic Depolymerization (BPD) of Kraft Lignin at Low pH**. *ChemistrySelect* 2018, **3**:11680–11686.

80. Wei Z, Zeng G, Huang F, Kosa M, Huang D, Ragauskas AJ: **Bioconversion of oxygen-pretreated Kraft lignin to microbial lipid with oleaginous Rhodococcus opacus DSM 1069**. *Green Chem* 2015, **17**:2784–2789.

81. Masai E, Katayama Y, Fukuda M: **Genetic and Biochemical Investigations on Bacterial Catabolic Pathways for Lignin-Derived Aromatic Compounds**. *Biosci Biotechnol Biochem* 2007, **71**:1–15.

82. Holder JW, Ulrich JC, DeBono AC, Godfrey PA, Desjardins CA, Zucker J, Zeng Q, Leach ALB, Ghiviriga I, Dancel C, et al.: **Comparative and Functional Genomics of Rhodococcus opacus PD630 for Biofuels Development**. *PLoS Genet* 2011, **7**:e1002219.

83. Linger JG, Vardon DR, Guarnieri MT, Karp EM, Hunsinger GB, Franden MA, Johnson CW, Chupka G, Strathmann TJ, Pienkos PT, et al.: **Lignin valorization through integrated biological funneling and chemical catalysis**. *Proc Natl Acad Sci* 2014, **111**:12013–12018.

84. Salvachúa D, Karp EM, Nimlos CT, Vardon DR, Beckham GT: **Towards lignin consolidated bioprocessing: Simultaneous lignin depolymerization and product**

generation by bacteria. *Green Chem* 2015, **17**:4951–4967.

85. Liu Z-H, Le RK, Kosa M, Yang B, Yuan J, Ragauskas AJ: **Identifying and creating pathways to improve biological lignin valorization**. *Renew Sustain Energy Rev* 2019, **105**:349–362.
86. Gadalla M, Olujić Ž, Jobson M, Smith R: **Estimation and reduction of CO2 emissions from crude oil distillation units**. *Energy* 2006, **31**:2398–2408.
87. Abdelaziz OY, Hosny WM, Gadalla MA, Ashour FH, Ashour IA, Hulteberg CP: **Novel process technologies for conversion of carbon dioxide from industrial flue gas streams into methanol**. *J CO2 Util* 2017, **21**:52–63.
88. Sheldon RA: **The E factor 25 years on: the rise of green chemistry and sustainability**. *Green Chem* 2017, **19**:18–43.
89. Sheldon RA, Sanders JPM: **Toward concise metrics for the production of chemicals from renewable biomass**. *Catal Today* 2015, **239**:3–6.
90. El-Halwagi MM: **Benchmarking Process Performance Through Overall Mass Targeting**. In *Sustainable Design Through Process Integration: Fundamentals and Applications to Industrial Pollution Prevention, Resource Conservation, and Profitability Enhancement*. Elsevier Inc.; 2017:73–125.
91. Turton R, Bailie RC, Whiting WB, Shaeiwitz JA: *Analysis, Synthesis, and Design of Chemical Processes*. Pearson Education; 2008.
92. Pinazo JM, Domine ME, Parvulescu V, Petru F: **Sustainability metrics for succinic acid production: A comparison between biomass-based and petrochemical routes**. *Catal Today* 2015, **239**:17–24.
93. Näyhä A, Pesonen H-L: **Diffusion of forest biorefineries in Scandinavia and North America**. *Technol Forecast Soc Change* 2012, **79**:1111–1120.
94. Rinesch T, Mottweiler J, Puche M, Concepción P, Corma A, Bolm C: **Mechanistic Investigation of the Catalyzed Cleavage for the Lignin β-O-4 Linkage: Implications for Vanillin and Vanillic Acid Formation**. *ACS Sustain Chem Eng* 2017, **5**:9818–9825.
95. Mottweiler J, Puche M, Räuber C, Schmidt T, Concepción P, Corma A, Bolm C: **Copper- and Vanadium-Catalyzed Oxidative Cleavage of Lignin using Dioxygen**. *ChemSusChem* 2015, **8**:2106–2113.
96. Sedai B, Tom Baker R: **Copper Catalysts for Selective C-C Bond Cleavage of β-O-4 Lignin Model Compounds**. *Adv Synth Catal* 2014, **356**:3563–3574.
97. Ma Y, Du Z, Liu J, Xia F, Xu J: **Selective oxidative C-C bond cleavage of a lignin model compound in the presence of acetic acid with a vanadium catalyst**. *Green Chem* 2015, **17**:4968–4973.
98. Hanson SK, Wu R, Silks LAP: **C-C or C-O Bond Cleavage in a Phenolic Lignin Model Compound: Selectivity Depends on Vanadium Catalyst**. *Angew Chemie - Int Ed* 2012, **51**:3410–3413.
99. Mathieu Y, Vidal JD, Arribas Martínez L, Abad Fernández N, Iborra S, Corma A: **Molecular Oxygen Lignin Depolymerization: An Insight into the Stability of Phenolic Monomers**. *ChemSusChem* 2020, **13**:4743–4758.

Paper I

Waste Biomass Valor (2017) 8:859–869
DOI 10.1007/s12649-016-9643-9

ORIGINAL PAPER

Physicochemical Characterisation of Technical Lignins for Their Potential Valorisation

Omar Y. Abdelaziz[1] · Christian P. Hulteberg[1]

Received: 24 March 2016 / Accepted: 25 July 2016 / Published online: 1 August 2016
© The Author(s) 2016. This article is published with open access at Springerlink.com

Abstract Lignin, the second most abundant natural polymer, has emerged as a potential alternative material to petroleum-based chemicals and renewable resource for the production of diverse forms of aromatics, biofuels, and bio-based materials. Thus, it is becoming important to understand its structure and properties to provide key features and insights for better/efficient lignin valorisation. In this work, the physicochemical characterisation of two types of industrial (technical) lignins, namely LignoBoost lignin and alkali-treated lignin was performed. Characterisation has been conducted using Brunauer–Emmett–Teller N_2 adsorption, particle size distribution, Fourier transform infrared spectroscopy, ultraviolet–visible absorption spectroscopy, gel permeation chromatography, and thermogravimetric analysis. It was found that the pretreatment severity considerably influenced the lignin composition and functional properties. The measured physicochemical properties helped in proposing potential valorisation routes for these lignins in the context of a biorefinery, focusing on their depolymerisation and subsequent biological conversion to value-added chemicals and fuels.

Keywords Lignin · Structural characterisation · Physicochemical properties · LignoBoost · Soda pulping · Biomass valorisation

✉ Christian P. Hulteberg
Christian.Hulteberg@chemeng.lth.se

[1] Department of Chemical Engineering, Lund University, P.O. Box 124, 221 00 Lund, Sweden

Introduction

Lignin is a complex biopolymer of phenylpropanoid subunits that accounts for approximately 15–35 % of the terrestrial lignocellulosic biomass, representing the most abundant renewable phenolic polymer on Earth and providing structural integrity to lignocellulosic material. It is expected that in the near future, the advent of new biorefineries, which convert cellulosic biomass into transportation biofuels, will introduce an excess supply of various lignins into the process streams, besides the substantial amounts of lignin produced annually from pulping [1]. This turns lignin into a potentially highly available and accessible renewable feedstock for the synthesis of bulk aromatic and phenolic compounds [2]. Also, in comparison with cellulose and hemicellulose, lignin carries the highest specific energy content within the organic matrix of woody materials [3]. Thus, it can be regarded as an attractive constituent of woody biomass for the production of advanced biofuels and value-added chemicals that can consequently help in meeting the future energy demands [4].

Lignin structure (Fig. 1a), content, and reactivity vary from one substrate to another, as they differ according to the origin and separation/pretreatment methods, generating a wide diversity of lignin aromatic biopolymers. The main building blocks of lignin are guaiacyl (G), syringyl (S), and *p*-hydroxyphenyl (H) that are produced throughout the dehydrogenative enzyme-initiated free-radical polymerisation of the monolignols (Fig. 1b) or so-called the major precursors [5]. Softwood lignins are predominantly formed from coniferyl alcohol and consist of G units. On the other hand, hardwood lignins constitute both coniferyl and sinapyl alcohol as monomer precursors and contain G, S, and H units in different ratios. Coniferyl, sinapyl, and

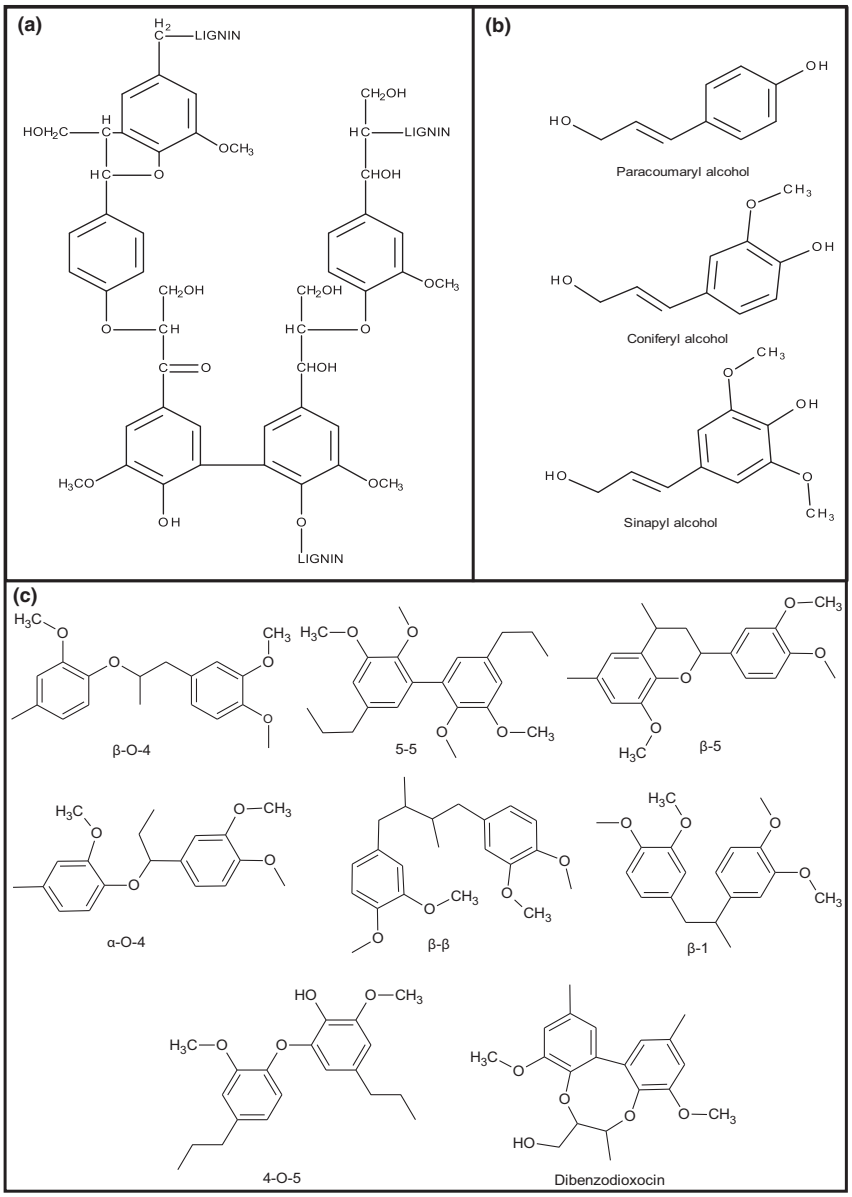


Fig. 1 Lignin, representative fragment (**a**), three major precursors (**b**), and common interunit linkages found in its structure (**c**)

coumaryl alcohol form the herbaceous (grass) lignins, where they also contain G, S, and H [6]. These structures are heterogeneously connected by interunit linkages that provide the biomass with inherent recalcitrance. The linkages (Fig. 1c) include 5-5, β-5, α-*O*-4, β-β, β-1, 4-*O*-5, dibenzodioxocin, and β-*O*-4 aryl glycerol ether which is considered dominant by constituting more than half of the lignin linkage structures [7].

The pulp and paper industry is now considered the largest prevailing lignocellulosic-based process that produces significant amount of lignin. Primarily, chemical pulping processes are used for producing paper and celluloses derivatives [8]. Kraft pulping is the main process that most of the paper pulp produced over the world is generated from [9]. Basically, wood is converted into wood pulp through treating with Na_2S/NaOH solution (white liquor) for several hours at a temperature range of 155–175 °C, where about 90–95 % of the lignin present in the starting material is easily dissolved. Lately, a novel process has been developed to efficiently separate lignin from kraft black liquor called LignoBoost. This process differs from the ordinary single-stage lignin separation process in that instead of washing the lignin filter cake directly after filtration, it is rather dispersed in a re-slurry tank, offering a better control of the pH and hence minimising the hydrogen ion concentration gradients during the washing stage [10]. Major advantages of the LignoBoost process comprise high lignin yield, low ash and carbohydrates contents, low investment costs, and low operational costs [11]. It is expected that this type of lignin would result in more value-added applications in future industrial installations and hasty capacity increase.

Another pulping process available, also producing high quantities of lignin, is the lignosulfonate/sulphite process. This process typically uses different sulphurous acid salts like sulphites and bisulphites, in which the lignin recovered contain about 4–8 % sulphur and are termed lignosulfonates, due to the sulfonate groups' presence in its structure [12]. Soda pulping is another existing pulping process, where biomass treatment made using an aqueous solution of NaOH or lime at temperatures of almost $\leq$160 °C. The lignin recovered is named alkali lignin and it is considered to be a good source of phenolics and aromatics [13]. Organic solvents have else been adopted in wood delignification, referred to as Organosolv pulping. Although this process offers benefits like producing high-quality lignin and lowering the enzyme cost, it still lack economic justifications [14]. A new biphasic Organosolv-like process also accounting for biomass pretreatment and lignin recovery called Organocat has been improved and proposed recently [15]. In principle, it uses an aqueous solution of 2-methyltetrahydrofuran (2-MTHF) as an organic solvent and oxalic acid as a catalyst, where effective separation of the primary constituents of the compact lignocellulosic material is attained in a single step [16]. To this end, the pretreatment of lignocellulosic biomass and the detailed understanding of their composition and structure are much-needed steps in order to devise efficient biomass and lignin valorisation strategies [17].

In the present work, two types of lignin obtained from different pulping processes, namely LignoBoost lignin and alkali-treated lignin were characterised for further use in their valorisation towards producing high-value chemicals. Characterisation was performed using Brunauer–Emmett–Teller (BET) to investigate the textural properties, particle size distribution (PSD) to tackle and report information about the size and range of lignin agglomerates, Fourier transform infrared spectroscopy (FT-IR) and ultraviolet–visible absorption spectroscopy (UV–Vis) to analyse the chemical structure, gel permeation chromatography (GPC) for determining the molecular weight distribution, and thermogravimetric analysis (TGA) to test the thermal degradation and stability. Applications were also proposed for better valorisation strategies with a special emphasis on the biological conversion of lignin.

Materials and Methods

Lignins

Two types of commercial technical lignin, namely LignoBoost lignin and alkali-treated lignin were investigated in this study. The LignoBoost lignin was obtained from Innventia's pilot plant at Bäckhammar, Sweden, while the alkali-treated lignin with low sulfonate content (4 % of sulphur) was purchased from Sigma-Aldrich. The LignoBoost lignin is fine powder and it is composed of several heterogeneous agglomerated molecules. The powder is light brown in appearance and is completely soluble in alkaline solutions. The sulphur present in the lignin is a mixture of inorganic, elemental, and organic bonds, where in approximate terms, 30 % of the sulphur is inorganic, 1 % is elemental, and the rest is organic. The sulphur content in the LignoBoost kraft lignin is normally of lower value between 1 and 3 %, with 1.8 % as a typical value of the sample studied. Besides, the lignin powder from the LignoBoost process exhibits about 30 % moisture content. The commercial alkali-treated lignin, on the other hand, is a black powder in appearance, more alkaline, pH 10.5, and contains no reducing sugars.

Textural Properties

The specific surface area and the pore size of both lignins were determined by the BET adsorption–desorption

method using a Micromeritics ASAP 2400 instrument (Norcross, GA, USA). Pore volume analysis was performed using the Barrett–Joyner–Halenda (BJH) method [18]. Before the analysis, the lignin samples were dried over 7 days and at a degassing temperature of 115 °C, under rough vacuum. Then, the measurements were conducted through the adsorption of nitrogen, at liquid nitrogen temperature, onto the biopolymer surface at different pressures. The desorption-isotherm was employed for the analysis and the values obtained are the average of two analysis runs.

Particle Size Analysis

The size distribution of the lignin particles was measured by laser diffraction with a Sympatec HELOS laser diffractometer equipped with the RODOS dispersing unit (Sympatec GmbH, Clausthal-Zellerfeld, Germany) in dry powder form after dispersing with compressed air (3 bar). The system uses a 632.8 nm HeNe laser for illuminating the particles and is capable of detecting particles in the dynamic size range of 0.5–875 μm. The lignins PSD were also characterized by the D_{10}, D_{50}, and D_{90} values, giving estimates for the percentage undersize, as well as the volume mean diameter (VMD), the sample volume weighted mean particle size; values were calculated based on the Fraunhofer theory and analysed in the standardised WINDOX software.

Spectroscopic Measurements

Fourier transform infrared (FT-IR) spectra of the lignins were obtained on a Bruker Alpha-P Platinum FT-IR spectrometer, equipped with a platinum attenuated total reflectance (ATR) sampling module hosting a diamond crystal (single bounce). For each sample, 24 scans were recorded in the wavenumber range of 4000–400 cm^{-1} in the transmittance mode with a resolution of 4 cm^{-1}.

The ultraviolet–visible (UV–Vis) absorption spectra of the lignin samples were recorded on a spectrophotometer (UV-160, Shimadzu Co., Kyoto, Japan). Following an established procedure [19], the samples were dissolved in a 0.1 M NaOH solution, diluted with deionised water, and the absorbance between 240 and 420 nm was measured.

Molecular Weight Distribution

The molecular weight distribution data of the lignin samples was determined by a GPC system. The system used was a Waters 600E chromatography system (Waters, Milford, MA, USA) equipped with a Waters 2414 refractive index (RI) detector, a Waters 486 UV absorbance detector and an analytical column packed with 30 cm of Superdex 30 and 30 cm of Superdex 200 (GE Healthcare, Uppsala, Sweden). The column was operated at ambient temperature and eluted with NaOH (analytical grade) as the mobile phase at a flowrate of 1.0 mL/min. Calibration was performed using polyethylene glycol (PEG) standards ranging from 400 to 35,000 g/mol in the eluent (Merck Schuchardt OHG, Hohenbrunn, Germany). The two lignins were dissolved at a concentration of 1 mg/mL in the eluent. The solution was further filtered using a 0.2 μm filter in order to remove any suspended matter, and 500 μL from the filtered solution was finally injected into the GPC system. Due to the comparison with PEG standard, both the molecular weight and the molecular number should be considered relative.

Thermogravimetric Analysis

The thermal stability studies for the lignins were performed by TGA using a TGA Q500 (TA Instruments) thermogravimetric analyser. Lignin samples of about 5 mg were used in both cases and placed in open alumina crucibles. Measurements were conducted in an inert atmosphere; the instrument was continuously flushed with a nitrogen flow of 60 mL/min. The thermal program consisted of an isothermal step at 150 °C for 10 min, accompanied by a 10 °C/min ramp from 25 to 600 °C. The objective of the isothermal step was to eliminate moisture (hygroscopic water), as it could interfere with the degradation steps at low temperatures and initiate an oxygen-promoted lignin decomposition.

Results and Discussion

Specific Surface Area and Pore Structure

The surface area and pore size of the lignins were calculated by applying the BET analysis. Technically speaking, the lignin surface properties are affected by the biomass substrate source and the pretreatment process conditions. Table 1 summarises the results generated from the nitrogen adsorption–desorption experiments.

The adsorption and desorption information acquired from each run was used to determine the lignins specific surface area (m^2/g), pore volume (cm^3/g), and pore size (Å), employing the BET and BJH models. The specific surface area data are presented as BET surface area (S_{BET}), Langmuir surface area (S_{LSA}), BJH surface area (S_{BJH}), and micropore area (S_{micro}). In addition, the single point surface areas of LignoBoost and alkali-treated lignins at P/P_o of 0.21 were calculated as 0.38 and 1.20 m^2/g, respectively.

Table 1 Surface area and pore structure parameters of lignins determined by BET analysis

Sample	Surface area (m^2/g)				Pore volume ($cm^3/g \times 10^3$)			Pore size (Å)	
	S_{BET}	S_{LSA}	S^a_{BJH}	S_{micro}	V^b_{total}	V^a_{BJH}	V^c_{micro}	D^d_{BET}	D^a_{BJH}
LignoBoost lignin	0.40	0.54	0.31	0.26	1.96	1.87	0.11	199	240
Alkali lignin	1.25	1.73	0.43	1.07	3.87	3.87	0.48	124	360

[a] Calculated using the cumulative desorption data between 17 and 3000 Å diameter by the Barrett–Joyner–Halenda (BJH) method

[b] Single point total pore volume of pores less than 3400 Å in diameter at $P/P_o = 0.99$

[c] Micropore volume calculated by the Horvath–Kawazoe (HK) method

[d] Average total pore diameter (4 V/A by BET)

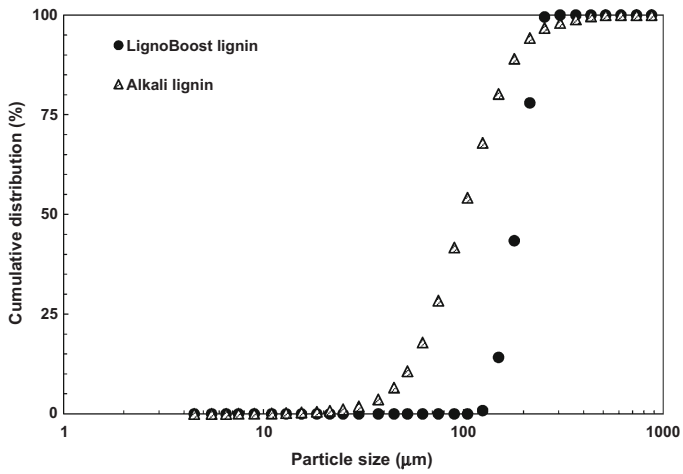


Fig. 2 Distribution of particle sizes for LignoBoost and alkali lignin samples

The purpose of comparing textural parameters from different pretreatment processes by this method is known to be useful [20]. Significant variations were observed with regard to the textural properties of both lignins (Table 1). Alkali-treated lignin exhibited to a higher specific surface area and pore volume than the LignoBoost lignin, suggesting an increase in the pretreatment severity of the applied process conditions for the alkali lignin. In the meanwhile, the alkali lignin BET results interestingly were comparable to another study [21]. However, to the best of the authors' knowledge, the BET parameters for LignoBoost lignin has not been previously reported.

Those results obtained suggest that alkali lignin provide a better candidate towards its biological valorisation. Within this scope, the fact that it has higher surface area and pore size would allow easier access of enzymes and microorganisms if applied to the lignin substrate. Hence, it could be biologically converted towards a wide platform of value-added chemicals via enzymatic depolymerisation and subsequent biological funnelling.

Distribution of Particle Sizes

PSD could provide information about the aggregation characteristics of lignin biomacromolecules. Figure 2 shows the cumulative PSD profiles for the two lignin samples, while the particle size characterisation data are outlined in Table 2.

The alkali lignin particles were considerably smaller than the LignoBoost lignin particles, as can be viewed in Fig. 2. It could be recognised that the pretreatment process does not result in similar size distributions of lignin macromolecules. Analysis also showed that the two lignin samples possessed a geometric PSD within the micron size range (Table 2), with VMD values of 188 μm for LignoBoost lignin and 113 μm for alkali lignin. It was revealed as well that the LignoBoost lignin exhibited a relatively narrower density distribution than the alkali lignin; this can be resulting from a higher degree of molecules cross-linking and aggregation. In addition, the pretreatment temperature seemed to influence the lignin

Table 2 Particle size distribution data for the lignins used. D_x indicates that x % in volume of the particles are smaller than the value stated

Sample	D_{10} (μm)	D_{50} (μm)	D_{85} (μm)	D_{90} (μm)	D_{99} (μm)	VMD (μm)
LignoBoost lignin	142.2	186.7	226.2	237.3	254.0	188.0
Alkali-treated lignin	51.2	100.0	162.8	186.3	373.3	113.0

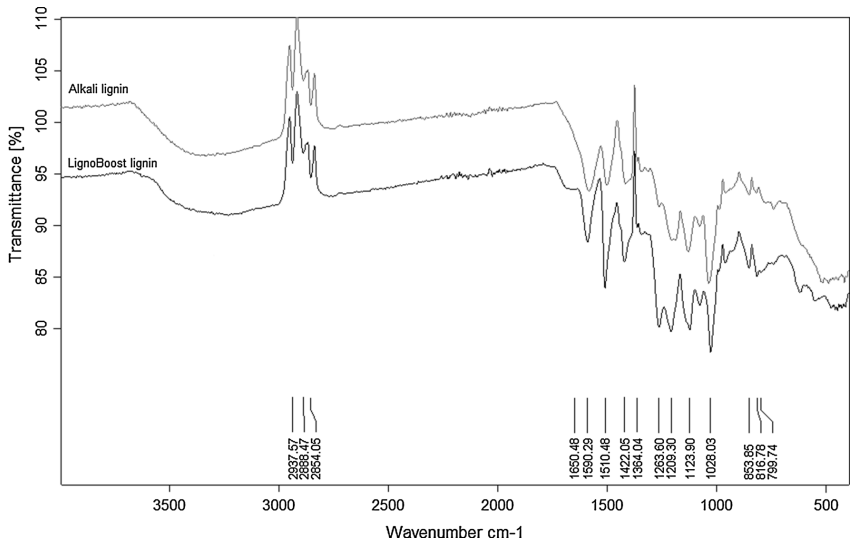


Fig. 3 FT-IR spectra of lignin samples with the wavenumber range 4000–400 cm^{-1}

particle size, as increasing temperature might lead to decreasing particle size. Those findings support the BET results, confirming that the alkali lignin would be a better substrate for biological valorisation. The fact of constituting smaller particle sizes would make it easier to depolymerise into smaller fragments. These low molecular weight fragments would serve as better carbon sources to be further hosted by various microbial cell factories, generating further numerous forms of value-added renewable chemicals.

FT-IR and UV Spectra

Variability in lignin composition and structural changes could possibly be identified using spectrophotometric methods. This is due to the specific absorbance of the individual phenolic constituents. Figure 3 presents the FT-IR spectra for both lignin samples.

As can be seen from the spectra, both lignins showed comparable behaviour, revealing the similarities of the functional groups found in them. Moreover, the corresponding bands and assignments for the two lignins are reported in Table 3. Here, we introduce an analysis of the spectra recorded for both lignins used in this study, based on the bands assignments previously reported in literature findings [22, 23].

Both lignins showed bands at 1600, 1515, and 1425 cm^{-1} that are corresponding to aromatic ring vibrations of the phenylpropane (C_9) skeleton, exhibiting the typical lignin absorption bands. In the wide absorption range between 3600 and 3000 cm^{-1}, similar bands appeared for the two lignins, which can be attributed to the hydroxyl groups in aromatic and aliphatic structures. The absorption band peaks at 2938 cm^{-1} for both lignins mainly corresponds to the C–H stretching in the methyl and methylene groups of the side chains, while the bands at 2854 cm^{-1} can be arising from the C–H stretching in the aromatic methoxyl groups. No bands were found for both lignins within the range between 1715 and 1705 cm^{-1} that originates from the unconjugated carbonyl–carboxyl stretching. The absence of such bands was found in agreement with previous work [24]. However, a strong band shoulder appeared at 1650 cm^{-1} for the LignoBoost lignin corresponding to the conjugated carbonyl–carboxyl

Table 3 FT-IR bands and assignments for LignoBoost and alkali lignins

Band (cm^{-1})	Vibration	Assignment	Band location (cm^{-1})	
			LignoBoost	Alkali
2960–2925	C–H stretching	$CH_3 + CH_2$	2938	2938
2850–2840	C–H stretching	OCH_3	2854	2854
1650	C=O stretching	Conjugated C=O	1650	–
1600	C–C stretching	Aromatic skeleton	1590	1585
1515	C–C stretching	Aromatic skeleton	1510	1501
1425	C–C stretching	Aromatic skeleton	1422	1417
1365	O–H in-plane deformation	Phenolic OH	1364	1364
1270	C–O stretching	G	1264	–
1220	C–O(H) + C–O(Ar) stretching	Phenolic OH + ether	1209	1189
1125	Ar–CH in-plane deformation	G	1124	1131
1030	C–O(H) + C–O(C) stretching	First order aliphatic OH + ether	1028	1037
855	Ar–CH out-of-plane deformation	G	854	854
810	Ar–CH out-of-plane deformation	G	817	819

stretching. This was not the case in that of the alkali-treated lignin, which can be due to the presence of more associated water or protein impurity. Considerable amounts of residual minerals is also expected to be present and they remain in the lignin fraction after pretreatment process. The analysis difficulty starts to increase below the 1400 cm^{-1} region because of the complex bands contributing from various modes of vibration. In spite of that, this spectral region constitutes specific vibrations to the monolignol precursors, allowing better lignin structural characterisation. The weak bands appearing at 1364 cm^{-1} for both samples can be originated from non-etherified phenolic OH groups, which is liberated from the cleavage of β-*O*-4 and α-*O*-4 linkages during the cooking process; this supports extensive phenol ether cleavage during pulping. The characteristic syringyl (S) bands for both lignins were not found, due to vanishing of the bands at 1326, 1115, and 825 cm^{-1}. Conversely, both samples revealed the characteristic vibrations of the guaiacyl (G) unit at around 1125, 855, and 810 cm^{-1}, but with different intensities, confirming that both lignins incorporated potential active sites towards polymerisation. More considerations should be taken into account regarding this point in the scope of better valorisation routes. For instance, incorporating mediators during enzymatic depolymerisation/biochemical pathway or capping agents throughout the chemical pathway.

UV spectroscopy was also adopted to monitor the lignins distribution variability and purity. Figure 4 shows the UV absorption spectra of both the LignoBoost and alkali-treated lignin samples.

No significant difference was noted within the acquired UV spectra for both lignin samples. It was found that both lignins exhibited an absorption maxima at around λ 280 nm, which is quite common for technical lignins, originating from the aromatic rings/non-conjugated phenolic groups present in the lignins structure and executed priory within the FT-IR spectra. However, LignoBoost lignin revealed a slightly higher absorbance strength than alkali lignin due to conducting the measurements in an alkaline medium [23]. It is also worth mentioning that absorption strength of both lignins were considered to be high for the visible solar wavelength range, which can be regarded to their deep/dark colours.

Molecular Weight

The molecular weight of lignin is a fundamental property that affects the biomass recalcitrance and lignin valorisation, where the most common characterisation technique employed in its measurement is the GPC [25]. Besides, the GPC technique has proven earlier to be reliable in determining the molecular weight distribution of kraft lignin and alkali lignin [26]. The GPC analysis using PEG standards and NaOH as eluent was performed to follow the molecular weight distribution of LignoBoost lignin and alkali-treated lignin samples. Figure 5 shows the gel permeation chromatograms for the lignin samples with a characteristic UV absorption measured at 280 nm.

Apparently, both lignin samples manifested different normalised GPC elution profiles. Alkali lignin exhibited higher molecular weight distribution values than the LignoBoost lignin. This can be attributed to the promotion of repolymerisation reactions during soda pulping process affecting the lignin molecular weight [22]. To give an instance, under the alkaline conditions, alkali-

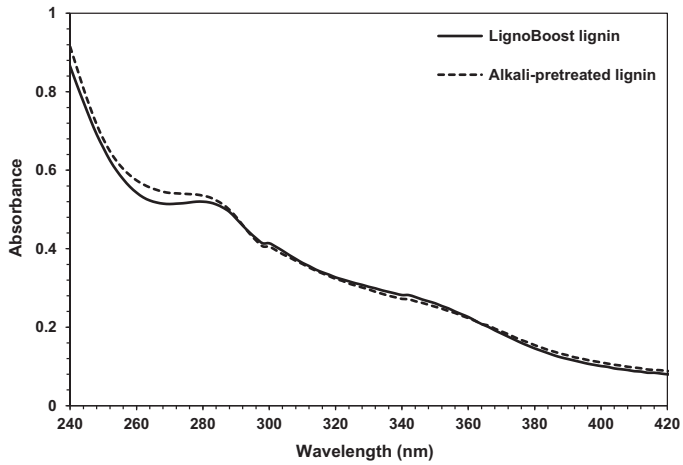


Fig. 4 UV–Vis absorption spectra of lignin samples under UV light

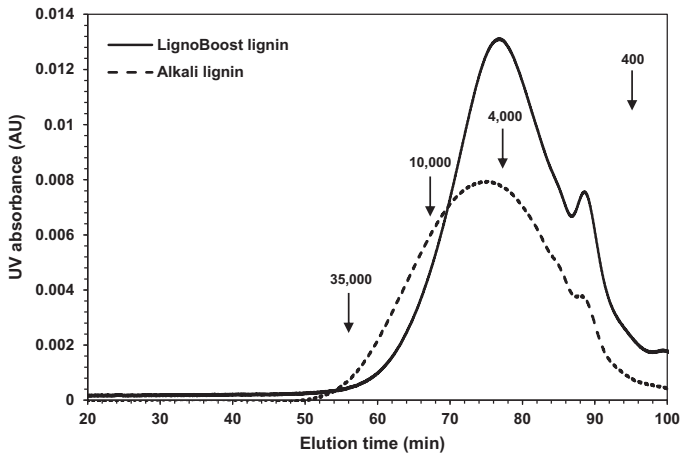


Fig. 5 Gel permeation chromatogram for LignoBoost and alkali lignin samples with characteristic UV absorption at 280 nm. The arrows indicate the molecular weight (Da) of the PEG standards that were used for calibration

stable methylene linkages are produced through the reaction of quinone methide intermediates (formed from α-hydroxyl groups) with other lignin fragments, leading to higher molecular weight distribution values.

From this perspective, it can be deduced that the LignoBoost lignin could be more readily depolymerised, whatever the pathway, than the alkali lignin owing to its lower molecular weight values. Although the BET analysis showed that the alkali lignin provided a better candidate for the biological conversion, here, the contrast occurred due to easier transformations and valorisation of low molecular weight lignin rather than high molecular weight ones.

Thermal Stability

Thermogravimetric analysis was conducted in order to compare the thermal stability of the lignin samples and the acquired characteristic results are given in Table 4. Furthermore, the thermogravimetric (TG) and first derivative thermogravimetric (DTG) curves are depicted in Fig. 6a, b, respectively.

TG curves represent the weight loss of lignin samples with respect to the thermal degradation temperature. Withal, the first derivative of the aforementioned curve (DTG) indicates the weight loss corresponding rate, where

Table 4 Thermal stability characteristics of lignin samples

Sample	Temperature of 40 % weight loss (°C)	DTG_{max} (°C)	Residue (%)
LignoBoost lignin	410	327	48
Alkali-treated lignin	488	307	57

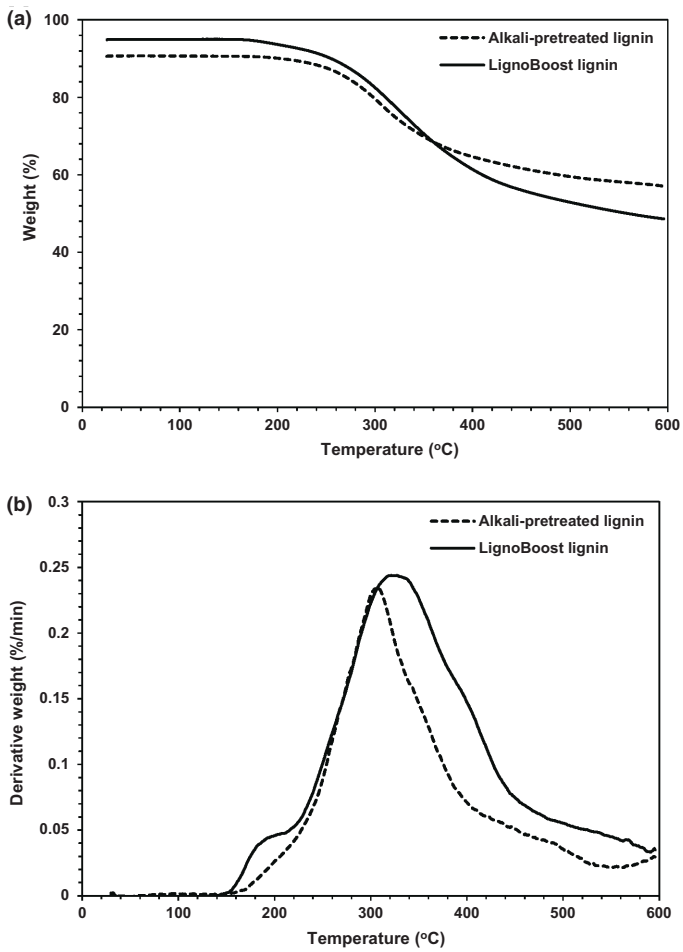


Fig. 6 TG curves (**a**) and DTG curves (**b**) for LignoBoost lignin and alkali-pretreated lignin

the peak of this curve (DTG_{max}) expresses the single decomposition temperature and can be used to demonstrate and compare the thermal stability characteristics of tested materials.

It can be noted that the thermal degradation of both lignin samples spans a wide range of temperature between 225 and 600 °C. At 40 % weight loss, the decomposition temperatures were estimated to be 410 and 488 °C for LignoBoost lignin and alkali-treated lignin, respectively. Nonetheless, the temperatures corresponding to the maximum rate of weight loss for LignoBoost lignin and alkali lignin appeared to be 327

and 307 °C, respectively. The DTG_{max} value of the alkali lignin is thus slightly lower than that of the LignoBoost lignin which may be attributed to different C–C linkages content of both lignins, though we found it in agreement with that value reported by Nadji et al. [27]. At 600 °C, the amounts of non-volatile residue were determined to be 48 and 57 % for LignoBoost and alkali lignins, respectively. These amounts of residue were incompletely burned and existed in the solid form, revealing the significant thermal stability properties of both lignins at high temperature and this could be allotted to the high degree of branching and the extremely condensed aromatic structures formation. This tendency could be accounted for, as the higher the lignin is condensed and complex, the more easily it is converted to charcoal owing to its great structural similarity [28]. Referring that both lignin samples come from two alkaline pulping processes, such alkaline conditions lead to the breakdown of protolignin, lignin fragments dissolution, and later subsequent recondensation. Also, at this point, the higher cross-linking capacity of alkali lignin at 600 °C can be observed, displaying the higher H structures content comparing to the LignoBoost sample.

For the sake of application purposes, these results show the potential of both lignins valorisation towards producing bio-oil [29] or biomaterials [30], for example, and biological conversion due to application at mild conditions. In contrast, they do not provide good candidates for phenol–formaldehyde resin synthesis, as the maximum rate loss within the nonmodified resins appears at 345 °C [22] or other adhesives [31].

Conclusions

Lignin is a key compound and the development of value-added products from it would greatly boost the economics of future biorefineries, highlighting the importance of understanding its complex nature. In this context, the physicochemical characterisation of two technical lignin samples from different pulping processes has been performed. Results have shown the notable influence of the pretreatment severity on the lignin chemical composition and functional properties. The insights gained in the technical lignins structure and properties helped in proposing better valorisation strategies. Potential applications have been finally suggested for both lignins with a particular focus on their depolymerisation and biological valorisation.

Acknowledgments This research is supported by the Swedish Foundation for Strategic Research (SSF), Grant RBP14-0052.

Open Access This article is distributed under the terms of the Creative Commons Attribution 4.0 International License (http://creativecommons.org/licenses/by/4.0/), which permits unrestricted use, distribution, and reproduction in any medium, provided you give appropriate credit to the original author(s) and the source, provide a link to the Creative Commons license, and indicate if changes were made.

References

1. Ragauskas, A.J., Beckham, G.T., Biddy, M.J., Chandra, R., Chen, F., Davis, M.F., Davison, B.H., Dixon, R.A., Gilna, P., Keller, M., Langan, P., Naskar, A.K., Saddler, J.N., Tschaplinski, T.J., Tuskan, G.A., Wyman, C.E.: Lignin valorization: improving lignin processing in the biorefinery. Science **344**, 1246843 (2014)
2. Gosselink, R.J.A., Teunissen, W., van Dam, J.E.G., de Jong, E., Gellerstedt, G., Scott, E.L., Sanders, J.P.M.: Lignin depolymerisation in supercritical carbon dioxide/acetone/water fluid for the production of aromatic chemicals. Bioresour. Technol. **106**, 173–177 (2012)
3. Azadi, P., Inderwildi, O.R., Farnood, R., King, D.A.: Liquid fuels, hydrogen and chemicals from lignin: a critical review. Renew. Sustain. Energy Rev. **21**, 506–523 (2013)
4. Tunå, P., Hulteberg, C.: Woody biomass-based transportation fuels: a comparative techno-economic study. Fuel **117**, 1020–1026 (2014)
5. Boeriu, C.G., Fiţigău, F.I., Gosselink, R.J.A., Frissen, A.E., Stoutjesdijk, J., Peter, F.: Fractionation of five technical lignins by selective extraction in green solvents and characterisation of isolated fractions. Ind. Crops Prod. **62**, 481–490 (2014)
6. Huber, G.W., Iborra, S., Corma, A.: Synthesis of transportation fuels from biomass: chemistry, catalysts, and engineering. Chem. Rev. **106**, 4044–4098 (2006)
7. Chakar, F.S., Ragauskas, A.J.: Review of current and future softwood kraft lignin process chemistry. Ind. Crops Prod. **20**, 131–141 (2004)
8. Sjöström, E.: Wood Chemistry: Fundamentals and Applications. Academic Press, San Diego (1993)
9. Moshkelani, M., Marinova, M., Perrier, M., Paris, J.: The forest biorefinery and its implementation in the pulp and paper industry: energy overview. Appl. Therm. Eng. **50**, 1427–1436 (2013)
10. Öhman, F., Theliander, H., Tomani, P., Axegard, P.: Method for separating lignin from black liquor, US patent 8486224 to Lignoboost AB (2013)
11. Tomani, P.: The LignoBoost process. Cellul. Chem. Technol. **44**, 53–58 (2010)
12. Calvo-Flores, F.G., Dobado, J.A., Isac-García, J., Martín-Martínez, F.J.: Lignin and Lignans as Renewable Raw Materials: Chemistry, Technology and Applications. Wiley, Chichester (2015)
13. Guo, D.L., Yuan, H.Y., Yin, X.L., Wu, C.Z., Wu, S.B., Zhou, Z.Q.: Effects of chemical form of sodium on the product characteristics of alkali lignin pyrolysis. Bioresour. Technol. **152**, 147–153 (2014)
14. Hergert, H.L.: Developments in organosolv pulping: an overview. In: Young, R.A., Akhtar, M. (eds.) Environmentally Friendly Technologies for the Pulp and Paper Industry. Wiley, New York (1998)
15. Abdelaziz, O.Y., Gadalla, M.A., El-Halwagi, M.M., Ashour, F.H.: A hierarchical approach for the design improvements of an Organocat biorefinery. Bioresour. Technol. **181**, 321–329 (2015)
16. vom Stein, T., Grande, P.M., Kayser, H., Sibilla, F., Leitner, W., Domínguez de María, P.: From biomass to feedstock one-step

fractionation of lignocellulose components by the selective organic acid-catalyzed depolymerization of hemicellulose in a biphasic system. Green Chem. **13**, 1772–1777 (2011)
17. Kalogiannis, K.G., Stefanidis, S., Marianou, A., Michailof, C., Kalogianni, A., Lappas, A.: Lignocellulosic biomass fractionation as a pretreatment step for production of fuels and green chemicals. Waste Biomass Valoriz. **6**, 781–790 (2015)
18. Barrett, E.P., Joyner, L.G., Halenda, P.P.: The determination of pore volume and area distributions in porous substances. I: computations from nitrogen isotherms. J. Am. Chem. Soc. **73**, 373–380 (1951)
19. Bu, L., Tang, Y., Gao, Y., Jian, H., Jiang, J.: Comparative characterization of milled wood lignin from furfural residues and corncob. Chem. Eng. J. **175**, 176–184 (2011)
20. Piccolo, C., Wiman, M., Bezzo, F., Lidén, G.: Enzyme adsorption on SO_2 catalyzed steam-pretreated wheat and spruce material. Enzyme Microb. Technol. **46**, 159–169 (2010)
21. Pareek, N., Gillgren, T., Jönsson, L.J.: Adsorption of proteins involved in hydrolysis of lignocellulose on lignins and hemicelluloses. Bioresour. Technol. **148**, 70–77 (2013)
22. Tejado, A., Peña, C., Labidi, J., Echeverria, J.M., Mondragon, I.: Physico-chemical characterization of lignins from different sources for use in phenol–formaldehyde resin synthesis. Bioresour. Technol. **98**, 1655–1663 (2007)
23. Ibrahim, M.N.M., Zakaria, N., Sipaut, C.S., Sulaiman, O., Hashim, R.: Chemical and thermal properties of lignins from oil palm biomass as a substitute for phenol in a phenol formaldehyde resin production. Carbohydr. Polym. **86**, 112–119 (2011)
24. Boeriu, C.G., Bravo, D., Gosselink, R.J.A., van Dam, J.E.G.: Characterisation of structure-dependent functional properties of lignin with infrared spectroscopy. Ind. Crops Prod. **20**, 205–218 (2004)
25. Tolbert, A., Akinosho, H., Khunsupat, R., Naskar, A.K., Ragauskas, A.J.: Characterization and analysis of the molecular weight of lignin for biorefining studies. Biofuels Bioprod. Biorefining **8**, 836–856 (2014)
26. Chen, F., Li, J.: Aqueous gel permeation chromatographic methods for technical lignins. J. Wood Chem. Technol. **20**, 265–276 (2000)
27. Nadji, H., Diouf, P.N., Benaboura, A., Bedard, Y., Riedl, B., Stevanovic, T.: Comparative study of lignins isolated from Alfa grass (*Stipa tenacissima* L.). Bioresour. Technol. **100**, 3585–3592 (2009)
28. Kim, J.-Y., Oh, S., Hwang, H., Kim, U.-J., Choi, J.W.: Structural features and thermal degradation properties of various lignin macromolecules obtained from poplar wood (*Populus albaglandulosa*). Polym. Degrad. Stab. **98**, 1671–1678 (2013)
29. Hua, W., Liu, C., Wu, S., Li, X.: Analysis of structural units and their influence on thermal degradation of alkali lignins. BioResources **11**, 1959–1970 (2016)
30. Monteil-Rivera, F., Phuong, M., Ye, M., Halasz, A., Hawari, J.: Isolation and characterization of herbaceous lignins for applications in biomaterials. Ind. Crops Prod. **41**, 356–364 (2013)
31. El Mansouri, N.-E., Salvadó, J.: Structural characterization of technical lignins for the production of adhesives: application to lignosulfonate, kraft, soda-anthraquinone, organosolv and ethanol process lignins. Ind. Crops Prod. **24**, 8–16 (2006)

Paper II

Biomass Conversion and Biorefinery (2018) 8:455–470
https://doi.org/10.1007/s13399-017-0294-2

ORIGINAL ARTICLE

Continuous catalytic depolymerisation and conversion of industrial kraft lignin into low-molecular-weight aromatics

Omar Y. Abdelaziz[1] · Kena Li[1] · Per Tunå[1] · Christian P. Hulteberg[1]

Received: 13 September 2017 / Revised: 14 September 2017 / Accepted: 15 November 2017 / Published online: 27 November 2017
© The Author(s) 2017. This article is an open access publication

Abstract
Base-catalysed depolymerisation of lignin using sodium hydroxide has been shown to be an effective approach towards exploiting industrial (technical) lignins within the pulp and paper industry. In the present work, a pine kraft lignin (Indulin AT) which is precipitated from black liquor of linerboard-grade pulp was depolymerised via base catalysis to produce low-molecular-mass aromatics without any organic solvent/capping agent in a continuous-flow reactor setup for the first time. The catalytic conversion of lignin was performed/screened at temperatures varying from 170 to 250 °C, using NaOH/lignin weight ratio ≈ 1 with 5 wt% lignin solids loadings for residence times of 1, 2 and 4 min, respectively, with comprehensive characterisation of substrate and produced reaction mixtures. The products were characterised using size exclusion chromatography (SEC), nuclear magnetic resonance spectroscopy (NMR) and supercritical fluid chromatography-diode array detector-tandem mass spectrometry (SFC-MS). The optimum operating conditions for such depolymerisation appeared to be at 240 °C and 30 h^{-1}, yielding the highest concentration of low-molecular-weight phenolics below the coking point. It was also found that the depolymerised lignin products exhibited better chemical stability during long-term storage at lower temperatures (~ 4 °C).

Keywords Biorefineries · Lignin valorisation · Lignin depolymerisation · Biomass conversion · Continuous-flow reactor system · Renewable chemicals

1 Introduction

Lignin, a complex and water-insoluble aromatic biopolymer, is attracting much attention owing to its potential as a renewable resource for the production of value-added chemicals, fuels, aromatics and bio-based materials. Conventionally, most large-scale industrial plants that utilise plant polysaccharides have burned lignin to generate the heat and power needed for biomass transformation and/or product drying. The emergence of biorefineries that convert cellulosic biomass into liquid biofuels will generate considerably more lignin than necessary to power the operation in addition to the lignin produced/combusted by the pulp and paper industry, and accordingly, efforts are underway to convert it into more valuable products [1]. It should be pointed out that lignin is the sole renewable available feedstock in nature that constitutes typical aromatic rings. Recent figures suggest that more than 130 million tons of lignin are presently liberated only from the pulp and paper industry, most of which is directly used on-site [2, 3]. Hence, the production of aromatic chemicals from lignin—the conversion process—is considered to be highly atom-economic; and the reason is that most of the carbon, hydrogen and oxygen atoms are well-reserved within the products. Designing new innovative processes/technologies to produce high-value products and subsequent scaling up of these technologies to produce such lignin-derived products at the commercial scale level and on a life cycle basis is a critical goal of many researchers currently working in the field of lignin utilisation [4, 5].

The challenges in employing lignin as an initial raw material for low-molecular-weight chemicals originate from the fact that the biopolymer is markedly heterogeneous—in many different aspects [3]. Firstly, lignin is heterogeneous in the sense that various plants build their lignin structures with different proportions of the constitutive building blocks. Basically, its streams differ in structure depending majorly

✉ Christian P. Hulteberg
Christian.Hulteberg@chemeng.lth.se

[1] Department of Chemical Engineering, Lund University, P.O. Box 124, SE-221 00 Lund, Sweden

on the method of isolation and source of plant [6]. Secondly, the cross-linking patterns are substantially stochastically created, and the lignin macromolecule is connected to the hemicellulose within the plant as well. There is therefore heterogeneity for lignin even from the same plant, highlighting the challenges towards finding efficient lignin valorisation strategies. Lignin can be specifically outlined as an amorphous biopolymer that is composed of three primary aromatic units—phenylpropane units—and termed as monolignols, namely *p*-coumaryl, coniferyl and sinapyl alcohols (Fig. 1). These units are linked together randomly by different types of ether/aryl ether (C–O) and carbon-carbon (C–C) bonds [7, 8], where the aryl ether linkages are spotted to be more easily cleaved [9] in comparison to the stable C–C linkages that are considered to be much more resistant towards chemical depolymerisation.

Depolymerisation of lignin hence requires the breaking of several types of bonds/linkages, which—if successful—will generate a complex mixture that is highly affected by the method/approach of depolymerisation adopted. In addition, and unlike cellulose, lignin is characterised by a diversity of distinct and chemically unalike bonding motifs, each requiring different cleavage conditions when selective depolymerisation and conversion attempts are targeted [2]. To add an insight, upon employing hydrothermal treatments for this refractory structure and aside from the phenolic monomers produced, a substantial amount of oligomeric compounds are also obtained, like dimers, trimers and high-molecular-mass oligomers, suggesting notable variations in the product. Due to such difficulties in the deconstruction step itself as well as in the product separation and based on the great potential of such a durable biopolymer in future renewable energy industries, lignin depolymerisation has become the gold-rush for numerous academics and key players within the bioenergy field worldwide [10]. In light of this, finding an efficient and cost-effective way of depolymerising such complex macromolecule into low-molecular-weight fragments that could be further utilised is thus pressing.

Studies on base-catalysed depolymerisation of lignin to produce phenolic compounds, in particular, have been conducted in various research efforts and are indeed current mainstay research [11–17]. The fact that soda is already adopted within the pulping processes promotes the potential of employing such homogeneous alkaline catalysis—from a process integration perspective. It is thus considered one of the primary state-of-the-art technologies available for lignin depolymerisation together with acid-catalysed depolymerisation, pyrolysis, gasification, hydrotreating, liquid-phase reforming and biodegradation. Miller et al. [13] investigated a collection of bases for depolymerising lignin and lignin model compounds within rapidly heated micro-autoclaves in the presence of alcohols. In their study, it was concluded that stronger bases, like CsOH, KOH and NaOH, are capable of producing higher yields of low-molecular-weight products than weaker bases, e.g. LiOH and $Ca(OH)_2$. Shabtai and co-workers [14] patented a two-step process for converting lignin into a suitable blending component for gasoline, where the initial step involved the base-catalysed lignin depolymerisation. This was subsequently followed by catalytic hydrodeoxygenation to generate gasoline-range aromatic fuels.

Going forward, Mahmood et al. [16] were successfully able to depolymerise kraft lignin into polyols through direct hydrolysis and using NaOH as a catalyst. The workable operating conditions seemed to be at 250 °C, NaOH/lignin ratio of 0.28 with 20 wt% substrate concentration and a 1-h reaction time, producing a suitable polyols replacement stream for rigid polyurethane foam synthesis. In another recent attempt, Dos Santos et al. [15] were able to produce bio-oil from base-catalysed depolymerisation of organosolv lignin at 300 °C and 40 min reaction time. The generated bio-oil solution was applied on wood and exhibited a good performance in improving its fungal resistance, introducing a new application for the produced reaction mixture from such process. In a very recent research effort by Katahira and co-workers [12], base-catalysed depolymerisation was applied on residual lignin-

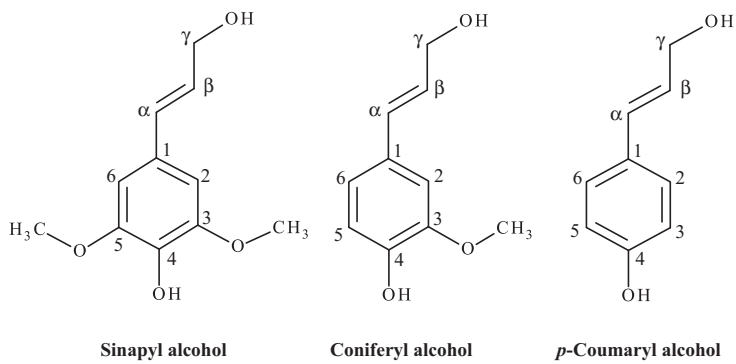


Fig. 1 Structures of the three primary building blocks of lignin (monolignols). The numbering of carbon atoms in the benzene ring and notation on the aliphatic propylene side chain are also depicted

rich biorefinery streams with 10 wt% solid loading, up to 4 wt% NaOH concentration, 40 min retention time and at temperature ranges of 270–330 °C. The study introduced some light on the viability of producing considerable yields of low-molecular-weight aromatics from such substrates and its potential valorisation and further upgrading to chemicals and fuels. It is worth to point out that the aforementioned research efforts were conducted in batch operation mode.

Certainly, repolymerisation reactions are believed to be one of the principal problems in the production of phenolic compounds during lignin depolymerisation. It is thus crucial to take into account decreasing the rate of repolymerisation/oligomerisation reactions during base-catalysed lignin depolymerisation, raising a key issue towards enhancing the yields of the low-molecular-weight products. Targeted research efforts [11, 18, 19] have tackled such problem via introducing capping agents in water with the aim of entrapping the available reactive fragments (e.g. phenolic compounds, formaldehyde) and masking the active sites (C_α present in the original lignin structure). In a very interesting research contribution, Roberts et al. [18] applied the usage of boric acid as a capping agent in such reaction with the aim of enhancing the product yields and suppressing the addition and condensation reactions of the initially formed products. The boric acid performed well as a protective agent during the hydrothermal lignin depolymerisation, minimising concurrent oligomerisation and polymerisation reactions and leading to higher product yields beyond 85%. Toledano et al. [11] also managed to overcome this problem via employing boric acid and phenol as capping agents and testing their nature and influence on base-catalysed lignin depolymerisation. An interesting point and provided that the capping agent/lignin ratio was optimised, phenol, in specific, appeared to boost the overall process through not only avoiding the repolymerisation phenomena but also favouring the production of more monomeric phenolic compounds, such as catechols, cresols and ferulic acid.

The use of H-donating reagents/solvents, such as formic acid and other stabilising compounds/alcohols have also been investigated in order to suppress the char formation problem and enhance the operation [20–23]. Gosselink et al. [20] tackled the addition of formic acid as hydrogen donor and experienced an increase in the yield of monomeric aromatics by stabilising the aromatic radicals, up to 12% based on lignin. Huang et al. [22] adopted the formic acid as well as an in situ hydrogen source during the depolymerisation of kraft lignin. It was demonstrated in this study that the formic acid is a more reactive hydrogen source than external hydrogen towards the reductive depolymerisation of technical lignin streams. It is speculated that the formic acid, in particular, is generated during the lignin pulping process (e.g. organosolv) and therefore can viably serve as an internal hydrogen donor with better hydrogen transfer protocols [24]. It is noteworthy that although lots of efforts have been made to develop efficient methods for lignin depolymerisation, the step to take this fundamental research to further industrial applications remains a major challenge.

The objective of this study is to screen the best reaction conditions for depolymerisation of technical lignin streams using base catalysis in continuous-mode operation, yielding the highest quantity of low-molecular-mass phenolic compounds. To the best of the authors' knowledge, the present contribution is the first of its nature to address the base-catalysed lignin depolymerisation using a novel continuous-mode operation system, identifying new regimes/conditions for such reaction. It is worth noting that most lignin depolymerisation reactions/processes are performed at temperatures of 250–650 °C, with or without catalysts, as critically reviewed by Zakzeski et al. [25] and Li et al. [4]; here in this paper, new milder conditions are introduced for such reaction typically below 240 °C in a continuous-mode operation and without exploiting any capping agents or hydrogen donors. The experimental/reaction conditions tested implied a temperature range of 170–250 °C, a pressure of 130 bar and residence time span of 1–4 min. Storage stability tests were investigated and product separation tasks were conducted on the obtained reaction mixture prior analysis. The lignin substrate and generated/depolymerised products were finally characterised using elementary analysis, size exclusion chromatography (SEC), nuclear magnetic resonance spectroscopy (NMR) and supercritical fluid chromatography-diode array detector-tandem mass spectrometry (SFC-DAD/MS).

2 Materials and methods

2.1 Materials

The commercial kraft lignin, Indulin AT, which is a pine softwood lignin that is precipitated from black liquor of linerboard-grade pulp, was obtained as dry powder from MeadWestvaco Corporation (Charleston Heights, SC) [26]. In this work, Indulin AT was used as the starting raw material in all experiments. This lignin stream has a moisture content of about 4.5 wt% and ash content of 3.5 wt%. The sample was analysed for its elemental composition at BELAB AB in Norrköping, Sweden; and full proximate, ultimate and compositional analyses for the lignin sample are reported in Table 1. The higher heating value (HHV) of the lignin sample was calculated based on the composition of main elements through an applied formula [27] with more than 90% predictions accuracy and in the range of ± 5% error (i.e. HHV (MJ/kg) = − 1.3675 + 0.3137 C + 0.7009 H + 0.0318 O*). The elemental compositions are in weight percentage, and O* is the sum of the contents of oxygen and other elements in the organic matter, including sulphur and nitrogen.

Table 1 Elementary analysis of Indulin AT lignin sample. The values are reported on a dry lignin basis, with available uncertainty (95% confidence interval). The oxygen content is calculated by difference

Analysis	Indulin AT lignin
Proximate analysis	
Ash (%)	3.5
Volatiles (%)	62.8
Fixed carbon (%)	33.7
Moisture (%)	4.5
HHV (MJ/kg	23.6
Ultimate analysis (% dry basis)	
C (%)	63.9[a]
H (%)	5.8[a]
N (%)	0.7[a]
S (%)	1.5[b]
O (%)	24.6

[a] Measured according to the SS-EN 15104 norm using a LECO Truspec CHN instrument

[b] Determined according to the SS-EN 15289 method with a LECO SC-144DR sulphur and carbon analyser

The feed was prepared prior to each experimental run and was composed typically of 5 wt% lignin substrate, 5 wt% NaOH and 90 wt% deionised (DI) water. Vacuum filtration for the feed was performed to ensure that no precipitation could occur in the pump and to prevent clogging problems within the pressure valve further after reaction. Sodium hydroxide, hydrochloric acid (37%) and all other chemicals were purchased from Sigma-Aldrich Sweden AB.

2.2 Depolymerisation apparatus and procedure

The base-catalysed lignin depolymerisation experiments were performed in a new-tailored continuous flow reactor (CFR), and a schematic diagram of the designed setup is presented in Fig. 2.

The system is composed of a Gilson 307 HPLC pump (Middleton, WI, USA), a Salamander tubular CFR reactor (Cambridge Reactor Design Ltd., Cottenham, UK) with a heated volume of 18 and 50 mL total system volume (ensured in safe reaction zone, i.e. max $P \times V = 8.15$ bar L < 20), and a specially assembled pressure control valve from nickel-molybdenum-chromium superalloy (Hastelloy C276; UNS N10276). The same material used in manufacturing the valve—Hastelloy C276—was also used for the reactor tubes to replace normal stainless steel tubes, offering excellent corrosion resistance in such severely basic environment. A filter was installed after the cooler in order to protect the pressure control valve from any char depositions if any. Before starting each experimental run, the setup was heated up and pressurised to the targeted operating conditions, keeping a continuous flow of DI water within the whole system. The feed was then continuously pumped to the reactor at volumetric flowrates of 10, 5 and 2.5 mL/min, respectively. These mixtures flowing through the reactor system typically correspond to residence times in the heating zone of about 1, 2 and 4 min, respectively. The experimental parameters and conditions are summarised in Table 2.

The experiments were conducted at different screening temperatures ranging from 170 to 250 °C, with 10 °C intervals, at pressures around 130 bar and retention times span of 1–4 min. For the reaction parameters, the temperature was set using a Eurotherm temperature controller (Eurotherm, Ashburn, Virginia, USA) and the pressure was adjusted through a backpressure regulator (Bronkhorst High-Tech B.V., Ruurlo, Netherlands). After exiting the reaction zone and expanding the product mixture to atmospheric pressure, the liquid products were continuously collected separately during the different operating conditions for workup and analysis purposes. The collected product samples were also divided into two cuts for storage stability testing, where one moiety was stored at room temperature and the other at 4 °C.

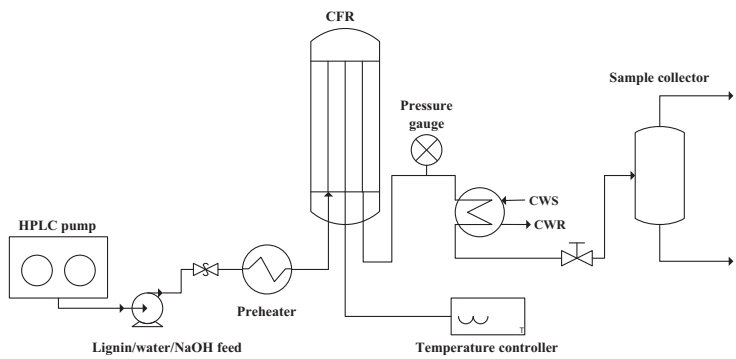


Fig. 2 Schematic diagram of the experimental setup

Table 2 Lignin depolymerisation experimental conditions

Parameter	Range tested
NaOH (wt%)	5
Lignin loading (wt%)	5
pH range	12–14
Temperature (°C)	170–250
Pressure (bar)	120–130
Time (min)	1–4

2.3 Molecular weight distribution

Following an established method [28], the molecular weight distributions of Indulin AT lignin as well as depolymerised lignin samples were determined and screened using a SEC system. The system used for the size screening studies was a Waters 600E chromatography system (Waters, Milford, MA, USA) equipped with a Waters 2414 refractive index (RI) detector, a Waters 486 UV absorbance detector and an analytical column packed with 30 cm of Superdex 30 and 30 cm of Superdex 200 (GE Healthcare, Uppsala, Sweden). The column was operated at ambient temperature and eluted with 125 mM NaOH solution (analytical grade) as the mobile phase at a flowrate of 1.0 mL/min. Calibration was performed using polyethylene glycol (PEG) standards ranging from 400 to 35,000 g/mol in the eluent (Merck Schuchardt OHG, Hohenbrunn, Germany). The samples were dissolved/diluted at concentrations of about 1 mg/mL in the eluent, and the solutions were further filtered using a 0.2-μm filter (Schleicher and Schuell, Dassel, Germany) in order to remove any suspended matter; and 500 μL from the filtered solution was lastly injected into the SEC system. Due to the comparison with PEG standards, both the molecular weight and the molecular number should be considered relative. For the storage stability tests, the feed mixture and the depolymerised lignin product samples (240 and 250 °C) were stored at different temperatures for periods of 1, 2 and 3 months before finally being analysed using the SEC system.

2.4 Characterisation approach

For detailed analysis of substrate and produced products, a workup procedure was developed for better characterisation results where separation tasks were involved. Basically, the product reaction mixture was first acidified with 6 M HCl to pH 1, which resulted in the precipitation of insoluble fragments. The supernatant—generated after acidification—was saved after centrifugal separation and extracted three times with ethyl acetate as extraction solvent. The ethyl acetate extract was then transferred quantitatively to a glass tube and evaporated under a gentle N_2 flow, where residue *A* (low-molecular-weight degradation products) was obtained. Residue *A* was finally stored for further SFC-MS analysis and subjection to a set of 2D ^{1}H–^{13}C HSQC NMR experiments. The acid-insoluble lignin product (residue *B*) originated after acidification was washed more than three times with DI water, freeze-dried for 24 h and stored for other analysis set.

For the SFC-DAD/MS analysis, residue *A* was first dissolved in 1 mL of methanol. The solution was then stored in a freezer at − 80 °C before being analysed. An ultra-high-performance supercritical fluid chromatography coupled with quadrupole-time-of-flight mass spectrometry method for the separation/analysis of major lignin-derived phenolic compounds was adopted in this sense, following a newly developed procedure [29]. Chromatographic separation and detection of the sample was performed with a Waters UltraPerformance Convergence Chromatography System (Milford, MA, USA) coupled to a Waters Xevo G2 Q-TOF mass spectrometer with electrospray ionisation (ESI) and atmospheric pressure chemical ionisation (APCI) (Waters, MS Technologies, Manchester, UK). The column employed was Waters Torus DIOL (1.7 μm, 3 × 100 mm) for target compounds separation. The mobile phase was composed of mainly CO_2 gas and methanol as co-solvent. The column temperature was set at 50 °C, and the pressure of the backpressure regulator was adjusted at 130 bar. A binary gradient elution program was employed with supercritical CO_2 and methanol as solvents. The mobile phase gradient started with 100:0 (CO_2/CH_3OH vol%) and ramped up to 91.5–8.5% of CO_2 solvent in 2.5 min, then ramped up to 75–25% of CO_2 solvent in 3 min and hold for 1 min and lastly decreased to the starting composition after 0.5 min. Ammonia (5 mM) in methanol was used as a makeup solvent, 0.2 mL/min. The data acquisition was done in a negative ion ESI mode. The data acquisition range was *m/z* 150–800. The capillary voltage was 3 kV, the extraction cone voltage was 4 V and the sampling cone voltage was 20 V. The source temperature was 120 °C, and the desolvation temperature was 600 °C with the desolvation gas flowrate of 1200 L/h. The cone gas flowrate was 40 L/h.

A set of ^{1}H and 2D ^{1}H–^{13}C HSQC NMR experiments for lignin and depolymerised products at 25 °C were acquired on Agilent VNMRS NMR spectrometers (Santa Clara, CA, USA) operating at 500 and 600 MHz, both equipped with a 5-mm HCN probe with triple-axis gradients. Typically, 50 mg of sample was dissolved in 0.5 mL of deuterated dimethyl sulfoxide-d_6 (DMSO-d_6) after stirring. Chemical shifts were referenced to the residual solvent signal at 2.5 and 39.5 ppm for ^{1}H and ^{13}C, respectively. The ^{1}H spectra were acquired using a 90° pulse angle, an acquisition time of 2 s, a relaxation delay of 2 s, 32 scans for the lignin sample and 4 scans for depolymerised products. The HSQC experiments were acquired using the Agilent pulse sequence gHSQC, a relaxation delay of 2 s, an acquisition time of 150 ms and 256 complex data points in the indirect dimension but were otherwise not acquired identically for the two samples. For the sample of depolymerised lignin residue, an edited experiment was used,

with spectral widths of 13.4 and 170 ppm for the ^{1}H and ^{13}C dimensions, respectively, and 64 transients. The total experimental time was 20 h. For the lignin sample, the experiment was run without editing, in order to maximise the signal intensities, with spectral widths of 12 and 170 ppm for the ^{1}H and ^{13}C dimensions, respectively, and 80 transients. The total experimental time was 25 h. The spectra were processed using VnmrJ software (v4.2).

3 Results and discussion

3.1 Size exclusion chromatography

Size exclusion chromatography (SEC) was performed to assess changes in the distribution of molecular mass of lignin samples before and after depolymerisation at temperatures ranging from 170 to 250 °C and, initially, with the flowrate of 10 mL/min. Figure 3a, b shows the corresponding UV absorbance chromatograms and refractive index elution profiles of different lignin samples, respectively. A flowrate of 10 mL/min was employed, corresponding to residence time of approximately 1 min in the reactor. As depicted in Fig. 3a, the initial molecular weight distribution profile of Indulin AT lignin generally distributed in a distinct wide region from 1 to 100 kDa with a peak around 4 kDa, illustrating that the main parts of Indulin AT are heavy compounds (heavier than 1 kDa). In addition, a small peak curve was also shown at approximately 0.9 kDa, representing a fraction of low-molecular-weight oligomers. The molecular weight distribution of the products gradually shifts towards lower molecular weight components with the increasing depolymerisation temperature (i.e. from 170 to 250 °C). The heaviest components with a molecular weight higher than 10 kDa almost disappeared when the temperature increased to 250 °C. It was noted that the bimodal curve distribution around 200–400 Da, which represents basically monomers and dimers, appeared when the temperature was above 220 °C. The higher depolymerisation

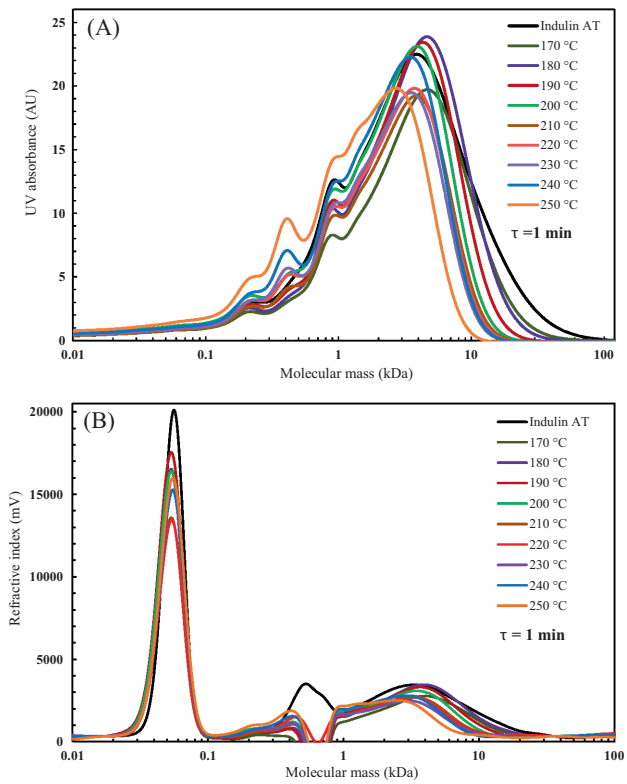


Fig. 3 Molecular weight distributions of Indulin AT and depolymerised lignin products, measured as **a** UV absorbance at 280 nm and **b** refractive index. The depolymerisation reaction sets were performed at temperatures ranging from 170 to 250 °C with the flowrate of 10 mL/min (reaction time of 1 min)

temperature yielded in turn substantially more monomers and dimers. Here, the lowest molecular mass distribution and the clearest peak at 200–400 Da were observed in the highest temperature (250 °C). The results at this juncture suggest that a more complete depolymerisation of lignin takes place with higher temperatures for such operation.

On the other hand, as shown in Fig. 3b, all the lignin samples had refractive index (RI) peaks at 40–70 Da, which comes from the sodium hydroxide. This illustrates that the hydrothermal depolymerisation reaction at such conditions is a sodium hydroxide consuming process. Such phenomenon was found to be comparable with other similar studies [25, 30], indicating/confirming that a high consumption of base is to be expected upon depolymerising lignin under alkaline conditions. Also during operation, the pH was lowered by two orders of magnitude confirming the consumption of alkali. A wide peak at about 1–10 kDa was also observed in the RI profiles (Fig. 3b). The peak weakened slightly with the increasing depolymerisation temperature, indicating the decrease of the molecular weight of Indulin AT lignin after depolymerisation.

Towards a better understanding of the reaction mechanism/behaviour and the CFR system performance, another screening attempt was performed at the same temperature range (170–250 °C) but with a lower feed flowrate of 5 mL/min, corresponding to a residence time of approximately 2 min. The UV absorbance chromatograms and the refractive index elution profiles for the lignin and depolymerised lignin samples at the aforementioned operating conditions are depicted as Fig. 4a, b, respectively.

Compared with the flowrate of 10 mL/min, a more thorough depletion of components over 10 kDa was observed from the temperature of 170 °C (Fig. 4a). Another stage of reduction happened when the temperature increased up to 190 °C. Accordingly, the peaks at around 400 Da and 1 kDa just get more and more distinct and higher above 190 °C. This represents a substantial increase in the production of monomers, dimers and other low-molecular-weight oligomers with the depolymerisation of Indulin AT kraft lignin. However, compared with 240 °C, an increase of the peak value at about 3 kDa was observed in the temperature of 250 °C. For the

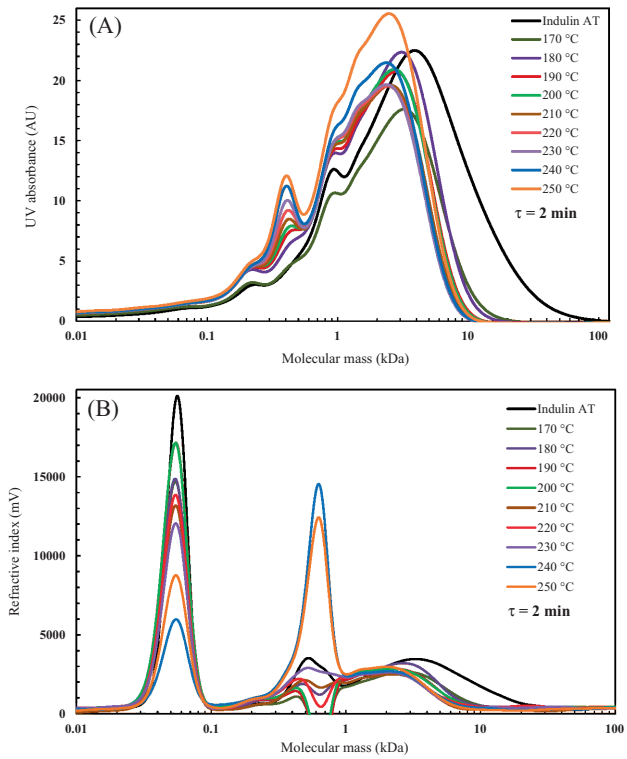


Fig. 4 Molecular weight distributions of Indulin AT and depolymerised lignin products, measured as **a** UV absorbance at 280 nm and **b** refractive index. The depolymerisation reaction sets were performed at temperatures ranging from 170 to 250 °C with the flowrate of 5 mL/min (reaction time of 2 min)

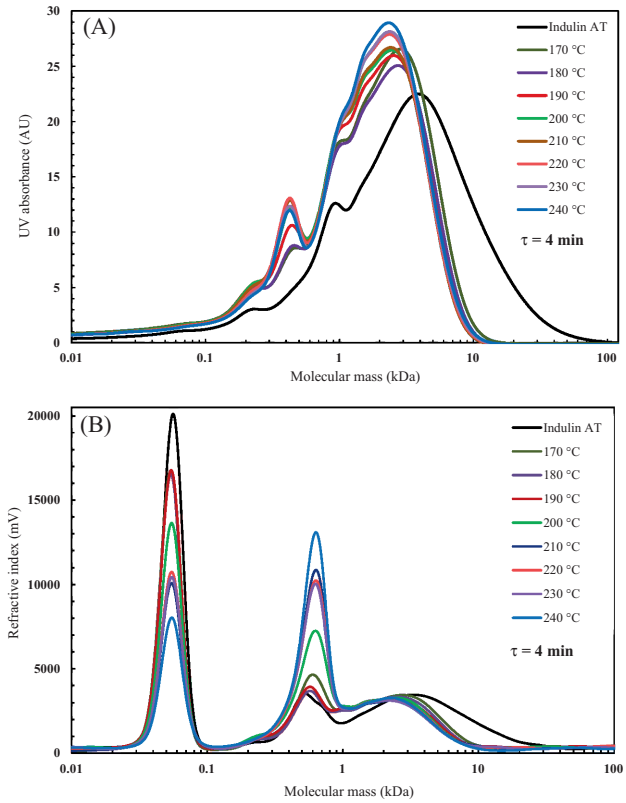


Fig. 5 Molecular weight distributions of Indulin AT and depolymerised lignin products, measured as **a** UV absorbance at 280 nm and **b** refractive index. The depolymerisation reaction sets were performed at temperatures ranging from 170 to 240 °C with the flowrate of 2.5 mL/min (reaction time of 4 min)

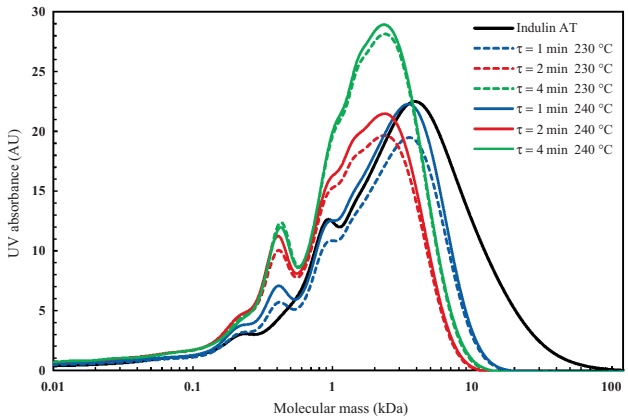


Fig. 6 Comparison of the molecular weight distributions of Indulin AT and depolymerised lignin products at temperatures of 230 and 240 °C (measured as UV absorbance at 280 nm) with the flowrate of 10, 5 and 2.5 mL/min

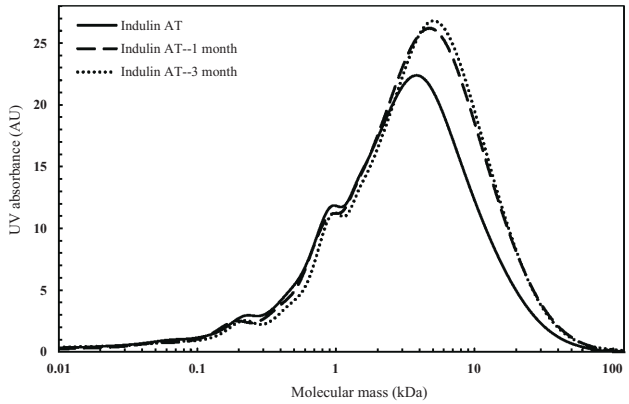


Fig. 7 Molecular weight distribution variations of Indulin AT lignin at different storage times testing the substrate stability

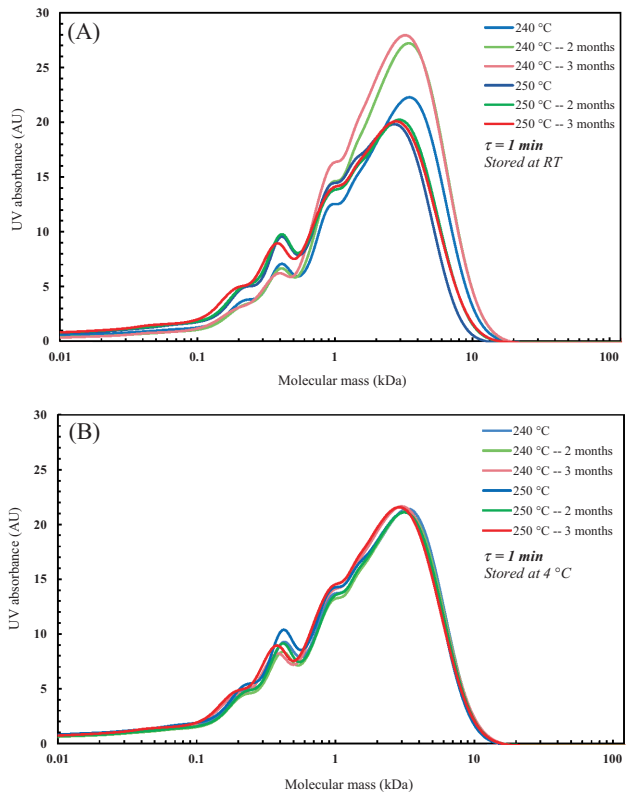


Fig. 8 Molecular weight distributions of depolymerised lignin samples at different storage times (measured as UV absorbance at 280 nm). The depolymerisation was performed with 10 mL/min flowrate at the temperatures 240 and 250 °C. The samples were stored at **a** room temperature (RT) and **b** 4 °C for periods of 2 and 3 months, respectively

experiments performed at 5 mL/min flowrate, char was experienced/formed at the temperature of 250 °C. The flowrate suddenly dropped, and the reactor tubing was plugged upon raising the temperature and feed flowrate, hindering any flow of feed solution throughout the CFR system. Therefore, temperature of 250 °C is not recommended for the continuous depolymerisation of Indulin AT lignin at a residence time of 2 min.

Figure 4b clearly shows the consumption of NaOH (40–70 kDa), i.e. lower refractive index exhibited, with the increased depolymerisation temperature. The results from the experiments at 240 and 250 °C displayed RI peaks at approximately 0.5–0.8 kDa which indicates the production of low-molecular-weight components tentatively at such conditions (Fig. 4b). In addition, the RI peaks at 1–10 kDa obviously decreased with the increasing depolymerisation temperature (170–250 °C), which indicates that more cleavage of the chemical bonds in the lignin molecules occurred under this operating conditions.

Final set of depolymerisation experiments was performed at a flowrate of 2.5 mL/min in the temperature range from 170 to 240 °C. At 2.5 mL/min feed flowrate, the residence time in the reactor was estimated to be 4 min. Under this condition, the heavy components with molecular weight higher than 10 kDa were totally depolymerised at different temperatures from 170 to 240 °C (Fig. 5a). There is also a remarkable growth in the amount of components with molecular mass between 1 and 5 kDa. A trend confirmed that UV absorbance and RI response increase with increased temperature was observed. However, no clear trend was experienced upon increasing the residence time, indicating that repolymerisation could be an issue at τ of 4 min (Fig. 5) in comparison to τ of 2 min (Fig. 4). More distinct peaks at 0.2–1 kDa were exhibited in UV absorbance and refractive index, which illustrates the production of more monomers, dimers and/or other oligomers (Fig. 5a, b).

To gain more comparative insights between different attained results, Fig. 6 was plotted showing different SEC

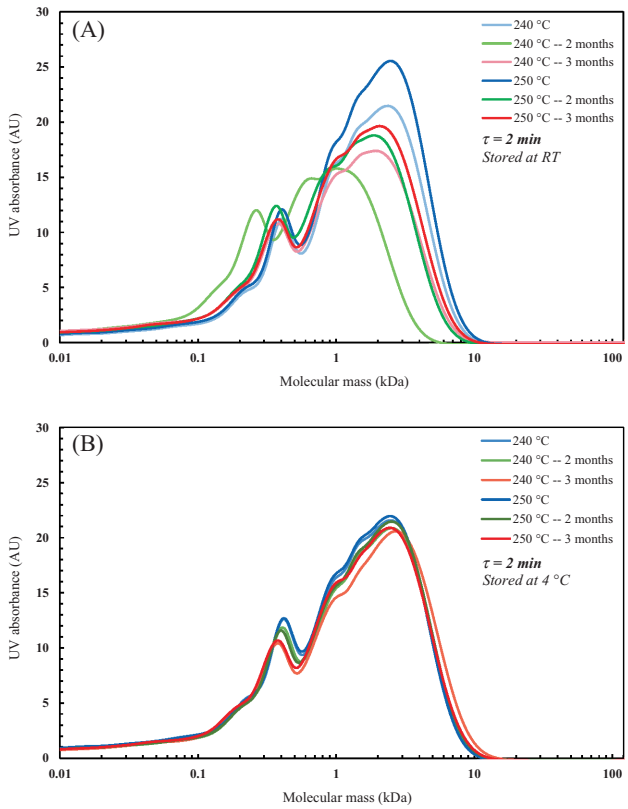


Fig. 9 Molecular weight distributions of depolymerised lignin samples at different storage times (measured as UV absorbance at 280 nm). The depolymerisation was performed with 5 mL/min flowrate at the temperatures 240 and 250 °C. The samples were stored at **a** room temperature (RT) and **b** 4 °C for periods of 2 and 3 months, respectively

profiles recorded for the three residence times tested (1, 2 and 4 min) at 230 and 240 °C (sweet depolymerisation spots). Comparing the changes encountered at different residence times under the same depolymerisation temperature, it can be deduced that longer residence time yields more low-molecular-mass oligomers, which can be demonstrated from Fig. 6. However, with 4 min of reaction time, the repolymerisation of Indulin AT became prominent. These phenomena can be visually seen in the comparative plot, where the curves for the experiments performed at temperatures of 230 and 240 °C exhibited a slight shift to the right when the residence increased from 2 to 4 min. The results here corresponded well with the changing of molecular mass distribution of lignin during autohydrolysis process [19]. Based on these results, for further investigation, we suggest 2 min residence time and 240 °C reaction temperature as the optimum operating conditions for Indulin AT base-catalysed depolymerisation in a continuous-mode processing.

The storage stability of lignin oils and lignin-derived bio-oils is a critical factor that would significantly influence the bio-oil applications—from an industrial point of view. In this context, the term "storage stability" may refer to the ability of the bio-oil to retain its initial chemical and physical properties in a relatively high temperature environment, i.e. thermal

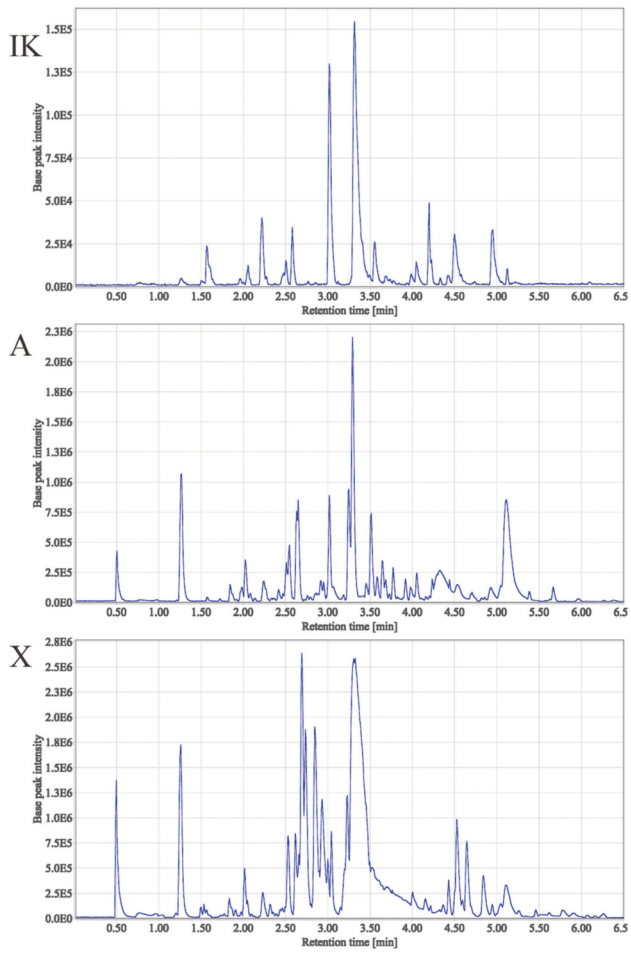


Fig. 10 Representative base peak intensity chromatograms obtained from the SFC-MS analysis for Indulin kraft lignin (IK), depolymerised lignin residues extracted from the runs performed at $T = 240$ °C and $\tau = 2$ min (A), and $T = 230$ °C and $\tau = 1$ min (X)

stability, or under atmospheric oxidation (oxidative stability) storage conditions [31]. The stability of lignin and lignin-derived bio-oils can be tested through storage time and/or storage temperature, and here, in the present study, we investigate both the long-term storage of lignin bio-oils and the effect of storage temperature on lignin and lignin oils' properties. Figure 7 presents the molecular weight distribution variations of Indulin AT lignin starting substrate (the mixture of 5% lignin with 5% NaOH and 90% distilled water) at room temperature and different storage times in order to assess the initial substrate stability. As can be seen, the lignin basic feed mixture appears to be very stable with time at normal storage conditions. This can be attributed to that there were no significant variations in size (molecular mass) encountered during this long-term storage.

The 240 and 250 °C (1 min of residence time) depolymerised lignin samples were first selected for the stability research and further compared with the ones obtained at 2 min reaction time, referring that the best depolymerisation results were experienced at these particular temperatures for such residence times. The molecular weight distribution of the first selected two depolymerised lignin samples which were stored at room temperature and refrigerated at 4 °C, respectively, were compared during 0–3 months of storage times (Fig. 8). In the condition of 4 °C, the molecular weight distribution of lignin samples was rarely changed after even 3 months' storage (Fig. 8b). This means that samples stored at 4 °C of storage condition were rather stable. However, it was clear that the peaks of the depolymerised lignin samples which were stored at room temperature moved to some extent at different storage periods (Fig. 8a). One explanation can be that the depolymerised components might have been repolymerised during such storage periods. Bearing in mind the capability of produced phenolic structures to react with available reactive sites in water during lignin conversion [32], cross-linking between the active sites and generated phenolic moieties in large fragments could take place, i.e. lignin could give in turn higher-molecular-weight fragments. Similar results can be observed in the other two depolymerised lignin samples at 240 and 250 °C with the residence time of 2 min (Fig. 9). It performed/revealed almost perfect stability in the 4 °C

Table 3 Most abundant chemical compounds identified by SFC-MS for Indulin kraft lignin starting material (IK), depolymerised lignin residues extracted from the runs performed at $T = 240$ °C and $\tau = 2$ min (A) and $T = 230$ °C and $\tau = 1$ min (X)

Sample	Compound	Retention time (min)	Calculated *m/z* ($[M\text{-}H]^-$)	Measured *m/z* ($[M\text{-}H]^-$)	Base peak intensity	MS^2 fragmentation	
						MS^2 transition	Lost fragment
IK	*p*-Hydroxybenzaldehyde	2.48	121.0290	121.0317	7.9E3	121 ➔ 92	CHO
	Vanillic acid	3.29	167.0345	167.0356	1.5E5	167 ➔ 152 167 ➔ 123 167 ➔ 108	CH_3 CO_2 $CH_3 + CO_2$
	p-Hydroxybenzoic acid	4.05	137.0239	137.0261	1.5E4	137 ➔ 93	CO_2
A	Guaiacol	0.50	123.0446	123.0442	1.4E6	123 ➔ 108	CH_3
	Vanillin	1.26	151.0395	151.0391	3.0E5	151 ➔ 136 151 ➔ 108	CH_3 $CH_3 + CO$
	Acetovanillone	1.26	165.0552	165.0553	1.7E6	165 ➔ 150 165 ➔ 122 165 ➔ 108	CH_3 $CH_3 + CO$ $CH_3 + COCH_2$
	p-Hydroxybenzaldehyde	2.49	121.0290	121.0290	1.2E5	121 ➔ 92	CHO
	p-Hydroxyacetophenone	2.53	135.0446	135.0441	8.2E5	135 ➔ 120 135 ➔ 108	CH_3 C_2H_3
X	Guaiacol	0.51	123.0446	123.0446	4.3E5	123 ➔ 108	CH_3
	Vanillin	1.27	151.0395	151.0397	5.1E5	151 ➔ 136 151 ➔ 108	CH_3 $CH_3 + CO$
	Acetovanillone	1.27	165.0552	165.0556	1.1E6	165 ➔ 150 165 ➔ 122 165 ➔ 108	CH_3 $CH_3 + CO$ $CH_3 + COCH_2$
	p-Hydroxybenzaldehyde	2.51	121.0290	121.0293	3.3E5	121 ➔ 92	CHO
	p-Hydroxyacetophenone	2.55	135.0446	135.0445	4.8E5	135 ➔ 120 135 ➔ 108	CH_3 C_2H_3
	Vanillic acid	3.29	167.0345	167.0356	2.2E6	167 ➔ 152 167 ➔ 123 167 ➔ 108	CH_3 CO_2 $CH_3 + CO_2$
	p-Hydroxybenzoic acid	4.05	137.0239	137.0251	2.5E5	137 ➔ 93	CO_2

refrigerator, while on the other end, some changes at room temperature were exhibited. The results here suggest that it is better/recommended to store the depolymerised lignin samples at lower temperatures for enhanced stability behaviour.

3.2 Supercritical fluid chromatography-mass spectrometry

The lignin starting material as well as the monomeric-rich fraction extracted from the depolymerised lignin products were qualitatively characterised using the newly introduced SFC-MS technique. Two samples from the depolymerised lignin streams produced where chosen beside the Indulin AT sample, residue *A* which entails the recommended/optimum operating conditions among all the runs performed (240 °C; 2 min) and the run performed at 230 °C and 1 min for the sake of drawing a comparative discussion. Figure 10 presents the typical base peak intensity chromatograms for the three investigated samples, and Table 3 reports the most abundant chemical compounds identified along with the MS/MS fragmentation data.

Seven major compounds were identified in the tested samples/fractions: guaiacol, vanillin, acetovanillone, *p*-hydroxyacetophenone, *p*-hydroxybenzaldehyde, vanillic acid and *p*-hydroxybenzoic acid, where the latter three compounds appeared in the starting Indulin kraft lignin sample. It was revealed from the analysis that guaiacol and vanillin are the main products generated from the current depolymerisation approach with higher concentrations/intensities for sample A over sample X, confirming/supporting the results acquired from the SEC attempts.

For the interesting sample A, it can be noted that the compounds exhibiting a retention time higher than 3 min were not identified due to the reason of being at low concentrations. These compounds may comprise vanillic acid and other distinct mono-aromatic moieties with aldehyde, acidic and methoxy functionalities. The decrease/disappearance of these particular compounds in the depolymerised lignin product obtained is due to the increasing severity of the reaction. This finding agrees well with results reported by Beauchet and coworkers [17]. In addition, the high selectivity towards guaiacol formation was attained for the higher reaction time (2 min). It can be suggested that the increase in the residence/reaction time (by lowering the feed pump flowrate) assisted in surging the guaiacol production which may have been generated not only from lignin itself but also from the extra depolymerisation of intermediate oligomers. The increased reaction severity also helped—to a great extent—in cleaving the acidic and aldehyde functions which were originally present in the initial starting lignin material. The depolymerised lignin products generated in the present study, i.e. guaiacol and vanillin, are known to have the potential of being key renewable aromatic building blocks for sustainable chemical industry [4, 33].

3.3 Nuclear magnetic resonance spectroscopy

The integrated ^{1}H NMR spectra obtained for Indulin Kraft starting material and depolymerised lignin samples are shown in Fig. 11. As can be seen, the increased intensities of proton chemical shifts (sharper peaks) of depolymerised lignin sample in comparison to the original lignin material suggest an increase in the degree of depolymerisation and higher formation of low-molecular-weight products.

The measurements on the produced depolymerised residue *A* show that the aliphatic compounds are rather present, but in very low concentrations. However, the main ^{1}H NMR peaks were assigned to typical aromatic protons (signals 6.0–8.0 ppm), besides the methoxyl and aldehyde groups, confirming the presence of small molecular entities within the depolymerised sample and supporting the findings of both SEC and SFC-MS.

It can be interpreted as well from the spectra that the methoxyl content, in particular, was dramatically decreased after the hydrothermal reaction, and this phenomenon agrees well with the reported literature on the hydrothermal treatment of lignin [34]. In addition, the large concentrations of

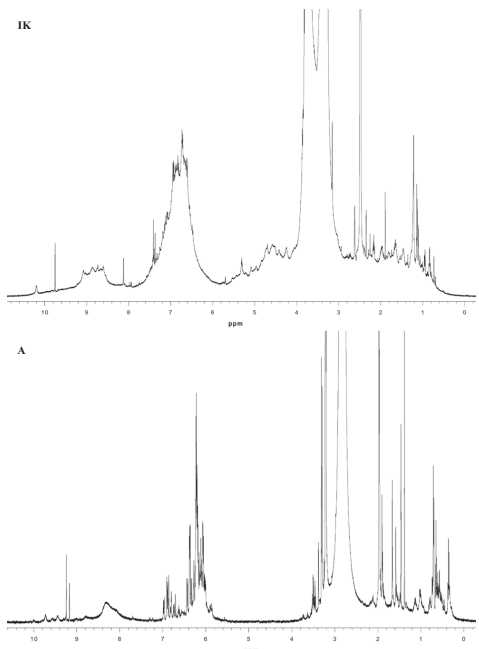


Fig. 11 Solid-state ^{1}H NMR spectra of Indulin AT lignin (IK) and depolymerised lignin residue extracted from the run performed at T = 240 °C and τ = 2 min (A)

hydroxyl and phenolic groups/protons in residue *A* can explain the increased hydrophilicity of produced aromatic compounds.

2D NMR spectroscopy was run on the depolymerised lignin residue *A* extracted from the run performed at $T = 240$ °C and $\tau = 2$ min which is considered to be optimum and compared with the untreated Indulin Kraft lignin sample. The measured spectra were interpreted qualitatively and divided into an aliphatic region (δ_C/δ_H 8.0–52.5/0.5–4.5 ppm), an inter-unit/oxygenated aliphatic region (δ_C/δ_H 52.5–90.0/2.8–5.7 ppm) and an aromatic region (δ_C/δ_H 105–155/6.0–9.2 ppm), as presented in Fig. 12 reporting different chemical shifts acquired. Tentative assignments of ^{13}C–^{1}H correlation signals/cross-peaks within the 2D NMR spectra were also identified for both lignin samples following recent literature reports [35, 36].

In general, guaiacol rings form about 95% of the major aromatic composition of lignin from softwood origin. Differences in the cross-peak patterns were detected for the two samples in the aliphatic 2D NMR region (Fig. 12; left compartment). The most characteristic cross-peaks of lignin macromolecule are found in the region of CH_2 groups (black rings), where they correspond to the primary aliphatic network present in lignin G–CH_2–CH_2–CH(R)–OH/R located at the α and β positions, bounded to the guaiacol ring. Most of the cross-peaks in the depolymerised fractions were found to be connected to an aromatic ring in the α-position, which suggests a shortening in the aliphatic chains within the bio-oil—residue *A*—in comparison to the Indulin AT substrate.

The inter-unit aliphatic region (also termed as oxygenated aliphatic region), shown in intermediate compartment of Fig. 12, is the region where carbon atoms bonded to alcohol, ether and Ar-methoxyl groups resonate. The known aliphatic inter-unit linkages β-O-4 (β-ether), β-β (pinoresinol), β-β (secoisolariciresinol) and β-5 (phenylcoumaran) were found for the Indulin AT lignin basic structure. However, the β-1 (diphenyl ethane), α-O-4 and dibenzodioxocine (5–5-α, β-O-4) structures were not found/detected, as they were probably hydrolysed during the kraft pulping process. From the visual inspection of the 2D NMR spectra for this region, it can be revealed that all the inter-unit/C–O linkages from Indulin AT lignin have disappeared post pretreatment reaction. This entails that the aliphatic C–O bonds have been cleaved under the tested reaction conditions (240 °C and 2 min residence time), i.e. in the known lignin inter-unit structures β-O-4, β-β, β-1 (weak signal) and β-5. This is indeed an important finding as it subsequently proves that all of the lignin starting material was reacted effectively under basic conditions in our CFR system. It also demonstrates that the amount of oxygen connected to the aliphatic carbons in depolymerised fraction is

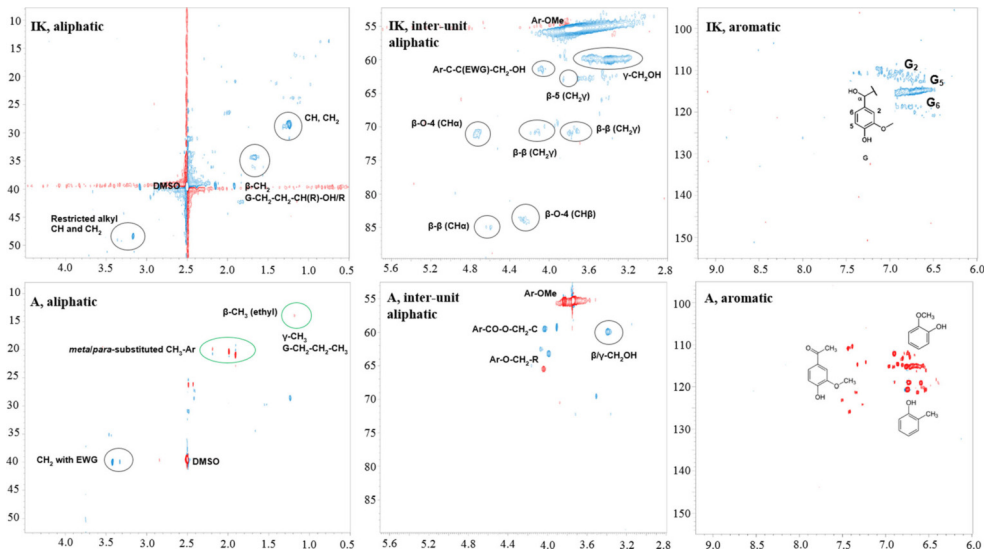


Fig. 12 The aliphatic δ_C/δ_H 8.0–52.5/0.5–4.5 ppm, inter-unit/oxygenated aliphatic δ_C/δ_H 52.5–90.0/2.8–5.7 ppm, and aromatic δ_C/δ_H 105–155/6.0–9.2 ppm regions of 2D NMR spectra obtained for Indulin AT lignin (IK) and depolymerised lignin residue extracted from the run performed at $T = 240$ °C and $\tau = 2$ min (A). Cross-peaks: CH, CH_2 and CH_3 (blue) for IK sample via normal HSQC and CH_2 (blue); CH/CH_3 (red) for sample *A* via edited HSQC experiments. Black rings correspond to lignin structural motifs, and green rings are new cross-peaks found in depolymerised lignin sample (colour figure online)

lowered. To note, the content of atomic oxygen comes almost exclusively from oxygen-containing groups (–OH and –OMe/R) connected to the aromatic ring, like phenols, guaiacols and other aromatic ethers.

Looking into the aromatic region, right compartment of Fig. 12, it was found that the main CH cross-peaks/signals of Indulin AT lignin correspond to the guaiacol ring (G) and the recognised substitution pattern of softwood kraft lignin, i.e. G_2, G_5 and G_6. It can further be seen that depolymerised lignin—residue *A*—exhibited a pattern of cross-peaks different than that of Indulin AT lignin. One of the principal reasons for this is that all monomeric/dimeric low-molecular-weight aromatics derived/produced ended up in this fraction. It was also confirmed from the SFC-MS analysis that phenol and phenol derivatives, e.g. guaiacol, dominate this residue/fraction, complementing such results.

4 Conclusions

Base-catalysed depolymerisation experiments on industrially generated lignin streams have been demonstrated using a new-tailored continuous flow reactor system. Kraft lignin was successfully converted into a phenolic bio-oil consisting of monomeric/oligomeric aromatic compounds. The optimum operating conditions for such conversion, yielding the highest concentration of low-molecular-weight aromatics and below the coking point, were achieved at 240 °C, 2 min, 5 wt% lignin loading and NaOH/lignin ratio ≈ 1 (*w*/*w*). The depolymerisation reaction appeared to be a NaOH consuming process, and this is directly proportional to the increase in reaction temperature and residence time, supported by RI profiles. The aliphatic C–O bonds have been cleaved under the tested reaction conditions in the lignin inter-unit structures (β-O-4, β-β, β-1, β-5), confirming that an effective lignin depolymerisation has been encountered. Controlling the reaction and storage temperatures is crucial for minimising char formation and preventing recondensation/repolymerisation reactions. Monomeric phenolic compounds (guaiacol, vanillin, apocynin, piceol) were identified from the current depolymerisation approach, generating a pool of chemically viable phenolic building blocks that can be considered for further high-value applications within the food and/or pharmaceutical industries. The present lignin depolymerisation reaction also enabled the production of partly deoxygenated dimeric/oligomeric fractions that could be utilised in liquid fuels applications and other renewable energy alternatives.

Acknowledgments Special thanks are due to Göran Carlström for assisting in NMR experiments, Jens Prothmann and Mingzhe Sun for helping in SFC-MS measurements and Johan Thuvander for the technical support with SEC.

Funding information This work was financed by the Swedish Foundation for Strategic Research (SSF) through the grant contract RBP14-0052. Financial supports from the Swedish Energy Agency (contract no. 41288-1), Preem, SunCarbon and Sveaskog are also acknowledged.

Open Access This article is distributed under the terms of the Creative Commons Attribution 4.0 International License (http://creativecommons.org/licenses/by/4.0/), which permits unrestricted use, distribution, and reproduction in any medium, provided you give appropriate credit to the original author(s) and the source, provide a link to the Creative Commons license, and indicate if changes were made.

References

1. Ragauskas AJ, Beckham GT, Biddy MJ, Chandra R, Chen F, Davis MF, Davison BH, Dixon RA, Gilna P, Keller M, Langan P, Naskar AK, Saddler JN, Tschaplinski TJ, Tuskan GA, Wyman CE (2014) Lignin valorization: improving lignin processing in the biorefinery. Science 344(6185):1246843. https://doi.org/10.1126/science.1246843
2. Rinaldi R, Jastrzebski R, Clough MT, Ralph J, Kennema M, Bruijnincx PCA, Weckhuysen BM (2016) Paving the way for lignin valorisation: recent advances in bioengineering, biorefining and catalysis. Angew Chemie Int Ed 55(29):8164–8215. https://doi.org/10.1002/anie.201510351
3. Abdelaziz OY, Brink DP, Prothmann J, Ravi K, Sun M, García-Hidalgo J, Sandahl M, Hulteberg CP, Turner C, Lidén G, Gorwa-Grauslund MF (2016) Biological valorization of low molecular weight lignin. Biotechnol Adv 34(8):1318–1346. https://doi.org/10.1016/j.biotechadv.2016.10.001
4. Li C, Zhao X, Wang A, Huber GW, Zhang T (2015) Catalytic transformation of lignin for the production of chemicals and fuels. Chem Rev 115(21):11559–11624. https://doi.org/10.1021/acs.chemrev.5b00155
5. Montazeri M, Eckelman MJ (2016) Life cycle assessment of catechols from lignin depolymerization. ACS Sustain Chem Eng 4(3):708–718. https://doi.org/10.1021/acssuschemeng.5b00550
6. Ayyachamy M, Cliffe FE, Coyne JM, Collier J, Tuohy MG (2013) Lignin: untapped biopolymers in biomass conversion technologies. Biomass Convers Biorefinery 3(3):255–269. https://doi.org/10.1007/s13399-013-0084-4
7. Sjöström E (1993) Wood chemistry: fundamentals and applications, 2nd edn. Academic Press, Inc., San Diego, California
8. Calvo-Flores FG, Dobado JA, Isac-García J, Martín-Martínez FJ (2015) Lignin and Lignans as renewable raw materials: chemistry, Technology and Applications. John Wiley & Sons, Ltd, Chichester. https://doi.org/10.1002/9781118682784
9. Yang L, Li Y, Savage PE (2014) Hydrolytic cleavage of C–O linkages in lignin model compounds catalyzed by water-tolerant Lewis acids. Ind Eng Chem Res 53(7):2633–2639. https://doi.org/10.1021/ie403545n
10. Xu C, Arancon RAD, Labidi J, Luque R (2014) Lignin depolymerisation strategies: towards valuable chemicals and fuels. Chem Soc Rev 43(22):7485–7500. https://doi.org/10.1039/C4CS00235K
11. Toledano A, Serrano L, Labidi J (2014) Improving base catalyzed lignin depolymerization by avoiding lignin repolymerization. Fuel 116:617–624. https://doi.org/10.1016/j.fuel.2013.08.071
12. Katahira R, Mittal A, McKinney K, Chen X, Tucker MP, Johnson DK, Beckham GT (2016) Base-catalyzed depolymerization of biorefinery lignins. ACS Sustain Chem Eng 4(3):1474–1486. https://doi.org/10.1021/acssuschemeng.5b01451

13. Miller JE, Evans L, Littlewolf A, Trudell DE (1999) Batch microreactor studies of lignin and lignin model compound depolymerization by bases in alcohol solvents. Fuel 78(11):1363–1366. https://doi.org/10.1016/S0016-2361(99)00072-1
14. Shabtai JS, Zmierczak WW, Chornet E (2001) Process for conversion of lignin to reformulated, partially oxygenated gasoline
15. Dos Santos PSB, Erdocia X, Gatto DA, Labidi J (2016) Bio-oil from base-catalyzed depolymerization of organosolv lignin as an antifungal agent for wood. Wood Sci Technol 50(3):599–615. https://doi.org/10.1007/s00226-015-0795-8
16. Mahmood N, Yuan Z, Schmidt J, Xu C (2013) Production of polyols via direct hydrolysis of kraft lignin: effect of process parameters. Bioresour Technol 139:13–20. https://doi.org/10.1016/j.biortech.2013.03.199
17. Beauchet R, Monteil-Rivera F, Lavoie JM (2012) Conversion of lignin to aromatic-based chemicals (L-chems) and biofuels (L-fuels). Bioresour Technol 121:328–334. https://doi.org/10.1016/j.biortech.2012.06.061
18. Roberts VM, Stein V, Reiner T, Lemonidou A, Li X, Lercher JA (2011) Towards quantitative catalytic lignin depolymerization. Chem - A Eur J 17(21):5939–5948. https://doi.org/10.1002/chem.201002438
19. Li J, Henriksson G, Gellerstedt G (2007) Lignin depolymerization/repolymerization and its critical role for delignification of aspen wood by steam explosion. Bioresour Technol 98(16):3061–3068. https://doi.org/10.1016/j.biortech.2006.10.018
20. Gosselink RJA, Teunissen W, van Dam JEG, de Jong E, Gellerstedt G, Scott e, Sanders JPM (2012) Lignin depolymerisation in supercritical carbon dioxide/acetone/water fluid for the production of aromatic chemicals. Bioresour Technol 106:173–177. https://doi.org/10.1016/j.biortech.2011.11.121
21. Rahimi A, Ulbrich A, Coon JJ, Stahl SS (2014) Formic-acid-induced depolymerization of oxidized lignin to aromatics. Nature 515(7526):249–252. https://doi.org/10.1038/nature13867
22. Huang S, Mahmood N, Tymchyshyn M, Yuan Z, Xu CC (2014) Reductive de-polymerization of kraft lignin for chemicals and fuels using formic acid as an in-situ hydrogen source. Bioresour Technol 171:95–102. https://doi.org/10.1016/j.biortech.2014.08.045
23. Huang X, Korányi TI, Boot MD, Hensen EJM (2014) Catalytic depolymerization of lignin in supercritical ethanol. ChemSusChem 7(8):2276–2288. https://doi.org/10.1002/cssc.201402094
24. Galkin MV, Samec JSM (2016) Lignin valorization through catalytic lignocellulose fractionation: a fundamental platform for the future biorefinery. ChemSusChem 9(13):1544–1558. https://doi.org/10.1002/cssc.201600237
25. Zakzeski J, Bruijnincx PCA, Jongerius AL, Weckhuysen BM (2010) The catalytic valorization of lignin for the production of renewable chemicals. Chem Rev 110(6):3552–3599. https://doi.org/10.1021/cr900354u
26. Hu Z, Du X, Liu J, Chang H, Jameel H (2016) Structural characterization of pine kraft lignin: BioChoice lignin vs Indulin AT. J. Wood Chem. Technol. 36(6):432–446. https://doi.org/10.1080/02773813.2016.1214732
27. Sheng C, Azevedo JLT (2005) Estimating the higher heating value of biomass fuels from basic analysis data. Biomass Bioenergy 28(5):499–507. https://doi.org/10.1016/j.biombioe.2004.11.008
28. Abdelaziz OY, Hulteberg CP (2017) Physicochemical characterisation of technical lignins for their potential valorisation. Waste Biomass Valoriz. 8(3):859–869. https://doi.org/10.1007/s12649-016-9643-9
29. Prothmann J, Sun M, Spégel P, Sandahl M, Turner C (2017) Ultra-high-performance supercritical fluid chromatography with quadrupole-time-of-flight mass spectrometry (UHPSFC/QTOF-MS) for analysis of lignin-derived monomeric compounds in processed lignin samples. Anal Bioanal Chem. https://doi.org/10.1007/s00216-017-0663-5
30. Brittain AD, Chrisandina NJ, Cooper RE, Buchanan M, Cort JR, Olarte MV, Sievers C (2017) Quenching of reactive intermediates during mechanochemical depolymerization of lignin. Catal Today. https://doi.org/10.1016/j.cattod.2017.04.066
31. Nguyen Lyckeskog H, Mattsson C, Åmand L-E, Olausson L, Andersson SI, Vamling L, Theliander H (2016) Storage stability of bio-oils derived from the catalytic conversion of softwood kraft lignin in subcritical water. Energy Fuel 30(4):3097–3106. https://doi.org/10.1021/acs.energyfuels.6b00087
32. Saisu M, Sato T, Watanabe M, Adschiri T, Arai K (2003) Conversion of lignin with supercritical water-phenol mixtures. Energy Fuel 17(4):922–928. https://doi.org/10.1021/ef0202844
33. Fache M, Boutevin B, Caillol S (2016) Vanillin production from lignin and its use as a renewable chemical. ACS Sustain Chem Eng 4(1):35–46. https://doi.org/10.1021/acssuschemeng.5b01344
34. Matsushita Y, Jo E-K, Inakoshi R, Yagami S, Takamoto N, Fukushima K, Lee SC (2013) Hydrothermal reaction of sulfuric acid lignin generated as a by-product during bioethanol production using lignocellulosic materials to convert bioactive agents. Ind Crop Prod 42:181–188. https://doi.org/10.1016/j.indcrop.2012.05.030
35. Mattsson C, Andersson S-I, Belkheiri T, Le Å, Olausson L, Vamling L, Theliander H (2016) Using 2D NMR to characterize the structure of the low and high molecular weight fractions of bio-oil obtained from LignoBoost™ kraft lignin depolymerized in subcritical water. Biomass Bioenergy 95:364–377. https://doi.org/10.1016/j.biombioe.2016.09.004
36. Constant S, Wienk HLJ, Frissen AE, Peinder P, Boelens R, van Es DS, Grisel RJH, Weckhuysen BM, Huijgen WJJ, Gosselink RJA, Bruijnincx PCA (2016) New insights into the structure and composition of technical lignins: a comparative characterisation study. Green Chem 18(9):2651–2665. https://doi.org/10.1039/C5GC03043A

Paper III

Bioresource Technology Reports 7 (2019) 100250

Contents lists available at ScienceDirect

Bioresource Technology Reports

journal homepage: www.journals.elsevier.com/bioresource-technology-reports

Membrane filtration of alkali-depolymerised kraft lignin for biological conversion

Omar Y. Abdelaziz[a], Krithika Ravi[a], Matthias Nöbel[a,b], Per Tunå[a], Charlotta Turner[c], Christian P. Hulteberg[a,*]

[a] Department of Chemical Engineering, Lund University, P.O. Box 124, SE-221 00 Lund, Sweden
[b] Australian Institute for Bioengineering and Nanotechnology, The University of Queensland, Brisbane, QLD 4072, Australia
[c] Department of Chemistry, Centre for Analysis and Synthesis, Lund University, P.O. Box 124, SE-221 00 Lund, Sweden

ARTICLE INFO

Keywords:
Lignocellulosic biorefinery
Lignin valorisation
Alkali depolymerisation
Nanofiltration
Pseudomonas
Bacterial conversion

ABSTRACT

In this study, we have investigated the possibility of membrane filtration as a means for obtaining a fraction containing mainly low-molecular-weight (LMW) compounds from depolymerised lignin (DL) for subsequent microbial conversion. A DL stream from continuous-mode alkali depolymerisation of a softwood kraft lignin produced at a temperature of 220 °C and a residence time of 2 min, using a NaOH/lignin weight ratio of 1 with 5 wt% lignin loading was fractionated using a polymeric membrane with a molecular weight cut-off of 500–700 Da. The permeate (DLP) volume recovery of LMW phenolics (250–450 Da) was 70% after filtration for 3.7 h. The DLP was used as a carbon source for growth of three bacterial strains; *Pseudomonas fluorescens*, *P. putida* EM42 and *Rhodococcus opacus*, and good growth was obtained by the first two microorganisms. This proof-of-concept study demonstrates a novel strategy for technical lignin valorisation by combining depolymerisation, nanofiltration and bioconversion.

1. Introduction

Lignin is regarded as the most abundant non-carbohydrate biopolymer on Earth, constituting a potential source of raw material for the production of renewable materials and value-added products. Despite this, it remains the most underutilised biomacromolecule due to its complexity and heterogeneity. Its efficient valorisation is thus an ongoing challenge within the biorefining industry (Ragauskas et al., 2014). Among the different strategies available for lignin valorisation, biological funnelling, or upgrading, has emerged as a promising approach to reduce the complexity of lignin fractions, enabling further transformation (Schutyser et al., 2018).

Depolymerisation of lignin is an essential step to obtain low-molecular-weight (LMW) compounds (monomers, dimers and possibly oligomers), as fragments of this size can serve as substrates for further cellular assimilation (Abdelaziz et al., 2016). To realise the concept of a lignin biorefinery, it has been proposed that kraft lignin, extracted from black liquor generated by pulping mills, be utilised as the starting material, to be fragmented into aromatic subunits with additional cleavage reactions and separation/upgrading, providing a commodity aromatics pool for the chemical industry (Hu et al., 2018). Depolymerised lignin (DL) for bioconversion should contain high concentrations (~100 g/L) of water-soluble LMW monomers (Beckham et al., 2016) that can be metabolised (Abdelaziz et al., 2016). However, these monomeric species are typically present in lignin streams at concentrations of only a few g/L (Linger et al., 2014), due to difficulties in the depolymerisation and separation steps. Improving methods of lignin solubilisation and concentration is thus key for further process integration (Beckham et al., 2016).

Membrane fractionation of DL streams represents a promising approach for product upgrading and selective separation of targeted molecules. In comparison to other available techniques for depolymerised lignin separation, e.g. acidification and solvent extraction, membranes have the advantage of separating compounds based on molecular weight. In the context of biorefineries, membrane separation can be characterised by its moderate cost-to-performance ratio, compactness and flexibility, mild processing conditions, low energy requirements and industrial scalability. Furthermore, it has the potential for integration into the production loop, enabling selective product purification and valuable co-product recovery from complex biomass streams, while minimising energy consumption (Dubreuil et al., 2017). Studies have been conducted previously on membrane separation of technical lignin (Aminzadeh et al., 2018) and oxidatively depolymerised lignin (Mota et al., 2018; Werhan et al., 2012). However, LMW

* Corresponding author.
E-mail address: christian.hulteberg@chemeng.lth.se (C.P. Hulteberg).

https://doi.org/10.1016/j.biteb.2019.100250
Received 14 March 2019; Received in revised form 24 May 2019; Accepted 28 May 2019
Available online 31 May 2019
2589-014X/ © 2019 The Authors. Published by Elsevier Ltd. This is an open access article under the CC BY-NC-ND license (http://creativecommons.org/licenses/BY-NC-ND/4.0/).

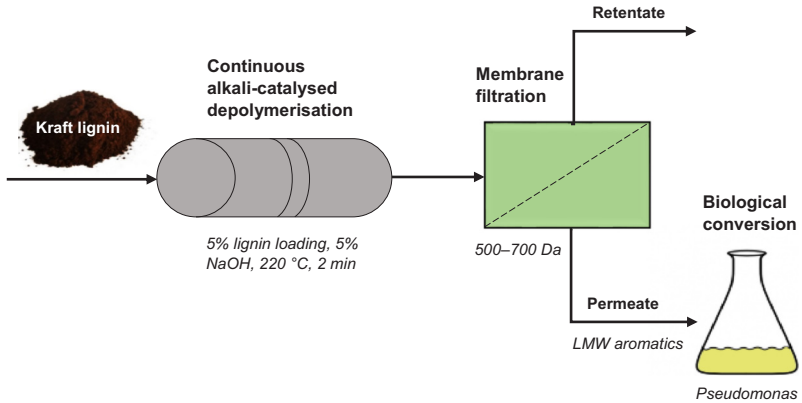


Fig. 1. An overview of the process concept.

lignin products from alkali-catalysed depolymerisation have not been considered as an opportunity for membrane separation to enable subsequent bioconversion.

In the present study, a LMW fraction was obtained from depolymerised lignin by membrane filtration, and assessed as a substrate for microbial conversion (Fig. 1). Nanofiltration (NF) was used to fractionate a DL from continuous alkali-catalysed depolymerisation of a technical softwood kraft lignin into permeate and retentate streams. The DL permeate was used in bacterial growth experiments employing strains belonging to the genera of *Pseudomonas* and *Rhodococcus* with known aromatic-metabolising capacity. A new process concept is introduced, and its potential for integration into existing pulp and paper mills is discussed.

2. Materials and methods

2.1. Depolymerised lignin

An aliquot of depolymerised lignin (DL) available from the study by Ravi et al. (2019) was used in the membrane filtration work. In short, the DL was based on a commercial lignin, Indulin AT (MeadWestvaco Corporation, currently Ingevity), which had been depolymerised using a continuous-flow reactor with an inflow containing lignin 5 wt% and NaOH 5 wt% according to the method described by Abdelaziz et al. (2018). The reaction operating conditions were: a temperature of 220 °C, a pressure of 120 bar and a volumetric flowrate of 5 mL/min (corresponding to 2 min residence time).

2.2. Membrane filtration

The DL stream was subjected to membrane filtration to separate the heavier fraction from the LMW fragments. An NP030 polymeric flat NF membrane (molecular weight cut-off 500–700 Da) was obtained from Microdyn-Nadir GmbH (Wiesbaden, Germany). This polymeric membrane was chosen to withstand the highly alkaline DL mixture (pH 13.5). The membrane was cut into 6.4 cm diameter circles and soaked in 0.5% (v/v) NaOH solution, then rinsed using deionised water before use.

Membrane filtration was conducted at 50 °C using a flat membrane test module (working volume 400 mL) coupled to a Trafag digital pressure gauge (Bubikon, Switzerland). The membrane module was placed on a Heidolph MR 2002 magnetic stirrer equipped with a heating plate (Heidolph Instruments, Schwabach, Germany). The chemically DL feed solution (200 mL batch operating volume) was stirred by a magnetic spin bar fitted in the module. A transmembrane pressure of 5.6 bar was applied using a N_2 gas flow, regulated via a pressure control valve. The average membrane flux, J (L/m^{2}h), was measured by weighing the permeate samples with a Mettler Toledo PL6001-S digital scale (Columbus, OH, USA) and estimated according to:

$$J = Q_p/A_m$$

where Q_p denotes the permeate flow rate through the membrane (L/h) and A_m the membrane surface area (m^2). The permeate was continuously collected and the accumulated weight was recorded every 20 s interval. The total filtration time was 3.7 h. The permeate and retentate fractions were stored at 4 °C prior to bacterial cultivation and analysis.

The molecular weight distributions of membrane-fractionated lignin samples were determined using size-exclusion chromatography (SEC), as described previously (Abdelaziz and Hulteberg, 2017). The original depolymerised lignin aliquot from Ravi et al. (2019) was reanalysed at the same time to ensure that no changes had occurred during storage. The highest UV absorbance response in each SEC chromatogram was normalised to 1 in order to enable visual comparison.

2.3. Shake flask cultivations

Bacterial shake flask cultivations were performed using the permeate fraction obtained from filtration of 50 g/L depolymerised lignin, after adjusting the pH to ~7 using H_2SO_4. The bacterial strains used were *Pseudomonas putida* KT2440 (DSM 6125), *Pseudomonas fluorescens* (DSM 50090) and *Rhodococcus opacus* (DSM 1069), purchased from the Deutsche Sammlung von Mikroorganismen und Zellkulturen, Braunschweig, Germany. M9 medium at pH 7 was used in all the experiments. The medium composition and cultivation conditions were as described previously (Ravi et al., 2019). Liquid culture experiments were performed in duplicate in 250 mL shake flasks containing 50 mL cultivation medium supplemented with 2 mL permeate as the sole carbon source. Cultivation proceeded for 7 days, with the addition of a further 1 mL of permeate on days 2 and 4. Bacterial growth was monitored spectrophotometrically by measuring the optical density (OD) at 620 nm.

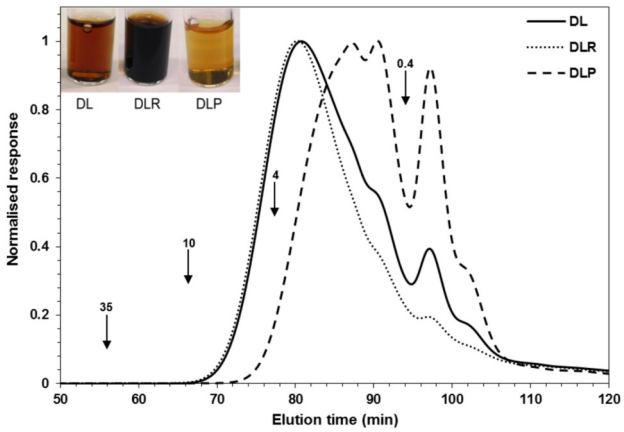


Fig. 2. Size-exclusion chromatograms of depolymerised lignin (DL) and the membrane filtered retentate (DLR) and permeate (DLP), showing characteristic UV absorption at 280 nm. The arrows indicate the molecular weights (kDa) of the PEG standards used for calibration. The change in colour between the permeate, retentate and depolymerised lignin can be seen.

3. Results and discussion

3.1. Molecular weight distribution and flux variation

NF was applied to the DL stream to separate high molecular and low molecular lignin fragments. The molecular weight distribution of the permeate (DLP) and the retentate (DLR) were measured using SEC to follow the size variations encountered. The ratio between LMW phenolic compounds and high molecular lignin were clearly different in the two fractions (Fig. 2). As desired, the LMW fraction of the depolymerised lignin mixture (reactor effluent) penetrated the membrane and appeared on the permeate side of the membrane, whereas the larger compounds were retained. This allows the DLP fraction – containing most of the LWM compounds – to be used at a higher concentration without precipitation of solids in biological conversion.

The volumetric fraction of permeate after almost 3.7 h was 70%, i.e. 140 mL was recovered on the permeate side and the rest of the DL batch was retained on the retentate side of membrane. It should be noted that the absorbance of the DLR was higher than that of DL and DLP. However, the UV absorbance curves were normalised to enable qualitative comparison in the same diagram. The retentate containing predominately the high-molecular-weight fraction of the DL stream complemented the DLP SEC curve. The initial small peak indicating LMW compounds (250–450 Da) was found on the permeate side of the membrane (Fig. 2), i.e. the ratio between the LMW depolymerised lignin species and the high-molecular-weight fragments changed. This will facilitate subsequent biological upgrading, since the LMW fraction contains mainly small oligomers and monomers, which would serve as readily available carbon sources for bacterial species. It also demonstrates that membrane filtration may be an attractive approach for improving the yield of LMW fractions in DL streams, compared to other alternatives such as acidification and solvent extraction.

The average membrane flux was monitored during DL separation to provide estimates of typical fluxes, and to evaluate the performance of the membrane (Fig. 3). No visible filter cake was formed on the membrane surface due to continuous magnetic stirring. The initial average permeate flux was found to be about 13 L/m^2 h. The flux then slowly decreased, reaching a minimum of about 8 L/m^2 h by the end of experiment. The slight decrease in the permeate flux may be attributed to the increasing concentration of high-molecular-weight material in the retentate. About 32% permeation of the initial lignin by weight was achieved over the entire filtration period.

Membrane flux decline is often a problem, and it is important to understand its underlying mechanisms to ensure the economic viability of the process (Mota et al., 2018). High permeation flux, in the range 25–30 L/m^2 h, has been reported when using ceramic membranes for the separation of lignin derivatives (Dubreuil et al., 2017), while lower permeate flux has been observed during the separation of lignin oxidation products due to membrane fouling (Werhan et al., 2012). Others have reported low fluxes, of 2.8–5.5 L/m^2 h, when using membranes with a cut-off of 1000 Da (Mota et al., 2018; Žabková et al., 2007). Based on the very few results available in the literature on the membrane separation of fragmented lignin fractions, the fluxes observed in this study (8–13 L/m^2 h) with a lignin concentration of 50 g/L were deemed to be adequate. The comparison with the literature on flux variations presented here is qualitative; however, the operating conditions and fluid properties should be unified to enable a quantitative comparison.

3.2. Bacterial conversion of the permeate stream

The higher solubility of the permeate fraction, compared to previously studied unfiltered depolymerisate (Ravi et al., 2019), enabled experiments on bioconversion to be carried out at a higher monomer concentration. An increase in OD of approximately 0.1 was seen in the *Pseudomonas* cultures on day 1 (Fig. 4), which is in line with our previous results for unfiltered depolymerisate (Ravi et al., 2019). The growth is likely due to the consumption of readily available monomers such as vanillin, vanillate and 4-hydroxybenzoate (Ravi et al., 2017). The OD of *Pseudomonas* cultures increased after the addition of more substrate (1 mL permeate on days 2 and 4), giving a final OD of 0.3. *P. fluorescens* formed aggregates on day 4, and hence it was not possible to monitor the growth by optical density. The tendency of *P. fluorescens* to form cell aggregates when exposed to toxic environments has been reported previously (Salvachúa et al., 2015), and has also been observed with unfiltered substrate (Ravi et al., 2019). In contrast to the other species, practically no growth was observed for *R. opacus* on the DLP. This is also in contrast to the results of our previous experiments with unfiltered depolymerisate, in which *R. opacus* showed some growth and was able to consume guaiacol, 4-HBA, vanillin and vanillate. However, the concentration of LMW compounds in the medium was lower in our previous study, and the poor growth on DLP in the present study may be due to inhibition by higher concentrations of LMW either phenolics, salts or other compounds present in the DLP

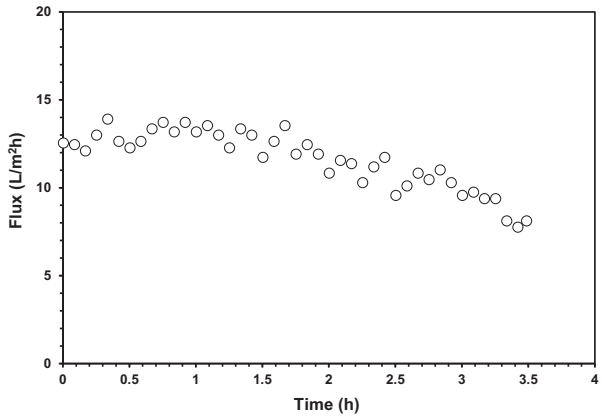


Fig. 3. Average transmembrane flux vs. time for the depolymerised lignin sample. The operating temperature was 50 °C and the transmembrane pressure was 5.6 bar.

medium.

3.3. Integration in pulp and paper mills

The suggested combination of chemical and microbial upgrading of lignin components could be integrated into an existing pulp and paper mill. A slipstream of black liquor could be heat treated to form additional smaller molecules. The heat treatment would reduce the amount of black liquor that needs to be filtered, reducing the membrane area required, and thus the operating and investment costs of filtration. The slipstream should preferably be taken downstream of tall oil separation, but before concentration to a high total solids content in the vaporiser section. The retentate stream could be sent directly back to the vaporising section, and the lignin could be further processed in the recovery boiler to produce process heat. The key to profitable operation is the downstream neutralisation of the permeate pH before bacterial upgrading, as this may disturb the sodium/sulphur balance in the mill. Therefore, after extraction of the fermentation product, the fermentation broth should be returned to the mill and the chemical recovery system. This concept study was performed using an existing kraft lignin product, but in a real application, a lignin powder would not be produced as an intermediate.

4. Conclusions

Membrane separation of depolymerised kraft lignin has been demonstrated as a possible approach to enable biological conversion of the low molecular compounds. The higher solubility of the permeate fraction, compared to the unfractionated stream, enabled bioconversion at increased concentrations. The technology suggested for combining chemical and microbial upgrading of technical lignin streams could be integrated into existing pulp and paper mills. The key to cost-effective operation is the downstream neutralisation of the permeate pH prior to biological conversion, as this may constrain the atomic balance in the mill.

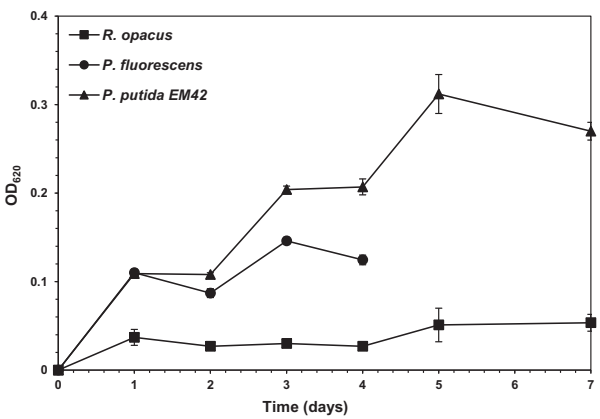


Fig. 4. Growth curves for *R. opacus, P. fluorescens* and *P. putida* EM42 with 2 mL permeate per 50 mL culture as the sole carbon source in M9 medium. An extra 1 mL of permeate was added on days 2 and 4. Permeate was obtained by filtering 50 g/L depolymerised lignin. Growth experiments were performed in duplicate and the error bars represent the standard deviation.

Acknowledgments

The authors are grateful for the financial support provided by the Swedish Foundation for Strategic Research (RBP14-0052) and the Swedish Energy Agency (41288-1). We thank Johan Thuvander for technical support with the membrane set-up, Kena Li for providing the depolymerisate, and Gunnar Lidén for comments on the work.

References

Abdelaziz, O.Y., Hulteberg, C.P., 2017. Physicochemical characterisation of technical lignins for their potential valorisation. Waste and Biomass Valorization 8, 859–869. https://doi.org/10.1007/s12649-016-9643-9.

Abdelaziz, O.Y., Brink, D.P., Prothmann, J., Ravi, K., Sun, M., García-Hidalgo, J., Sandahl, M., Hulteberg, C.P., Turner, C., Lidén, G., Gorwa-Grauslund, M.F., 2016. Biological valorization of low molecular weight lignin. Biotechnol. Adv. 34, 1318–1346. https://doi.org/10.1016/j.biotechadv.2016.10.001.

Abdelaziz, O.Y., Li, K., Tunå, P., Hulteberg, C.P., 2018. Continuous catalytic depolymerisation and conversion of industrial kraft lignin into low-molecular-weight aromatics. Biomass Convers. Biorefinery 8, 455–470. https://doi.org/10.1007/s13399-017-0294-2.

Aminzadeh, S., Lauberts, M., Dobele, G., Ponomarenko, J., Mattsson, T., Lindström, M.E., Sevastyanova, O., 2018. Membrane filtration of kraft lignin: structural charactristics and antioxidant activity of the low-molecular-weight fraction. Ind. Crops Prod. 112, 200–209. https://doi.org/10.1016/j.indcrop.2017.11.042.

Beckham, G.T., Johnson, C.W., Karp, E.M., Salvachúa, D., Vardon, D.R., 2016. Opportunities and challenges in biological lignin valorization. Curr. Opin. Biotechnol. 42, 40–53. https://doi.org/10.1016/j.copbio.2016.02.030.

Dubreuil, M.F.S., Servaes, K., Ormerod, D., Van Houtven, D., Porto-Carrero, W., Vandezande, P., Vanermen, G., Buekenhoudt, A., 2017. Selective membrane separation technology for biomass valorization towards bio-aromatics. Sep. Purif. Technol. 178, 56–65. https://doi.org/10.1016/j.seppur.2016.12.033.

Hu, J., Zhang, Q., Lee, D.-J., 2018. Kraft lignin biorefinery: a perspective. Bioresour. Technol. 247, 1181–1183. https://doi.org/10.1016/J.BIORTECH.2017.08.169.

Linger, J.G., Vardon, D.R., Guarnieri, M.T., Karp, E.M., Hunsinger, G.B., Franden, M.A., Johnson, C.W., Chupka, G., Strathmann, T.J., Pienkos, P.T., Beckham, G.T., 2014. Lignin valorization through integrated biological funneling and chemical catalysis. Proc. Natl. Acad. Sci. 111, 12013–12018. https://doi.org/10.1073/pnas.1410657111.

Mota, I.F., Pinto, P.R., Ribeiro, A.M., Loureiro, J.M., Rodrigues, A.E., 2018. Downstream processing of an oxidized industrial kraft liquor by membrane fractionation for vanillin and syringaldehyde recovery. Sep. Purif. Technol. 197, 360–371. https://doi.org/10.1016/j.seppur.2018.01.001.

Ragauskas, A.J., Beckham, G.T., Biddy, M.J., Chandra, R., Chen, F., Davis, M.F., Davison, B.H., Dixon, R.A., Gilna, P., Keller, M., Langan, P., Naskar, A.K., Saddler, J.N., Tschaplinski, T.J., Tuskan, G.A., Wyman, C.E., 2014. Lignin valorization: improving lignin processing in the biorefinery. Science 344, 1246843.

Ravi, K., García-Hidalgo, J., Gorwa-Grauslund, M.F., Lidén, G., 2017. Conversion of lignin model compounds by Pseudomonas putida KT2440 and isolates from compost. Appl. Microbiol. Biotechnol. 101, 5059–5070. https://doi.org/10.1007/s00253-017-8211-y.

Ravi, K., Abdelaziz, O.Y., Nöbel, M., García-Hidalgo, J., Gorwa-Grauslund, M.F., Hulteberg, C.P., Lidén, G., 2019. Bacterial conversion of depolymerized Kraft lignin. Biotechnol. Biofuels 12, 56. https://doi.org/10.1186/s13068-019-1397-8.

Salvachúa, D., Karp, E.M., Nimlos, C.T., Vardon, D.R., Beckham, G.T., 2015. Towards lignin consolidated bioprocessing: simultaneous lignin depolymerization and product generation by bacteria. Green Chem. 17, 4951–4967. https://doi.org/10.1039/C5GC01165E.

Schutyser, W., Renders, T., Van den Bosch, S., Koelewijn, S.-F., Beckham, G.T., Sels, B.F., 2018. Chemicals from lignin: an interplay of lignocellulose fractionation, depolymerisation, and upgrading. Chem. Soc. Rev. 47, 852–908. https://doi.org/10.1039/C7CS00566K.

Werhan, H., Farshori, A., Rudolf von Rohr, P., 2012. Separation of lignin oxidation products by organic solvent nanofiltration. J. Memb. Sci. 423–424, 404–412. https://doi.org/10.1016/j.memsci.2012.08.037.

Žabková, M., da Silva, E.A.B., Rodrigues, A.E., 2007. Recovery of vanillin from lignin/vanillin mixture by using tubular ceramic ultrafiltration membranes. J. Memb. Sci. 301, 221–237. https://doi.org/10.1016/j.memsci.2007.06.025.

Paper IV

Topics in Catalysis (2019) 62:639–648
https://doi.org/10.1007/s11244-019-01146-5

ORIGINAL PAPER

Oxidative Depolymerisation of Lignosulphonate Lignin into Low-Molecular-Weight Products with Cu–Mn/δ-Al_2O_3

Omar Y. Abdelaziz[1,2] · Sebastian Meier[3] · Jens Prothmann[4] · Charlotta Turner[4] · Anders Riisager[2] · Christian P. Hulteberg[1]

Published online: 5 March 2019
© The Author(s) 2019

Abstract
Lignin depolymerisation receives great attention due to the pressing need to find sustainable alternatives to fossil sources for production of fuels and chemicals. In this study, alumina-supported Cu–Mn and Ni–Mo catalysts were tested for oxidative depolymerisation of a technical lignin stream—sodium lignosulphonates—to produce valuable low-molecular-weight aromatics that may be considered for applications in the fuels and chemicals sector. The reactions were performed at elevated temperature and oxygen pressure, and the product mixtures were analysed by size exclusion chromatography, two-dimensional nuclear magnetic resonance spectroscopy and supercritical fluid chromatography mass spectrometry. The best performance was obtained with Cu–Mn/δ-Al_2O_3, which was thoroughly characterised before and after use by nitrogen physisorption, scanning electron microscopy, energy dispersive spectroscopy, powder X-ray diffraction, thermal gravimetric analysis, inductively coupled plasma optical emission spectrometry and X-ray photoelectron spectroscopy. Major products identified were vanillin, *p*-hydroxybenzaldehyde, vanillic acid and *p*-hydroxybenzoic acid as well as smaller aliphatic aldehydes, acids and lactones.

Keywords Catalytic oxidation · Cu–Mn/Al_2O_3 catalyst · Heterogeneous catalysis · Lignin valorisation · Sodium lignosulphonates

1 Introduction

Utilisation of renewable raw materials as a source of energy, chemicals and materials is expected to increase in the near future. This supports emerging biorefinery strategies and new circular bioeconomy concepts moving towards better valorisation of lignocellulosic biomass. Lignin is one of the main constituents (polymeric wood components) of terrestrial plant biomass, together with the carbohydrate polymers cellulose and hemicellulose. It is a complex biopolymer consisting of phenylpropanoid subunits and accounts for approximately 15–30% of the woody biomass dry weight, providing structural integrity to the terrestrial lignocellulosic material [1–3]. Lignin is recognised as the third most abundant biopolymer available on Earth after cellulose and chitin, providing a potential source for production of renewable materials and high-value products [3, 4]. Large amounts of this heterogeneous substrate are already generated each year as a low-value by-product of the pulp and paper industry; transforming it into homogeneous and usable fractions with higher value is of great importance.

Electronic supplementary material The online version of this article (https://doi.org/10.1007/s11244-019-01146-5) contains supplementary material, which is available to authorized users.

✉ Omar Y. Abdelaziz
omar.abdelaziz@chemeng.lth.se

✉ Anders Riisager
ar@kemi.dtu.dk

✉ Christian P. Hulteberg
christian.hulteberg@chemeng.lth.se

[1] Department of Chemical Engineering, Lund University, P.O. Box 124, 221 00 Lund, Sweden

[2] Centre for Catalysis and Sustainable Chemistry, Department of Chemistry, Technical University of Denmark, 2800 Kgs. Lyngby, Denmark

[3] Department of Chemistry, Technical University of Denmark, 2800 Kgs. Lyngby, Denmark

[4] Centre for Analysis and Synthesis, Department of Chemistry, Lund University, P.O. Box 124, 221 00 Lund, Sweden

Despite its potential, lignin remains a greatly underutilised biopolymer in contrast to other lignocellulosic polymeric components [5], and its efficient valorisation presents an ongoing challenge. It is most commonly used as a low-cost fuel for heat and power generation, since it has the highest specific energy content available in the organic matrix of lignocellulosic materials due to its more reduced carbons [6]. In contrast, only a minor portion is being commercialised and transformed to other valuable products and applications.

The challenges in using lignin as a raw material for low-molecular-weight (LMW) chemicals production [7] result from the fact that the polymer is markedly heterogeneous, hindering the disassembling of its phenolic building blocks. Technical (industrial) lignins are particularly challenging compared to other native lignin streams. A principal reason is that such streams contain primarily C–C inter-unit bonds having high bond dissociation energy [8, 9], unlike C–O ether bonds, which are more easy to cleave.

Sulphur-containing lignin streams are generated in large scale on-site pulp mills, such as in sulphate (Kraft) and sulphite pulping. Lignin from sulphite processes is denoted as lignosulphonates, and is produced by means of sulphurous acid and/or a sulphite salt containing ammonium, magnesium, calcium, or sodium at different pH levels [10]. Lignosulphonates are less pure, have a higher molecular weight and contain higher sulphur contents than Kraft lignin. However, lignosulphonates have a unique property that makes them different from other available lignin streams: they are water-soluble. Due to the presence of sulphonated groups, lignosulphonates are negatively charged and water-soluble at neutral pH. A fragment representing the structure of sodium lignosulphonate lignin (used in this study) is schematically shown in Fig. 1.

Various lignin depolymerisation and conversion methods have been described in the literature, each approach having its own advantages and limitations. Examples comprise acid-catalysed [11, 12], base-catalysed [13, 14], thermochemical [15, 16], biochemical [1, 17], reductive [18, 19] and oxidative [20–22] lignin depolymerisation. Oxidative depolymerisation, in particular, emerges as a promising route among the deconstruction strategies, as it can produce highly functionalised chemicals under relatively mild operating conditions. Numerous efforts concerning oxidative depolymerisation of lignin model compounds have been reported, while only a few have considered real lignin substrates (raw lignin) as an option to investigate new functionalities and structures of the formed monomers, oligomers and organic acids [23, 24]. Heterogeneous catalysts may offer a number of advantages for oxidative depolymerisation of lignin, not only in terms of easy separation and recyclability, but also when the reactions are performed in the presence of molecular O_2 or other viable oxidants.

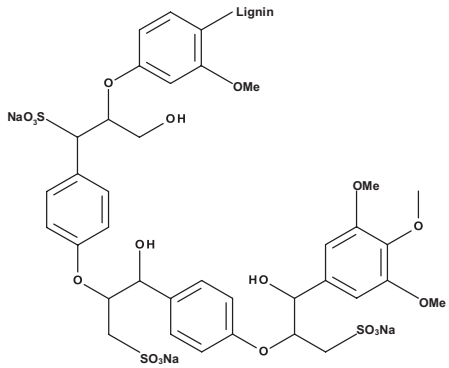


Fig. 1 Representative chemical structure of sodium lignosulphonate lignin

In the present study, different heterogeneous catalysts were tested for their ability to depolymerise sodium lignosulphonates—a technical lignin stream—into LMW aromatics using molecular O_2 without additional solvent. The catalyst performance was evaluated using various characterisation techniques, and the product mixtures were thoroughly analysed to elucidate structural features.

2 Experimental

2.1 Chemicals and Materials

Sodium lignosulphonate lignin (LS) was kindly provided by Domsjö Fabriker AB (Örnsköldsvik, Sweden) and used as starting raw material. Proximate and ultimate analyses as well as the high heating value of LS substrate are reported in Table 1. Oxygen gas (≥ 99.5%) was obtained from AGA, Denmark, methanol and ethyl acetate (LC–MS grades) purchased from Merck, Germany, and ammonia (2 M in methanol) purchased from Fisher Scientific, USA. Unless otherwise mentioned, all other chemicals and reagents were purchased from Sigma-Aldrich or VWR and used as received without further purification.

2.2 Catalyst Preparation

The catalysts used were all based on an extruded δ-Al_2O_3 support crushed to 20–30 mesh (1–2 mm). Cu–Mn/δ-Al_2O_3 (Cat A) was prepared by incipient wetness impregnation (IWI) of a mixture of the Cu and Mn acetate salts, repeated twice. The samples were dried and calcined at 350 °C for 1 h after each impregnation, resulting in a catalyst composition

Table 1 Elementary analysis and higher heating value of lignosulphonate lignin. The values are reported on a dry basis, with available uncertainty (95% confidence interval). The oxygen content was calculated by difference

Analysis	Lignosulphonate lignin (LS)
Proximate analysis	
Ash (%)	26.9
Volatiles (%)	60.3
Fixed carbon (%)	12.8
Moisture (%)	3.3
HHV (MJ kg^{-1})	16
Ultimate analysis (% dry basis)	
C	42.9
H	4.4
N	0.8
S	7.9
O	17.1

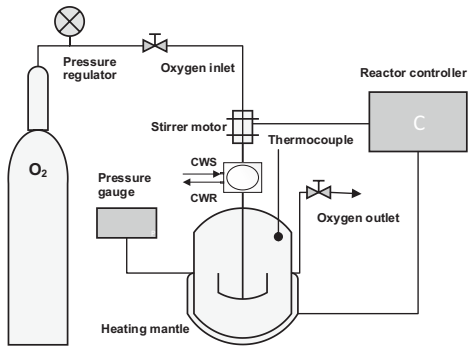


Fig. 2 Schematic illustration of setup used for lignin oxidative depolymerisation experiments

of 3% Cu and 6% Mn. Ni–Mo/δ-Al_2O_3 (Cat B) was also prepared by IWI using the nitrate salts of Ni and Mo, starting with Mo impregnation, calcination at 500 °C for 2 h and then Ni impregnation, followed by calcination at 500 °C for 2 h, resulting in a catalyst composition of 3% Ni and 6% Mo. Sulphided Ni–Mo/δ-Al_2O_3 (Cat C) was prepared by treating Cat B with 100 ppm H_2S in N_2 for 16 h (GHSV 400 h^{-1}) using a temperature ramp from 25 to 400 °C followed by a hold time of 10 h. After sulphidation, the catalyst was waxed using a C_{18} saturated hydrocarbon (octadecane) to ensure the sulphidated catalyst remain intact.

2.3 Catalytic Oxidation Reactions

The oxidative depolymerisation experiments were carried out in a 100 mL mechanically stirred Parr reactor equipped with a 4843 PID temperature controller (Parr Instruments Company, Moline, Illinois, USA). Three heterogeneous catalysts and the support were screened and tested for their ability to depolymerise the LS substrate under O_2 pressure. A schematic diagram of the experimental setup used in this study is shown in Fig. 2.

Typically, in a single run, the reactor was loaded with 30 mL of deionised water (DI), 600 mg of LS substrate and 300 mg of catalyst (catalyst-to-lignin ratio = 1:2 w/w). The reactor was purged (at least twice) and pressurised with molecular O_2 to 15 bar, where after the reactor under stirring (400 rpm) was heated to the reaction temperature of 160 °C. The reaction time was counted from the onset of the set temperature (heating time ~ 40 min). After completion of the reaction, the reactor was directly quenched in an ice bath and depressurised at room temperature (cooling time ~ 5 min).

2.4 Analysis of Products

The product mixtures were analysed using size exclusion chromatography (SEC), 2D nuclear magnetic resonance (NMR) spectroscopy and supercritical fluid chromatography mass spectrometry (SFC-MS).

2.4.1 SEC Analysis

The molecular weight distribution (MWD) and sizes of LS substrate and produced reaction mixtures were determined using a SEC system, as described in our previously developed method for technical lignin samples [25]. In brief, the system was a Waters 600E high-performance liquid chromatography setup (Waters, Milford, MA, USA) fitted with a Waters 2414 refractive index detector, a Waters 486 ultraviolet (UV) absorbance detector and an analytical column packed with 60 cm of Superdex 30 and 200 prep grade (GE Healthcare, Uppsala, Sweden). The column was operated at room temperature and eluted with 125 mM NaOH solution at a flowrate of 1.0 mL/min. Calibration was done using polyethylene glycol (PEG) standards ranging from 0.4 to 35 kDa (Merck Schuchardt OHG, Hohenbrunn, Germany). The samples were diluted at concentrations of 0.5 g/L in the eluent and the solutions were filtered using a 0.2 µm filter (Schleicher and Schuell, Dassel, Germany) to remove any suspended matter. The filtered solution (500 µL) was injected into the SEC system for data acquisition. Due to comparison with PEG standards, the molecular weight and the molecular number should be interpreted relatively.

2.4.2 NMR Spectroscopy

NMR samples of LS substrate and reaction products were prepared by mixing 500 µL substrate or product solution with 50 µL D_2O (Sigma-Aldrich, 99.9% D) in 5 mm NMR sample tubes. For product identification, ^{1}H–^{13}C HSQC and ^{1}H–^{1}H TOCSY spectra were acquired for product mixtures and for authentic reference compounds of acetaldehyde, formaldehyde, methanol, acetic acid, β-hydroxy-γ-butyrolactone, α-hydroxy-γ-butyrolactone, succinic acid, malic acid and maleic acid at 25 °C on a Bruker Avance III 800 MHz spectrometer equipped with a TCI CryoProbe. The ^{1}H–^{13}C HSQC spectra had a carrier offset of 75 ppm and a spectral width of 165 ppm in the ^{13}C dimension. ^{1}H–^{13}C HSQC spectra were recorded as data matrices of 2048 × 256 complex data points sampling the NMR signal for 159 and 7.7 ms in the ^{1}H and ^{13}C dimensions, respectively. A multiplicity-edited ^{1}H–^{13}C HSQC spectrum was acquired on the product mixture in order to gain additional structural insight by distinguishing CH, CH_2 and CH_3 groups. ^{1}H–^{1}H TOCSY spectra were acquired as data matrices of 1024 × 256 complex data points sampling the NMR signal for 128 and 32 ms in the direct and indirect ^{1}H dimension, respectively. The ^{1}H–^{1}H TOCSY spectra were acquired with a spectral width of 10 ppm in both dimensions around a carrier offset of 4.7 ppm using a 10 kHz spin lock field during a mixing time of 80 ms. A double quantum-filtered ^{1}H–^{1}H COSY spectrum of the water soluble product was acquired as a data matrix of 1024 × 256 complex data points with a spectral width of 13.3 ppm in both dimensions, sampling the NMR signal for 96 and 24 ms in the direct and indirect ^{1}H dimension, respectively. All spectra were processed with a shifted sine-bell apodisation function and extensive zero filling in both dimensions in Topspin 3.5.

2.4.3 SFC-MS Analysis

The LS substrate and reaction products were analysed using SFC-MS to reveal monomeric compounds present. Prior to analysis, the sample preparation was performed as described in our previously published method for the analysis of lignin monomers [26]; 10 mL of LS sample and the reaction product were acidified to pH 1 using 6 M HCl, and precipitates removed by centrifugation. The supernatants were extracted with 10 mL ethyl acetate (2 × 3 mL + 1 × 4 mL), and the corresponding extracts combined and the ethyl acetate evaporated under a nitrogen stream. The solid residues were redissolved in 3 mL ethyl acetate and filtered with a 0.2 µm polytetrafluoroethylene membrane syringe filter.

A Waters Ultra Performance Convergence Chromatography System (Waters, Milford, MA, USA) equipped with a Waters Torus DIOL (1.7 µm, 3 mm × 100 mm) and a Waters Torus Van-Guard pre-column (1.7 µm, 2.1 mm × 5 mm) was connected via a flow splitter (ACQUITY UPC^2 splitter, Waters) to a Waters XEVO-G2 QTOF-MS (Waters). A modified method of our previously published approach for the identification of lignin monomers using ultra-high-performance supercritical fluid chromatography/high resolution mass spectrometry (UHPSFC/HRMS) was used for analysis [26]. In short, a DIOL column was used with a column temperature of 50 °C, a flow rate of 2 mL and a backpressure of 130 bar. For the elution, a gradient was used starting with 0% B (vol%) and then ramped to 8.5% (vol%) until 2.5 min. Then B was increased to 25% (vol%) until 5.5 min and then held for 2 min. Then B was reduced in 0.5 min to 0% (vol%) and the column was equilibrated for 2 min with the starting condition before the next injection. The solvents were CO_2 (A) and methanol (B) and the injection volume was 1.5 µL. As a makeup solvent, methanol with 5 mM ammonia was used with a flow rate of 0.4 mL/min. The electrospray ionisation source was used in negative mode with a source temperature of 120 °C, a desolvation gas temperature of 600 °C, a desolvation gas flow of 1200 L/h, a cone voltage of 20 V and a capillary voltage of 3 kV. Both samples were analysed in full scan mode and in MS^2 mode. For the MS^2 mode, a collision induced dissociation energy ramp from 10 to 35 V was used.

2.5 Characterisation of Catalysts

The fresh and spent samples of best performing catalyst were characterised with Brunauer–Emmett–Teller (BET) nitrogen adsorption–desorption, scanning electron microscopy (SEM), energy dispersive spectroscopy (EDS) elemental mapping, powder X-ray diffraction (XRD), thermal gravimetric analysis (TGA), inductively coupled plasma optical emission spectrometry (ICP-OES) and X-ray photoelectron spectroscopy (XPS).

N_2 nitrogen physisorption measurements were performed at − 196 °C using an ASAP 2020 Micromeritics instrument (Norcross, GA, USA) for examining surface areas and porous structures of the catalyst samples. The samples were degassed at 200 °C under vacuum for 4 h prior to measurements, and the specific surface areas were estimated according to the BET method.

The morphology of the catalyst samples was examined through a high-resolution SEM (FEI Quanta 200F), fitted with an Everhart–Thornley detector (ETD). The images were recorded at low accelerating voltage (2 kV), with a spot size of 3, and with 1000 times magnification. EDS was used in connection with SEM for the elemental mapping and map sum spectra acquisition. The elemental mapping was collected using the same spectrophotometer.

Powder XRD analysis was performed with a Huber G670 diffractometer using Cu$K_{\alpha 1}$ radiation (λ = 1.54 Å) within a

2θ range of 3–100°, emitting from a focusing quartz monochromator. The radiation exposure time was 60 min.

TGA was carried out in a dynamic air environment using a Mettler Toledo Star^e thermal analyser (model TGA/DSC 1) in the temperature interval 25–600 °C with a constant heating rate of 10 °C/min. The thermal program was paused at 600 °C for 1 h during measurement.

The samples used for ICP-OES analysis (500 mg of catalyst per analysis) were dissolved in 7 mL of HNO_3 and 3 mL of water in a Mar5 microwave oven in a closed Teflon vessel, in which both temperature and pressure were controlled. The samples were then diluted 5 times with deionised water before analysis using an Optima 8300 from PerkinElmer (Waltham, MA, USA).

XPS spectra were acquired with a Thermo Scientific system at room temperature using monochromated AlK_α radiation (1484.6 eV). The base pressure in the analysis chamber was maintained at 2×10^{-7} mbar. The numbers of scans were 20, 20, 10 and 4 for Mn, Cu, Al and O, respectively.

3 Results and Discussion

3.1 Molecular Weight and Structural Features

To examine the variations between the lignin substrate and produced reaction products, the samples were analysed and compared in terms of molecular weight distribution and chemical structure. Figure 3 depicts the SEC curves of the initial LS substrate and the product mixtures generated from different experimental runs.

As can be seen, the Cu–Mn/δ-Al_2O_3 catalyst showed superior performance for converting the high-molecular-weight LS material into LMW products (M_p ~ 1.4 kDa).

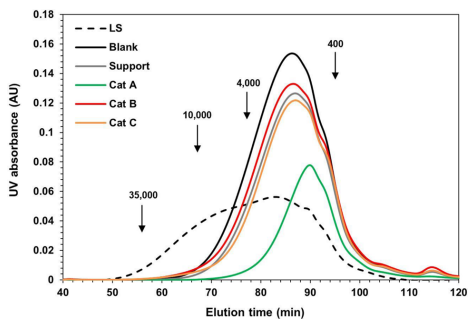


Fig. 3 Size exclusion chromatograms of lignosulphonate lignin and depolymerised samples with characteristic UV absorption at 280 nm. The arrows point to the molecular weight (Da) of the PEG standards that were used for calibration

In comparison to other investigated catalysts, the higher catalytic performance of Cu–Mn/δ-Al_2O_3 can be explained by the ability of transition metal ions – Mn and Cu – to form highly oxidised metallo–oxo complexes upon reaction with the molecular O_2. The product fractions also exhibited much narrower molecular weight distributions in comparison to the starting material, which exhibited a rather broad peak constituting exceedingly heavy molecules. The product fraction generated over Cu–Mn/δ-Al_2O_3, on the other hand, showed a maximum range of 10 kDa for heaviest contained molecules, suggesting that an effective depolymerisation process was achieved. The products generated over alumina support, Ni–Mo/δ-Al_2O_3 and sulphided Ni–Mo/δ-Al_2O_3 showed slightly better performance (molecular weight reductions) than the blank experiment. However, the changes were not significant, and Cu–Mn/δ-Al_2O_3 was thus selected for further detailed analysis.

In addition, it was revealed from the NMR measurements that there were notable differences in the chemical compositions of the LS sample and the product sample generated utilising Cu–Mn/δ-Al_2O_3 catalyst, particularly in the inter-unit/oxygenated aliphatic region. Figure 4 compares 2D ^{1}H–^{13}C HSQC spectra acquired in water of the original LS lignin (Fig. 4a) and of the product mixture obtained upon oxidative depolymerisation using Cu–Mn/δ-Al_2O_3 catalyst (Fig. 4b; see supplementary material Fig. S1 for a full overlay of substrate and product spectra). The spectra validate that LS is rich in guaiacyl content and low in syringyl content, with some residual xylan likely present from original pretreatment. Spectral comparison shows that oxidative depolymerisation vastly abolishes methoxy group signals (δ^1H ~ 3.5–4 ppm, δ^{13}C ~ 55 ppm) as well as other signals in the side-chain interunit linkage region (aliphatic oxygenated groups at δ^{13}C ~ 60–90 ppm). As C–C linkages constitute a considerable fraction of the interunit linkages present in technical lignin, the findings here suggest that Cu–Mn/δ-Al_2O_3 catalyst is capable of catalysing C–C bond cleavage of the propyl side-chain in the LS lignin structural units.

Consistent with recent reports for a chelator-mediated Fenton reaction [27], the water-soluble post-reaction material is also largely devoid of aromatic ^{1}H–^{13}C HSQC signals in our depolymerisation system. A variety of product signals can be observed. These products were characterised by the use of authentic reference standards and homonuclear assignment spectra (^{1}H–^{1}H TOCSY spectra) as well as multiplicity-edited ^{1}H–^{13}C HSQC to identify spin systems and structural motifs in the product molecules. Figure 4b shows an assigned ^{1}H–^{13}C HSQC spectrum with some molecules in the product mixture highlighted. Consistent with the loss of methoxy signal, the product mixture included methanol and its oxidation products formaldehyde (detected as the hydrate form) and formic acid as well as acetaldehyde (detected as hydrate and free aldehyde form) and acetic acid.

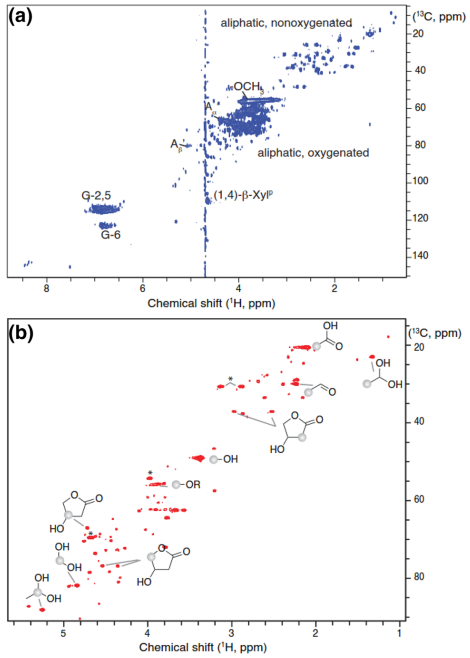


Fig. 4 Two-dimensional ^{1}H–^{13}C HSQC NMR spectrum of lignosulphonate lignin substrate (**a**) and spectrum of identified reaction products in oxidatively depolymerised sample using Cu–Mn/δ-Al_2O_3 catalyst, with the sphere indicating the CH group corresponding to indicated spectral signals (**b**). Products include methanol, formaldehyde, formic acid, acetaldehyde, acetic acid and β-hydroxy-γ-butyrolactone. The asterisk indicates a major mixture component that is tentatively assigned to the β-sulphonate derivative of γ-butyrolactone

The presence of these aldehydes in the product mixture indicates a stepwise reaction with aldehydes formed as highly populated intermediates. Notably, the product mixture also included larger polyhydroxylated carbonyl containing compounds such as β-hydroxy-γ-butyrolactone in addition to the β-sulphonate derivative of γ-butyrolactone (Fig. 4b). In a recent study, lactone species were identified as key condensation product in technical lignin streams [28], consistent with the presence of novel lactone markers. Unlike β-hydroxy-γ-butyrolactone, α-hydroxy-γ-butyrolactone was not observed in significant amount in the product mixture.

SFC-MS analysis was done to achieve qualitative molecular information about the samples. The base peak ion chromatograms of the LS and the oxidatively depolymerised lignosulphonate after reaction with Cu–Mn/δ-Al_2O_3 (Cat A) are shown in Fig. 5.

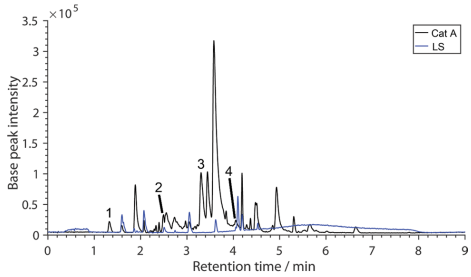


Fig. 5 Base peak ion chromatograms obtained from the SFC-MS analysis for lignosulphonate lignin (LS) substrate and oxidatively depolymerised product using Cu–Mn/δ-Al_2O_3 catalyst (Cat A). Peak identities: vanillin (1), *p*-hydroxybenzaldehyde (2), vanillic acid (3) and *p*-hydroxybenzoic acid (4)

Comparing the chromatograms, it can be seen that the catalytically treated sample showed more monomers than the LS sample and only vanillic acid was identified in the latter based on the retention time, exact mass and observed fragments (Table S1). In contrast, the four lignin monomers vanillin, *p*-hydroxybenzaldehyde, vanillic acid and *p*-hydroxybenzoic acid were identified by the same identification criteria in the catalytically depolymerised sample (Table S1). Vanillic acid was identified in both samples, but the significant difference in the peak intensities in the extracted ion chromatograms (Figs. S2 and S11) showed that additional vanillic acid was produced during the course of the oxidation reaction. The extracted ion chromatograms, mass spectra and MS^2 spectra for all identified compounds are shown in Figs. S2 to S16 (supplementary material).

3.2 Catalyst Characterisation

The δ-Al_2O_3 support used for the experiments had a specific surface area as measured by nitrogen physisorption of 128 m^2/g and a pore volume of 0.54 cm^3/g. The calculated average pore size (assuming cylindrical pores) was 16.7 nm. The rather open pore system was quite well in line with the sizes of lignin macromolecules reported, which are in the 1–40 nm range depending on source and extraction method [29], indicating that all catalyst inventory was available for reaction. Adding the active phase to the support slightly lowered the measured surface area (118 m^2/g for the Cu/Mn-catalyst and 116 m^2/g for the Ni/Mo-catalyst). The spent catalysts showed higher surface area than the fresh ones, probably due to carbon deposits in the catalyst pores. Due to the wax used in conserving the sulphided Ni–Mo catalyst, it was not possible to perform accurate BET analysis for Cat C. All properties as derived from the nitrogen physisorption measurements are summarised in Table 2.

Table 2 Textural properties as calculated by BET analysis

Catalyst	Specific surface area ($m^2\ g^{-1}$)	Pore size (nm)	Pore volume ($cm^3\ g^{-1}$)
δ-Al_2O_3 fresh	128.4	16.7	0.54
δ-Al_2O_3 spent	129.8	14.4	0.47
Cu–Mn/δ-Al_2O_3 fresh	118.1	15.6	0.46
Cu–Mn/δ-Al_2O_3 spent	145.3	11.8	0.43
Ni–Mo/δ-Al_2O_3 fresh	115.7	13.7	0.40
Ni–Mo/δ-Al_2O_3 spent	141.8	12.8	0.45

SEM images were obtained for the δ-Al_2O_3 catalyst support (Fig. 6a), the fresh Cu–Mn/δ-Al_2O_3 (Fig. 6b) and the spent Cu–Mn/δ-Al_2O_3 (Fig. 6c) to visualise the morphology of the materials. The images of the alumina support and the fresh catalyst showed only minor differences between the materials before and after the addition of the active phase on the 100 µm scale, whereas significant differences were found between the two fresh samples and the spent catalyst. Thus, in the spent catalyst, an uneven top-layer (dark grey areas) with islands of catalyst appeared to rise above the support surface.

TG analysis (Fig. 7) of the fresh and spent catalysts were quite different with the spent material losing much more weight between 300 and 450 °C – almost 10 wt% – compared to the fresh catalyst. This difference was attributed to vaporisation of heavier organic compounds, thermal decomposition of polymers and, at higher temperatures, oxidation of solid carbon, thus likely corresponding to the top-layer, which also induced a lowering of the BET surface area as discussed above.

SEM–EDS images with corresponding elemental spectra of the fresh and spent Cu–Mn/δ-Al_2O_3 catalyst, respectively (Fig. 8), further revealed a significant increase in the sulphur

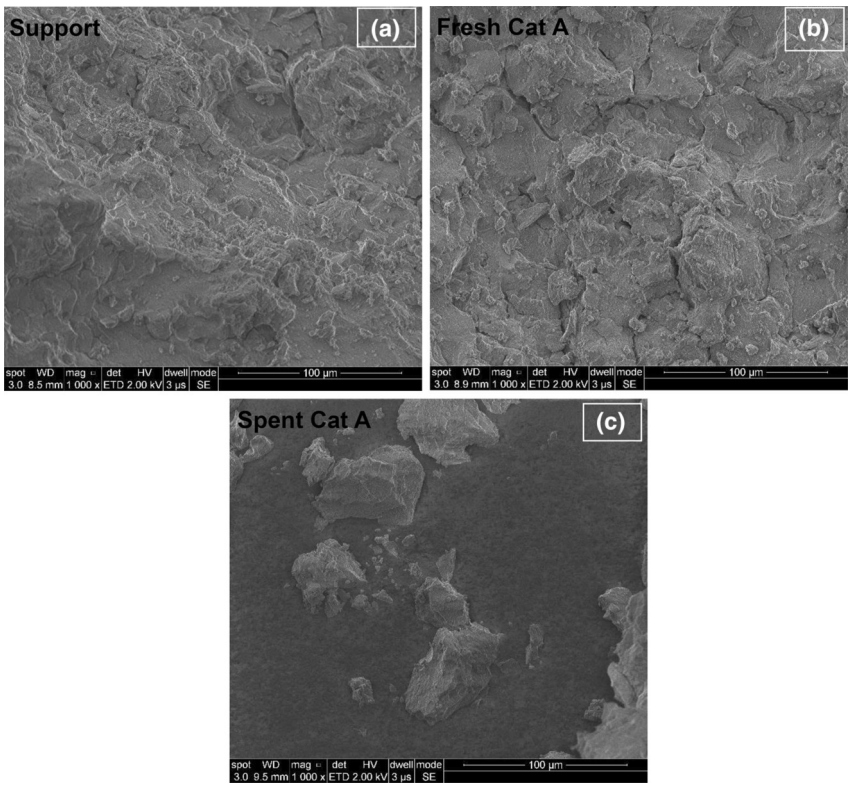


Fig. 6 SEM images of the **a** δ-Al_2O_3 support, **b** fresh Cu–Mn/δ-Al_2O_3 catalyst and **c** spent Cu–Mn/δ-Al_2O_3 catalyst

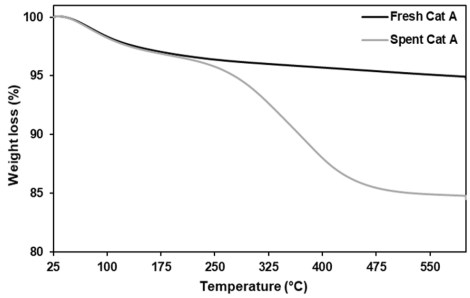


Fig. 7 TGA curves of the fresh and spent Cu–Mn/δ-Al_2O_3 catalyst

amount in the spent catalyst compared to the fresh catalyst. In addition, the signal intensity with respect to Mn and Cu appeared to be lower in the spent catalyst, which may be due to the previously mentioned top-layer. Notably, no changes in the bulk of the catalyst were indicated from the powder X-ray diffraction patterns of the materials (Fig. 9), which revealed only diffractions peaks consistent with δ-Al_2O_3 at 2θ of 32, 36, 45, 61, 67 and 85° [30].

The catalyst surface composition was further investigated using XPS and revealed several differences between the fresh and spent catalysts according to the analysis in Table 3. First, a high surface sulphur content of 1.7 atomic% was found for the spent catalyst after the lignin oxidative depolymerisation reaction. Second, the spent catalyst had a significantly lower surface concentration of Mn (0.4 atomic% against 3.3 atomic% in the fresh catalyst), whereas the surface Cu concentration remained almost unchanged. The decrease in Mn content clearly indicated leaching of Mn from the supported catalyst during operation, which may also have contributed to the observed catalytic activity as Mn ions have been reported to be active for lignin depolymerisation reactions [31].

The leaching of Mn was confirmed and quantified using ICP-OES analysis. The measured composition of the fresh

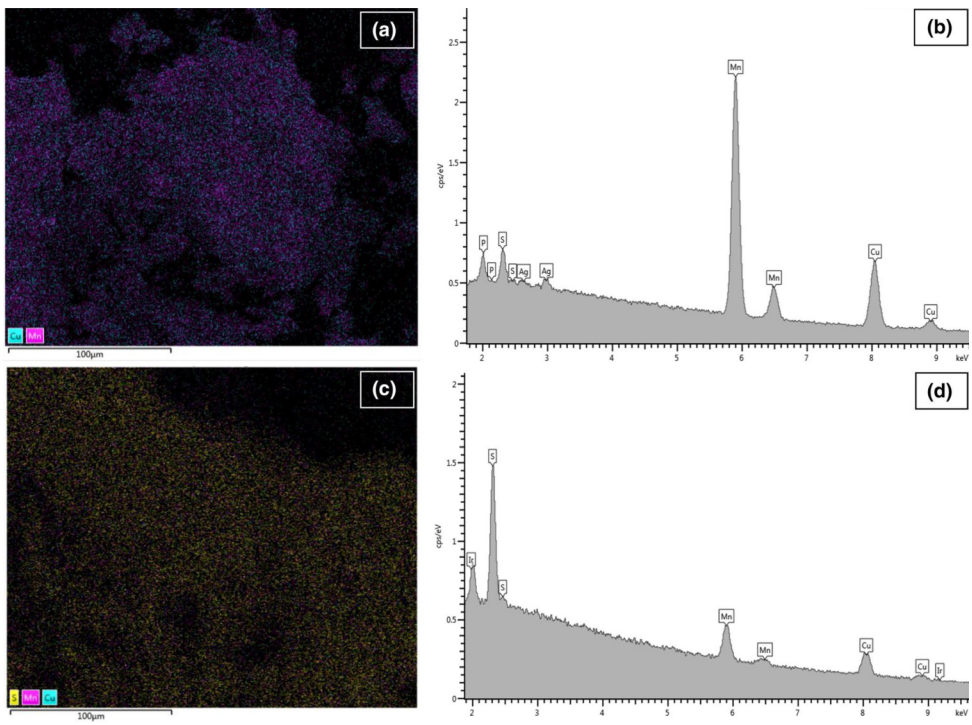


Fig. 8 SEM–EDS elemental mapping and map sum spectra of the **a, b** fresh Cu–Mn/δ-Al_2O_3 catalyst and **c, d** spent Cu–Mn/δ-Al_2O_3 catalyst

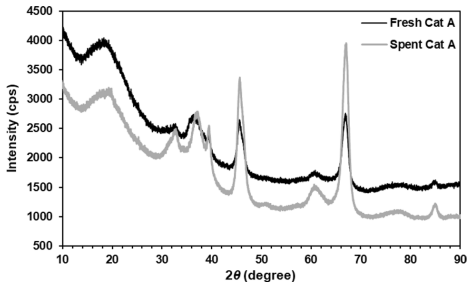


Fig. 9 XRD patterns of the fresh and spent Cu–Mn/δ-Al_2O_3 catalyst

Table 3 Surface elemental composition (% atomic concentration) as determined by XPS

Catalyst	Al2p	O1s	Cu2p	Mn2p	S2p
Cu–Mn/δ-Al_2O_3 fresh	38.1	58.3	0.3	3.3	–
Cu–Mn/δ-Al_2O_3 spent	38.3	59.2	0.4	0.4	1.7

Cu–Mn/δ-Al_2O_3 catalyst was 3.15 wt% Mn and 2.29 wt% Cu; the catalyst contained no or very low amounts of sulphur. After the oxidative depolymerisation, the metal content in the catalyst were lowered to 0.34 wt% Mn and 0.48 wt% Cu, revealing that also Cu had leached from the catalyst even though the surface concentration apparently remained unchanged as found by XPS. Moreover, the sulphur content had increased considerably to 0.42 wt%. Combined, these results showed that the catalyst was not stable under the operating conditions tested, hindering the performance of recyclability tests and the investigation of catalyst reusability. Further optimisation is required to ensure long-term, stable operation.

4 Conclusions

Alumina-supported Cu–Mn and Ni–Mo catalysts were tested for their ability to depolymerise sodium lignosulphonates, a technical lignin stream generated from sulphite pulping. Under O_2 pressure, Cu–Mn/δ-Al_2O_3 showed a surpassing performance in converting LS into LMW compounds. Major compounds identified were vanillin, *p*-hydroxybenzaldehyde, vanillic acid and *p*-hydroxybenzoic acid in addition to smaller aliphatic aldehydes, acids and lactones. Such product streams can potentially be utilised in a diverse form of value-added applications in current fast-growing chemical and bio-based industries. Unfortunately, the long-term performance and the stability of the most active Cu–Mn/δ-Al_2O_3 catalyst was influenced negatively by the operating conditions, resulting in deposits of carbon- and sulphur-containing compounds on the catalyst surface as well as leaching of Mn and Cu ions. Hence, optimisation of catalyst durability remains a key for future work and possible successful industrial operation.

Acknowledgements This work was financed by the Swedish Foundation for Strategic Research (SSF) through grant contract RBP14-0052. O.Y. Abdelaziz acknowledges the internal funding of Lund University and Technical University of Denmark. Thanks to Hulteberg Chemistry & Engineering AB for providing the catalysts used in this study, and Gunnar Lidén for supplying the sodium lignosulphonates from Domsjö Fabriker AB. Bodil Fliis Holten, Sofia Mebrahtu Wisén, Leonhard Schill, Lise-Lotte Jespersen and Berit Wenzell are acknowledged for technical support with characterisation of the catalysts. 800 MHz NMR spectra were recorded by using the spectrometer of the NMR centre DTU supported by the Villum Foundation.

Open Access This article is distributed under the terms of the Creative Commons Attribution 4.0 International License (http://creativecommons.org/licenses/by/4.0/), which permits unrestricted use, distribution, and reproduction in any medium, provided you give appropriate credit to the original author(s) and the source, provide a link to the Creative Commons license, and indicate if changes were made.

References

1. Gall DL, Ralph J, Donohue TJ, Noguera DR (2017) Biochemical transformation of lignin for deriving valued commodities from lignocellulose. Curr Opin Biotechnol 45:120–126. https://doi.org/10.1016/j.copbio.2017.02.015
2. Sjöström E (1993) Wood chemistry: fundamentals and applications, 2nd edn. Academic Press, San Diego
3. Calvo-Flores FG, Dobado JA, Isac-García J, Martín-Martínez FJ (2015) Lignin and lignans as renewable raw materials: chemistry, technology and applications. Wiley, Chichester
4. Bruijnincx PCA, Rinaldi R, Weckhuysen BM (2015) Unlocking the potential of a sleeping giant: lignins as sustainable raw materials for renewable fuels, chemicals and materials. Green Chem 17:4860–4861. https://doi.org/10.1039/c5gc90055g
5. Ragauskas AJ, Beckham GT, Biddy MJ et al (2014) Lignin valorization: improving lignin processing in the biorefinery. Science 344:1246843
6. Azadi P, Inderwildi OR, Farnood R, King DA (2013) Liquid fuels, hydrogen and chemicals from lignin: a critical review. Renew Sustain Energy Rev 21:506–523. https://doi.org/10.1016/j.rser.2012.12.022
7. Abdelaziz OY, Brink DP, Prothmann J et al (2016) Biological valorization of low molecular weight lignin. Biotechnol Adv 34:1318–1346. https://doi.org/10.1016/j.biotechadv.2016.10.001
8. Rinaldi R, Jastrzebski R, Clough MT et al (2016) Paving the way for lignin valorisation: recent advances in bioengineering, biorefining and catalysis. Angew Chemie Int Ed 55:8164–8215. https://doi.org/10.1002/anie.201510351
9. Guadix-Montero S, Sankar M (2018) Review on catalytic cleavage of C–C inter-unit linkages in lignin model compounds: towards lignin depolymerisation. Top Catal 61:183–198. https://doi.org/10.1007/s11244-018-0909-2
10. Aro T, Fatehi P (2017) Production and application of lignosulfonates and sulfonated lignin. ChemSusChem 10:1861–1877. https://doi.org/10.1002/cssc.201700082

11. Güvenatam B, Heeres EHJ, Pidko EA, Hensen EJM (2016) Lewis-acid catalyzed depolymerization of protobind lignin in supercritical water and ethanol. Catal Today 259:460–466. https://doi.org/10.1016/j.cattod.2015.03.041
12. Lahive CW, Deuss PJ, Lancefield CS et al (2016) Advanced model compounds for understanding acid-catalyzed lignin depolymerization: identification of renewable aromatics and a lignin-derived solvent. J Am Chem Soc 138:8900–8911. https://doi.org/10.1021/jacs.6b04144
13. Chaudhary R, Dhepe PL (2017) Solid base catalyzed depolymerization of lignin into low molecular weight products. Green Chem 19:778–788. https://doi.org/10.1039/C6GC02701F
14. Abdelaziz OY, Li K, Tunå P, Hulteberg CP (2018) Continuous catalytic depolymerisation and conversion of industrial kraft lignin into low-molecular-weight aromatics. Biomass Convers Biorefinery 8:455–470. https://doi.org/10.1007/s13399-017-0294-2
15. Pandey MP, Kim CS (2011) Lignin depolymerization and conversion: a review of thermochemical methods. Chem Eng Technol 34:29–41
16. Amen-Chen C, Pakdel H, Roy C (2001) Production of monomeric phenols by thermochemical conversion of biomass: a review. Bioresour Technol 79:277–299. https://doi.org/10.1016/S0960-8524(00)00180-2
17. Wu W, Dutta T, Varman AM et al (2017) Lignin valorization: two hybrid biochemical routes for the conversion of polymeric lignin into value-added chemicals. Sci Rep 7:8420. https://doi.org/10.1038/s41598-017-07895-1
18. Feghali E, Carrot G, Thuéry P et al (2015) Convergent reductive depolymerization of wood lignin to isolated phenol derivatives by metal-free catalytic hydrosilylation. Energy Environ Sci 8:2734–2743
19. Huang S, Mahmood N, Tymchyshyn M et al (2014) Reductive de-polymerization of kraft lignin for chemicals and fuels using formic acid as an in-situ hydrogen source. Bioresour Technol 171:95–102. https://doi.org/10.1016/j.biortech.2014.08.045
20. Rodrigues Pinto PC, Borges da Silva EA, Rodrigues AE (2011) Insights into oxidative conversion of lignin to high-added-value phenolic aldehydes. Ind Eng Chem Res 50:741–748. https://doi.org/10.1021/ie102132a
21. Ma R, Guo M, Zhang X (2018) Recent advances in oxidative valorization of lignin. Catal Today 302:50–60. https://doi.org/10.1039/9781788010351-00128
22. Tarabanko VE, Tarabanko N (2017) Catalytic oxidation of lignins into the aromatic aldehydes: general process trends and development prospects. Int J Mol Sci 18:2421. https://doi.org/10.3390/ijms18112421
23. Behling R, Valange S, Chatel G (2016) Heterogeneous catalytic oxidation for lignin valorization into valuable chemicals. What results? What limitations? What trends? Green Chem 18:1839–1854. https://doi.org/10.1039/c5gc03061g
24. Vangeel T, Schutyser W, Renders T, Sels BF (2018) Perspective on lignin oxidation: advances, challenges, and future directions. Top Curr Chem. https://doi.org/10.1007/s41061-018-0207-2
25. Abdelaziz OY, Hulteberg CP (2017) Physicochemical characterisation of technical lignins for their potential valorisation. Waste Biomass Valorization 8:859–869. https://doi.org/10.1007/s12649-016-9643-9
26. Prothmann J, Sun M, Spégel P et al (2017) Ultra-high-performance supercritical fluid chromatography with quadrupole-time-of-flight mass spectrometry (UHPSFC/QTOF-MS) for analysis of lignin-derived monomeric compounds in processed lignin samples. Anal Bioanal Chem 409:7049–7061. https://doi.org/10.1007/s00216-017-0663-5
27. Kent MS, Zeng J, Rader N et al (2018) Efficient conversion of lignin into a water-soluble polymer by a chelator-mediated Fenton reaction: optimization of H_2O_2 use and performance as a dispersant. Green Chem 20:3024–3037. https://doi.org/10.1039/c7gc03459h
28. Lancefield CS, Wienk HLJ, Boelens R et al (2018) Identification of a diagnostic structural motif reveals a new reaction intermediate and condensation pathway in kraft lignin formation. Chem Sci 9:6348–6360. https://doi.org/10.1039/c8sc02000k
29. Vainio U, Maximova N, Hortling B et al (2004) Morphology of dry lignins and size and shape of dissolved kraft lignin particles by X-ray scattering. Langmuir 20:9736–9744. https://doi.org/10.1021/la048407v
30. Sieber M, Mehner T, Dietrich D et al (2014) Wear-resistant coatings on aluminium produced by plasma anodising—a correlation of wear properties, microstructure, phase composition and distribution. Surf Coat Technol 240:96–102. https://doi.org/10.1016/j.surfcoat.2013.12.021
31. Ziebell A (2008) Modelling lignin depolymerisation using size exclusion chromatography. Swinburne University of Technology, Hawthorn

Publisher's Note Springer Nature remains neutral with regard to jurisdictional claims in published maps and institutional affiliations.

Paper V

This is an open access article published under an ACS AuthorChoice License, which permits copying and redistribution of the article or any adaptations for non-commercial purposes.

ACS Sustainable Chemistry & Engineering

Cite This: ACS Sustainable Chem. Eng. 2019, 7, 11640−11652

Research Article

pubs.acs.org/journal/ascecg

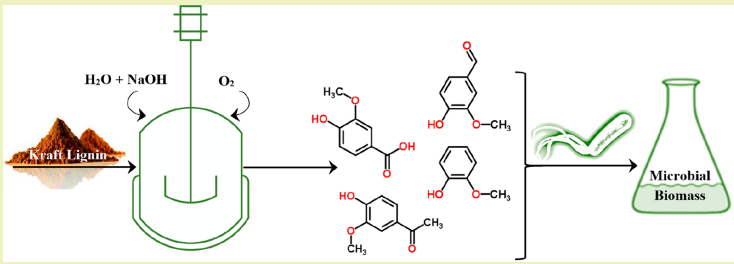
Oxidative Depolymerization of Kraft Lignin for Microbial Conversion

Omar Y. Abdelaziz,[†,‡] Krithika Ravi,[†] Fabian Mittermeier,[†] Sebastian Meier,[‡] Anders Riisager,[‡] Gunnar Lidén,[†] and Christian P. Hulteberg*[,†]

[†]Department of Chemical Engineering, Lund University, Naturvetarvägen 14, 221 00 Lund, Sweden

[‡]Department of Chemistry, Technical University of Denmark, Kemitorvet 207, 2800 Kgs. Lyngby, Denmark

Supporting Information



ABSTRACT: The valorization of lignin is being increasingly recognized as crucial to improve the economic viability of integrated biorefineries. Because of its inherent heterogeneity and recalcitrance, lignin has been treated as a waste product in the pulp and paper industry, but new technologies are now being explored to transform lignin into a sustainable resource and enhance its value chain. In the present study, alkaline oxidative depolymerization was investigated as a potential form of pretreatment to enable further biological conversion of LignoBoost kraft lignin (LB). LB lignin oxidation reactions were studied at various temperatures (120−200 °C) and O_2 partial pressures (3−15 bar) to identify the optimal conditions for obtaining a biocompatible, oxidatively depolymerized lignin (ODLB) stream. The low molecular weight compounds resulting from this treatment consisted mainly of aromatic monomers and carboxylic acids. The highest yield of aromatic monomers, 3 wt %, was obtained at 160 °C and 3 bar O_2. The yield of carboxylic acids increased with both increasing temperature and O_2 pressure, exceeding 13% under the harshest conditions investigated. The growth of four aromatic-catabolizing bacterial strains was examined on reaction product mixtures, all of which showed growth on agar plates utilizing ODLB as the sole source of carbon and energy. *Rhodococcus opacus* and *Sphingobium* sp. SYK-6 were found to consume most of the aromatic monomers present in the ODLB (e.g., vanillin, vanillate, acetovanillone, and guaiacol). The findings of this study indicate that pretreatment by oxidative depolymerization has potential in the biological valorization of technical lignin streams, for the production of valuable chemicals and materials.

KEYWORDS: *Alkaline oxidation, Aromatic monomers, Bacterial conversion, Lignin valorization, LignoBoost, Softwood, Sustainable resources*

INTRODUCTION

Lignin is considered the most abundant terrestrial non-carbohydrate biopolymer, comprising 15−30 wt % of dry lignocellulosic biomass.[1−4] As a raw material, lignin has considerable potential in a lignocellulosic biorefinery but also poses significant challenges.[5,6] The valorization of lignin would improve the economics of biomass conversion, as the use of lignin today is primarily limited to combustion for energy recovery in pulp mills. Apart from economic considerations, environmental concerns must also be taken into account in the development of future lignin biorefinery concepts, and the principles of green chemistry should be adopted in lignin processing and conversion.[7]

Kraft pulping is the process most commonly used to produce paper pulp worldwide.[8] In this operation, wood is transformed into wood-pulp by treatment with a Na_2S/NaOH solution, so-called white liquor, at temperatures of 155−175 °C for several hours,[9] during which 90−95% of the lignin in the starting material is dissolved.[10] The annual production of kraft pulp worldwide is about 130 million tons,[11] and the kraft lignin black liquor generated represents the largest share of the biofuel sector in the Swedish and the Finnish energy matrices.[12] LignoBoost is a well-proven technology for commercial-scale kraft lignin

Received: March 21, 2019
Revised: May 6, 2019
Published: June 13, 2019

 © 2019 American Chemical Society

DOI: 10.1021/acssuschemeng.9b01605
ACS Sustainable Chem. Eng. 2019, 7, 11640−11652

recovery.[13,14] This process enables high-purity lignin production with rather low ash and carbohydrate contents. Considering the dominant role of kraft processes,[15] and that lignin is an abundant, inexpensive resource of aromatics, new applications based on utilizing kraft lignin from black liquor are desirable.

The challenges associated with the utilization and conversion of (technical) kraft lignin into bulk or specialty chemicals are the result of the highly complex and heterogeneous nature of this biomacromolecule. The condensed structures, highly recalcitrant linkages, and presence of sulfur render kraft lignin a difficult raw material to process and transform.[16,17] The development of efficient methods of depolymerization will thus play a central role in the valorization of kraft lignin for the production of valuable platform chemicals.[18]

The depolymerization of technical lignin is a demanding task, as processing, such as kraft cooking, usually results in significant changes in the lignin structure. Condensation of reactive intermediate motifs via C−C bond formation and the cleavage of aryl ether bonds (predominantly β-O-4 linkages)[4,19] during the cooking process make it structurally different from native lignin and more resistant to break down. Lignin depolymerization approaches reported in the literature include thermal,[20] biochemical,[21−23] acid-catalyzed,[24] base-catalyzed,[25−27] oxidative,[28−31] and reductive[32,33] methods. Among these, the oxidation approach represents an energy-efficient means of lignin decomposition, while generating targeted products in a selective way, including valuable chemicals such as phenolic aldehydes, phenolic acids, and carboxylic acids.[34−37] Oxidation also allows the pH of reaction product mixtures to be controlled, by monitoring the yields of aliphatic carboxylic acids, while reducing the recalcitrance of lignin structures. Therefore, chemochemical oxidative depolymerization may be a valuable pretreatment step in biochemical lignin conversion.

Microbial funneling, i.e., the use of converging microbial pathways toward a common intermediate, is a promising approach to tackle the multitude of compounds in lignin-derived streams.[38−40] Several microorganisms have been utilized in previous studies for the bioconversion of pretreated lignin streams. Microbial growth and the accumulation of intracellular storage compounds have been investigated in alkaline-pretreated liquor from corn stover using several bacteria. In a study including 14 bacterial strains, *Amycolatopsis* sp., *Pseudomonas putida*, and *Acinetobacter* ADP1 were reported to depolymerize and catabolize 30% of the initial lignin present.[22] In another recent study on the conversion of depolymerized kraft lignin employing base catalysis, *Pseudomonas fluorescens* was reported to break down high molecular weight lignin, and *Rhodococcus opacus* was reported to consume most of the available aromatic monomers.[41] The intracellular accumulation of lipids in *R. opacus* growing on oxygen-treated kraft lignin has also been assessed, showing an accumulation of 0.07 g/L microbial lipids, mainly composed of palmitic and stearic acids.[42] The ability of bacterial species to metabolize depolymerized lignin depends on several factors, including the plant origin of the lignin, whether the lignin is technical or native, the type and severity of pretreatment, and the complexity of the product mixture. It is therefore important to screen for, and select, the appropriate microorganism for a given substrate. In contrast, the mode of lignin separation, such as LignoBoost, LignoForce, or similar commercially available methods, is not believed to greatly influence the suitability with respect to biocompatibility.

In the present work, alkaline oxidative depolymerization of an industrial lignin stream (LignoBoost softwood kraft) was examined, and the effect of reaction severity on molecular weight distribution and the formation of low molecular weight products was evaluated. Microbial conversion of the depolymerized products was further assessed to identify the treatment conditions that provided a biocompatible product stream with the potential for bacterial conversion. The growth of four aromatic-catabolizing bacterial species: *P. putida* KT2440, *P. fluorescens*, *R. opacus*, and *Sphingobium* sp. SYK-6, on various product mixtures was evaluated. High-cell-density liquid cultivations were performed using lignin treated at a selected condition to analyze the consumption of monomers and possible effects on molecular weight by enzymatic degradation. The study demonstrates the potential of oxidative depolymerization as a means of pretreatment toward the microbial conversion of technical lignin and is, to the best of our knowledge, the first integrated study exploring the parameter space of oxidative depolymerization and the resulting effect on lignin conversion by multiple bacterial species.

EXPERIMENTAL SECTION

Chemicals and Materials. LignoBoost lignin (LB), a softwood kraft technical lignin, was obtained as a dry powder from Innventia's pilot plant located in Bäckhammar, Sweden. Oxygen gas ($O_2 \geq 99.5\%$) was supplied by AGA Industrial Gases, Denmark. The bacterial species *Pseudomonas putida* KT2440 (DSM 6125), *Pseudomonas fluorescens* (DSM 50090), and *Rhodococcus opacus* (DSM 1069) were purchased from Deutsche Sammlung von Mikroorganismen and Zellkulturen (Braunschweig, Germany). *Sphingobium sp.* SYK-6 (JCM 17495) was purchased from the Japan Collection of Microorganisms (Tsukuba, Japan). M9 mineral medium was used for all the plate and liquid culture experiments. The medium consisted of the following buffer salts (per L): 6 g of Na_2HPO_4, 3 g of KH_2PO_4, 1 g of NH_4Cl, 0.5 g of NaCl, 2 mM $MgSO_4$, 100 μM $CaCl_2$, and 10 mL of trace element mixture.[43] Sterile/aseptic conditions were maintained throughout the cultivations. LB or oxidatively depolymerized LB was used as the sole carbon source at a concentration of 2−10 g/L. Before being added to the culture media, the substrates were acidified (if necessary) to pH ≈ 9 using sulfuric acid and were sterile filtered. The initial pH of cultivation media was 7. All chemicals and reagents were of analytical grade and were used as received without further purification, unless otherwise stated.

Oxidative Depolymerization of LB. The oxidative depolymerization reactions were conducted in a 100 mL mechanically stirred Parr reactor equipped with a 4843 PID temperature controller (Parr Instruments Company, Moline, Illinois, USA). In a typical run, the reactor was loaded with 30 mL of 0.2 M NaOH aqueous solution (deionized water) and 600 mg of LB substrate. The reactor was purged (three times) and pressurized with pure O_2 to the target pressure and then heated to the desired reaction temperature (±3 °C) while stirring (500 rpm) and was maintained at this temperature for a reaction time of 30 min. The heating time was ∼30−40 min, depending on the reaction temperature. A matrix of nine experiments with various combinations of reaction temperature (120−200 °C) and O_2 partial pressure (3−15 bar) was investigated. After the desired reaction time, the reactor was rapidly quenched in an ice bath and depressurized at room temperature (cooling time ≤5 min). The liquid products were finally collected for analysis and bacterial screenings.

To produce sufficient substrate for further microbial conversion experiments, upscaled oxidative depolymerization was performed using a similar method to that described above, with a 300 mL mechanically stirred Parr reactor equipped with a 4848 PID controller (featuring autotuning capability for precise temperature/pressure control and minimum overshoot). The reactor was loaded with 100 mL of NaOH aqueous solution (0.2 M; deionized water) and 2 g of LB substrate. The selected reaction conditions were 160 °C (±2 °C), 3 bar O_2, and 30 min reaction time under stirring (500 rpm). The product is henceforth denoted ODLB.

DOI: 10.1021/acssuschemeng.9b01605
ACS Sustainable Chem. Eng. 2019, 7, 11640−11652

Biochemical Conversion of ODLB. Glycerol stocks (at −80 °C) containing the bacteria were streaked on nutrient-rich medium plates and incubated at 30 °C for 24 h. M9 medium plates (with 1.5% agar), supplemented with 2 g/L lignin, were then inoculated with a single colony from the nutrient-rich medium plates and incubated at 30 °C for 7 days. All plate experiments were carried out in duplicate. The plates were regularly checked, and growth was documented by visual inspection.

Liquid culture experiments were carried out in 250 mL shake flasks containing 50 mL of culture media. M9 media with 10 g/L glucose were used for precultures of *P. putida*, *P. fluorescens*, and *R. opacus*. *Sphingobium* sp. SYK-6 was precultured in Trypticase soy broth supplemented with yeast extract. All precultures were inoculated from a single colony from the respective rich-media plates and incubated overnight at 30 °C with orbital shaking (180 rpm). Cells from the precultures were then washed with saline and subsequently used to inoculate flasks containing a sufficient amount of lignin to achieve an initial optical density of ∼4. All shake flask experiments were performed in duplicate. Samples were withdrawn at regular intervals to monitor growth, changes in molecular weight, and the consumption of aromatic monomers. Biomass growth was determined by measuring the optical density at 620 nm (OD_{620}). The samples were diluted with saline when required to ensure that the optical density remained in the linear range of 0.03−0.3. As the color of lignin is dark, the respective culture supernatants were used as blanks prior to biomass measurements. The cells were then removed by centrifugation (3 min at 12300*g*), and the supernatants were stored at −20 °C for chemical analysis.

Characterization and Product Analysis. Size exclusion chromatography (SEC) was used to determine the molecular weight distribution (MWD), the weight-average molecular weight (M_w), and the number-average molecular weight (M_n) of LB and the ODLB products. The SEC system consisted of an AZURA high-performance liquid chromatography (HPLC) setup (Knauer, Berlin, Germany) with UV (UVD 2.1L) and RI (RID 2.1L) detectors, and a P 6.1L pump. Samples were injected with a Smartline Autosampler 3950, and the system was controlled, and peak evaluations were managed, using ClarityChrom 6.1.0 software. Two Superdex 10/300 GL columns, Peptide and 200 Increase (GE Healthcare Bio-Sciences AB, Uppsala, Sweden) were used to ensure high resolution over a large range of molecular weights (one column was used at a time). Analysis was performed at ambient temperature, under isocratic conditions, with a linear velocity of 23 cm/h. Calibration was carried out using nine different sodium polystyrene sulfonate standards, with molecular weights in the range of 200 Da to 150 kDa. Each sample was diluted with 0.1 M NaOH to a concentration of 0.5−1 g/L and filtered (0.22 μm) to remove any suspended matter. The volume of filtered solution injected was 50 μL, and elution was performed for 100 min using an aqueous solution containing 0.1 M NaOH.

Changes in the MWD of the samples after fermentation were analyzed using another SEC system, as described previously.[44] This consisted of a Waters 600E chromatography system with an analytic column packed with 30 cm Superdex 30 and 30 cm Superdex 200 coupled to a Waters 2414 RI detector and a Waters 486 UV detector. The mobile phase used was 0.5 wt % NaOH at a flow rate of 1 mL/min (isocratic elution). The samples were centrifuged to remove the cells, and the supernatants were filtered and diluted (final concentration 0.5 g/L) before analysis. The injection volume was 500 μL, and the total run time for each sample was 180 min. Lignin samples were compared before and after bioconversion by overlaying the SEC chromatograms obtained.

An ultraperformance liquid chromatography (UPLC) system (Waters Acquity) equipped with a photodiode array detector (Waters, Milford, MA, USA) was used for identification and quantification of the aromatic monomers in the lignin samples. The column used for separation was ethylene-bridged hybrid C_{18} with an internal diameter of 2.1 mm, 100 mm length, and 1.7 μm particle size. The temperature of the column was maintained at 50 °C. The mobile phase used was a mixture of 3% acetonitrile, 96.5% water, 0.5% acetic acid (fraction A), and 86.5% acetonitrile, 13% water, 0.5% acetic acid (fraction B). The lignin samples were diluted with mobile phase (fraction A) to a final concentration of 0.5 g/L, and a volume of 2.5 μL was injected. Gradient elution at a flow rate of 0.6 mL/min was used for analysis. The method started with 100% A, decreased to 90% A over 5 min, held at 90% A for 2 min, and decreased to 25% A over 4.5 min. After each sample was analyzed, the column was washed with 100% B for 5 min and then equilibrated with 100% A for 5 min. An Acquity UPLC Console was used to control the system, and Empower 3 was used to process the data. The compounds were identified by comparing the retention time and UV spectra (if necessary) with the corresponding standards. Peaks were quantified using the area under the curve against their respective calibration standards. The yields of aromatic monomers (in %) were calculated based on the initial weight of lignin (estimated analysis deviation ±5%).

A Waters Acquity HPLC system equipped with a UV and RI detector (Water, Milford, MA, USA) was used for the identification and quantification of nonaromatic acids. The column used for separation was an Aminex HPX-87H, at a temperature of 60 °C. The mobile phase was 5 mM H_2SO_4 at a flow rate of 0.6 mL/min (isocratic elution). The sample injection volume was 20 μL, and the total run time for each sample was 50 min. The data were reviewed and processed using Empower 3 software, and the compounds were identified by comparing the retention time with the respective standards. Peaks were quantified using the area under the curve against their respective calibration standards. The yields of nonaromatic acids (in %) were calculated based on the initial weight of lignin (estimated analysis deviation ±5%).

Nuclear magnetic resonance (NMR) spectroscopy was used to analyze samples of the LB substrate and ODLB product by mixing 100 mg of the substrate or product with 600 μL of DMSO-d_6 (Sigma-Aldrich, 99.9% D) and transferring the resultant samples to 5 mm NMR sample tubes. Two-dimensional $^1H-^{13}C$ correlation spectra of the substrate and product mixtures were recorded at 50 °C on a Bruker Avance III 800 MHz spectrometer equipped with a TCI CryoProbe. The $^1H-^{13}C$ heteronuclear multiple-bond correlation (HMBC) spectra had a carrier offset of 110 ppm and a spectral width in the ^{13}C dimension of 220 ppm. These $^1H-^{13}C$ HMBC spectra were recorded as data matrices of 2048 × 128 complex data points sampling the NMR signal for 197 and 2.9 ms in the ^1H and ^{13}C dimensions, respectively. An interscan recycle delay of 1.5 s and the accumulation of 128 scans per increment were employed, resulting in an analysis time of 16.5 h per HMBC spectrum. $^1H-^{13}C$ heteronuclear single-quantum correlation (HSQC) spectra with a carrier offset of 90 ppm and a spectral width in the ^{13}C dimension of 180 ppm were recorded as data matrices of 1024 × 160 complex data points sampling the NMR signals for 106 and 4.4 ms in the ^1H and ^{13}C dimensions, respectively. An interscan recycle delay of 1.5 s and the accumulation of 32 scans per increment were used, which resulted in an analysis time of 4.5 h per HSQC spectrum. All spectra were processed with extensive zero filling in both dimensions with Topspin 3.5.

High-resolution scanning electron microscopy (SEM) was used to visualize the morphologies of the lignin samples using an FEI Quanta 200F microscope. The instrument was operated in low-vacuum mode to obtain charge contrast imaging data using a large field detector. Before measurements, the samples were gold coated using a current of 20 mA and 10 s sputter time (Quorum Q150T ES, Quorum Technologies Ltd., Laughton, UK) in order to minimize charging effects. Images were recorded at a low accelerating voltage (3 kV), with a spot size of 3.0, and magnification of 10 000 times.

Nitrogen adsorption−desorption isotherms were measured on an ASAP 2020 Micromeritics instrument (Norcross, GA, USA) to examine the surface areas and porous structures of the lignin samples. The samples were degassed at 110 °C under high vacuum for 4 h prior to measurements. The Brunauer−Emmet−Teller (BET) and Barrett−Joyner−Halenda methods[45,46] were applied in the analysis to obtain the surface area (estimated deviation ±0.2 m^2/g) and pore volume (estimated deviation ±0.001 cm^3/g), respectively.

RESULTS AND DISCUSSION

Oxidative Depolymerization of LB − Effects on Molecular Weight Distribution. The molecular weight is a

DOI: 10.1021/acssuschemeng.9b01605
ACS Sustainable Chem. Eng. 2019, 7, 11640−11652

fundamental property of lignin and lignin-derived fractions, as it greatly impacts the recalcitrance and thus the valorization, of lignin. The most common characterization method used is SEC,[47] which has proven reliable in determining the M_w and MWD of kraft lignin and its depolymerized fractions.[17,27,33,48,49] SEC was used to evaluate the changes in molecular weight of lignin samples produced under different reaction conditions. The reaction numbers indicating the different conditions used are given in Table 1, and the variation in molecular weight and

Table 1. Product Yields and pH Values from the Oxidative Depolymerization of LB Lignin

run[a]	temperature (°C)	P_{O_2} (bar)	monophenols + acids (%)[b]	pH
1	120	3	5.2	13.1
2	120	9	6.3	12.6
3	120	15	9.4	10.1
4	160	3	8.3	12.3
5	160	9	10.5	8.3
6	160	15	10.4	7.6
7	200	3	6.8	12.0
8	200	9	13.1	8.4
9	200	15	14.2	7.0
blank	–	–	3.2	13.4

[a]Fixed reaction parameters: 20 g/L LB, 0.2 M NaOH aqueous solution, 30 min. [b]Basedon the total lignin substrate.

the relative mass abundance of corresponding oxygen-treated kraft lignin samples are shown in Figure 1. The SEC profiles of the substrate and product samples are shown in Figures S1–S2 in the Supporting Information.

The lignin starting material, LB (blank), exhibited a broad MWD with a dispersity index of 2.5 and an average molecular weight of about 48 kDa. A significant reduction in molecular size and narrower distributions were obtained after oxidative depolymerization (Figure 1a). For example, at a temperature of 120 °C, M_w values of 33.4, 14.6, and 8.8 kDa were obtained at O_2 pressures of 3, 9, and 15 bar, respectively (reactions 1–3). Increasing the temperature to 160 and 200 °C resulted in further size reductions, with average M_w values of 6.4, 4.4, and 4.2 kDa (reactions 4–6), and 3.3, 2.4, and 2.5 kDa (reactions 7–9) at analogous O_2 pressures. It is worth noting that, at the higher reaction temperatures, only a negligible effect on M_w was seen for P_{O_2} > 9 bar, suggesting that the reaction was not limited by the gas accessibility under such conditions. The lowest dispersity index (~1.3) was also obtained following the harshest reaction conditions, indicating that high temperature and O_2 pressure favored lignin breakdown into low molecular weight products.

A further illustration of the effects of the reaction conditions on the molecular size distribution and relative mass abundance is given in Figure 1b. Approximately half of the untreated LB lignin consisted of macromolecules with M_w > 10 kDa, while the low molecular weight portion (<1 kDa) represented less than 1% of the total abundance. When the reactions were performed at higher temperatures (160–200 °C), a substantial shift in mass distribution was seen toward smaller lignin fragments. For instance, the fraction of higher oligomers (1–3 kDa) increased gradually from 49 to 75% (reactions 4–9), compared to the blank sample (19%). Similarly, the portion rich in phenolic monomers, dimers, and trimers (<1 kDa) increased to 4–12%, confirming that both pressurized oxygen and higher temperature were needed to effectively depolymerize the LB lignin into low molecular weight products. Importantly, the abundance of high molecular weight fractions (>10 kDa) was generally below 5% under these conditions, and none were found after reactions at 200 °C (reactions 7–9).

Oxidative Depolymerization of LB – Effects on Monomer Formation. Product distribution and yields resulting from lignin oxidative depolymerization are known to vary depending on the lignin source,[37,50] operating conditions,[51,52] and even the kind of pretreatment prior to oxidation.[53] All product mixtures from oxidative depolymerization reactions in the present work were subjected to liquid chromatographic analysis to identify and quantify the phenolic monomers and carboxylic acids produced (Figure 2). The pH values of the mixtures were also determined to complement the characterization of the samples produced under different treatment conditions (Table 1).

The main aromatic monomeric compounds identified in the oxygen-treated samples were vanillin, vanillic acid, guaiacol, and acetovanillone (Figure 2a); the highest total yield of 3.2 wt % being observed after treatment at 160 °C and 3 bar O_2 (reaction 4). The higher yields obtained for vanillin and vanillic acid than in the blank sample (up to 5-fold increase), confirmed that oxygen promoted their formation.[54] The yields obtained are in agreement with those reported by Singh and co-workers (3–5 wt %) upon depolymerizing kraft lignin with alkaline hydrogen peroxide for further bioconversion.[55] The amount of guaiacol produced also increased with increasing depolymerization temperature. Conversely, at fixed temperature, the guaiacol fraction decreased with increasing O_2 pressure, suggesting that oxygen probably converted the guaiacol formed into either its corresponding aromatic aldehydes[56] or predominantly carboxylic acids via ring opening.[57]

Formic and acetic acids, together with minor amounts of succinic acid (<0.5 wt %), were the predominant organic acids found in the depolymerized samples (4–13 wt %, Figure 2b). The formation of carboxylic acids was especially pronounced at high temperature and O_2 pressure, probably due to the oxidation of the aromatics under severe conditions, as mentioned above. This finding is consistent with the reaction being consecutive, such that the nonaromatic carboxylic acids are formed as breakdown products from the monophenol type compounds. Consecutive breakdown is supported by the positive effect of introducing additional O_2 on monomeric aromatics at the lowest temperature (120 °C) as opposed to the effect at higher temperatures with higher reaction rates (≥160 °C). A high ratio of organic acids to monoaromatic products was likewise reported by Lyu et al.[28] in oxidative cracking of ammonia-extracted lignin from corn stover at high temperatures and oxygen pressures. Furthermore, Schutyser et al.[29] found that vanillin could be further oxidized to nonaromatic carboxylic acids during alkaline aerobic oxidation, resulting predominantly in formic, malonic, and acetic acids, in line with the results of the present study. Notably, the formation of carboxylic acids lowered the pH of the depolymerized product mixtures from the initial pH of the untreated LB sample (13.4). Interestingly, almost neutral pH values (7.6 and 7.0) were observed in the product solutions after reactions at 15 bar O_2 and temperatures of 160 and 200 °C, respectively (reactions 6 and 9). This is an important observation, as near-neutral pH conditions are preferable for bacterial cultivation. In addition, a reduction in the pH of the product mixtures due to the oxygen treatment led to an increase in the level of soluble lignin components, thus enabling bioconversion at higher concentrations.

DOI: 10.1021/acssuschemeng.9b01605
ACS Sustainable Chem. Eng. 2019, 7, 11640–11652

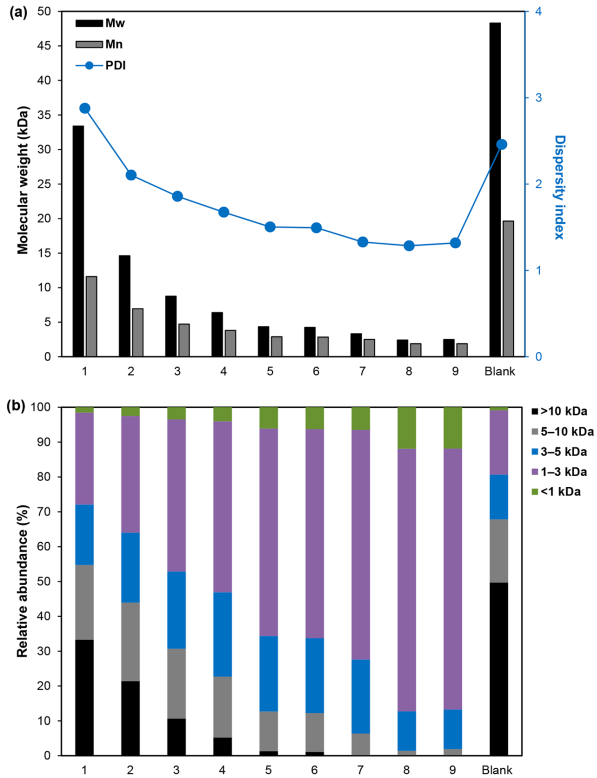


Figure 1. Molecular weight distribution and dispersity index (a) and relative mass abundance (b) for different depolymerized lignin samples. M_w is the weight-average molecular weight, M_n the number-average molecular weight, and PDI is the dispersity index. The reaction number according to Table 1 is given on the abscissa.

Overall, depolymerization of LB at 160 °C and 3 bar O_2 pressure (reaction 4) provided the most favorable product mixture, with a high yield of aromatic monomers (3.2 wt %) and a rather low content of highly oxidized compounds (i.e., carboxylic acids). This sample was thus deemed interesting for detailed chemical analysis using NMR, SEM, and BET, and for use in microbial liquid cultivation experiments. Hence, the reactor was scaled up to prepare a larger batch of the product under these conditions.

Characterization of ODLB. Heteronuclear NMR analysis at a high magnetic field was used to reveal structural variations between the native LB and ODLB lignin samples and to identify functional groups and molecular species in the product material. Figure 3 shows the two-dimensional $^1H-^{13}C$ HMBC NMR spectra obtained from the initial substrate and depolymerized product.

The presence of aromatic aldehydes, ketones, and carboxylic acids detected by UPLC/HPLC analysis was confirmed by 2D HMBC NMR. This method enabled visualization of such functional groups and demonstrated the changes between LB (Figure 3a) and ODLB (Figure 3b), especially regarding aliphatic and aromatic aldehydes, ketones, and acids ($\delta^{13}C \sim 170-215$ ppm). The functional groups and molecules identified included, among others, aromatic aldehydes (α-aldehydes, $\delta^{13}C$ 190.5 ppm), aromatic α-ketones ($\delta^{13}C$ 194.5−198.4 ppm, with lower values indicative of an aromatic and an ether group adjacent to the keto group and higher values indicative of a rather short-chain substituent ketone), aromatic acetyl esters ($\delta^{13}C$ 169.7 ppm), aromatics with aliphatic functionalization (and HMBC correlations from δ^1H 2.4 ppm to aromatic carbon atoms), intact aromatic methyl ether signals, aliphatic acids including acetate, formate, lactate, and longer hydroxy acids, as well as aliphatic ketones and α-keto acids ($\delta^{13}C$ 177.6 and 203.9 ppm).

The structural motifs in the LB and ODLB samples were also compared using 2D $^1H-^{13}C$ HSQC analysis (Figure S3). The spectra indicated variations between the materials, mostly in the interunit (oxygenated) aliphatic region. In addition, parts of the signals corresponding to nonoxygenated aliphatic moieties ($\delta^{13}C/\delta^1H$ 8.0−52.5/0.5−2.5 ppm) disappeared after oxidative depolymerization. The HSQC data also showed a decrease in the methoxy resonance at $\delta^{13}C/\delta^1H \approx 56/3.7$ ppm, whereas the

DOI: 10.1021/acssuschemeng.9b01605
ACS Sustainable Chem. Eng. 2019, 7, 11640−11652

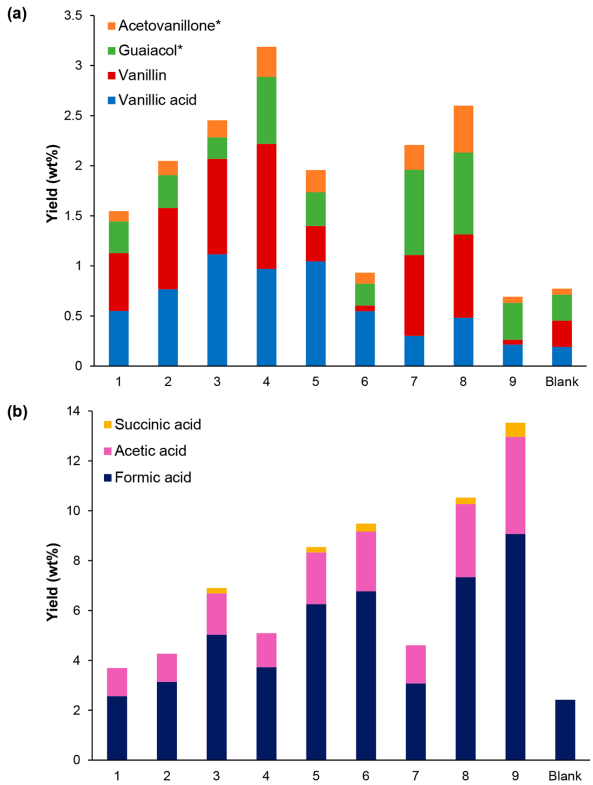


Figure 2. Impact of reaction temperature and oxygen pressure on the yield of (a) monophenols and (b) other carboxylic acids from the oxidative depolymerization of LB lignin. Reaction conditions: 20 g/L LB, 0.2 M NaOH aqueous solution, 30 min. (*: Including coeluting compound, quantified with guaiacol and acetovanillone standards, respectively). The reaction number according to Table 1 is given on the abscissa.

aromatic chemical structures ($\delta^{13}C/\delta^{1}H$ 105−140/6.0−8.0 ppm) were apparently rather resistant to degradation under the treatment conditions applied. This stability indicates that it is possible to achieve depolymerization without oxidative breakage of the aromatic rings under suitably tuned conditions.

SEM characterization was carried out to gain insight into changes in the surface morphology of the LB after oxidative depolymerization. The SEM images obtained for LB and the ODLB lignin samples are shown in Figure 4.

The LB had a rather smooth surface emphasizing the high recalcitrance of the untreated lignin (Figure 4a). However, the surface of the ODLB product was considerably changed by the reaction, where the smooth surface was broken into smaller particles, accompanied by the appearance of needle-like structures and multilayer eroded parts (Figure 4b). Such morphological changes are consistent with the results reported by Wei and co-workers,[42] and probably reduce the surface integrity of the native LB, making it more accessible to subsequent microbial conversion.

Nitrogen physisorption measurements were performed to provide quantitative estimates of the changes in surface area and pore structure of the lignin during the depolymerization process. The textural properties of the LB and ODLB lignin samples are summarized in Table 2. The N_2 adsorption−desorption isotherms of the substrate and product samples are also shown in Figure S4 in the Supporting Information.

The original lignin had a specific surface area of 1.23 m^2/g and a modest pore volume of 0.0015 cm^3/g. The calculated average pore size, assuming cylindrical pores, was 4.9 nm. In comparison, the ODLB sample showed an almost 4-fold increase in specific surface area (4.35 m^2/g) together with an increase in pore size (5.49 nm) and pore volume (0.0060 cm^3/g), all of which are consistent with the structural interpretation of the SEM images discussed above.

The comparison of textural parameters resulting from the pretreatment of woody biomass by BET analysis has been shown to be useful.[58] Although the mechanisms for the enzymatic degradation of cellulose and lignin differ, the fact that the ODLB sample had a higher surface area and pore size may allow easier access of enzymes and reactive mediators, which can facilitate further microbial lignin conversion.

DOI: 10.1021/acssuschemeng.9b01605
ACS Sustainable Chem. Eng. 2019, 7, 11640−11652

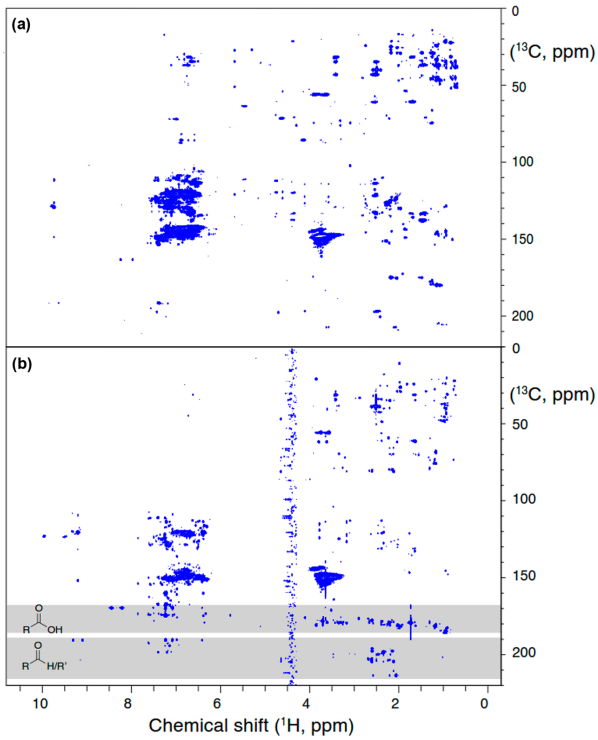


Figure 3. ^{1}H−^{13}C HMBC NMR spectra of (a) LB and (b) ODLB lignin samples. The increased presence of aliphatic and aromatic aldehydes, ketones, and carboxylic acids is indicated by a highlight of characteristic spectral regions in panel b. Reaction conditions: 20 g/L LB, 0.2 M NaOH aqueous solution, 160 °C, 3 bar O_2, 30 min.

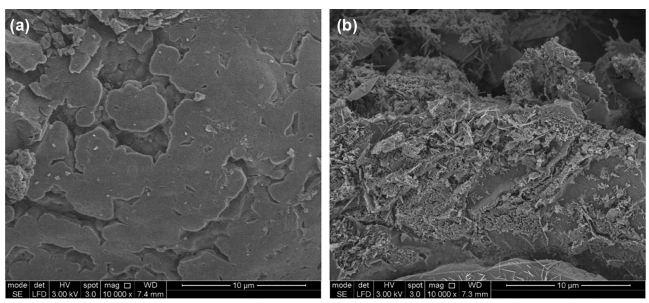


Figure 4. SEM images of (a) LB and (b) ODLB lignin samples. Reaction conditions: 20 g/L LB, 0.2 M NaOH aqueous solution, 160 °C, 3 bar O_2, 30 min.

Bacterial Growth on Depolymerized LB. Microbial growth on the produced lignin samples was evaluated on M9 agar plates using LB and LB treated under different conditions (reactions 1−9 and blank, Table 1) as the sole source of carbon and energy. The bacterial strains *Pseudomonas putida* KT2440, *Pseudomonas fluorescens*, *Rhodococcus opacus*, and *Sphingobium* sp. strain SYK-6 have previously been reported to metabolize similar lignin substrates or related lignin monomers.[42,59] These experiments allowed us to determine whether any of the unknown compounds in the depolymerized products were toxic,

DOI: 10.1021/acssuschemeng.9b01605
ACS Sustainable Chem. Eng. 2019, 7, 11640−11652

Table 2. Textural Properties of Lignin Samples Calculated using BET Analysis

sample	BET surface area (m^2/g)	pore size (nm)	pore volume (cm^3/g)
LB	1.23	4.90	0.0015
ODLB[a]	4.35	5.49	0.0060

[a]Reaction conditions: 20 g/L LB, 0.2 M NaOH aqueous solution, 160 °C, 3 bar O_2, 30 min.

in particular to microbial growth at the given concentrations. Both *Pseudomonas* species showed abundant growth on most of the treated lignin samples already after 120 h (data not shown), indicating that these strains could easily metabolize the compounds present. After 7 days of incubation, *R. opacus* and *Sphingobium* sp. SYK-6 were also able to grow on the agar plates, including those containing the untreated LB lignin (Table 3).

The results presented in Table 3 suggest that neither LB nor the depolymerized products obtained under different conditions was toxic to bacterial growth at the concentrations present. Less growth was seen on the untreated LB substrate than on the depolymerized lignin samples (Table 3), which is in line with the lower amount of readily available monomers for direct consumption in LB (Table 1; Figure 2). The reason for abundant growth on the substrates treated under harsh conditions (i.e., high temperature and oxygen pressure) may be the higher acid concentrations (up to 13.5%, Figure 2b), as some of the organisms used in this study have previously demonstrated the ability to grow on similar acids.[38,60]

Shake Flask Experiments with ODLB. High-cell-density inoculations (OD ≈ 3.5−4) were performed to assess the utilization of low molecular weight compounds in ODLB as carbon sources, as well as possible enzymatic effects on the molecular size of the lignin. All four organisms tested in the plate screening experiments were used for liquid cultivations in shake flasks, with a lignin concentration of 2 g/L as the sole carbon source and incubation for about 150 h.

After inoculation, a slight decrease in OD was observed for all organisms, after which *P. putida* KT2440, *R. opacus*, and *Sphingobium* sp. SYK-6 showed maintained OD throughout the cultivation (Figure 5). In the case of *P. fluorescens*, a decrease in OD (from 3.7 to 2.5) was seen during the first 45 h, which was probably caused by the formation of cell aggregates, which could be seen by microscopic examination. This response of *P. fluorescens* has previously been reported and described as a reaction to toxic shock.[22] In addition, the formation of a biofilm was observed at the air−liquid interface in the shake flasks for all organisms.

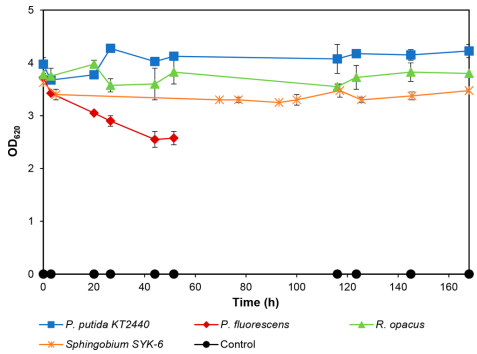


Figure 5. Cell density of bacterial species cultivated on M9 medium supplemented with 2 g/L ODLB lignin (160 °C and 3 bar O_2) as the sole source of carbon and energy. Cultivations were performed in duplicate, and the data points represent the average, and the error bars the standard deviation.

Furthermore, *P. putida* KT2440 and *Sphingobium* sp. SYK-6 were cultivated in higher lignin concentrations (10 g/L ODLB) together with lower initial cell densities (OD < 0.01). The results showed a clear growth of these organisms on lignin with a maximum OD of around 0.45 (Figure S5). The consumption of monomers by the organisms was in agreement with the high-cell-density experiments (detailed below).

The consumption of aromatic monomers by the bacterial strains was analyzed using UPLC. Both the *Pseudomonas* strains and *Sphingobium* sp. SYK-6 were able to convert vanillin to vanillic acid and eventually consume all the vanillic acid available and produced in less than 50 h (Figure 6). The conversion of toxic aldehydes, such as vanillin, to their respective acids has been described previously.[61] In contrast, *R. opacus* converted vanillin to vanillyl alcohol as an intermediate, after which vanillin, vanillic acid, and vanillyl alcohol were completely consumed within 21 h. The detoxification of vanillin to its corresponding alcohol has mostly been reported in yeast, but also in a few bacteria, such as *Gluconacetobacter xylinus* and *Pseudomonas* sp. isolate 9.1.[62−64] The accumulation of vanillyl alcohol instead of vanillic acid in *R. opacus* might be due to the poor expression of the gene encoding for the vanillin dehydrogenase enzyme.[65]

Table 3. Growth of Bacterial Strains on M9 Agar Plates with LB Lignin (2 g/L) Treated under Different Conditions[a]

Temperature (°C)	120						160						200						Untreated	
Pressure O_2 (bar)	3		9		15		3		9		15		3		9		15			
Organism	I	II	I	II	I	II	I	II	I	II	I	II	I	II	I	II	I	II	I	II
P. putida KT2440	++	+	++	+	++	++	++	++	++	++	++	++	++	++	++	++	++	++	+	+
P. fluorescens	+	+	+	+	++	+	+	++	++	++	++	++	+	++	++	++	++	++	+	+
R. opacus	+	+	+	+	+	+	+	+	++	+	+	+	-	-	+	+	++	++	+	+
Sphingobium SYK-6	+	+	++	+	++	++	+	+	+	+	++	+	++	+	+	++	+	+	+	+

[a]The plates were incubated at 30 °C for 7 days. Biological duplicates are indicated by I and II (++ abundant growth; + growth; - no growth).

DOI: 10.1021/acssuschemeng.9b01605
ACS Sustainable Chem. Eng. 2019, 7, 11640−11652

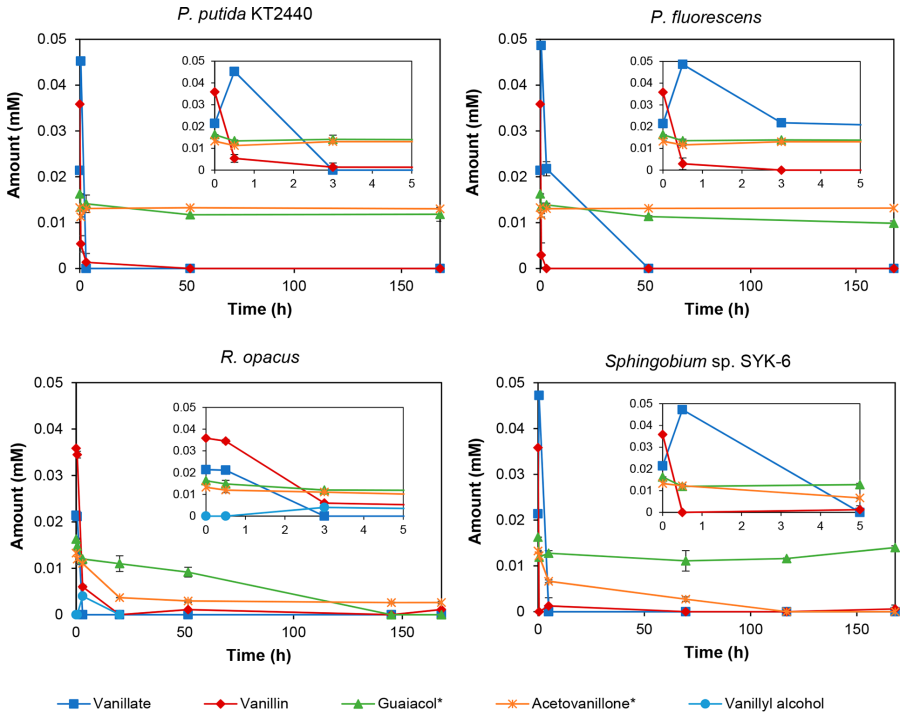


Figure 6. Consumption of aromatic monomers in the high-cell-density cultivations on ODLB lignin (2 g/L) as a function of time. (* + coeluting substance, quantified using guaiacol and acetovanillone standards, respectively). The first 5 h are enlarged for better readability in the initial cultivation phases. Data points represent the average of the duplicate experiments and the error bars the standard deviation.

The UPLC peaks eluting at 4.7 and 5.0 min are believed to be guaiacol and acetovanillone, respectively, based on their retention times. However, the UV spectra of these compounds suggest that the peaks coelute with some other unidentified compounds. *R. opacus* was the only organism to consume guaiacol and its coeluting compound within 150 h (Figure 6). Besides *R. opacus*, a few Gram-positive bacteria have been reported to be able to grow on guaiacol as the sole carbon source.[66] The enzyme cytochrome P450 monooxygenase responsible for the demethylation of guaiacol to catechol has been described in both Gram-positive and Gram-negative bacteria, such as *Rhodococcus rhodochrous*, *Amycolatopsis* sp., and *Moraxella* sp.[67−69] Neither the *Pseudomonas* strains nor *Sphingobium* sp. SYK-6 was able to assimilate guaiacol within 150 h (Figure 6). Although *P. putida* KT2440 has been reported to possess the pathway for catechol degradation, growth was not observed in this study. *Sphingobium* sp. SYK-6 has β-etherase genes that cleave the β-aryl ether linkages in lignin dimers to generate guaiacol, but the assimilation of guaiacol has not been reported.[59]

Sphingobium sp. SYK-6 was the only organism able to metabolize acetovanillone and its coeluting compound in around 100 h (Figure 6). In a recent study, we found that *R. opacus* was unable to assimilate acetovanillone,[41] which suggests that the coeluting compound was consumed within 20 h in this case, leaving the acetovanillone in the culture medium unconsumed for 150 h (Figure 6). The bioconversion of some compounds, such as ferulic acid and 4-vinyl guaiacol, to acetovanillone has been described in a few organisms,[70] but the consumption of acetovanillone as the sole carbon source has not been reported. None of the *Pseudomonas* species included in the current study were able to assimilate acetovanillone in 150 h (Figure 6), despite the high cell density, which suggests the absence of the required enzymes.

SEC analysis was performed to assess changes in the dissolved higher molecular weight lignin fraction present in the substrate, caused by the action of extracellular enzymes, such as laccases and peroxidases. A noninoculated control flask was monitored to see if the changes in molecular weight were also observed in the absence of microbial action. On the basis of related work,[41] it is suggested that the peaks at long retention times (around 105 and 94 min) represented low molecular weight monomers or short oligomers, whereas the broad peak at 89 min represents larger lignin fractions (Figure 7).

After 70 h, the monomer peaks disappeared in all cultivations, suggesting the consumption of most of the available monomers. At the end of cultivation (168 h), all organisms showed an increase in the intensity of the polymer peak, the highest absorption being measured for *P. fluorescens* (0.18). After 168 h, there was also a slight increase in the polymer peak of the

DOI: 10.1021/acssuschemeng.9b01605
ACS Sustainable Chem. Eng. 2019, 7, 11640−11652

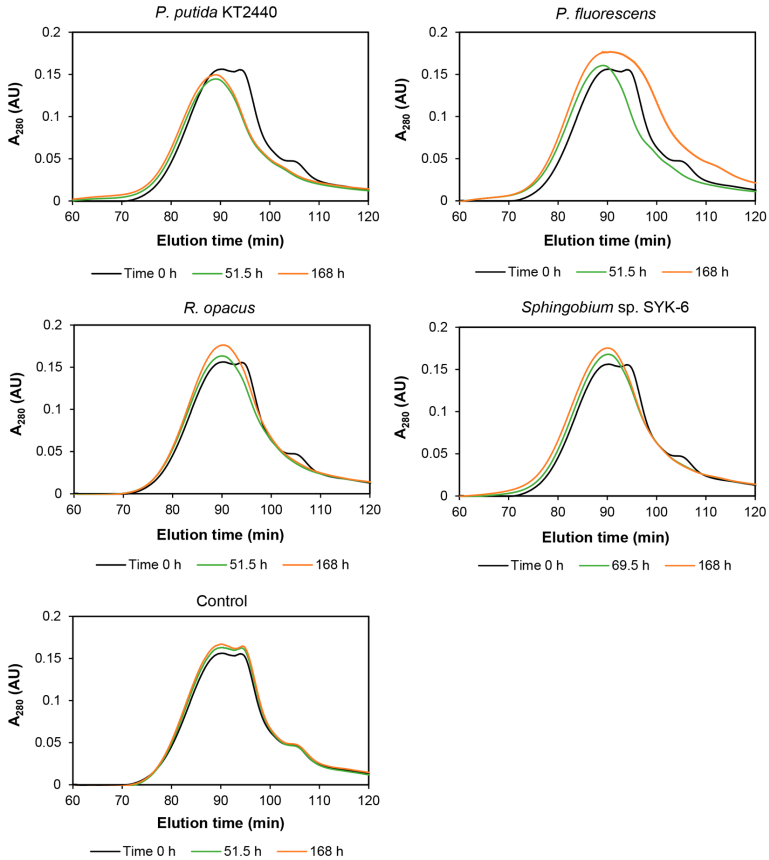


Figure 7. SEC chromatograms of samples from high-cell-density cultivations on 2 g/L ODLB lignin (160 °C and 3 bar O_2) and from a noninoculated control. Results are shown for samples collected at 0, 51.5, and 168 h (*P. putida* KT2440, *P. fluorescens*, *R. opacus*, and control) or at 0, 69.5, and 168 h (*Sphingobium sp.* SYK-6). Elution time (min) and absorbance at 280 nm are indicated. AU, arbitrary units.

noninoculated control (Figure 7), which was probably due to the condensation of unstable lignin fragments. Apart from the increase in peak height, a peak shift/widening toward higher molecular weight was also observed in the inoculated flasks (except in the case of *R. opacus*), but not in the control flask (Figure 7). These observations suggest that repolymerization of polymeric lignin is stronger in the presence of bacterial species, which might be due to the secretion of extracellular enzymes. All the organisms included in this study have previously been reported to secrete extracellular lignin-degrading/polymerizing enzymes.[22,71,72] The action of these enzymes in the polymerization or depolymerization of a particular substrate depends on various factors, such as the reaction temperature/time, the structure of the lignin, substrate loading, the presence of a mediator, and the origin of the enzyme.

In conclusion, the results presented in this study show that oxidative depolymerization of technical lignin, under rather mild operating conditions, can produce low molecular weight fractions that are amenable to microbial conversion. The work adds to the state of the art within lignin refining by including novel investigations on oxidation reaction parameters and multiple microbial species, thus allowing obtaining an approach that is more green and benign than previously reported. This approach can hopefully be broadly applied to enable the production of various bioproducts based on industrial kraft lignin streams. However, the depolymerization and fermentation conditions should be optimized to allow scalability and process/product development.

■ ASSOCIATED CONTENT

Supporting Information

The Supporting Information is available free of charge on the ACS Publications website at DOI: 10.1021/acssuschemeng.9b01605.

DOI: 10.1021/acssuschemeng.9b01605
ACS Sustainable Chem. Eng. 2019, 7, 11640−11652

SEC chromatograms of the untreated LB substrate and the oxidatively depolymerized lignin products generated at different reaction conditions; 2D $^{1}H-^{13}C$ HSQC NMR spectra showing aliphatic, interunit, and aromatic regions for the LB and the ODLB lignin samples as well as their N_2 adsorption−desorption isotherms; growth curves for *Pseudomonas putida* KT2440 and Sphingobium sp. SYK-6 with 10 g/L ODLB (PDF)

AUTHOR INFORMATION

Corresponding Author

*E-mail: christian.hulteberg@chemeng.lth.se.

ORCID

Omar Y. Abdelaziz: 0000-0002-3530-3509
Sebastian Meier: 0000-0003-3761-3217
Anders Riisager: 0000-0002-7086-1143
Christian P. Hulteberg: 0000-0002-3502-5529

Notes

The authors declare no competing financial interest.

ACKNOWLEDGMENTS

This work was financed by the Swedish Foundation for Strategic Research (RBP14-0052). O.Y.A. acknowledges internal funding from Lund University and the Technical University of Denmark. We thank Anders Arkell, Arkell Innovations AB, for SEC measurements. The 800 MHz NMR spectra were recorded using the spectrometer at the DTU NMR Center, supported by the Villum Foundation.

REFERENCES

(1) Zakzeski, J.; Bruijnincx, P. C. A.; Jongerius, A. L.; Weckhuysen, B. M. The Catalytic Valorization of Lignin for the Production of Renewable Chemicals. *Chem. Rev.* **2010**, *110* (6), 3552−3599.

(2) Li, C.; Zhao, X.; Wang, A.; Huber, G. W.; Zhang, T. Catalytic Transformation of Lignin for the Production of Chemicals and Fuels. *Chem. Rev.* **2015**, *115* (21), 11559−11624.

(3) Abdelaziz, O. Y.; Brink, D. P.; Prothmann, J.; Ravi, K.; Sun, M.; García-Hidalgo, J.; Sandahl, M.; Hulteberg, C. P.; Turner, C.; Lidén, G.; et al. Biological Valorization of Low Molecular Weight Lignin. *Biotechnol. Adv.* **2016**, *34* (8), 1318−1346.

(4) Schutyser, W.; Renders, T.; Van den Bosch, S.; Koelewijn, S.-F.; Beckham, G. T.; Sels, B. F. Chemicals from Lignin: An Interplay of Lignocellulose Fractionation, Depolymerisation, and Upgrading. *Chem. Soc. Rev.* **2018**, *47*, 852−908.

(5) Ragauskas, A. J.; Beckham, G. T.; Biddy, M. J.; Chandra, R.; Chen, F.; Davis, M. F.; Davison, B. H.; Dixon, R. A.; Gilna, P.; Keller, M.; et al. Lignin Valorization: Improving Lignin Processing in the Biorefinery. *Science* **2014**, *344* (6185), 1246843.

(6) Key, R. E.; Bozell, J. J. Progress toward Lignin Valorization via Selective Catalytic Technologies and the Tailoring of Biosynthetic Pathways. *ACS Sustainable Chem. Eng.* **2016**, *4* (10), 5123−5135.

(7) Gillet, S.; Aguedo, M.; Petitjean, L.; Morais, A. R. C.; da Costa Lopes, A. M.; Łukasik, R. M.; Anastas, P. T. Lignin Transformations for High Value Applications: Towards Targeted Modifications Using Green Chemistry. *Green Chem.* **2017**, *19* (18), 4200−4233.

(8) Moshkelani, M.; Marinova, M.; Perrier, M.; Paris, J. The Forest Biorefinery and Its Implementation in the Pulp and Paper Industry: Energy Overview. *Appl. Therm. Eng.* **2013**, *50* (2), 1427−1436.

(9) Sjöström, E. *Wood Chemistry: Fundamentals and Applications*, 2nd ed., Academic Press, Inc.: San Diego, CA, 1993.

(10) Calvo-Flores, F. G.; Dobado, J. A.; Isac-García, J.; Martín-Martínez, F. J. *Lignin and Lignans as Renewable Raw Materials: Chemistry, Technology and Applications*; John Wiley & Sons, Ltd: Chichester, UK, 2015.

(11) Rinaldi, R.; Jastrzebski, R.; Clough, M. T.; Ralph, J.; Kennema, M.; Bruijnincx, P. C. A.; Weckhuysen, B. M. Paving the Way for Lignin Valorisation: Recent Advances in Bioengineering, Biorefining and Catalysis. *Angew. Chem., Int. Ed.* **2016**, *55* (29), 8164−8215.

(12) Jönsson, J.; Pettersson, K.; Berntsson, T.; Harvey, S. Comparison of Options for Utilization of a Potential Steam Surplus at Kraft Pulp Mills-Economic Performance and CO2 Emissions. *Int. J. Energy Res.* **2013**, *37* (9), 1017−1035.

(13) Tomani, P. The LignoBoost Process. *Cellul. Chem. Technol.* **2010**, *44* (1−3), 53−58.

(14) Öhman, F.; Theliander, H.; Tomani, P.; Axegard, P. *Method for Separating Lignin from Black Liquor*. U.S. Patent 8,486,224, 2013.

(15) Hu, J.; Zhang, Q.; Lee, D.-J. Kraft Lignin Biorefinery: A Perspective. *Bioresour. Technol.* **2018**, *247*, 1181−1183.

(16) Bruijnincx, P. C. A.; Rinaldi, R.; Weckhuysen, B. M. Unlocking the Potential of a Sleeping Giant: Lignins as Sustainable Raw Materials for Renewable Fuels, Chemicals and Materials. *Green Chem.* **2015**, *17* (11), 4860−4861.

(17) Aminzadeh, S.; Lauberts, M.; Dobele, G.; Ponomarenko, J.; Mattsson, T.; Lindström, M. E.; Sevastyanova, O. Membrane Filtration of Kraft Lignin: Structural Charactristics and Antioxidant Activity of the Low-Molecular-Weight Fraction. *Ind. Crops Prod.* **2018**, *112*, 200−209.

(18) Sun, Z.; Fridrich, B.; De Santi, A.; Elangovan, S.; Barta, K. Bright Side of Lignin Depolymerization: Toward New Platform Chemicals. *Chem. Rev.* **2018**, *118* (2), 614−678.

(19) Pu, Y.; Hu, F.; Huang, F.; Ragauskas, A. J. Lignin Structural Alterations in Thermochemical Pretreatments with Limited Delignification. *BioEnergy Res.* **2015**, *8* (3), 992−1003.

(20) Pandey, M. P.; Kim, C. S. Lignin Depolymerization and Conversion: A Review of Thermochemical Methods. *Chem. Eng. Technol.* **2011**, *34* (1), 29−41.

(21) Gall, D. L.; Ralph, J.; Donohue, T. J.; Noguera, D. R. Biochemical Transformation of Lignin for Deriving Valued Commodities from Lignocellulose. *Curr. Opin. Biotechnol.* **2017**, *45*, 120−126.

(22) Salvachúa, D.; Karp, E. M.; Nimlos, C. T.; Vardon, D. R.; Beckham, G. T. Towards Lignin Consolidated Bioprocessing: Simultaneous Lignin Depolymerization and Product Generation by Bacteria. *Green Chem.* **2015**, *17*, 4951−4967.

(23) Zhao, C.; Xie, S.; Pu, Y.; Zhang, R.; Huang, F.; Ragauskas, A. J.; Yuan, J. S. Synergistic Enzymatic and Microbial Lignin Conversion. *Green Chem.* **2016**, *18* (5), 1306−1312.

(24) Sturgeon, M. R.; Kim, S.; Lawrence, K.; Paton, R. S.; Chmely, S. C.; Nimlos, M.; Foust, T. D.; Beckham, G. T. A Mechanistic Investigation of Acid-Catalyzed Cleavage of Aryl-Ether Linkages: Implications for Lignin Depolymerization in Acidic Environments. *ACS Sustainable Chem. Eng.* **2014**, *2* (3), 472−485.

(25) Katahira, R.; Mittal, A.; McKinney, K.; Chen, X.; Tucker, M. P.; Johnson, D. K.; Beckham, G. T. Base-Catalyzed Depolymerization of Biorefinery Lignins. *ACS Sustainable Chem. Eng.* **2016**, *4* (3), 1474−1486.

(26) Chaudhary, R.; Dhepe, P. L. Solid Base Catalyzed Depolymerization of Lignin into Low Molecular Weight Products. *Green Chem.* **2017**, *19* (3), 778−788.

(27) Abdelaziz, O. Y.; Li, K.; Tunå, P.; Hulteberg, C. P. Continuous Catalytic Depolymerisation and Conversion of Industrial Kraft Lignin into Low-Molecular-Weight Aromatics. *Biomass Convers. Biorefin.* **2018**, *8* (2), 455−470.

(28) Lyu, G.; Yoo, C. G.; Pan, X. Alkaline Oxidative Cracking for Effective Depolymerization of Biorefining Lignin to Mono-Aromatic Compounds and Organic Acids with Molecular Oxygen. *Biomass Bioenergy* **2018**, *108*, 7−14.

(29) Schutyser, W.; Kruger, J. S.; Robinson, A. M.; Katahira, R.; Brandner, D. G.; Cleveland, N. S.; Mittal, A.; Peterson, D. J.; Meilan, R.; Román-Leshkov, Y.; et al. Revisiting Alkaline Aerobic Lignin Oxidation. *Green Chem.* **2018**, *20* (16), 3828−3844.

(30) Ma, R.; Guo, M.; Zhang, X. Recent Advances in Oxidative Valorization of Lignin. *Catal. Today* **2018**, *302*, 50−60.

(31) Abdelaziz, O. Y.; Meier, S.; Prothmann, J.; Turner, C.; Riisager, A.; Hulteberg, C. P. Oxidative Depolymerisation of Lignosulphonate

DOI: 10.1021/acssuschemeng.9b01605
ACS Sustainable Chem. Eng. 2019, 7, 11640−11652

Lignin into Low-Molecular-Weight Products with Cu-Mn/δ-Al2O3. *Top. Catal.* **2019**. DOI: 10.1007/s11244-019-01146-5.
(32) Feghali, E.; Carrot, G.; Thuéry, P.; Genre, C.; Cantat, T. Convergent Reductive Depolymerization of Wood Lignin to Isolated Phenol Derivatives by Metal-Free Catalytic Hydrosilylation. *Energy Environ. Sci.* **2015**, *8*, 2734−2743.
(33) Huang, S.; Mahmood, N.; Tymchyshyn, M.; Yuan, Z.; Xu, C. C. Reductive De-Polymerization of Kraft Lignin for Chemicals and Fuels Using Formic Acid as an in-Situ Hydrogen Source. *Bioresour. Technol.* **2014**, *171*, 95−102.
(34) Behling, R.; Valange, S.; Chatel, G. Heterogeneous Catalytic Oxidation for Lignin Valorization into Valuable Chemicals: What Results? What Limitations? What Trends? *Green Chem.* **2016**, *18* (7), 1839−1854.
(35) Santos, S. G.; Marques, A. P.; Lima, D. L. D.; Evtuguin, D. V.; Esteves, V. I. Kinetics of Eucalypt Lignosulfonate Oxidation to Aromatic Aldehydes by Oxygen in Alkaline Medium. *Ind. Eng. Chem. Res.* **2011**, *50* (1), 291−298.
(36) Tarabanko, V. E.; Tarabanko, N. Catalytic Oxidation of Lignins into the Aromatic Aldehydes: General Process Trends and Development Prospects. *Int. J. Mol. Sci.* **2017**, *18* (11), 2421.
(37) Rodrigues Pinto, P. C.; Borges Da Silva, E. A.; Rodrigues, A. E. Insights into Oxidative Conversion of Lignin to High-Added-Value Phenolic Aldehydes. *Ind. Eng. Chem. Res.* **2011**, *50* (2), 741−748.
(38) Linger, J. G.; Vardon, D. R.; Guarnieri, M. T.; Karp, E. M.; Hunsinger, G. B.; Franden, M. A.; Johnson, C. W.; Chupka, G.; Strathmann, T. J.; Pienkos, P. T.; et al. Lignin Valorization through Integrated Biological Funneling and Chemical Catalysis. *Proc. Natl. Acad. Sci. U. S. A.* **2014**, *111* (33), 12013−12018.
(39) Beckham, G. T.; Johnson, C. W.; Karp, E. M.; Salvachúa, D.; Vardon, D. R. Opportunities and Challenges in Biological Lignin Valorization. *Curr. Opin. Biotechnol.* **2016**, *42*, 40−53.
(40) Rodriguez, A.; Salvachúa, D.; Katahira, R.; Black, B. A.; Cleveland, N. S.; Reed, M.; Smith, H.; Baidoo, E. E. K.; Keasling, J. D.; Simmons, B. A.; et al. Base-Catalyzed Depolymerization of Solid Lignin-Rich Streams Enables Microbial Conversion. *ACS Sustainable Chem. Eng.* **2017**, *5* (9), 8171−8180.
(41) Ravi, K.; Abdelaziz, O. Y.; Nöbel, M.; García-Hidalgo, J.; Gorwa-Grauslund, M. F.; Hulteberg, C. P.; Lidén, G. Bacterial Conversion of Depolymerized Kraft Lignin. *Biotechnol. Biofuels* **2019**, *12*, 56.
(42) Wei, Z.; Zeng, G.; Huang, F.; Kosa, M.; Huang, D.; Ragauskas, A. J. Bioconversion of Oxygen-Pretreated Kraft Lignin to Microbial Lipid with Oleaginous Rhodococcus Opacus DSM 1069. *Green Chem.* **2015**, *17* (5), 2784−2789.
(43) Pfennig, N.; Lippert, K. D. Über Das Vitamin B12-Bedürfnis Phototropher Schwefelbakterien. *Arch. Microbiol.* **1966**, *55* (3), 245−256.
(44) Abdelaziz, O. Y.; Hulteberg, C. P. Physicochemical Characterisation of Technical Lignins for Their Potential Valorisation. *Waste Biomass Valorization* **2017**, *8* (3), 859−869.
(45) Brunauer, S.; Emmett, P. H.; Teller, E. Adsorption of Gases in Multimolecular Layers. *J. Am. Chem. Soc.* **1938**, *60* (2), 309−319.
(46) Barrett, E. P.; Joyner, L. G.; Halenda, P. P. The Determination of Pore Volume and Area Distributions in Porous Substances. I. Computations from Nitrogen Isotherms. *J. Am. Chem. Soc.* **1951**, *73* (1), 373−380.
(47) Tolbert, A.; Akinosho, H.; Khunsupat, R.; Naskar, A. K.; Ragauskas, A. J. Characterization and Analysis of the Molecular Weight of Lignin for Biorefining Studies. *Biofuels, Bioprod. Biorefin.* **2014**, *8* (6), 836−856.
(48) Domínguez-Robles, J.; Tamminen, T.; Liitiä, T.; Peresin, M. S.; Rodríguez, A.; Jääskeläinen, A. S. Aqueous Acetone Fractionation of Kraft, Organosolv and Soda Lignins. *Int. J. Biol. Macromol.* **2018**, *106*, 979−987.
(49) Belkheiri, T.; Andersson, S.-I.; Mattsson, C.; Olausson, L.; Theliander, H.; Vamling, L. Hydrothermal Liquefaction of Kraft Lignin in Subcritical Water: Influence of Phenol as Capping Agent. *Energy Fuels* **2018**, *32* (5), 5923−5932.
(50) Das, A.; Rahimi, A.; Ulbrich, A.; Alherech, M.; Motagamwala, A. H.; Bhalla, A.; da Costa Sousa, L.; Balan, V.; Dumesic, J. A.; Hegg, E. L.; et al. Lignin Conversion to Low-Molecular-Weight Aromatics via an Aerobic Oxidation-Hydrolysis Sequence: Comparison of Different Lignin Sources. *ACS Sustainable Chem. Eng.* **2018**, *6* (3), 3367−3374.
(51) Araújo, J. D. P.; Grande, C. A.; Rodrigues, A. E. Vanillin Production from Lignin Oxidation in a Batch Reactor. *Chem. Eng. Res. Des.* **2010**, *88* (8), 1024−1032.
(52) Pacek, A. W.; Ding, P.; Garrett, M.; Sheldrake, G.; Nienow, A. W. Catalytic Conversion of Sodium Lignosulfonate to Vanillin: Engineering Aspects. Part 1. Effects of Processing Conditions on Vanillin Yield and Selectivity. *Ind. Eng. Chem. Res.* **2013**, *52* (25), 8361−8372.
(53) Yao, S. G.; Mobley, J. K.; Ralph, J.; Crocker, M.; Parkin, S.; Selegue, J. P.; Meier, M. S. Mechanochemical Treatment Facilitates Two-Step Oxidative Depolymerization of Kraft Lignin. *ACS Sustainable Chem. Eng.* **2018**, *6* (5), 5990−5998.
(54) Bjelić, S.; Garbuio, L.; Arturi, K. R.; van Bokhoven, J. A.; Jeschke, G.; Vogel, F. Oxidative Biphasic Depolymerization (BPD) of Kraft Lignin at Low PH. *Chemistry Select* **2018**, *3* (41), 11680−11686.
(55) Wu, W.; Dutta, T.; Varman, A. M.; Eudes, A.; Manalansan, B.; Loqué, D.; Singh, S. Lignin Valorization: Two Hybrid Biochemical Routes for the Conversion of Polymeric Lignin into Value-Added Chemicals. *Sci. Rep.* **2017**, *7*, 8420.
(56) Zakzeski, J.; Dębczak, A.; Bruijnincx, P. C. A.; Weckhuysen, B. M. Catalytic Oxidation of Aromatic Oxygenates by the Heterogeneous Catalyst Co-ZIF-9. *Appl. Catal., A* **2011**, *394* (1−2), 79−85.
(57) Fernandes, M. R. C.; Huang, X.; Abbenhuis, H. C. L.; Hensen, E. J. M. Lignin Oxidation with an Organic Peroxide and Subsequent Aromatic Ring Opening. *Int. J. Biol. Macromol.* **2019**, *123*, 1044−1051.
(58) Piccolo, C.; Wiman, M.; Bezzo, F.; Lidén, G. Enzyme Adsorption on SO2 Catalyzed Steam-Pretreated Wheat and Spruce Material. *Enzyme Microb. Technol.* **2010**, *46* (3−4), 159−169.
(59) Masai, E.; Katayama, Y.; Fukuda, M. Genetic and Biochemical Investigations on Bacterial Catabolic Pathways for Lignin-Derived Aromatic Compounds. *Biosci., Biotechnol., Biochem.* **2007**, *71* (1), 1−15.
(60) Holder, J. W.; Ulrich, J. C.; DeBono, A. C.; Godfrey, P. A.; Desjardins, C. A.; Zucker, J.; Zeng, Q.; Leach, A. L. B.; Ghiviriga, I.; Dancel, C.; et al. Comparative and Functional Genomics of Rhodococcus Opacus PD630 for Biofuels Development. *PLoS Genet.* **2011**, *7* (9), No. e1002219.
(61) Ravi, K.; García-Hidalgo, J.; Gorwa-Grauslund, M. F.; Lidén, G. Conversion of Lignin Model Compounds by Pseudomonas Putida KT2440 and Isolates from Compost. *Appl. Microbiol. Biotechnol.* **2017**, *101* (12), 5059−5070.
(62) Zhang, S.; Winestrand, S.; Guo, X.; Chen, L.; Hong, F.; Jönsson, L. J. Effects of Aromatic Compounds on the Production of Bacterial Nanocellulose by Gluconacetobacter Xylinus. *Microb. Cell Fact.* **2014**, *13*, 62.
(63) Ravi, K.; García-Hidalgo, J.; Nöbel, M.; Gorwa-Grauslund, M. F.; Lidén, G. Biological Conversion of Aromatic Monolignol Compounds by a Pseudomonas Isolate from Sediments of the Baltic Sea. *AMB Express* **2018**, *8*, 32.
(64) Wang, X.; Liang, Z.; Hou, J.; Bao, X.; Shen, Y. Identification and Functional Evaluation of the Reductases and Dehydrogenases from Saccharomyces Cerevisiae Involved in Vanillin Resistance. *BMC Biotechnol.* **2016**, *16*, 31.
(65) Chen, H.-P.; Chow, M.; Liu, C.-C.; Lau, A.; Liu, J.; Eltis, L. D. Vanillin Catabolism in Rhodococcus Jostii RHA1. *Appl. Environ. Microbiol.* **2012**, *78* (2), 586−588.
(66) Karlson, U.; Dwyer, D. F.; Hooper, S. W.; Moore, E. R. B.; Timmis, K. N.; Eltis, L. D. Two Independently Regulated Cytochromes P-450 in a Rhodococcus Rhodochrous Strain That Degrades 2-Ethoxyphenol and 4-Methoxybenzoate. *J. Bacteriol.* **1993**, *175* (5), 1467−1474.
(67) Eltis, L. D.; Karlson, U.; Timmis, K. N. Purification and Characterization of Cytochrome P450RR1 from Rhodococcus Rhodochrous. *Eur. J. Biochem.* **1993**, *213* (1), 211−216.

DOI: 10.1021/acssuschemeng.9b01605
ACS Sustainable Chem. Eng. 2019, 7, 11640−11652

(68) Sutherland, J. B. Demethylation of Veratrole by Cytochrome P-450 in Streptomyces Setonii. *Appl. Environ. Microbiol.* **1986**, *52* (1), 98−100.
(69) Dardas, A.; Gal, D.; Barrelle, M.; Sauret-Ignazi, G.; Sterjiades, R.; Pelmont, J. The Demethylation of Guaiacol by a New Bacterial Cytochrome P-450. *Arch. Biochem. Biophys.* **1985**, *236* (2), 585−592.
(70) Max, B.; Tugores, F.; Cortés-Diéguez, S.; Domínguez, J. M. Bioprocess Design for the Microbial Production of Natural Phenolic Compounds by Debaryomyces Hansenii. *Appl. Biochem. Biotechnol.* **2012**, *168* (8), 2268−2284.
(71) de Gonzalo, G.; Colpa, D. I.; Habib, M. H. M.; Fraaije, M. W. Bacterial Enzymes Involved in Lignin Degradation. *J. Biotechnol.* **2016**, *236*, 110−119.
(72) Brzonova, I.; Kozliak, E. I.; Andrianova, A. A.; LaVallie, A.; Kubátová, A.; Ji, Y. Production of Lignin Based Insoluble Polymers (Anionic Hydrogels) by C. Versicolor. *Sci. Rep.* **2017**, *7*, 17507.

DOI: 10.1021/acssuschemeng.9b01605
ACS Sustainable Chem. Eng. 2019, 7, 11640−11652

Paper VI

This is an open access article published under a Creative Commons Attribution (CC-BY) License, which permits unrestricted use, distribution and reproduction in any medium, provided the author and source are cited.

ACS AUTHORCHOICE

ACS Sustainable Chemistry & Engineering

pubs.acs.org/journal/ascecg

Research Article

Conceptual Design of a Kraft Lignin Biorefinery for the Production of Valuable Chemicals via Oxidative Depolymerization

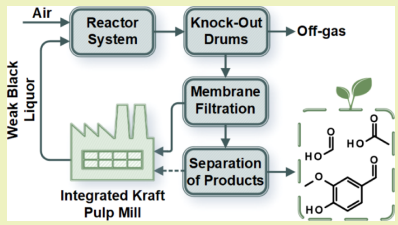
Omar Y. Abdelaziz, Abdulrahman A. Al-Rabiah, Mahmoud M. El-Halwagi, and Christian P. Hulteberg*

Cite This: *ACS Sustainable Chem. Eng.* 2020, 8, 8823−8829

Read Online

ACCESS | Metrics & More | Article Recommendations | Supporting Information

ABSTRACT: Lignin is the most abundant aromatic biopolymer on Earth, and its aromatic structure makes it a promising platform for the production of biobased chemicals and other valuable building blocks. The valorization of lignin into chemicals currently presents a challenge, and its facilitation is key in the development of viable lignocellulosic biorefinery processes. This study presents a conceptual design for a recently demonstrated process for lignin oxidative depolymerization. Modeling, simulation, and analysis were performed based on experimental data to assess the viability of the process. Mass and energy balances and main design data were determined for a 700 t/y kraft lignin biorefinery. The production capacity of aromatic chemicals, including vanillin, vanillic acid, guaiacol, and acetovanillone, was 0.3 kg aromatics/kg net lignin use. A heat-integrated process design is suggested, and the energy demands and the CO_2 emissions are evaluated and compared. Assuming an interest rate of 10% and a plant lifetime of 10 years, the return on investment was calculated to be 14%, indicating that such a biorefinery is viable. A sensitivity analysis was carried out to assess the impact of the vanillin selling price and the cost of lignin on the profitability of the process. A quantitative investigation of process sustainability resulted in an E-factor of ∼1.6 for the entire synthetic route, that is, 38% material efficiency. The findings of this study underline the need for further research to develop efficient lignin conversion technologies with attractive yields in order to increase profitability on an industrial scale.



KEYWORDS: *biobased chemicals, biomass valorization, biorefinery systems, lignin conversion, process simulation, sustainable resources, techno-economic analysis*

INTRODUCTION

Lignin is the largest source of aromatic building blocks in nature and has significant potential as a raw material for the production of biobased products, allowing the replacement of fossil-derived materials.[1,2] It is found in most terrestrial plants, constituting 15−40% dry weight, and purveys structural integrity.[3,4] Because of its heterogeneity and recalcitrance, lignin is often treated as a waste byproduct and burned to produce energy. However, the efficient valorization of lignin is key in realizing more sustainable and competitive biorefineries, and the utilization of lignin as a resource for the production of chemicals offers an attractive opportunity.[5] The development of efficient process technologies for the conversion of lignin into value-added chemicals is thus of the utmost importance in biorefinery research.[6,7]

Kraft pulping is the main process used to produce paper pulp. Wood is transformed into pulp by cooking in a solution of Na_2S/NaOH, the so-called white liquor, at a temperature of 155−175 °C for several hours.[8] About 90−95% of the lignin in the starting material can be dissolved through this process.[9] It has recently been estimated that the annual production of kraft pulp worldwide is about 130 million tons,[10] from which approximately 50 million tons of degraded lignin are liberated.[11,12] Lignin from kraft black liquor also represents a large share of the bioenergy sector in Sweden and Finland,[13,14] and new product chains based on exploiting kraft lignin from black liquor as a renewable source of aromatics are being encouraged.

Techno-economic evaluation of lignocellulosic biorefineries in general, and lignin biorefinery concepts in particular, is required to assess the commercial viability of novel and emerging technologies. Examples of such technologies include bio-oil stabilization and upgrading,[15] levulinic acid conversion,[16] the production of monosugars,[17] 5-hydroxymethylfurfural,[18] butadiene from furfural,[19] biodiesel from algal oil,[20] glycerol valorization,[21] and lignocellulosic ethanol.[22] Such studies revealed considerable variability in the feedstock and products derived from different biorefinery processes.

Received: April 20, 2020
Revised: May 19, 2020
Published: June 5, 2020



ACS Publications

© 2020 American Chemical Society

A limited number of studies have recently been carried out on the technical design and viability of novel lignin valorization processes. Energy and exergy calculations have been performed on catechol production based on lignin extracted from olive tree pruning.[23] Process intensification has been combined with simulation to compare different strategies for the production of vanillin/methyl vanillate from kraft lignin, for example, extraction with organic solvents, nanofiltration, and adsorption with zeolite; the last alternative shows additional savings in energy and cost of 0.2 and 7.4%, respectively.[24] Capacity design and risk analysis of biophenol/resin production from kraft lignin have also been presented,[25,26] demonstrating that the viability of such a biorefinery depends on the selling price of the product on the market and variations in the cost of lignin. The techno-economics of large-scale production of colloidal lignin particles, involving solubilization with tetrahydrofuran and ethanol, has also been assessed, where an internal rate of return of 17% was reported.[27] In another study, the feasibility of synthesizing lignin micro- and nanoparticles via an aerosol/atomization method has been evaluated, where manufacturing costs were quoted as being in the range of 600−1170 $/t.[28] Three lignin conversion routes to biobased aromatics have been analyzed: noncatalytic pyrolysis, hydrothermal upgrading, and direct hydrodeoxygenation; the last route is found to be the most economically promising.[29]

Life cycle assessment (LCA) studies have also been carried out on lignin-based processes to assess their environmental impact. An LCA of catechol production from lignin contained in candlenut shells has been performed,[30] showing an overall reduction in the environmental footprint of this route, compared to the conventional production from petrochemicals. LCA of adipic acid production from lignin has also been performed, in which reductions in greenhouse gas emissions of 62−78% were predicted for the biobased route, compared to conventional production of adipic acid.[31] Techno-economic analysis and LCA are essential when introducing a developing technology onto the market, to provide information for investment purposes, and to identify whether additional research is needed prior to implementation.

In the present study, the experimental work reported by Abdelaziz et al.[32] was used as a basis for the design and techno-economic evaluation of large-scale production of valuable chemicals from lignin. The oxidative depolymerization of industrial kraft lignin, extracted using the LignoBoost technology, to provide low-molecular-weight compounds suitable for microbial conversion was described. We investigate the viability of chemical production preceding biological funneling as another possible route for lignin processing. Novel process configurations were developed using Aspen Plus software. Economic and environmental analyses were performed, and process profitability was evaluated using different price ranges of lignin and products.

METHODS

The process design was based on first-hand experimental data, obtained from a study on the oxidative depolymerization of kraft lignin as a means of pretreatment for microbial conversion.[32] Briefly, kraft lignin precipitated using the LignoBoost technology was treated with molecular oxygen under different reaction conditions to identify the best conditions for obtaining a biocompatible, oxidatively depolymerized lignin stream. The reactions were also performed under mild alkaline conditions to ensure solubilization of the lignin. However, the addition of sodium hydroxide was not included in process simulation because of the possibility of using the sodium hydroxide material stream available in a pulp mill as an active cooking chemical. The feed to the process was rather assumed to be in the form of weak black liquor. The highest yield of aromatic monomers was obtained at 160 °C and 3 bar oxygen partial pressure (Table S1), and this product slate was found to be suitable for conversion by several microbial species. Carboxylic acids were also generated from the reaction and are treated here as useful coproducts.

An opportunity for scaling up the production of biobased chemicals from the lignin material was investigated to enable assessing the economic viability of such a biorefinery. The underlying goal was to identify the process limitations and to determine whether the process would be of commercial interest. The major aromatic compounds generated by this process include vanillin, vanillic acid, acetovanillone, and guaiacol, while the carboxylic acids were primarily composed of formic and acetic acids. This process was designed to be integrated into an existing pulp and paper mill. A simplified block flow diagram of the proposed process modeled in this study is presented in Figure 1.

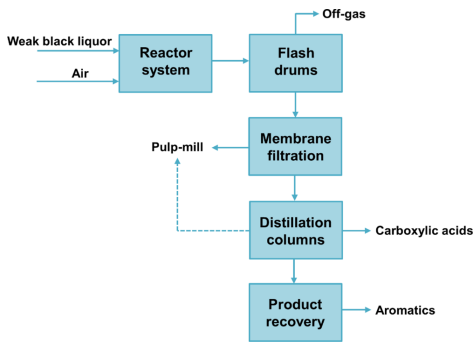


Figure 1. Simplified block flow diagram of the lignin oxidative depolymerization process.

Process Simulation. Aspen Plus V10 software was used to simulate the process of oxidative depolymerization of lignin into aromatic chemicals and carboxylic acids. Mass and energy balances were calculated in the Aspen Plus simulation environment after specifying the input streams and unit operations. The proposed biorefinery was assumed to have an input of about 700 metric tons of lignin per annum, excluding feedstock streams recovered within the process, which is almost 10% of the production from LignoBoost lignin. The RISE lignin plant (LignoDemo), located at Bäckhammar in Sweden, can produce up to 8000 t/y of high-quality LignoBoost kraft lignin (the raw material used in our experimental work), which is then used as a raw material for the production of biofuels, chemicals, and other materials.

The phenolic compound 2-methoxy-4-propylphenol ($C_{10}H_{14}O_2$) was used as a model for lignin.[33] The thermodynamic model used to describe the phase equilibrium between different components of the process was the nonrandom two-liquid (NRTL) property model. Simulations included the Mixer, Pump, Compr, Heater, HeatX, Valve, RStoic, Flash2, Sep, and RadFrac modules. The main reactions defined for the stoichiometric reactor simulation were as follows

$$C_{10}H_{14}O_2 + 10.7O_2 \rightarrow 3.6CH_2O_2 + 6.4CO_2 + 3.4H_2O \quad (1)$$

$$C_{10}H_{14}O_2 + 6.96O_2 \rightarrow 2.77C_2H_4O_2 + 4.46CO_2 + 1.46H_2O \quad (2)$$

$$C_{10}H_{14}O_2 + 7.565O_2 \rightarrow 1.41C_4H_6O_4 + 4.36CO_2 + 2.77H_2O \quad (3)$$

https://dx.doi.org/10.1021/acssuschemeng.0c02945
ACS Sustainable Chem. Eng. 2020, 8, 8823−8829

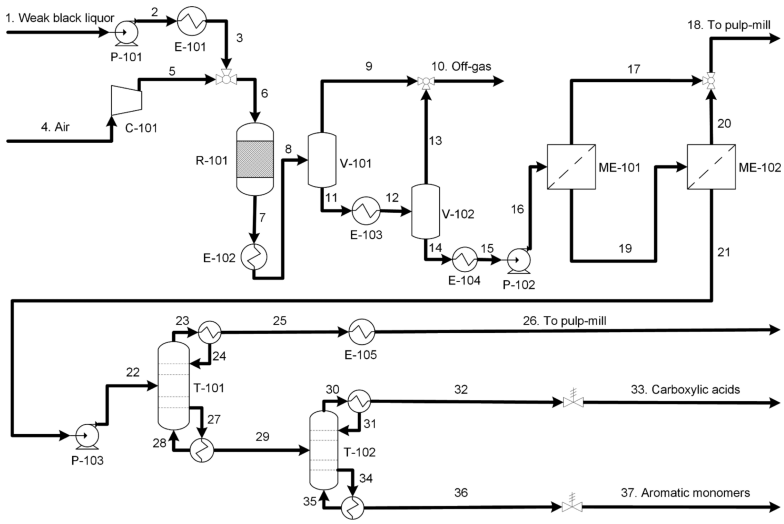


Figure 2. Process flow diagram for the conversion of lignin to aromatics and acids via oxidative depolymerization.

$$C_{10}H_{14}O_2 + 4.58O_2 \rightarrow 0.99C_8H_8O_4 + 2.08CO_2 + 3.04H_2O \quad (4)$$

$$C_{10}H_{14}O_2 + 1.78O_2 \rightarrow 1.34C_7H8O_2 + 0.62CO_2 + 1.64H_2O \quad (5)$$

$$C_{10}H_{14}O_2 + 3.235O_2 \rightarrow 1.09C_8H_8O_3 + 1.28CO_2 + 2.64H_2O \quad (6)$$

$$C_{10}H_{14}O_2 + 2.5O_2 \rightarrow C_9H_{10}O_3 + CO_2 + 2H_2O \quad (7)$$

Energy and Environmental Analyses. The total utility requirements to satisfy the heating and cooling demands in the process flowsheets were calculated using Aspen Energy Analyzer. In the design of the base case, the available energy savings were identified by comparing the actual energy demands with the energy targets. Furthermore, a heat integration scheme was proposed with the objective of maximizing the process-to-process heat recovery, thus minimizing the total utility requirements.

The amount of CO_2 emitted corresponding to burning a certain amount of fuel, Q_{fuel}, was estimated for the base case and the heat-integrated design using the equation below

$$[CO_2]_{emitted} = (Q_{fuel}/NHV) \times (C\ \%/100) \times \alpha \quad (8)$$

where α is the ratio of the molar masses of CO_2 and carbon (=3.67). NHV denotes the net heating value, and values of 39,771 and 51,600 kJ/kg were used for heavy fuel oil and natural gas, respectively, while the carbon contents C % (dimensionless) were set to 86.5 and 75.4, respectively.[34,35]

Economic Evaluation. Stoichiometric−economic targeting (also referred to as stoichionomic targeting) was used to provide benchmarks for the flows of reactants and products.[36] Together with chemical pricing data, this tool is useful in making early-stage decisions regarding a proposed process design. The metric for inspecting sales and reactants (MISR) was used to determine whether the process had the potential for economic viability or not, defined as

$$MISR = \frac{\sum_{p=1}^{N_{products}} F_p \times S_p}{\sum_{r=1}^{N_{reactants}} F_r \times C_r} \quad (9)$$

where F_p is the annual production rate of product p, S_p is the selling price of product p, F_r is the annual feed rate of reactant r, and C_r is the cost price of reactant r. If MISR >1, the process may be considered for more detailed analysis, although higher values of MISR are desirable. If MISR <1, the process is not desirable from an economic perspective.

CAPCOST, a software tool for capital cost estimation based on the equipment module costing method,[37] was used for detailed analysis to calculate the total capital and operating costs and to assess the economic viability of the proposed process designs. The direct and indirect project expenses were included in the capital cost estimates by multiplying a bare module factor by the cost of the purchased equipment. All costs were estimated in US dollars (US$) and updated to 2019 prices, considering the annual Chemical Engineering Plant Cost Index (CEPCI). As the plant was assumed to be geographically located in Sweden, a corporate tax rate of 21.4% was applied. The return on investment (ROI) and net present value (NPV) were the indices calculated to assess the profitability of the proposed process designs. The major assumptions used in the techno-economic evaluation are summarized in Table S2.

RESULTS AND DISCUSSION

Mass and Energy Balances. A computer simulation model was developed to perform the mass and energy balance calculations, based on the block flow diagram in Figure 1. The process includes several parts, that is, lignin conversion, gas and solid separation, membrane filtration, and product recovery. The process flow diagram is depicted in Figure 2.

The lignin, in the form of weak black liquor (stream 1 in Figure 2), is heated to 174 °C before mixing with air at a pressure of 8.5 bar (stream 5). The combined stream (stream 6) is sent to a reactor (R-101), which is operated at about 160 °C and 8 bar. The reactor effluent (stream 7) is cooled to 100 °C in a heat exchanger (E-102). The effluent stream is then flashed in two flash drums (V-101 and V-102) to separate the noncondensable gases from the liquid products, while the off-gas (stream 10) is possibly sent for purification.

https://dx.doi.org/10.1021/acssuschemeng.0c02945
ACS Sustainable Chem. Eng. 2020, 8, 8823−8829

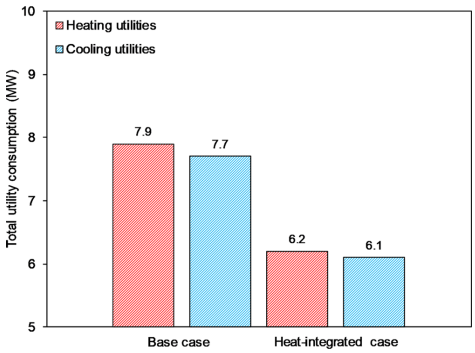


Figure 3. Energy demands in the lignin oxidative depolymerization process in the base case and heat-integrated design.

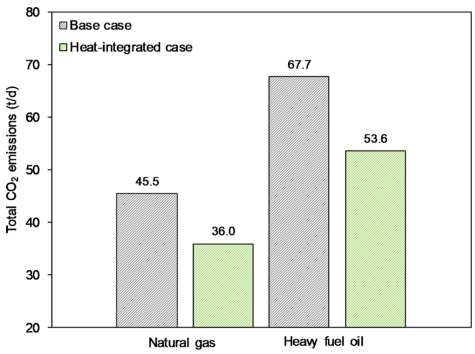


Figure 4. Daily CO_2 emissions from the lignin oxidative depolymerization process in the base case and the heat-integrated design.

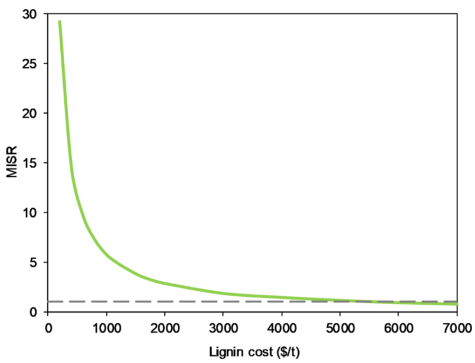


Figure 5. Effect of the cost of lignin on MISR in the oxidative depolymerization process.

The liquid product mixture (stream 16) is sent to a membrane filtration unit (ME-101), where any unreacted lignin is recovered as retentate (stream 17). The permeate is sent to a hydrophobic membrane separator (ME-102) that selectively removes the organics from the aqueous stream. Such a membrane technology concept has been a subject of interest in recent research owing to the highly efficient separation of organics and ease of operation.[29] The retentate from ME-102 (stream 20) is combined with stream 17 and recycled to the pulp mill. The remaining organic fraction in aqueous solution (stream 21) is separated from water in a distillation column (T-101), and the water is returned to the mill (stream 26). The bottoms (stream 29) are sent to a second distillation column (T-102), where the carboxylic acids (formic and acetic acid, stream 33) are separated from the low-molecular-weight aromatic products (stream 37).

Based on the simulations obtained from the model, mass and energy balances were evaluated for the oxidative lignin depolymerization process. Data related to the main process streams of the base case, including component flows, conditions, and so forth, are given in Table S3.

Heat integration was then applied to the base case, and an additional heat exchanger unit was added to recover the excess energy in the process. The location of the new heat exchanger was upstream of E-101 for the cold-side fluid and upstream of E-102 for the hot-side fluid. Consequently, E-101 could be operated at a lower heating duty requirement, and the cooling duty of E-102 was reduced.

Process Analysis and Sustainability. The energy and environmental performance of the various process configurations were analyzed and compared. A considerable proportion of the process operating costs is attributed to the heating and cooling duties, both of which can be minimized by means of heat integration. Figure 3 shows the total utility consumption of the base case and the heat-integrated case.

Table 1. Summary of Key Economic Results for the Lignin Oxidative Depolymerization Process

parameter	base case	heat-integrated design
total capital cost (MM$)	6.53	6.69
cost of raw materials (MM$/y)	0.17	0.17
utilities (MM$/y)	1.63	1.28
product sales (MM$/y)	4.06	4.06
NPV (MM$)	3.58	4.97
ROI (%)	10.36	13.87

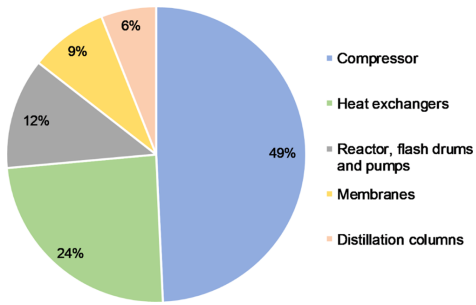


Figure 6. Contributions of various pieces of equipment to the fixed capital investment.

https://dx.doi.org/10.1021/acssuschemeng.0c02945
ACS Sustainable Chem. Eng. 2020, 8, 8823−8829

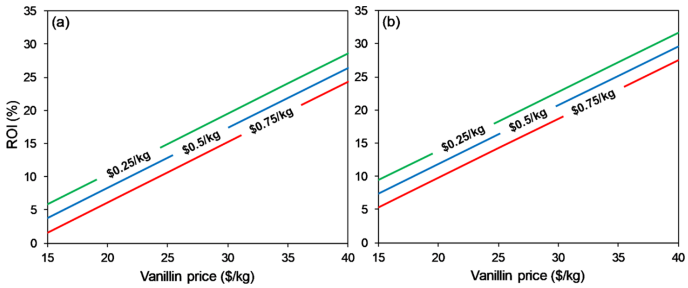


Figure 7. Sensitivity analysis for the ROI of (a) the base case and (b) the heat-integrated design, for various lignin costs.

Heat integration reduced the energy demands for heating and cooling utilities by 22% and 21%, respectively.

Furthermore, heat integration led to a reduction in CO_2 emissions (Figure 4). The environmental analysis was based on the amount of CO_2 emitted by the combustion of fuels powering the process. The reduction in CO_2 emissions, compared to the base case, was 9500 or 14,100 kg/d, depending on whether the fuel used was natural gas or heavy fuel oil, respectively. The heat-integrated process design of this lignin biorefinery thus provides a more sustainable option from both the energy and environmental perspectives.

Sheldon's environmental factor (E-factor) was used to quantify the sustainability and greenness of the proposed process.[38] The amount of waste generated per kg of the product produced can be calculated with the E-factor, allowing the material efficiency, a metric used for the production of commodity chemicals from biomass, to be estimated. Material efficiency is defined as the total mass of useful products divided by the total mass of useful products + waste.

The useful products in this study were defined as the carboxylic acids (formic and acetic acid) and the aromatic monomers (vanillin, vanillic acid, guaiacol, and acetovanillone). The main waste steam in the process was stream 10, the off-gas, where the CO_2 emission amounted to 2138 kg/d. This corresponds to an E-factor of ∼1.6, a value in the range of a bulk chemical sector.[38] This gave a material efficiency of 38%, which is an acceptable value for a biomass-based synthetic route.[39] Other metrics, such as ozone depletion, acidification, smog formation, and societal impact, can be evaluated through a detailed LCA, but this was beyond the scope of this study. Nonetheless, it should be stressed that the use of lignin as a renewable feedstock for biobased chemical production, rather than petroleum, is encouraging from a sustainability perspective.

Profitability Assessment. To assess the economic potential of this oxidative depolymerization process based on actual stoichiometric calculations, the stoichionomic indicator MISR was used. Actual product yields and separation losses were taken into account in these stoichiometric calculations. The effect of lignin cost on the MISR for the process is shown in Figure 5.

The value at which the process becomes economically infeasible is at a lignin cost of 5600 $/ton. Under reasonable price scenarios for kraft lignin (250−750 $/ton), high values of MISR (>8) were obtained. A more detailed economic analysis, involving other costs, that is, capital cost, utilities, and so forth, was thus undertaken. The profitability of the two process schemes was evaluated based on the ROI and NPV. The key economic results for both scenarios are summarized in Table 1.

The total capital cost of the heat-integrated design was estimated to be about 2.5% higher than that in the base case. Figure 6 shows a cost breakdown, illustrating the contribution from each unit operation to the fixed capital investment. The air compressor unit was the most expensive component, contributing 49% to the total capital cost, followed by the heat exchangers, which contributed 24%. The main reason for the high cost of the air compressor was that a spare unit was included in the economic evaluation to provide operational flexibility.

On the other hand, a notable reduction in the cost of utilities was achieved by applying heat integration (22% compared to the base case), which in turn affected the overall profitability of the process. The NPV and the ROI of the base case were $3.6MM and 10.4%, respectively, while the corresponding values for the heat-integrated design were $5MM and 14%, respectively. Acceptable values of ROI for forest-based biorefineries have been reported to be 10−15%.[40] The acceptable value is considerably lower in Scandinavia than in other countries, indicating the potential of establishing forest biorefinery concepts.

A sensitivity analysis was performed to assess the impact of changes in the cost of feedstock and product selling price on the profitability of the process (Figure 7). The ROI is plotted against the selling price of vanillin, ranging from $15/kg to $40/kg, and a lignin cost ranging from $0.25/kg to $0.75/kg, for the two designs considered.

Under pessimistic conditions, that is, a lignin cost of $0.75/kg and a vanillin selling price of $15/kg, rather low, but still positive, ROIs were obtained: 1.6% for the base case and 5.3% for the heat-integrated design. The selling price of vanillin had a strong influence on the ROIs of both process configurations. In a favorable scenario (a lignin cost of $0.25/kg and a vanillin selling price of $40/kg), the ROI was quite high for both configurations (≥29%). The heat-integrated design exhibited an average increase in ROI of approximately 3.4% compared to the base case at the higher lignin cost.

The process described in this study is still in its infancy, and there is a rather high degree of uncertainty concerning the value of the products generated. The commercial application of lignin depolymerization and upgrading technologies is still limited, which can lead to uncertainties in the modeling and investment cost calculations.[29,41] However, the assessment of such early-stage technologies is desirable as this could provide insights into potential drivers, barriers, targets, and impacts on

https://dx.doi.org/10.1021/acssuschemeng.0c02945
ACS Sustainable Chem. Eng. 2020, 8, 8823−8829

further technological development. The present work contributes to the knowledge on the thermochemical transformation of lignin to value-added chemicals, which will be useful in the subsequent improvement of the process in the context of environmental and economic sustainability.

CONCLUSIONS

The substitution of nonrenewable fossil resources with renewable biomass as the principal raw material for producing chemicals is a crucial goal of green chemistry and engineering. In this study, we have evaluated the techno-economic viability of biochemical production from kraft lignin as a renewable feedstock via oxidative depolymerization. Process synthesis, simulation, and integration formed the basis of the analysis and the assessment of the potential viability with respect to vanillin production. The process was evaluated on a scale of 700 t/y of fresh lignin feed. After heat integration, and assuming a cost of lignin of $250/ton, the process was deemed economically viable, with values of ROI in the range of 9−32%, based on the product selling price. It is suggested that the process be colocated and integrated with an existing pulp and paper mill, as this will significantly reduce the overall operating costs. Work is ongoing to improve the yield and selectivity toward vanillin employing different catalytic systems. This early-stage process analysis provides a sounder base for the practical realization of an integrated facility for valorizing lignin waste streams into value-added chemicals, which also speaks for providing environmental benefits.

ASSOCIATED CONTENT

Supporting Information

The Supporting Information is available free of charge at https://pubs.acs.org/doi/10.1021/acssuschemeng.0c02945.

Data related to the product parameters, the techno-economic assumptions, and the various streams in the lignin oxidative depolymerization process (PDF)

AUTHOR INFORMATION

Corresponding Author

Christian P. Hulteberg − *Department of Chemical Engineering, Lund University, 221 00 Lund, Sweden;* orcid.org/0000-0002-3502-5529; Email: christian.hulteberg@chemeng.lth.se

Authors

Omar Y. Abdelaziz − *Department of Chemical Engineering, Lund University, 221 00 Lund, Sweden;* orcid.org/0000-0002-3530-3509

Abdulrahman A. Al-Rabiah − *Department of Chemical Engineering, King Saud University, Riyadh 11421, Saudi Arabia*

Mahmoud M. El-Halwagi − *The Artie McFerrin Department of Chemical Engineering, Texas A&M University, College Station, Texas 77843-3122, United States;* orcid.org/0000-0002-0020-2281

Complete contact information is available at: https://pubs.acs.org/10.1021/acssuschemeng.0c02945

Notes

The authors declare no competing financial interest.

ACKNOWLEDGMENTS

This work was supported by the Swedish Foundation for Strategic Research (RBP14-0052), the Swedish Energy Agency (45241-1 and 49701-1), and the Södra Research Foundation (2019-149). A.A.A. acknowledges financial support from the Research Center at the College of Engineering, Deanship of Scientific Research, King Saud University.

REFERENCES

(1) Sun, Z.; Fridrich, B.; De Santi, A.; Elangovan, S.; Barta, K. Bright Side of Lignin Depolymerization: Toward New Platform Chemicals. *Chem. Rev.* **2018**, *118*, 614−678.

(2) Zhu, P.; Abdelaziz, O. Y.; Hulteberg, C. P.; Riisager, A. New Synthetic Approaches to Biofuels from Lignocellulosic Biomass. *Curr. Opin. Green Sustain. Chem.* **2020**, *21*, 16−21.

(3) Ragauskas, A. J.; Beckham, G. T.; Biddy, M. J.; Chandra, R.; Chen, F.; Davis, M. F.; Davison, B. H.; Dixon, R. A.; Gilna, P.; Keller, M.; Langan, P.; Naskar, A. K.; Saddler, J. N.; Tschaplinski, T. J.; Tuskan, G. A.; Wyman, C. E. Lignin Valorization: Improving Lignin Processing in the Biorefinery. *Science* **2014**, *344*, 1246843.

(4) del Río, J. C.; Rencoret, J.; Gutiérrez, A.; Elder, T.; Kim, H.; Ralph, J. Lignin Monomers from beyond the Canonical Monolignol Biosynthetic Pathway: Another Brick in the Wall. *ACS Sustainable Chem. Eng.* **2020**, *8*, 4997−5012.

(5) Schutyser, W.; Renders, T.; Van den Bosch, S.; Koelewijn, S.-F.; Beckham, G. T.; Sels, B. F. Chemicals from Lignin: An Interplay of Lignocellulose Fractionation, Depolymerisation, and Upgrading. *Chem. Soc. Rev.* **2018**, *47*, 852−908.

(6) Key, R. E.; Bozell, J. J. Progress toward Lignin Valorization via Selective Catalytic Technologies and the Tailoring of Biosynthetic Pathways. *ACS Sustainable Chem. Eng.* **2016**, *4*, 5123−5135.

(7) Sudarsanam, P.; Duolikun, T.; Babu, P. S.; Rokhum, L.; Johan, M. R. Recent Developments in Selective Catalytic Conversion of Lignin into Aromatics and Their Derivatives. *Biomass Conversion and Biorefinery*; 2019.

(8) Sjöström, E. *Wood Chemistry: Fundamentals and Applications*, 2nd ed.; Academic Press, Inc.: San Diego, California, 1993.

(9) Calvo-Flores, F. G.; Dobado, J. A.; Isac-García, J.; Martín-Martínez, F. J. *Lignin and Lignans as Renewable Raw Materials: Chemistry, Technology and Applications*; John Wiley & Sons, Ltd: Chichester, U.K., 2015.

(10) Rinaldi, R.; Jastrzebski, R.; Clough, M. T.; Ralph, J.; Kennema, M.; Bruijnincx, P. C. A.; Weckhuysen, B. M. Paving the Way for Lignin Valorisation: Recent Advances in Bioengineering, Biorefining and Catalysis. *Angew. Chem., Int. Ed.* **2016**, *55*, 8164−8215.

(11) Bruijnincx, P. C. A.; Rinaldi, R.; Weckhuysen, B. M. Unlocking the Potential of a Sleeping Giant: Lignins as Sustainable Raw Materials for Renewable Fuels, Chemicals and Materials. *Green Chem.* **2015**, *17*, 4860−4861.

(12) Hu, J.; Zhang, Q.; Lee, D.-J. Kraft Lignin Biorefinery: A Perspective. *Bioresour. Technol.* **2018**, *247*, 1181−1183.

(13) Jönsson, J.; Pettersson, K.; Berntsson, T.; Harvey, S. Comparison of Options for Utilization of a Potential Steam Surplus at Kraft Pulp Mills-Economic Performance and CO2 Emissions. *Int. J. Energy Res.* **2013**, *37*, 1017−1035.

(14) Abdelaziz, O. Y.; Li, K.; Tunå, P.; Hulteberg, C. P. Continuous Catalytic Depolymerisation and Conversion of Industrial Kraft Lignin into Low-Molecular-Weight Aromatics. *Biomass Convers. Biorefin.* **2018**, *8*, 455−470.

(15) Li, W.; Dang, Q.; Smith, R.; Brown, R. C.; Wright, M. M. Techno-Economic Analysis of the Stabilization of Bio-Oil Fractions for Insertion into Petroleum Refineries. *ACS Sustainable Chem. Eng.* **2017**, *5*, 1528−1537.

(16) Braden, D. J.; Henao, C. A.; Heltzel, J.; Maravelias, C. C.; Dumesic, J. A. Production of Liquid Hydrocarbon Fuels by Catalytic Conversion of Biomass-Derived Levulinic Acid. *Green Chem.* **2011**, *13*, 1755−1765.

(17) van den Bergh, J.; Babich, I. V.; O'Connor, P.; Moulijn, J. A. Production of Monosugars from Lignocellulosic Biomass in Molten Salt Hydrates: Process Design and Techno-Economic Analysis. *Ind. Eng. Chem. Res.* **2017**, *56*, 13423−13433.
(18) de Carvalho, E. G. L.; Rodrigues, F. d. A.; Monteiro, R. S.; Ribas, R. M.; da Silva, M. J. Experimental Design and Economic Analysis of 5-Hydroxymethylfurfural Synthesis from Fructose in Acetone-Water System Using Niobium Phosphate as Catalyst. *Biomass Convers. Biorefin.* **2018**, *8*, 635−646.
(19) Kuznetsov, A.; Kumar, G.; Ardagh, M. A.; Tsapatsis, M.; Zhang, Q.; Dauenhauer, P. J. On the Economics and Process Design of Renewable Butadiene from Biomass-Derived Furfural. *ACS Sustainable Chem. Eng.* **2020**, *8*, 3273−3282.
(20) Pokoo-Aikins, G.; Nadim, A.; El-Halwagi, M. M.; Mahalec, V. Design and Analysis of Biodiesel Production from Algae Grown through Carbon Sequestration. *Clean Technol. Environ. Policy* **2010**, *12*, 239−254.
(21) D'Angelo, S. C.; Dall'Ara, A.; Mondelli, C.; Pérez-Ramírez, J.; Papadokonstantakis, S. Techno-Economic Analysis of a Glycerol Biorefinery. *ACS Sustainable Chem. Eng.* **2018**, *6*, 16563−16572.
(22) da Silva, A. R. G.; Giuliano, A.; Errico, M.; Rong, B.-G.; Barletta, D. Economic Value and Environmental Impact Analysis of Lignocellulosic Ethanol Production: Assessment of Different Pretreatment Processes. *Clean Technol. Environ. Policy* **2019**, *21*, 637−654.
(23) Mabrouk, A.; Erdocia, X.; Alriols, M. G.; Labidi, J. Economic Analysis of a Biorefinery Process for Catechol Production from Lignin. *J. Clean. Prod.* **2018**, *198*, 133−142.
(24) Wongtanyawat, N.; Lusanandana, P.; Khwanjaisakun, N.; Kongpanna, P.; Phromprasit, J.; Simasatitkul, L.; Amornraksa, S.; Assabumrungrat, S. Comparison of Different Kraft Lignin-Based Vanillin Production Processes. *Comput. Chem. Eng.* **2018**, *117*, 159−170.
(25) Dessbesell, L.; Yuan, Z.; Hamilton, S.; Leitch, M.; Pulkki, R.; Xu, C. C. Bio-based Polymers Production in a Kraft Lignin Biorefinery: Techno-economic Assessment. *Biofuels, Bioprod. Bioref.* **2018**, *12*, 239−250.
(26) Dessbesell, L.; Yuan, Z.; Leitch, M.; Paleologou, M.; Pulkki, R.; Xu, C. C. Capacity Design of a Kraft Lignin Biorefinery for Production of Biophenol via a Proprietary Low-Temperature/Low-Pressure Lignin Depolymerization Process. *ACS Sustainable Chem. Eng.* **2018**, *6*, 9293−9303.
(27) Ashok, R. P. B.; Oinas, P.; Lintinen, K.; Sarwar, G.; Kostiainen, M. A.; Österberg, M. Techno-Economic Assessment for the Large-Scale Production of Colloidal Lignin Particles. *Green Chem.* **2018**, *20*, 4911−4919.
(28) Abbati de Assis, C.; Greca, L. G.; Ago, M.; Balakshin, M. Y.; Jameel, H.; Gonzalez, R.; Rojas, O. J. Techno-Economic Assessment, Scalability, and Applications of Aerosol Lignin Micro- and Nanoparticles. *ACS Sustainable Chem. Eng.* **2018**, *6*, 11853−11868.
(29) Vural Gursel, I.; Dijkstra, J. W.; Huijgen, W. J. J.; Ramirez, A. Techno-Economic Comparative Assessment of Novel Lignin Depolymerization Routes to Bio-Based Aromatics. *Biofuels, Bioprod. Bioref.* **2019**, *13*, 1068−1084.
(30) Montazeri, M.; Eckelman, M. J. Life Cycle Assessment of Catechols from Lignin Depolymerization. *ACS Sustainable Chem. Eng.* **2016**, *4*, 708−718.
(31) Corona, A.; Biddy, M. J.; Vardon, D. R.; Birkved, M.; Hauschild, M. Z.; Beckham, G. T. Life Cycle Assessment of Adipic Acid Production from Lignin. *Green Chem.* **2018**, *20*, 3857−3866.
(32) Abdelaziz, O. Y.; Ravi, K.; Mittermeier, F.; Meier, S.; Riisager, A.; Lidén, G.; Hulteberg, C. P. Oxidative Depolymerization of Kraft Lignin for Microbial Conversion. *ACS Sustainable Chem. Eng.* **2019**, *7*, 11640−11652.
(33) Hanaoka, T.; Fujimoto, S.; Yoshida, M. Efficiency Estimation and Improvement of the 1,3-Butadiene Production Process from Lignin via Syngas through Process Simulation. *Energy Fuels* **2017**, *31*, 12965−12976.
(34) Gadalla, M.; Olujic, Z.; Jobson, M.; Smith, R. Estimation and Reduction of CO2 Emissions from Crude Oil Distillation Units. *Energy* **2006**, *31*, 2398−2408.
(35) Abdelaziz, O. Y.; Hosny, W. M.; Gadalla, M. A.; Ashour, F. H.; Ashour, I. A.; Hulteberg, C. P. Novel Process Technologies for Conversion of Carbon Dioxide from Industrial Flue Gas Streams into Methanol. *J. CO2 Util.* **2017**, *21*, 52−63.
(36) El-Halwagi, M. M. Benchmarking Process Performance Through Overall Mass Targeting. *Sustainable Design through Process Integration: Fundamentals and Applications to Industrial Pollution Prevention, Resource Conservation, and Profitability Enhancement*; Elsevier Inc., 2017; pp 73−125.
(37) Turton, R.; Bailie, R. C.; Whiting, W. B.; Shaeiwitz, J. A. *Analysis, Synthesis, and Design of Chemical Processes*, 3rd ed.; Pearson Education: Boston, MA, 2008.
(38) Sheldon, R. A. The E Factor 25 Years on: The Rise of Green Chemistry and Sustainability. *Green Chem.* **2017**, *19*, 18−43.
(39) Pinazo, J. M.; Domine, M. E.; Parvulescu, V.; Petru, F. Sustainability Metrics for Succinic Acid Production: A Comparison between Biomass-Based and Petrochemical Routes. *Catal. Today* **2015**, *239*, 17−24.
(40) Näyhä, A.; Pesonen, H.-L. Diffusion of Forest Biorefineries in Scandinavia and North America. *Technol. Forecast. Soc. Change* **2012**, *79*, 1111−1120.
(41) Huang, K.; Fasahati, P.; Maravelias, C. T. System-Level Analysis of Lignin Valorization in Lignocellulosic Biorefineries. *iScience* **2020**, *23*, 100751.

https://dx.doi.org/10.1021/acssuschemeng.0c02945
ACS Sustainable Chem. Eng. 2020, 8, 8823−8829

Paper VII

Catalysis Science & Technology

ROYAL SOCIETY OF CHEMISTRY

PAPER

View Article Online
View Journal

Check for updates

Cite this: DOI: 10.1039/d0cy02158j

Oxidative depolymerization of Kraft lignin to high-value aromatics using a homogeneous vanadium–copper catalyst†

Florian Walch, [a] Omar Y. Abdelaziz, [b] Sebastian Meier, [c] Saša Bjelić, [d] Christian P. Hulteberg [b] and Anders Riisager *[a]

Lignin, the world's most abundant biopolymer with high aromaticity, has huge potential as a renewable feedstock replacing petroleum for the production of chemicals, fuels and functional materials. The enhanced utilization of lignin would improve the economic viability of existing pulp and paper mills, as well as lignocellulosic biorefineries, where lignin is highly available, but mostly incinerated for energy recovery. Catalysis could be of crucial importance to improve current depolymerization strategies, and hence contribute to a more sustainable and responsible use of terrestrial resources. In the present study, the impact of different homogeneous transition-metal catalysts on the oxidative depolymerization of a technical softwood Kraft lignin was investigated. The reactions were carried out using molecular oxygen under rather mild operating conditions and the produced aromatic monomers included, among others, vanillin, vanillic acid and acetovanillone. The best performing system incorporated a $VO(acac)_2$–$Cu(OAc)_2$ (V–Cu) catalyst, resulting in a bio-oil yield of approximately 50% and a total increase in aromatic monomers of 27%, on a weight basis. Moreover, a favorable combined effect between $VO(acac)_2$ and $Cu(OAc)_2$ was suggested by NMR spectroscopy. UHPLC-HRMS and corresponding statistical analysis revealed a more than 30-fold increase in two aromatic molecules with an oxoacetic functionality and oxalic acid as well as a focusing effect on selected molecules, when employing the V–Cu catalyst. The findings of this study indicate that the V–Cu catalyst system is promising for the efficient conversion of technical lignin into value-added aromatic chemicals. However, catalyst recycling and reuse must be demonstrated, for successful implementation under industrial conditions.

Received 6th November 2020,
Accepted 14th January 2021

DOI: 10.1039/d0cy02158j

rsc.li/catalysis

Introduction

The valorization of biomass represents a promising and sustainable alternative for the production of platform chemicals, fine chemicals, functional materials and fuels, compared to petroleum-based processes.[1–4] Lignin, the most abundant non-carbohydrate polymer in biomass, is of particular interest, as it comprises the world's largest renewable source of aromatic compounds. Lignin makes up 10–40% of the dry weight of woody biomass and grasses.[4–7] The biopolymer is composed of three aromatic moieties, namely *p*-hydroxyphenyl (H), guaiacyl (G), and syringyl (S) units (Fig. 1). These units are cross-linked *via* different carbon–carbon and/or carbon–oxygen bonds, of which the β-O-4′ and 5–5′ bonds appear most often, with respective abundances of 45–50% and 18–25% in softwood. However, the fraction of H-, G- and S-units and the proportion of linkages varies considerably between hardwood, softwood and grasses.[8–10] Moreover, the composition of lignin is dependent on the extraction process used to separate it from cellulose and hemicellulose,[11–15] where the fraction of C–C bonds is typically higher in technical lignins as compared to native

[a] Centre for Catalysis and Sustainable Chemistry, Department of Chemistry, Technical University of Denmark, Kemitorvet 207, 2800 Kgs. Lyngby, Denmark. E-mail: ar@kemi.dtu.dk
[b] Department of Chemical Engineering, Lund University, Naturvetarvägen 14, 221 00 Lund, Sweden
[c] Department of Chemistry, Technical University of Denmark, Kemitorvet 207, 2800 Kgs. Lyngby, Denmark
[d] Laboratory for Bioenergy and Catalysis, Paul Scherrer Institute, Forschungsstrasse 111, 5232 Villigen, Switzerland

† Electronic supplementary information (ESI) available. See DOI: 10.1039/d0cy02158j

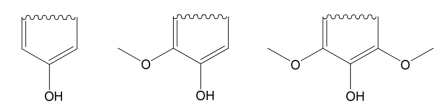


Fig. 1 Chemical structure of the three aromatic moieties of lignin, *p*-hydroxyphenyl (H), guaiacyl (G), and syringyl (S) residues.

lignins due to condensation.[16,17] Despite the heterogeneity of lignin causing several difficulties, its unique chemical structure and the high bioavailability of this renewable, non-edible feedstock offers a huge potential towards industrial implementation.[18] However, in pulp and paper mills as well as in lignocellulosic biorefineries, where lignin is generated in large quantities, the focus currently lies on the valorization of carbohydrates. In contrast, lignin is mainly utilized for heat and power generation.[19,20]

To fully exploit the potential of lignin and to make it more attractive to the pulp and paper industry and lignocellulosic biorefineries, catalysis could play a key role in depolymerizing lignin into value-added aromatic monomers.[21] In order to keep the native functional groups of the aromatic moieties and add functionality, oxidative depolymerization strategies seem most promising.[1,4,22,23] Typical depolymerization products are platform or fine chemicals, such as phenolic aldehydes and acids, fractionated into a viscous bio-oil by solvent extraction.[4,24,25] A wide range of homogeneous and heterogeneous catalysts has previously been evaluated, including metal salts, metal oxides, coordination complexes, composites of metal oxides, polyoxometalates, organometallics, metal–organic frameworks, organocatalysts and enzymes.[8,12,21,26–28] However, the nature of the obtained compounds is dependent on the used lignin (or lignin model compound), reaction conditions and media or oxidant. Therefore, it is rather difficult to effectively compare the performance of the aforementioned catalysts.

Among homogeneous catalysts, Cu-, Mn-, Co-, Fe- and V-based catalysts showed promising catalytic activity in depolymerizing lignin into valuable aromatic compounds.[4,19,29–32] Copper and vanadium catalysts have shown to selectively cleave the C–C bonds in the oxidative depolymerization reactions.[33–35] Reaction mechanisms for vanadium-catalyzed oxidative cleavages have been proposed.[35–37] Yet, most of the studies have dealt with lignin model compounds or native lignin, whereas investigations on technical lignin are rather seldom.[38] As model compounds often represent one specific type of lignin linkage,[4,23] studies on real complex feedstocks, including technical lignin, should be preferred to gain insights into representative product functionalities.

In the present study, we address the gap in technical lignin conversion by investigating the oxidative depolymerization of a technical LignoBoost (LB) Kraft lignin from softwood. The objective was to produce high-value aromatic monomers and high-quality bio-oil under rather mild conditions, using oxygen gas as the environmentally benign primary oxidant and an alkaline water solution as the solvent. Different homogeneous catalysts were tested, and their performance was assessed. A potential combined effect on the cleavage of different lignin linkages by a vanadium–copper-based catalyst was suggested, and the system was further optimized. Compared to previous studies dealing with a related catalytic system,[30,31] this study rather focused on the identification and quantification of the major reaction products that could be generated from a real industrial lignin stream than on gaining mechanistic insights from the conversion of model compounds. In addition, the reaction medium used in this study was a NaOH aqueous solution, whereas in the related studies, organic solvents, such as pyridine or toluene, had been used. The possibility of using the NaOH available in a Kraft pulp mill as an active cooking chemical renders the proposed approach attractive from a process integration perspective.[39]

Experimental

Chemicals and materials

$VO(acac)_2$ (95%), $Cu(OAc)_2{\cdot}H_2O$, vanillin (99%), vanillic acid (97%), 4-hydroxybenzaldehyde (98%), acetovanillone (98%), HCl (aq. solution, 37 wt%), NaOH (98%) and DMSO-d_6 (99.9%) were purchased from Sigma-Aldrich. Ethyl acetate (EtOAc, HPLC grade), acetone (HPLC grade), Na_2SO_4 anhydrous (99.8%) and qualitative filter paper 413 (55 mm) were purchased from VWR International. 4-Hydroxybenzoic acid (99%) was purchased from Fluka Chemical, and $Mn(OAc)_2$ (98%) was purchased from Merck. Oxygen gas (99.5%) was purchased from Air Liquide Denmark. LB softwood Kraft lignin was obtained as a dry powder from the LignoBoost demonstration plant in Bäckhammar, Sweden. LB is characterized by its rather low ash and carbohydrate contents and a sulfur content usually in the range of 1–3%.[40] Deionized water was used throughout all experiments. All materials were used as received, without further purification.

Depolymerization reactions

In a typical experiment, an autoclave (Parr Instrument Company, 300 mL, equipped with a Parr 4848 reactor controller and a Teflon insert) was loaded with 60 mL of an aqueous 25 g L^{-1} lignin in 2 M NaOH solution and the respective amount of catalyst. The reactor was sealed and purged with oxygen gas three times and pressurized to the desired O_2 partial pressure. Stirring (700 rpm) was applied and the reactor was heated up to the desired temperature (45 min to reach 150 °C). Reaction time was considered to start after the desired reaction temperature was reached.

After the completion of the reaction, the autoclave was quenched in an ice bath to cool it down to room temperature, which typically took 30 min. The reactor was then opened, the liquid product mixture was collected and was stored in a freezer (−20 °C), in order to inhibit possible condensation reactions. Solid residues remaining in the reaction chamber were rinsed with water and were then stored at −20 °C until further usage.

Workup procedure

An aliquot of 20 mL of the product mixture (pH $>$ 13) was acidified with aqueous HCl to pH $\leq$ 1, leading to the precipitation of heavy lignin fragments. In order to separate

This journal is © The Royal Society of Chemistry 2021

the two phases, the resulting mixture was centrifuged (3900 rpm) for 20 min. After centrifugation, the liquid phase was transferred to a separation funnel. Residual solvent in the remaining solid fraction (precipitate) was evaporated in a freeze-dryer (Scanvac Coolsafe 110-4 Pro) until dryness, the solid was weighed and stored in the fridge at 4 °C until further analysis. The liquid phase was extracted with EtOAc three times (2 × 15 mL, 1 × 30 mL) and the remaining aqueous fraction was collected and stored in the fridge at 4 °C until further analysis. The combined organic phases were dried over anhydrous Na_2SO_4. EtOAc was evaporated with a rotary evaporator (IKA RV 10) at 40 °C and approximately 210 mbar to yield a brownish bio-oil. The yield of bio-oil was calculated gravimetrically based on the initial lignin weight fed into the reactor, as shown in eqn (1).

$$\text{Bio-oil yield [wt\%]} = \frac{m(\text{Bio-oil}) \times 3}{m(\text{Lignin})} \times 100 \quad (1)$$

The resulting dry bio-oil was then analyzed. Typically, about 50 mg of bio-oil were used instantaneously for the quantification of monomers. The remaining bio-oil was dissolved in *ca.* 5 mL acetone, sealed and stored in the fridge at 4 °C until further use.

A schematic flowchart of the workup procedure is shown in Fig. 2. Selected reactions were performed in duplicate or triplicate, and eqn (2) was used to calculate the yields of monomers.

$$\text{Monomer yield [wt\%]} = \frac{m(\text{Monomer})_{\text{NMR}}}{m(\text{Bio-oil})_{\text{NMR}}} \times \text{Bio-oil yield} \quad (2)$$

Size-exclusion chromatography (SEC)

SEC was used to determine the molecular weight distribution (MWD), the weight-average molecular weight (M_w), and the number-average molecular weight (M_n) of the unreacted LB lignin and the oxidatively depolymerized lignin products. The SEC system consisted of a Waters Alliance 2695 high-performance liquid chromatography (HPLC) setup (Milford, MA, USA) with a Waters 2487 UV detector. The system was controlled and peak evaluations were managed using Waters Empower 3 chromatography data software. A Superdex 200 Increase 10/300 GL column (GE Healthcare Bio-Sciences AB, Uppsala, Sweden) was used to ensure high resolution over a large range of molecular weights. Calibration was carried out using different sodium polystyrene sulfonate standards from Polymer Standards Service GmbH (Mainz, Germany). Each sample was diluted with 0.1 M NaOH to a concentration of 0.5 g L^{-1} and filtered (0.2 μm) to remove any suspended matter. The volume of filtered solution injected into the SEC system was 10 μL and elution was performed for 60 min using an aqueous solution containing 0.1 M NaOH.

Nuclear magnetic resonance (NMR)

Samples for NMR analysis were prepared by redissolving 50 mg bio-oil in 550 μL DMSO-d_6 and transferring the samples to a 5 mm NMR tube. All spectra were acquired at 25 °C using an 800 MHz Bruker Avance III instrument equipped with a TCI cryoprobe and a SampleJet sample changer. One-dimensional ^{13}C spectra were acquired with 30 s of recycle delay, sampling 64k complex data points during 1.36 s of acquisition time. ^{1}H–^{13}C heteronuclear single quantum coherence (HSQC) NMR spectra with 140 ppm spectral width in the ^{13}C dimension were acquired as data matrices of 1024(^{1}H) × 256(^{13}C) complex data points to probe the linkage region and the chemical composition of the substrate. Reaction products were identified and quantified as detailed below by the acquisition of ^{1}H–^{13}C HSQC NMR spectra of 60 ppm spectral width centered in the aromatic spectral region, sampling 2048(^{1}H) × 512(^{13}C) complex data points with 2 accumulations per increment, a recycle delay of 1.2 seconds and non-uniform sampling of 50% of the data points in the indirect dimension. All NMR spectra were processed with ample zero filling and baseline corrections in all dimensions using Bruker Topspin 3.5 pl 7 and were integrated into the same software.

Quantitative ^{1}H–^{13}C NMR

Conventional one-dimensional NMR spectroscopy is inherently quantitative, if precautions are taken to ensure that full recovery occurs between accumulated transients. Such a quantitative NMR (qNMR) approach is not always

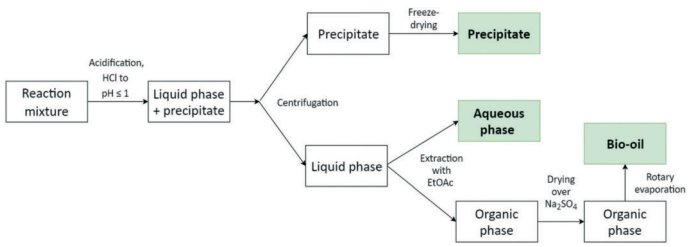


Fig. 2 Schematic depiction of the workup procedure upon oxidative depolymerization of LB Kraft lignin.

viable for quantification in complex reaction material, however, it has been concluded in previous studies that two-dimensional NMR-based quantifications can be superior to ^{1}H NMR-based quantifications in complex mixtures, specifically when using highly-resolved ^{1}H–^{13}C HSQC NMR spectra.[41] HSQC NMR spectra are not inherently quantitative due to relaxation during transfer periods and as signal amplitude modulates with scalar coupling between ^{1}H and ^{13}C. These problems can be circumvented, when using the ^{1}H–^{13}C HSQC NMR spectrum as a detection modality, while calibrating the response through gravimetrically defined reference compounds.

Standard solutions were prepared by dissolving vanillin, vanillic acid, 4-hydroxybenzaldehyde, acetovanillone and 4-hydroxybenzoic acid in DMSO-d_6 (about 5 mg in 550 μL), and transferred to a 5 mm NMR tube. Standards were used both for identification and quantification with high-resolution ^{1}H–^{13}C spectra. Reference samples were gravimetrically prepared in DMSO-d_6 and analyzed under identical conditions for identification and quantification. The estimated deviation resulting from the signal-to-noise ratio in the NMR determinations was ±0.01 wt%.

Ultra high-performance liquid chromatography (UHPLC)-high-resolution mass spectrometry (HRMS)

For UHPLC-HRMS analysis, 1 μL of the 100 times diluted sample with water was injected into a liquid chromatography-mass spectrometry system. The time-resolved separation of the analytes was performed in a Dionex Ultimate 3000 Series RS system (Thermo Scientific, Basel, Switzerland) including a pump, a column compartment and an auto-sampler. The column and pre-column were Thermo Scientific Accucore RP-MS (150 mm × 2.1 mm, particle size 2.6 μm). The following program with mobile phase A (1 vol% MeOH, 1 vol% CH_3CN and 0.2 vol% HCOOH in high purity water) and mobile phase B (100 vol% MeOH) was applied: 1% B (0–1 min) 1 to 99% B (1–6 min), 99% B (6–8 min), followed by equilibration step and 99 to 1% B (8–8.2 min), 1% B (8.2–10 min). The flow was set to 0.7 mL min^{-1}, while the temperature of the column was kept constant at 50 °C. Heated electrospray ionization (ESI, 3.5 kV spray voltage) in positive and negative mode was used for the ionization of the analytes.

Data acquisition was performed using a Thermo Scientific Q Exactive hybrid quadrupole-Orbitrap mass spectrometer controlled by Xcalibur 4.1 software. Mass spectra were acquired in full scan mode with an isolation window of 1 m/z from 50–750 m/z. The resolution was 70 000. The raw mass spectral data files were collected in triplicate. The UHPLC-HRMS data were imported into Compound Discoverer 3.1 software (Thermo Scientific, Switzerland) and processed with standard settings except for mass tolerance (set to 2.5 ppm). Chromatographic peaks detected in one of the input files, but missing in others, were checked by the "Fill Gaps" option. The composition (of a general formula $C_cH_hO_o$) was predicted based on exact mass and isotopic patterns and evaluated against MS/MS spectra. The cutoff value for the area was set to 5×10^6. The identity of the compounds was determined with mzCloud, where possible. Only features yielding formulas present in ChemSpider were used. Tentative identification was performed using the FISh score algorithm (Fig. S1, ESI†).

The statistical significance of perturbations between different runs was assessed using volcano plots, which specify $\log_2$ of the fold-change on the x-axis *versus* significance ($-\log_{10}$ of the p-value from a post-hoc ANOVA analysis) on the y-axis. The fold change was calculated as the ratio of the area under the peak from corresponding runs. Statistically relevant changes in the composition can be found where the following conditions are met: p-value < 0.05 as well as $\log_2 < -2$ or $\log_2 > 2$ for significantly downregulated and significantly upregulated species, respectively. In the absence of strict rules, a value of $\log_2 = 2$ as cutoff value is widely accepted.[42,43]

Results and discussion

Screening of homogeneous catalysts

A screening of homogeneous transition-metal based catalysts was performed to evaluate their ability to catalyze the oxidative depolymerization of lignin to monomeric aromatic compounds. Five different catalytic systems were tested. The catalysts were primarily assessed based on their selectivity towards vanillin and vanillic acid. The reaction conditions were kept constant throughout the screening, and the quantification of the monomeric aromatic products was carried out by ^{1}H–^{13}C HSQC NMR spectroscopy. Representative spectra used in the identification and quantification of selected compounds in the post-reaction material are presented in Fig. S2, ESI.† The concentration of NaOH (2 M) was chosen to maintain pH > 13 for the entire reaction. Maintaining a high pH is important, as acidic products of depolymerization could lower the pH, hence influencing the degradation of produced vanillin due to oxidation.[44] However, the usage of even higher NaOH concentrations has been reported to lead to operational problems.[19]

In terms of selectivity towards vanillin, the $Cu(OAc)_2$ and $VO(acac)_2$–$Cu(OAc)_2$ (V–Cu) catalyst systems showed higher vanillin yields of about 3.5%, compared to the control reaction (no added catalyst) and the other catalysts tested, where yields in the range of 1.5–3% were obtained (Fig. 3). Comparing these two systems, the yields obtained for acetovanillone, 4-hydroxybenzoic acid and 4-hydroxybenzaldehyde were rather similar. However, the V–Cu catalyst provided a higher yield in vanillic acid than $Cu(OAc)_2$ catalyst alone. Hence, either $VO(acac)_2$ seemed to inhibit the formation of vanillin or, more likely, promote its further oxidation into vanillic acid, as the obtained yield in vanillin was considerably lower than for the control reaction. For the combined V–Cu catalyst system, a combined effect

This journal is © The Royal Society of Chemistry 2021

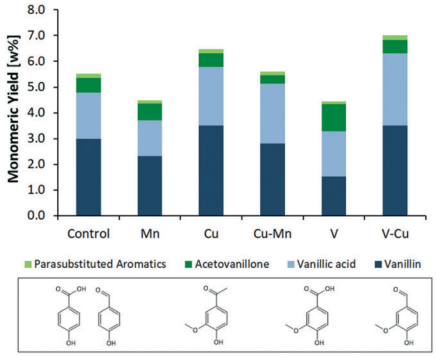


Fig. 3 Yields of the identified monomeric aromatic compounds and their respective chemical structures during oxidative depolymerization. "Parasubstituted Aromatics" describes a combination of the small yields of 4-hydroxybenzoic acid and 4-hydroxybenzaldehyde. Reaction conditions: 150 °C, 10 min, 5 bar initial O_2, 60 mL of 25 g L^{-1} lignin in 2 M NaOH. Mn: $Mn(OAc)_2$, Cu: $Cu(OAc)_2$, V: $VO(acac)_2$. Monomer yields given in mass of respective monomer per mass of initial lignin. The control reaction was performed in triplicate, the V–Cu-catalyzed reaction in duplicate, and the respective average values are given. Amounts and ratios of the respective catalysts are summarized in Table S1, ESI.†

between the components was observed, as the selectivity towards vanillin was enhanced by catalysis with $VO(acac)_2$ and the yield in vanillic acid increased relative to catalysis by $Cu(OAc)_2$.

Due to the aforementioned differences in the yields of vanillin and vanillic acid, the total amount of the five quantified aromatic monomers (vanillin, vanillic acid, acetovanillone, 4-hydroxybenzoic acid and 4-hydroxybenzaldehyde) increased up to 7.0% upon V–Cu catalysis, compared to 5.5% in the control reaction and 6.5% in the Cu-catalyzed reaction. This corresponds to an improvement in the total monomer yield of 27% and 18% comparing the V–Cu- and the Cu-catalyzed reactions to the control reaction, respectively. Conversely, the catalyst composed of $Cu(OAc)_2$ and $Mn(OAc)_2$ did not show similar combined effects, as the yield of vanillin (2.8%) ranged between the yields observed when using the individual catalysts (3.5% for $Cu(OAc)_2$ and 2.3% for $Mn(OAc)_2$).

The combined effect of V–Cu catalysis is in line with previous observations on lignin model compounds[30,31] and lignin.[31] The reaction mechanisms probably proceed *via* a combination of C–C and C–O bond cleavages. Nonetheless, selective C–C bond cleavages have been shown employing Cu[34] or V-catalysis.[33] The selectivity between C–C or C–O bond cleavage has also been shown to be dependent on the nature of the employed V-catalyst.[35] However, to elucidate specific cleavages of interunit linkages and reaction mechanisms, studies on lignin model compounds seem more appropriate. Lignin model compounds resemble common linkages found in the lignin polymer in a simpler molecule, aiming to facilitate analysis of the reaction pathways.[4,45] A recent study has also shown the stability of the obtained aromatic products (*e.g.* vanillin) under alkaline oxidative depolymerization conditions to be crucial.[46] Overall, the reaction pathways are dependent on several parameters, such as the chemical nature of V- and Cu-catalysts, reaction conditions and solvent, and require further research.

SEC was carried out in order to follow the degree of depolymerization and MWDs for the respective catalytic oxidative reactions. As indicated in Fig. 4, depolymerization was clearly successful in the two catalyzed reactions using $Cu(OAc)_2$ and V–Cu catalysts and in the control reaction. This observation is also reflected by a decrease in the MWD (Table S2, ESI†). The M_w decreased from a very broad distribution of 5980 Da (unprocessed lignin feed) to 1135 Da (V–Cu), and the M_n analogously decreased from 1668 Da to 790 Da. In consequence, a narrower distribution of molecular weight was achieved, as confirmed by the polydispersity index (PDI), which decreased from 3.58 for the unprocessed lignin to ≤1.44 for the oxidatively depolymerized samples.

The obtained values for M_w and M_n were slightly lower for the catalyzed depolymerization reactions than for the control reaction. However, the signal at the peak ranging between 160 and 200 Da was higher for the two catalyzed reactions than for the control reaction (Fig. 4). This observation is consistent with higher amounts of the aromatic monomers; vanillin, vanillic acid and acetovanillone produced within the catalyzed reactions, as the aromatic monomers should be observed in this region. Although the performance of V–Cu and $Cu(OAc)_2$ in terms of producing monomeric and dimeric products was rather similar according to SEC, a higher concentration of oligomeric products was observed in the case of V–Cu, which is indicated by higher absorbance in the region of 700–800 Da.

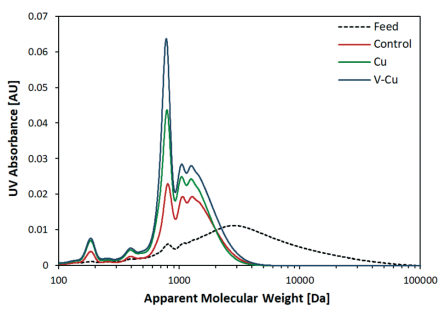


Fig. 4 Molecular weight distributions of the unprocessed lignin feed, the control and the selected catalyzed samples after oxidative depolymerization. Reaction conditions: 150 °C, 10 min, 5 bar initial O_2, 60 mL of 25 g L^{-1} lignin in 2 M NaOH. Cu: $Cu(OAc)_2$, V: $VO(acac)_2$. Amounts and ratios of respective catalysts are given in Table S1, ESI.†

NMR analysis

$^{1}H–^{13}C$ HSQC NMR spectroscopy was performed on the LB substrate and on the bio-oils obtained after the catalytic reactions (Fig. 5). The main linkages identified in the feedstock are displayed in Fig. 6, deriving from β-aryl-ether (β-O-4) (A), phenylcoumaran (β-5) (B) and resinol (β–β) (C) units. Regarding the aromatic region, the most prominent peaks were obtained from guaiacyl (G) units, which is characteristic for softwood lignin. Guaiacyl units are of major importance for the formation of vanillin, vanillic acid and acetovanillone. Additionally, *p*-hydroxyphenyl (H) units were detected, albeit in significantly lower amounts than guaiacyl units.

The NMR spectra of the bio-oils obtained upon V–Cu catalysis (green), $Cu(OAc)_2$ catalysis (blue), $VO(acac)_2$ catalysis (red) and the control reaction (dark blue), as well as the substrate (gray) are compared in Fig. 7. Most of the linkages detected in the substrate disappeared in both the catalyzed and the control samples, suggesting the cleavage of those bonds as well as the efficient separation of monomers from higher oligomers during the workup procedure. Moreover, different structural motifs were formed in the spectra of the $Cu(OAc)_2$- and $VO(acac)_2$-catalyzed reactions, as highlighted by the black boxes in Fig. 7. The signals for the motifs were situated within the oxygenated aliphatic region for the Cu-catalyzed bio-oil. For the bio-oil obtained by the V catalyst, signals were detected that did not emerge in the control or in the Cu-catalyzed reactions. The spectrum of the reaction employing bimetallic V–Cu catalysis contained signals for characteristic structural motifs of individual spectra for both catalysts, suggesting a combined effect. The observation that different reactivity patterns can be obtained by V–Cu catalysis compared to their monometallic analogues indicates the potential of the catalytic system for the oxidative cleavage of complex lignin macromolecules, supporting previous studies on lignin model compounds.[47] However, detailed insights into the combined effect and probable V–Cu interactions will require a dedicated mechanistic study. A favorable effect of

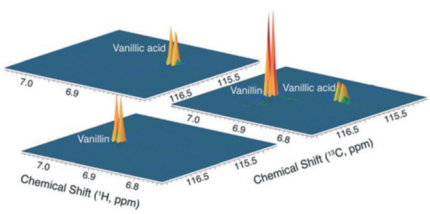


Fig. 5 Graphical representation of selected signals used in $^{1}H–^{13}C$ HSQC NMR for identification and quantification (using the response for gravimetrically defined reference amounts). Front: vanillin standard, back: vanillic acid standard, right: products in bio-oil of the V–Cu-catalyzed reaction. Reaction conditions: 150 °C, 10 min, 5 bar initial O_2, 60 mL of 25 g L^{-1} lignin in 2 M NaOH, 1.4 mmol $VO(acac)_2$–$Cu(OAc)_2$ (V : Cu ratio = 0.75).

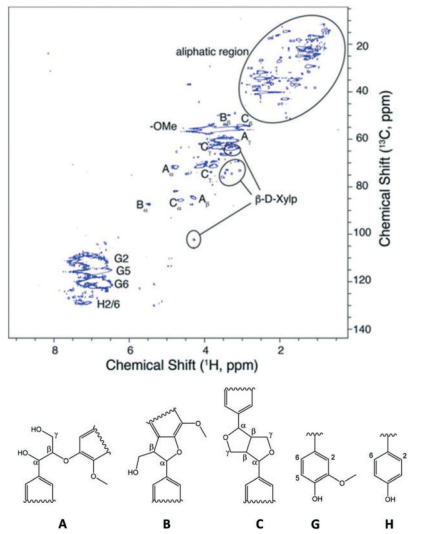


Fig. 6 $^{1}H–^{13}C$ HSQC NMR spectrum of the LB substrate (top) and chemical structures of the respective units (bottom). A: β-Aryl-ether (β-O-4), B: phenylcoumaran (β-5), resinol (β–β), G: guaiacyl, H: *p*-hydroxyphenyl, β-D-Xylp: β-D-xylopyranoside.

V–Cu interactions towards oxidation was suggested not only by the emergence of characteristic structural motifs in the linkage region but also by a higher amount of HCO_3^-

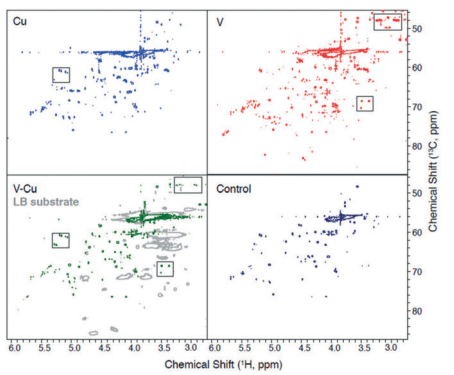


Fig. 7 Comparison of $^{1}H–^{13}C$ HSQC NMR spectra of the LB substrate and the bio-oils obtained upon $Cu(OAc)_2$ catalysis, $VO(acac)_2$ catalysis and $VO(acac)_2$–$Cu(OAc)_2$-catalysis in comparison to bio-oil obtained in the control process. Reaction conditions: 150 °C, 10 min, 5 bar initial O_2, 60 mL of 25 g L^{-1} lignin in 2 M NaOH. Amounts and ratios of respective catalysts are given in Table S1, ESI† and an enlarged version of Fig. 7 can be found in Fig. S4, ESI.†

This journal is © The Royal Society of Chemistry 2021

produced upon V–Cu catalysis relative to formic acid if compared to the other catalysts tested (Fig. S3, ESI†). A complimentary method that provides insight into the oxidative formation of other compounds with few CH groups was used in UHPLC-HRMS analysis of the corresponding post-reaction materials.

UHPLC-HRMS analysis

Ultra-high pressure reversed-phase liquid chromatography was performed on the LB substrate, the product from the control experiment and the organic (bio-oil) and aqueous fractions obtained upon V–Cu catalysis. After data reduction and filtering, 168 different organic molecules could be identified. The chemical similarity between different streams was firstly elucidated using hierarchical cluster analysis (Fig. 8). The prevalence of the particular molecule between the samples is denoted by the blue color (the more intense the color, the higher is the relative concentration of the particular species). The differentiation of the clusters is depicted with the corresponding dendrograms.

Clustering analysis revealed a clear separation of the aqueous samples from LB and organic samples (vertical separation). Separation, according to the chemical species (horizontal separation), showed that the vast majority of the organic species present in the feed were successfully converted during the process, which is in agreement with the observations from NMR spectroscopy and demonstrated by high bio-oil yields. The control and V–Cu catalyzed organic samples had a similar composition, but the V–Cu-catalyzed sample showed a focus that was more pronounced on fewer, selected species (see Fig. 9 and 10). The same focusing trend was also evident in the aqueous samples. In essence, the control samples comply with the majority of the detected species, whereas the V–Cu sample showed district clustering, which is further characterized below.

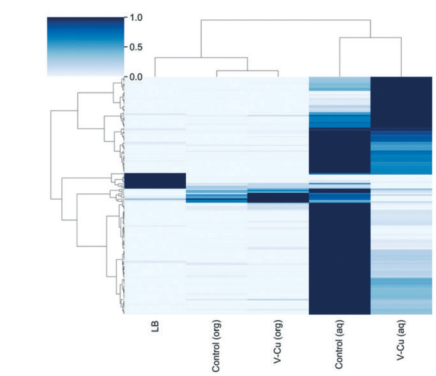


Fig. 8 Hierarchical cluster analysis of organic and aqueous LB as well as samples from control and V–Cu catalyzed reactions using Ward's method and Euclidean metric.

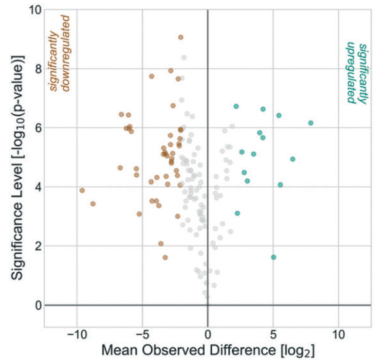


Fig. 9 Volcano plot of V–Cu catalyzed *vs.* control aqueous sample.

UHPLC-HRMS characterization of the products in aqueous phase

The volcano plot (common negative logarithm of the *p*-value *versus* the binary logarithm of the ratio between two samples) of the HRMS data for the aqueous phases resulting from V–Cu and control samples is shown in Fig. 9. Providing a rigorous statistical analysis, the volcano plot is dividing the chemical species into significantly upregulated (significantly present in V–Cu), significantly downregulated (significantly present in control samples), and non-affected (statistically

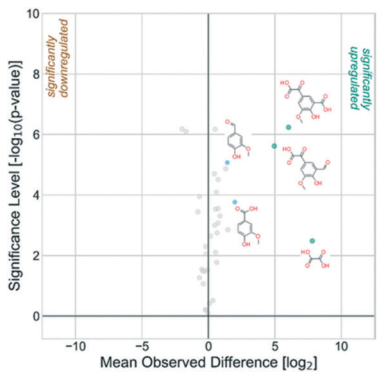


Fig. 10 Volcano plot of V–Cu catalyzed *vs.* control organic sample. Significantly upregulated species and corresponding tentative structures are shown with a green dot. Vanillin and vanillic acid are shown with a light-blue dot for comparison. Note that the two aromatic species possessing an oxoacetic functionality are tentative structures.

non-separable between samples) species. In total, 161 chemical species passed the cutoff criteria and were classified into 14 mainly present in the V–Cu-derived fraction, 56 mostly present in the control sample and 91 species that were statistically indistinguishable between the samples.

The chemical nature of those groups was assessed by van Krevelen and 2D-kernel density analysis[48] (Fig. S5, ESI†). The aqueous control sample was characterized by a maximum in molecular weight around 200 Da with a prominent shoulder around 110 Da, simultaneously having a double peak of double bond equivalents (DBE) around 2.5 and 6.5.

The van Krevelen plot showed clustering around 1 H/C and 0.6 O/C ratios, indicating the presence of oxygenated and aromatic species. The non-affected species had a wide distribution, ranging from 0.5–2.0 H/C and 0.5–1.25 O/C. The MWD showed a Gaussian distribution near 120 Da and a DBE of 1.8, with a shoulder reaching to higher DBE values. In contrast, the V–Cu-catalyzed aqueous sample had a sharp peak at a DBE of 2 and a MWD plateau between 120 and 180 Da. The van Krevelen plot revealed aliphatic oxygenated species clustering around 1.6 H/C and 0.8 O/C.

UHPLC-HRMS characterization of the products in organic phase

The volcano plots of control *vs.* LB, V–Cu *vs.* LB, and V–Cu *vs.* control samples are shown in Fig. S6 and S7, ESI† and Fig. 10, respectively. As observed in the cluster analysis (Fig. 8), most of the species present in LB were converted. With the help of volcano plots, the detailed characterization of those changes could be described. The control experiment yielded 12 out of 37 molecular species into 9 new species, leaving 16 species as statistically indistinguishable. The V–Cu-catalyzed reaction was able to produce 13 new species, reducing the number of indistinguishable species from 16 to 12. Those species could either result from different depolymerization pathways, or conversion from already depolymerized oligo- or monomers. A combination of both presenting strategies is also possible.

The volcano plot of V–Cu catalyzed *vs.* control reaction (Fig. 10) emphasizes that a few chemical species surpassed the criteria being statistically indistinguishable between the control and V–Cu samples. These species may be primarily produced by temperature- and pH-induced conversion of LB and may only be affected by the catalyst to a minor extent. The chemical nature of the statistically indistinguishable species was characterized using van Krevelen analysis (Fig. S8, ESI†). The characteristic of these species is given by H/C ratio of 1 and O/C ratio ranging from 0.25–0.7, thus representing typical oxygenated aromatic species. These species are monomeric as could be deduced from the MWD plots, with a maximum in MWD at about 160 Da (Fig. S9, ESI†). Vanillin and vanillic acid were clearly upregulated, albeit with $\log_2$-values at 1.4 and 1.8 for vanillin and vanillic acid, respectively, thus not matching the criteria to be significantly upregulated.

The selectivity of the employed V–Cu catalyst is demonstrated by the chemical nature of the upregulated species (chemical structures depicted with green dots in Fig. 10, confirmed structure of oxalic acid and tentative structures for aromatic molecules). These species exceeded a 30-fold increase in the V–Cu-catalyzed sample. Although the structures of the upregulated species are tentative, the presence of the oxoacetic group in their structure is certain. All structures present in the ChemSpider database having the proposed formula, and which collision-induced fragment structure could be explained using the FiSH scoring algorithm, have an oxoacetic group (Fig. S10, ESI†). Similar to vanillin and vanillic acid, oxalic acid was identified independently, using authentic standards. The ability of the V–Cu catalyst to prevent further degradation of the oxoacetic group thus potentially opens a specific route towards the production of platform-relevant aromatic species with an oxoacetic functional group.

Optimization of reaction parameters

The initial screening identified V–Cu as the most promising of the investigated catalyst systems. The performance of the system was further optimized in order to enhance the yield in vanillin and vanillic acid and to contribute to a deeper understanding of the catalytic system itself. Several parameters concerning the reaction conditions and the composition of the catalyst were investigated, including oxygen pressure, temperature, reaction time, V : Cu ratio and catalyst-to-lignin ratio (Fig. 11).

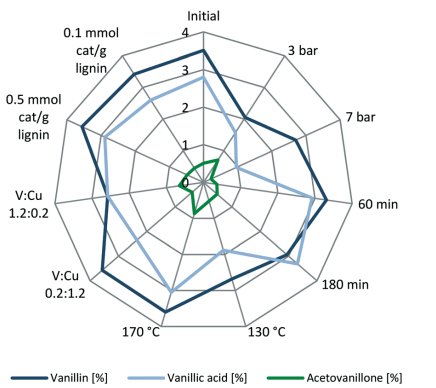


Fig. 11 Yields obtained for vanillin, vanillic acid and acetovanillone at different reaction conditions. Variations from initial reaction conditions are indicated. Initial reaction conditions: 150 °C, 10 min, 5 bar initial O_2, 60 mL of 25 g L^{-1} lignin in 2 M NaOH, 1.4 mmol $VO(acac)_2$–$Cu(OAc)_2$ (V : Cu ratio = 0.75).

This journal is © The Royal Society of Chemistry 2021

In terms of initial oxygen partial pressure, neither a decrease of the pressure to 3 bar nor an increase to 7 bar yielded higher amounts of vanillin or vanillic acid compared to reactions conducted in the presence of 5 bar O_2 partial pressure. However, a trend was observed regarding amounts of acetovanillone, which showed higher yields at lower oxygen partial pressure. In contrast, the yield in bio-oil was found to be highly dependent on partial pressure, obtaining higher yields with increasing pressure ranging from 34% (3 bar) to 56% (7 bar), as shown in Table S1, ESI.†

Upon increasing the reaction time from 10 min to 60 min and 180 min, a trend towards the production of more vanillic acid and less vanillin was observed. Changes in vanillin and vanillic acid showed opposite trends, with vanillin yields decreasing from 3.5% (10 min) to 3.3% (60 min) and 2.9% (180 min), while yields of vanillic acid increased from 2.8% (10 min) to 2.9% (60 min) and 3.3% (180 min). This observation is thus consistent with the oxidation of vanillin to vanillic acid over time.[44] Bio-oil formation was clearly favored by increasing the reaction times, with yields up to 60% (both 60 and 180 min) compared to 48% (10 min). SEC analysis of the reaction mixtures produced at different reaction times resulted in similar MWDs, as displayed in Fig. S11, ESI.† Again, the values for M_w and M_n were slightly lower than for the control reaction, while the obtained absorbance signal was significantly higher for the catalyzed samples.

Decreasing the reaction temperature from 150 to 130 °C resulted in a considerable decrease in yields of both vanillin and vanillic acid. Such observations are consistent with previous results,[19] where a drop in the yields of vanillin and vanillic acid was reported upon changing the reaction temperature from 150 to 125 °C. Oppositely, increasing the reaction temperature from 150 to 170 °C led to an increase in the obtained yield of vanillin from 3.5 to 3.6% and of vanillic acid from 2.8 to 3.1%, respectively. Although the yield increased, the effect was not as pronounced, which is consistent with recent reports on the oxidation of native lignin.[19] Noticeably, the yield in acetovanillone was not affected by lowering the temperature, while a rise to 170 °C increased the yield from 0.5% to 0.9%. However, due to the rather long heating time of the autoclave (*ca.* 45 min to 150 °C), it remained difficult to distinguish the effects of reaction temperature and time.

Altering the ratio of $VO(acac)_2$ and $Cu(OAc)_2$ (*i.e.* V : Cu molar ratio) in the reaction, while maintaining the metal-to-lignin ratio, yielded results that support a possible synergistic effect of $VO(acac)_2$ and $Cu(OAc)_2$, as the highest yields of vanillin and vanillic acid were found in the presence of comparable amounts of both catalysts. An increase in the fraction of $Cu(OAc)_2$ led to a decrease in the yield of vanillic acid, whereas the amount of produced vanillin remained rather constant when decreasing the V : Cu ratio relative to initial conditions with V : Cu = 0.75 (0.6 : 0.8 molar ratio). On the other hand, increasing the V : Cu ratio both decreased the yield of vanillin and vanillic acid, while the yield of acetovanillone was slightly increased.

Influence of catalyst amount and catalyst reuse

To address the technical viability of the reaction system, the catalyst-to-lignin ratio was further investigated. As the initial amount of catalyst to lignin was rather high compared to previously reported studies,[19,33] only lower amounts of catalyst-to-lignin were considered. No major changes in the amount of produced vanillin and vanillic acid could be observed when reducing the amount of catalyst from 0.9 mmol g^{-1} lignin (1.4 mmol V–Cu) to 0.5 mmol g^{-1} lignin. When employing 0.1 mmol catalyst per g lignin, the yield in vanillin and vanillic acid decreased slightly, but only by approximately 0.2–0.3%. These data suggest that, in order to improve the viability of a possible industrial implementation, a lower amount of catalyst may be utilized without a drastic reduction in vanillin/vanillic acid yield. Ideal conditions for implementation in production thus remain to be established.

After reaction, the V–Cu catalyst was separated by EtOAc extraction into an aqueous phase containing NaCl that originates from the LB substrate and the HCl acidification step (Fig. 2). A preliminary experiment was performed to assess the sensitivity of the catalyst to recycling in the presence of increasing concentrations of NaCl, when recycling was carried out according to the procedure proposed in Fig. S12, ESI.† Unfortunately, the recycled catalyst showed rather poor activity, with a yield in vanillin that was even lower than in the control experiment (1.9 compared to 3.0%, respectively). Apart from the yield in vanillic acid, which was slightly higher, all the other quantified aromatic compounds yielded comparable amounts as in the control. Problems within the proposed recycling procedure may result from the increasing concentrations of NaCl as a consequence of acidification and subsequent basification. This problem could be addressed by using an alternative acid that forms less problematic salts, or by separation of the formed salts, *e.g.* through ion exchange or membrane filtration. Another significant aspect is the impact of the recycling procedure on the catalyst. The harsh changes in pH possibly change the chemical composition of the catalyst, in this way affecting its activity towards vanillin and vanillic acid. Characterization of the recycled catalyst and a comparison to the fresh catalyst might give insight into reasons for the lower catalytic activity. Overall, the challenges in recyclability represent a possible starting point for future research and should be considered for potential future adaptations in the design of catalytic system.

Conclusions

The ability to catalyze the oxidative depolymerization of technical lignin with different homogeneous transition-metal catalysts was investigated, with $VO(acac)_2$–$Cu(OAc)_2$ showing the most promising results. The obtained aromatic monomers included vanillin, vanillic acid and acetovanillone, and effective depolymerization to low molecular weight compounds was confirmed by SEC-UV. Optimization of reaction parameters indicated 5 bar initial oxygen pressure

and a molar V : Cu ratio of 0.75 to be optimal, whereas higher temperature and reaction time only had a minor influence on the monomer yield. However, with increasing oxygen partial pressure and reaction time, bio-oil yields increased up to 60%.

A combined effect of $VO(acac)_2$ and $Cu(OAc)_2$ on the product yield was observed as characteristic products of both catalysts were identified in reaction mixtures upon combined V–Cu catalysis. The statistical analysis illustrated a focusing effect of the examined catalyst towards selected products, highlighting a more than 30-fold increase in three molecules possessing an oxoacetic group. This may open new routes towards producing platform chemicals with oxoacetic functionalities. Catalyst recycling indicates that implementation under industrially relevant conditions remains a subject for future research. Such implementation bears promise, as the findings of this study underline the opportunity of sustainably producing high-value aromatics from industrial lignin streams.

Conflicts of interest

There are no conflicts to declare.

Acknowledgements

This research project was supported by the Technical University of Denmark, Lund University, the Swedish Foundation for Strategic Research (RBP14-0052), the Södra Foundation for Research, Development and Education (2019-149), the Swedish Energy Agency (45241-1 and 49701-1), and the Swiss Innovation Agency Innosuisse in the framework of the Swiss Competence Center for Energy Research (SCCER BIOSWEET). We thank Henrik Almqvist for technical support with SEC. The 2D NMR spectra were recorded using the 800 MHz spectrometer at the NMR Center DTU, supported by the Villum Foundation. Part of this work was supported by and performed within the Energy System Integration platform at the Paul Scherrer Institute.

References

1 Z. Sun, B. Fridrich, A. De Santi, S. Elangovan and K. Barta, *Chem. Rev.*, 2018, **118**, 614–678.
2 S. Gillet, M. Aguedo, L. Petitjean, A. R. C. Morais, A. M. da Costa Lopes, R. M. Lukasik and P. T. Anastas, *Green Chem.*, 2017, **19**, 4200–4233.
3 P. Zhu, O. Y. Abdelaziz, C. P. Hulteberg and A. Riisager, *Curr. Opin. Green Sustain. Chem.*, 2020, **21**, 16–21.
4 J. Zakzeski, P. C. A. Bruijnincx, A. L. Jongerius and B. M. Weckhuysen, *Chem. Rev.*, 2010, **110**, 3552–3599.
5 G. De Gonzalo, D. I. Colpa, M. H. M. Habib and M. W. Fraaije, *J. Biotechnol.*, 2016, **236**, 110–119.
6 V. K. Ponnusamy, D. D. Nguyen, J. Dharmaraja, S. Shobana, J. R. Banu, R. G. Saratale, S. W. Chang and G. Kumar, *Bioresour. Technol.*, 2019, **271**, 462–472.
7 A. J. Ragauskas, G. T. Beckham, M. J. Biddy, R. Chandra, F. Chen, M. F. Davis, B. H. Davison, R. A. Dixon, P. Gilna, M. Keller, P. Langan, A. K. Naskar, J. N. Saddler, T. J. Tschaplinski, G. A. Tuskan and C. E. Wyman, *Science*, 2014, **344**, 1246843.
8 F. G. Calvo-Flores, J. A. Dobado, J. Isac-García and F. J. Martín-Martínez, *Lignin and Lignans as Renewable Raw Materials: Chemistry, Technology and Applications*, 2015.
9 C. Mattsson, S. Andersson, T. Belkheiri, L. Åmand, L. Olausson, L. Vamling and H. Theliander, *Biomass Bioenergy*, 2016, **95**, 364–377.
10 G. L. F. Gellerstedt and E. G. Henriksson, in *Monomers, Polymers and Composites from Renewable Resources*, 2008, pp. 201–224.
11 P. Azadi, O. R. Inderwildi, R. Farnood and D. A. King, *Renewable Sustainable Energy Rev.*, 2013, **21**, 506–523.
12 H. Lange, S. Decina and C. Crestini, *Eur. Polym. J.*, 2013, **49**, 1151–1173.
13 J. C. Biermann, *Handbook of pulping and papermaking*, 2nd edn, 1996.
14 J. C. Carvajal, Á. Gómez and C. A. Cardona, *Bioresour. Technol.*, 2016, **214**, 468–476.
15 C. G. Boeriu, D. Bravo, R. J. A. Gosselink and J. E. G. Van Dam, *Ind. Crops Prod.*, 2004, **20**, 205–218.
16 L. Shuai and B. Saha, *Green Chem.*, 2017, **19**, 3752–3758.
17 S. Guadix and M. Meenakshisundaram, *Top. Catal.*, 2018, **61**, 183–198.
18 J. J. Bozell, *Top. Curr. Chem.*, 2014, **353**, 229–256.
19 W. Schutyser, J. S. Kruger, A. M. Robinson, R. Katahira, D. G. Brandner, N. S. Cleveland, A. Mittal, D. J. Peterson, R. Meilan, Y. Román-Leshkov and G. T. Beckham, *Green Chem.*, 2018, **20**, 3828–3844.
20 O. Y. Abdelaziz, K. Ravi, F. Mittermeier, S. Meier, A. Riisager, G. Lidén and C. P. Hulteberg, *ACS Sustainable Chem. Eng.*, 2019, **7**, 11640–11652.
21 R. Ma, M. Guo and X. Zhang, *Catal. Today*, 2018, **302**, 50–60.
22 T. Vangeel, W. Schutyser, T. Renders and B. F. Sels, *Top. Curr. Chem.*, 2018, **376**, 1–18.
23 R. Behling, S. Valange and G. Chatel, *Green Chem.*, 2016, **18**, 1839–1854.
24 N. Abad-Fernández, E. Pérez and M. J. Cocero, *Green Chem.*, 2019, **21**, 1351–1360.
25 E. Pérez and C. O. Tuck, *Eur. Polym. J.*, 2018, **99**, 38–48.
26 O. Y. Abdelaziz, S. Meier, J. Prothmann, C. Turner, A. Riisager and C. P. Hulteberg, *Top. Catal.*, 2019, **62**, 639–648.
27 H. Wang, M. Tucker and Y. Ji, *J. Appl. Chem.*, 2013, **2013**, 1–9.
28 S. Bjelić, L. Garbuio, K. R. Arturi, J. A. van Bokhoven and F. Vogel, *ChemistrySelect*, 2018, **3**, 11680–11686.
29 P. J. Deuss and K. Barta, *Coord. Chem. Rev.*, 2016, **306**, 510–532.
30 T. Rinesch, J. Mottweiler, M. Puche, A. Corma and C. Bolm, *ACS Sustainable Chem. Eng.*, 2017, **5**, 9818–9825.
31 J. Mottweiler, M. Puche, C. Räuber, T. Schmidt, P. Concepción, A. Corma and C. Bolm, *ChemSusChem*, 2015, **8**, 2106–2113.
32 E. B. Clatworthy, J. L. Picone-Murray, A. K. L. Yuen, R. T. Maschmeyer, A. F. Masters and T. Maschmeyer, *Catal. Sci. Technol.*, 2019, **9**, 384–397.

 This journal is © The Royal Society of Chemistry 2021

33 Y. Ma, Z. Du, J. Liu, F. Xia and J. Xu, *Green Chem.*, 2015, **17**, 4968–4973.
34 B. Sedai and R. Tom Baker, *Adv. Synth. Catal.*, 2014, **356**, 3563–3574.
35 S. K. Hanson, R. Wu and L. A. P. Silks, *Angew. Chem.*, 2012, **124**, 3410–3413.
36 Y. Ma, Z. Du, F. Xia, J. Ma, J. Gao and J. Xu, *RSC Adv.*, 2016, **6**, 110229–110234.
37 S. K. Hanson, R. T. Baker, J. C. Gordon, B. L. Scott and D. L. Thorn, *Inorg. Chem.*, 2010, **49**, 5611–5618.
38 W. Schutyser, T. Renders, S. Van Den Bosch, S.-F. Koelewijn, G. T. Beckham and B. F. Sels, *Chem. Soc. Rev.*, 2018, **47**, 852–908.
39 O. Y. Abdelaziz, A. A. Al-Rabiah, M. M. El-Halwagi and C. P. Hulteberg, *ACS Sustainable Chem. Eng.*, 2020, **8**, 8823–8829.
40 P. Tomani, *Cellul. Chem. Technol.*, 2010, **44**, 53–58.
41 I. A. Lewis, S. C. Schommer, B. Hodis, K. A. Robb, M. Tonelli, W. M. Westler, M. R. Sussman and J. L. Markley, *Anal. Chem.*, 2007, **79**, 9385–9390.
42 K. R. Arturi, S. Kucheryavskiy, R. P. Nielsen, M. Maschietti, F. Vogel, S. Bjelić and E. G. Søgaard, *J. Supercrit. Fluids*, 2019, **143**, 211–222.
43 W. Jia, Y. Li, A. Du, Z. Fan, R. Zhang, L. Shi, C. Luo, K. Feng, J. Chang and X. Chu, *Food Chem.*, 2020, **315**, 126308.
44 E. A. B. da Silva, M. Zabkova, J. D. Araújo, C. A. Cateto, M. F. Barreiro, M. N. Belgacem and A. E. Rodrigues, *Chem. Eng. Res. Des.*, 2009, **87**, 1276–1292.
45 L. Yang, K. Seshan and Y. Li, *Catal. Today*, 2017, **298**, 276–297.
46 Y. Mathieu, J. D. Vidal, L. Arribas Martínez, N. Abad Fernández, S. Iborra and A. Corma, *ChemSusChem*, 2020, **13**, 4743–4758.
47 B. Sedai, C. Díaz-Urrutia, R. T. Baker, R. Wu, L. A. P. Silks and S. K. Hanson, *ACS Catal.*, 2011, **1**, 794–804.
48 S. Bjelić, J. Yu, B. B. Iversen, M. Glasius and P. Biller, *Energy Fuels*, 2018, **32**, 3579–3587.

Printed by Media-Tryck, Lund 2021 NORDIC SWAN ECOLABEL 3041 0903



ISBN: 978-91-7422-782-6

Department of Chemical Engineering
Faculty of Engineering, LTH
Lund University

